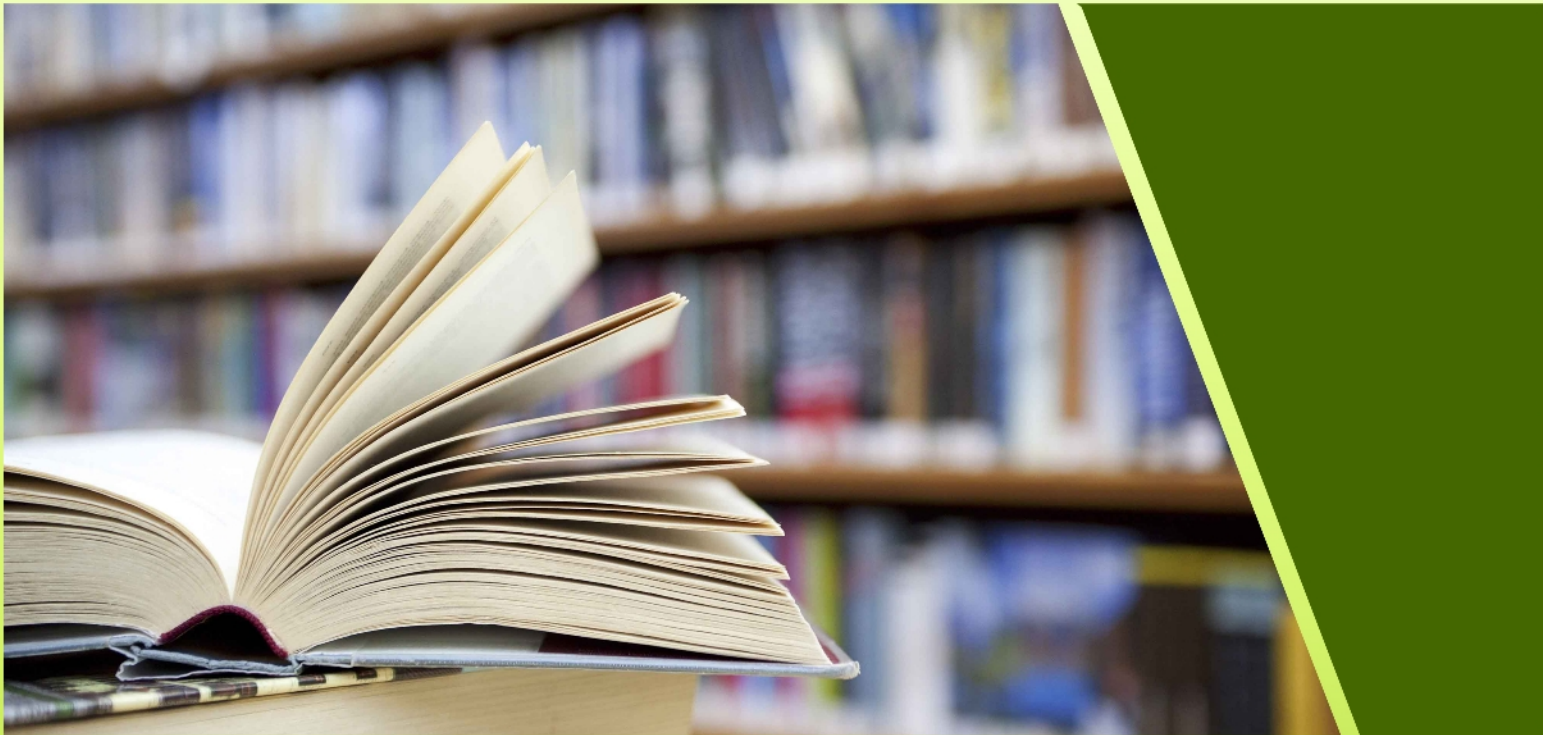




# **Atmospheric Pollution & Climate Change (APCC) Environmental Information System (ENVIS) Resource Partner**

(Sponsored by Ministry of Environment, Forest & Climate Change, Govt. of India)



## **ABSTRACTS India & Global**

**2019-20**

**INDIAN INSTITUTE OF TROPICAL METEOROLOGY  
PUNE - 411 008**

*Contributed by*

**Dr. Gufran Beig**

**Mr. Samir Dhapare**

**Mr. Gaurav Shinde**

**Ms. Bhagyashri Katre**

**Ms. Darshana Jadhav**

Environmental Information System (ENVIS) Resource Partner on Atmospheric Pollution & Climate Change (APCC) at Indian Institute of Tropical Meteorology (IITM), Pune is compiling the abstracts of new research done in the field air pollution and climate change categories, for the year 2019. This book has those abstracts which would help scientists, environmentalists and conservationists regarding monitoring, & controlling for atmospheric pollution and climate change.

## CONTENTS

Sr. No.	Title	Page No.
<b>1.</b>	<b>Aerosol and Air Quality research</b>	
1.	Aerosol Climate Change Connection (AC3) Special Issue: An Overview	1
2.	Aerosol Characteristics over the Northwestern Indo-Gangetic Plain: Clear-Sky Radiative Forcing of Composite and Black Carbon Aerosol	1
3.	Surface PM <sub>2.5</sub> Estimate Using Satellite-Derived Aerosol Optical Depth over India	2
4.	Two-Way Relationship between Aerosols and Fog: A Case Study at IGI Airport, New Delhi	3
5.	Quantification of Carbonaceous Aerosol Emissions from Cookstoves in Senegal	3
6.	Identification of Sources from Chemical Characterization of Fine Particulate Matter and Assessment of Ambient Air Quality in Dhaka, Bangladesh	4
7.	Aerosol Chemical Characterization and Contribution of Biomass Burning to Particulate Matter at a Residential Site in Islamabad, Pakistan	5
8.	Aerosol Chamber Characterization for Commercial Particulate Matter (PM) Sensor Evaluation	6
9.	Impacts of New Particle Formation on Short-term Meteorology and Air Quality as Determined by the NPF-explicit WRF-Chem in the Midwestern United States	7
10.	Chemical Composition of Particulate Matter from Traffic Emissions in a Road Tunnel in Xi'an, China	7
11.	Pollution Characterization, Source Identification, and Health Risks of Atmospheric-Particle-Bound Heavy Metals in PM <sub>10</sub> and PM <sub>2.5</sub> at Multiple Sites in an Emerging Megacity in the Central Region of China	8
12.	Airborne Particulate Pollution Measured in Bangladesh from 2014 to 2017	9
23.	Characterization of the Air Quality Index for Urumqi and Turfan Cities, China	10
14.	Air Pollution Profiles and Health Risk Assessment of Ambient Volatile Organic Compounds above a Municipal Wastewater Treatment Plant, Taiwan	11
15.	Health Benefit Assessment of China's National Action Plan on Air Pollution in the Beijing-Tianjin-Hebei Area	11
16.	On the Contribution of Particulate Matter (PM <sub>2.5</sub> ) to Direct Radiative Forcing over Two Urban Environments in India	12
17.	Emission Characteristics of Regulated and Unregulated Air Pollutants from Heavy Duty Diesel Trucks and Buses	13
18.	Construction and Characterization of an Indoor Smog Chamber for Measuring the Optical and Physicochemical Properties of Aging Biomass Burning Aerosols	13
19.	Monitoring of Emission of Particulate Matter and Air Pollution using Lidar in Belgorod, Russia	14

20.	Spatial and Temporal Variations of Gaseous and Particulate Pollutants in Six Sites in Tibet, China, during 2016–2017	15
21.	Particulate Matter Source Contributions for Raipur-Durg-Bhilai Region of Chhattisgarh, India	16
22.	Measurement of Black Carbon Concentration and Comparison with PM <sub>10</sub> and PM <sub>2.5</sub> Concentrations Monitored in Chungcheong Province, Korea	16
23.	The Geological Availability and Emissions of Sulfur and SO <sub>2</sub> from the Typical Coal of China	17
24.	Study on Influencing Mechanism of Outdoor Plant-related Particles on Indoor Environment and its Control Measures during Transitional Period in Nanjing	18
25.	Sources of High Sulfate Aerosol Concentration Observed at Cape Hedo in Spring 2012	19
26.	Various Sources of PM <sub>2.5</sub> and their Impact on the Air Quality in Tainan City, Taiwan	19
27.	Comparison of Discharging Electrodes for the Electrostatic Precipitator as an Air Filtration System in Air Handling Units	20
28.	Development and Validation of a Novel Particle Source for Nano-sized Test Aerosols	21
29.	Spatial and Temporal Variations of PM <sub>2.5</sub> in North Carolina	21
30.	Source Apportionment and Macro Tracer: Integration of Independent Methods for Quantification of Woody Biomass Burning Contribution to PM <sub>10</sub>	22
31.	Differential Probability Functions for Investigating Long-term Changes in Local and Regional Air Pollution Sources	23
32.	Variation in Airborne Particulate Levels at a Newly Opened Underground Railway Station	24
33.	Characterization of the Air Quality Index in Southwestern Taiwan	24
34.	Ambient Endotoxin and Chemical Pollutant (PM <sub>10</sub> , PM <sub>2.5</sub> , and O <sub>3</sub> ) Levels in South Korea	25
35.	Black Carbon Aerosol in the Industrial City of Xuzhou, China: Temporal Characteristics and Source Appointment	25
36.	Evaluation of Indoor Air Pollution during Decorating Process and Inhalation Health Risks in Xi'an, China: A Case Study	26
37.	Characteristics of PM <sub>2.5</sub> -bound PAHs at an Urban Site and a Suburban Site in Jinan in North China Plain	27
38.	Effects of Surface Properties of Vertical Textiles Indoors on Particle Deposition: A Small-scale Chamber Study	27
39.	Trends of Fog and Visibility in Taiwan: Climate Change or Air Quality Improvement?	28
40.	Characteristics of Air Pollutants and Greenhouse Gases at a Regional Background Station in Southwestern China	29
41.	Applicability of Optical and Diffusion Charging-Based Particulate Matter Sensors to Urban Air Quality Measurements	30

42.	Aerosol Impacts on Meteorological Elements and Surface Energy Budget over an Urban Cluster Region in the Yangtze River Delta	31
43.	Fine Particulate Matter-induced Toxic Effects in an Animal Model of <i>Caenorhabditis elegans</i>	31
44.	Bioaerosol Concentrations and Size Distributions during the Autumn and Winter Seasons in an Industrial City of Central China	32
45.	The Effect of Sampling Inlet Direction and Distance on Particle Source Measurements for Dispersion Modelling	33
46.	Responses of Secondary Inorganic PM <sub>2.5</sub> to Precursor Gases in an Ammonia Abundant Area In North Carolina	33
47.	Synoptic Weather Patterns and Associated Air Pollution in Taiwan	34
48.	Effects of Wind Direction on the Airflow and Pollutant Dispersion inside a Long Street Canyon	35
49.	Effect of Large-scale Biomass Burning on Aerosol Optical Properties at the GAW Regional Station Pha Din, Vietnam	36
50.	Impact of Biomass Burning in South and Southeast Asia on Background Aerosol in Southwest China	36
51.	Climatology and Chemistry of Surface Ozone and Aerosol under Alpine Conditions in East Siberia	37
52.	Evaluation of WRF-Chem Model Forecasts of a Prolonged Saharan Dust Episode over the Eastern Alps	38
53.	Aerosol Optical Properties over Gurushikhar, Mt. Abu: A High Altitude Mountain Site in India	39
54.	Variability of Aerosol Optical Properties Observed at a Polluted Marine (Gosan, Korea) and a High-altitude Mountain (Lulin, Taiwan) Site in the Asian Continental Outflow	39
55.	Characteristics and Formation Mechanisms of Sulfate and Nitrate in Size-segregated Atmospheric Particles from Urban Guangzhou, China	40
56.	Aerosol Pollution Characterization before Chinese New Year in Zhengzhou in 2014	41
57.	Impact of Extreme Meteorological Events on Ozone in the Pearl River Delta, China	42
58.	Chemical Characteristics and Source Apportionment of PM <sub>2.5</sub> during Winter in the Southern Part of Urumqi, China	43
59.	Heavy Particulate Matter Pollution during the 2014–2015 Winter in Tianjin, China	43
60.	Effects of Retarding Fuel Injection Timing on Toxic Organic Pollutant Emissions from Diesel Engines	44
61.	Inhalation Health Risk Assessment for the Human Tracheobronchial Tree under PM Exposure in a Bus Stop Scene	45
62.	Evaluation of Different Machine Learning Approaches to Forecasting PM <sub>2.5</sub> Mass Concentrations	46
63.	Chemical Characterization of Fine Particulate Matter in Gasoline and Diesel Vehicle Exhaust	46

64.	Analysis of Chemical Composition, Source and Processing Characteristics of Submicron Aerosol during the Summer in Beijing, China	47
65.	Coarse and Fine Particulate Matter Components of Wildland Fire Smoke at Devils Postpile National Monument, California, USA	48
66.	Investigating the Role of Meteorological Factors in the Vertical Variation in PM <sub>2.5</sub> by Unmanned Aerial Vehicle Measurement	48
67.	Biological and Chemical Air Pollutants in an Urban Area of Central Europe: Co-exposure Assessment	49
68.	Emissions of PM <sub>2.5</sub> -bound Polycyclic Aromatic Hydrocarbons and Metals from a Diesel Generator Fueled with Biodiesel Converted from Used Cooking Oil	50
69.	Emission of Carbonyl Compounds from Cooking Oil Fumes in the Night Market Areas	50
70.	Dominant Factors Influencing the Concentrations of Particulate Matters inside Train Carriages Traveling in Different Environments in the Taipei Mass Rapid Transit System	51
71.	Regional Air Quality Forecast Using a Machine Learning Method and the WRF Model over the Yangtze River Delta, East China	52
72.	Black Carbon Emissions from Light-duty Passenger Vehicles Using Ethanol Blended Gasoline Fuels	53
73.	Testing of an Indoor Air Cleaner for Particulate Pollutants under Realistic Conditions in an Office Room	53
74.	Elemental Composition, Morphology and Sources of Fine Particulates (PM <sub>2.5</sub> ) in Hefei City, China	54
75.	Characteristics of Single Aerosol Particles during Pollution in Winter in an Urban Area of Ningbo, China	55
76.	A Big Data Analysis of PM <sub>2.5</sub> and PM <sub>10</sub> from Low Cost Air Quality Sensors near Traffic Areas	56
77.	Characteristics and Formation Mechanism of Surface Ozone in a Coastal Island of Southeast China: Influence of Sea-land Breezes and Regional Transport	57
78.	Emission Factors of NO <sub>x</sub> , SO <sub>2</sub> , PM and VOCs in Pharmaceuticals, Brick and Food Industries in Shanxi, China	57
79.	Effects of Ambient PM <sub>2.5</sub> Collected Using Cyclonic Separator from Asian Cities on Human Airway Epithelial Cells	58
80.	Speciated PM Composition and Gas and Particle Emission Factors for Diesel Construction Machinery in China	59
81.	Meteorological Parameters and Gaseous Pollutant Concentrations as Predictors of Ground-level PM <sub>2.5</sub> Concentrations in the Beijing-Tianjin-Hebei Region, China	59
82.	Characteristics of Carbon Dioxide Emissions from a Seismically Active Fault	60
83.	Review of Effluents and Health Effects of Cooking and the Performance of Kitchen Ventilation	61

84.	Characteristics, Formation Mechanisms and Potential Transport Pathways of PM <sub>2.5</sub> at a Rural Background Site in Chongqing, Southwest China	61
85.	Spatial Distribution and Multiscale Transport Characteristics of PM <sub>2.5</sub> in China	62
86.	Source Apportionment of PM <sub>2.5</sub> at Urban and Suburban Sites in a Port City of Southeastern China	63
87.	Emissions of NO <sub>x</sub> , PM, SO <sub>2</sub> , and VOCs from Coal-fired Boilers Related to Coal Washing, Iron-steel Production, and Lime and Gypsum Making in Shanxi, China	63
88.	Seasonal Variations, Source Apportionment, and Health Risk Assessment of Heavy Metals in PM <sub>2.5</sub> in Ningbo, China	64
89.	Is Morning or Evening Better for Outdoor Exercise? An Evaluation Based on Nationwide PM <sub>2.5</sub> Data in China	65
90.	Multifractal Cascade Analysis on the Nature of Air Pollutants Concentration Time Series over China	66
91.	Performance Evaluation of a Very-low-volume Sampler for Atmospheric Particulate Matter	66
92.	On the Performance Parameters of PM <sub>2.5</sub> and PM <sub>1</sub> Size Separators for Ambient Aerosol Monitoring	67
93.	Chemical Characteristics, Sources Apportionment, and Risk Assessment of PM <sub>2.5</sub> in Different Functional Areas of an Emerging Megacity in China	68
94.	Current Status of Fine Particulate Matter (PM <sub>2.5</sub> ) in Vietnam's Most Populous City, Ho Chi Minh City	69
95.	Chemical Composition and Health Risk of PM <sub>2.5</sub> from Near-ground Firecracker Burning in Micro Region of Eastern Taiwan	69
96.	Molecular Compositions and Sources of Organic Aerosols from Urban Atmosphere in the North China Plain during the Wintertime of 2017	70
97.	Comparative Study of PAHs in PM <sub>1</sub> and PM <sub>2.5</sub> at a Background Site in the North China Plain	71
98.	Analysis of PAHs Associated with PM <sub>10</sub> and PM <sub>2.5</sub> from Different Districts in Nanjing	72
99.	Fine Particulate Matter and Ozone Pollution in the 18 Cities of the Sichuan Basin in Southwestern China: Model Performance and Characteristics	72
100.	A Novel Method of Collecting and Chemically Characterizing Milligram Quantities of Indoor Airborne Particulate Matter	73
101.	Characterization and Source Analysis of Water-soluble Ions in Atmospheric Particles in Jinzhong, China	74
102.	Vertical Distribution of Particulate Matter and its Relationship with Planetary Boundary Layer Structure in Shenyang, Northeast China	75
103.	PM <sub>2.5</sub> Associated PAHs and Inorganic Elements from Combustion of Biomass, Cable Wrapping, Domestic Waste, and Garbage for Power Generation	76
104.	Source Identification on High PM <sub>2.5</sub> Days Using SEM/EDS, XRF, Raman, and Windblown Dust Modeling	76



105.	A Dynamic Dust Emission Allocation Method and Holiday Profiles Applied to Emission Processing for Improving Air Quality Model Performance	77
106.	Simulation-based Design of Regional Emission Control Experiments with Simultaneous Pollution of O <sub>3</sub> and PM <sub>2.5</sub> in Jinan, China	78
107.	Sources and Characteristics of Particulate Matter at Five Locations in an Underground Mine	79
108.	High Loadings of Water-Soluble Oxalic Acid and Related Compounds in PM <sub>2.5</sub> Aerosols in Eastern Central India: Influence of Biomass Burning and Photochemical Processing	79
109.	Inter-correlation of Chemical Compositions, Transport Routes, and Source Apportionment Results of Atmospheric PM <sub>2.5</sub> in Southern Taiwan and the Northern Philippines	80
110.	Relieved Air Pollution Enhanced Urban Heat Island Intensity in the Yangtze River Delta, China	81
111.	Climate Impacts of the Biomass Burning in Indochina on Atmospheric Conditions over Southern China	82
112.	Characteristics of PM <sub>10</sub> Levels Monitored for More than a Decade in Subway Stations in South Korea	83
113.	Air Pollution Characteristics and Meteorological Correlates in Lin'an, Hangzhou, China	83
114.	Effects of Blending Ethanol with Gasoline on the Performance of Motorcycle Catalysts and Airborne Pollutant Emissions	84
115.	Infants' Neurodevelopmental Effects of PM <sub>2.5</sub> and Persistent Organohalogen Pollutants Exposure in Southern Taiwan	85
116.	Identifying Leading Nodes of PM <sub>2.5</sub> Monitoring Network in Taiwan with Big Data-oriented Social Network Analysis	86
<b>2.</b>	<b>Atmosphere Chemistry and Physics</b>	
117.	Characterization of black carbon-containing fine particles in Beijing during wintertime	87
118.	Vertical characterization of aerosol optical properties and brown carbon in winter in urban Beijing, China	88
119.	Devastating Californian wildfires in November 2018 observed from space: the carbon monoxide perspective	89
120.	On what scales can GOSAT flux inversions constrain anomalies in terrestrial ecosystems?	89
121.	Tropical Pacific Climate Variability under Solar Geoengineering: Impacts on ENSO Extremes	90
122.	Seasonal and diurnal variability in O <sub>3</sub> , black carbon, and CO measured at the Rwanda Climate Observatory	91
123.	Direct radiative effect of dust-pollution interactions	92
124.	Future climatic drivers and their effect on PM <sub>10</sub> components in Europe and the Mediterranean Sea	93
125.	Anthropogenic aerosol forcing under the Shared Socioeconomic Pathways	94
126.	Effective densities of soot particles and their relationships with the mixing state at an urban site of the Beijing mega-city in the winter of 2018	95

127.	Quantifying snow darkening and atmospheric radiative effects of black carbon and dust on the South Asian monsoon and hydrological cycle: experiments using variable-resolution CESM	96
128.	Estimating global surface ammonia concentrations inferred from satellite retrievals	97
<b>3.</b>	<b>Atmospheric Environment - 3.629</b>	
129.	Investigating horizontal and vertical pollution gradients in the atmosphere associated with an urban location in complex terrain, Reno, Nevada, USA	98
130.	A modelling study of the terrain effects on haze pollution in the Sichuan Basin	99
131.	Synoptic and local circulations associated with events of high particulate pollution in Valparaiso, Chile	99
132.	Atmospheric emission inventory of SO <sub>3</sub> from coal-fired power plants in China in the period 2009–2014	100
133.	Urban land use regression models: can temporal deconvolution of traffic pollution measurements extend the urban LUR to suburban areas?	101
134.	Spatio-temporal variation of wind influence on distribution of fine particulate matter and its precursor gases	102
135.	Seasonal variation, sources and health risk assessment of polycyclic aromatic hydrocarbons in different particle fractions of PM <sub>2.5</sub> in Beijing, China	103
136.	Applying machine learning methods in managing urban concentrations of traffic-related particulate matter (PM <sub>10</sub> and PM <sub>2.5</sub> )	103
137.	PM <sub>2.5</sub> and its ionic components at a roadside site in Wuhan, China	104
138.	Analyses of regional pollution and transportation of PM <sub>2.5</sub> and ozone in the city clusters of Sichuan Basin, China	105
139.	Sources of indoor air pollution at a New Zealand urban primary school; a case study	105
140.	Sources of indoor air pollution at a New Zealand urban primary school; a case study	106
141.	On-road measurements and modelling of vehicular emissions during traffic interruption and congestion events in an urban traffic corridor	107
142.	Bottom-up emission inventories of multiple air pollutants from open straw burning: A case study of Jiangsu province, Eastern China	107
143.	Dust emission from crushing of hard rock aggregates	108
144.	Simulation analysis of atmospheric SO <sub>2</sub> contributions from different regions in China	109
145.	Air quality, emissions, and source contributions analysis for the Greater Bengaluru region of India	110
146.	PM <sub>2.5</sub> emission characteristics of coal-fired power plants in Beijing-Tianjin-Hebei region, China	110
147.	Effects of meteorology and emission reduction measures on air pollution in Beijing during heating seasons	111

148.	Identification of industrial point sources of airborne dust particles in an urban environment by a combined mineralogical and meteorological analyses: A case study from the Upper Silesian conurbation, Poland	112
149.	Long-term measurements of planetary boundary layer height and interactions with PM2.5 in Shanghai, China	112
150.	Health risk assessment for highway toll station workers exposed to PM2.5-bound heavy metals	113
151.	Determinants of commuter exposure to PM2.5 and CO during long-haul journeys on national highways in India	114
152.	Enhancing source identification of hourly PM2.5 data in Seoul based on a dataset segmentation scheme by positive matrix factorization (PMF)	115
153.	VOC characteristics and source apportionment at a PAMS site near an industrial complex in central Taiwan	116
154.	Exposure to traffic-related particulate matter and deposition dose to auto rickshaw driver in Dhanbad, India	116
155.	The pollution characteristics of PM10 and PM2.5 during summer and winter in Beijing, Suning and Islamabad	117
156.	Correlations of PM10 concentrations in urban areas with vehicle fleet development, rain precipitation and diesel fuel sales	118
157.	severe fog-haze episode in Beijing-Tianjin-Hebei region: Characteristics, sources and impacts of boundary layer structure	118
158.	Temporospatial variations and Spearman correlation analysis of ozone concentrations to nitrogen dioxide, sulfur dioxide, particulate matters and carbon monoxide in ambient air, China	119
159.	Particulate matter size distribution in air surface layer of Middle Ural and Arctic territories	120
160.	Chemical speciation of water-soluble ionic components in PM2.5 derived from peatland fires in Sumatra Island	120
161.	Exploring the stratospheric source of ozone pollution over China during the 2016 Group of Twenty summit	121
162.	Analysis and visualization of multidimensional time series: Particulate matter (PM10) from São Carlos-SP (Brazil)	122
163.	Airborne PM10 and lead concentrations at selected traffic junctions in Khyber Pakhtunkhwa, Pakistan: Implications for human health	122
164.	Trace elements bound to airborne PM10 in a heavily industrialized site nearby Athens: Seasonal patterns, emission sources, health implications	123
165.	Spatial-temporal characteristics of the air quality in the Guangdong–Hong Kong–Macau Greater Bay Area of China during 2015–2017	124
166.	Role of the position of the North Atlantic jet in the variability and odds of extreme PM10 in Europe	124
167.	Particulate matter bound polycyclic aromatic hydrocarbons: Toxicity and health risk assessment of exposed inhabitants	125
168.	Relationship between long-range transported atmospheric black carbon and carbon monoxide at a high-altitude background station in East Asia	126
169.	Distribution, source and transport of the aerosols over Central Asia	127

170.	PM2.5 and PM10 oxidative potential at a Central Mediterranean Site: Contrasts between dithiothreitol- and ascorbic acid-measured values in relation with particle size and chemical composition	128
171	Spatial and temporal distribution of open bio-mass burning in China from 2013 to 2017	129
172.	Impact of emission controls on air quality in Beijing during APEC 2014: Implications from water-soluble ions and carbonaceous aerosol in PM2.5 and their precursors	129
173.	New method for evaluating winter air quality: PM2.5 assessment using Community Multi-Scale Air Quality Modeling (CMAQ) in Xi'an	130
174.	Measurement-based assessment of the regional contribution and drivers of reduction in annual and daily fine particulate matter impact metrics in Paris, France (2009–2018)	131
175.	An advanced spatio-temporal model for particulate matter and gaseous pollutants in Beijing, China	132
176.	Meteorological parameters and gaseous pollutant concentrations as predictors of daily continuous PM2.5 concentrations using deep neural network in Beijing–Tianjin–Hebei, China	133
177.	Fine and ultrafine particles concentrations in vape shops	134
178.	Short-term responses of greenhouse gas emissions and ecosystem carbon fluxes to elevated ozone and N fertilization in a temperate grassland	134
179.	Multiple perspectives for modeling regional PM2.5 transport across cities in the Beijing–Tianjin–Hebei region during haze episodes	135
180.	Design and application of a hybrid assessment of air quality models for the source apportionment of PM2.5	136
181.	Assessment and mitigation of indoor human exposure to fine particulate matter (PM2.5) of outdoor origin in naturally ventilated residential apartments: A case study	137
182.	China's black carbon emission from fossil fuel consumption in 2015, 2020, and 2030	137
183.	Influence of atmospheric PM2.5, PM10, O3, CO, NO2, SO2, and meteorological factors on the concentration of airborne pollen in Guangzhou, China	138
184.	Collective impacts of biomass burning and synoptic weather on surface PM2.5 and CO in Northeast China	139
185.	Oral bioavailability estimation of toxic and essential trace elements in PM10	140
186.	The transport of PM10 over Cape Town during high pollution episodes	140
187.	Investigating secondary organic aerosol formation pathways in China during 2014	141
188.	A high-resolution inventory of air pollutant emissions from crop residue burning in China	142
189.	Analysis of aerosol scattering properties and PM10 concentrations at a mountain site influenced by mineral dust transport	143
190.	Regional air pollution mixtures across the continental US	144

191.	Analysis of PM <sub>2.5</sub> pollution episodes in Beijing from 2014 to 2017: Classification, interannual variations and associations with meteorological features	144
192.	Understanding the washoff processes of PM <sub>2.5</sub> from leaf surfaces during rainfall events	145
193.	Study on the contribution of transport to PM <sub>2.5</sub> in typical regions of China using the regional air quality model RAMS-CMAQ	146
194.	Contributions of local and regional sources to PM <sub>2.5</sub> and its health effects in north India	147
195.	Assessing PM <sub>2.5</sub> model performance for the conterminous U.S. with comparison to model performance statistics from 2007-2015	147
196.	Characteristics of six criteria air pollutants before, during, and after a severe air pollution episode caused by biomass burning in the southern Sichuan Basin, China	148
197.	Analysis of exposure to fine particulate matter using passive data from public transport	149
198.	A study on the short-term impact of fine particulate matter pollution on the incidence of cardiovascular diseases in Beijing, China	150
199.	Surveillance efficiency evaluation of air quality monitoring networks for air pollution episodes in industrial parks: Pollution detection and source identification	151
200.	Characterization of pollutants emitted during burning of eight main tree species in subtropical China	151
201.	Numerical assessment of PM <sub>2.5</sub> and O <sub>3</sub> air quality in Continental Southeast Asia: Impacts of potential future climate change	152
202.	Characteristics and sources of volatile organic compounds (VOCs) in Shanghai during summer: Implications of regional transport	153
203.	Emission inventory of key sources of air pollution in Lebanon	154
204.	Emission inventory research of typical agricultural machinery in Beijing, China	155
205.	Traffic source impacts on chlorinated polycyclic aromatic hydrocarbons in PM <sub>2.5</sub> by short-range transport	155
206.	Performance evaluation of twelve low-cost PM <sub>2.5</sub> sensors at an ambient air monitoring site	156
207.	Investigation of long-range transported PM <sub>2.5</sub> events over Northern Taiwan during 2005–2015 winter seasons	157
208.	Effects of meteorological factors to reduce large-scale PM <sub>10</sub> emission estimation errors on unpaved roads	158
209.	Characteristics and sources of PM <sub>2.5</sub> and reactive gases near roadways in two metropolitan areas in Canada	159
210.	Monitoring on-road air quality and measuring vehicle emissions with remote sensing in an urban area	160
211.	Interactions between rainfall and fine particulate matter investigated by simultaneous chemical composition measurements in downtown Beijing	160

212.	Mode-specific, semi-volatile chemical composition of particulate matter emissions from a commercial gas turbine aircraft engine	161
213.	Source identification of personal exposure to fine particulate matter (PM <sub>2.5</sub> ) among adult residents of Hong Kong	161
214.	Insights into the temporal and spatial characteristics of PM <sub>2.5</sub> transport flux across the district, city and region in the North China Plain	162
215.	Black carbon and PM <sub>2.5</sub> monitoring campaign on the roadside and residential urban background sites in the city of Tehran	163
216.	Age-specific seasonal associations between acute exposure to PM <sub>2.5</sub> sources and cardiorespiratory hospital admissions in California	164
217.	Primary particulate matter emissions and estimates of secondary organic aerosol formation potential from the exhaust of a China V diesel engine	165
218.	Reducing PM <sub>2.5</sub> and secondary inorganic aerosols by agricultural ammonia emission mitigation within the Beijing-Tianjin-Hebei region, China	165
219.	Numerical assessment of PM <sub>2.5</sub> and O <sub>3</sub> air quality in continental Southeast Asia: Baseline simulation and aerosol direct effects investigation	166
220.	A fast forecasting method for PM <sub>2.5</sub> concentrations based on footprint modeling and emission optimization	167
<b>4.</b>	<b>Atmospheric Research- 3.778</b>	
221.	Carbonaceous components and major ions in PM <sub>10</sub> from the Amazonian Basin	168
222.	Background concentrations of PMs in Xinjiang, West China: An estimation based on meteorological filter method and Eckhardt algorithm	169
223.	Comparing the impact of strong and weak East Asian winter monsoon on PM <sub>2.5</sub> concentration in Beijing	170
224.	Natural and anthropogenic contributions to long-term variations of SO <sub>2</sub> , NO <sub>2</sub> , CO, and AOD over East China	170
225.	Atmosphere boundary layer height and its effect on air pollutants in Beijing during winter heavy pollution	171
226.	Consensus in climate classifications for present climate and global warming scenarios	172
227.	Sources and spatial distribution of PM <sub>2.5</sub> -bound polycyclic aromatic hydrocarbons in Zhengzhou in 2016	173
228.	Open cut black coal mining: Empirical verification of PM <sub>2.5</sub> air emission estimation techniques	174
229.	Variation tendency of pollution characterization, sources, and health risks of PM <sub>2.5</sub> -bound polycyclic aromatic hydrocarbons in an emerging megacity in China: Based on three-year data	174
230.	Characteristics of gaseous and particulate ammonia and their role in the formation of secondary inorganic particulate matter at Delhi, India	175
231.	Weekly cycle assessment of PM mass concentrations and sources, and impacts on temperature and wind speed in Southern Italy	176

232.	Temporal distribution and source apportionment of PM2.5 chemical composition in Xinjiang, NW-China	177
233.	Characterization of individual particles and meteorological conditions during the cold season in Zhengzhou using a single particle aerosol mass spectrometer	178
234.	Long-term variations of the PM2.5 concentration identified by MODIS in the tropical rain forest, Southeast Asia	178
235.	Impacts of urban expansion on fog types in Shanghai, China: Numerical experiments by WRF model	179
236.	Comparing mountain breezes and their impacts on CO <sub>2</sub> mixing ratios at three contrasting areas	180
237.	Regional CO emission estimated from ground-based remote sensing at Hefei site, China	181
238.	Characterizing the regional contribution to PM10 pollution over northern France using two complementary approaches: Chemistry transport and trajectory-based receptor models	182
239.	C-Sr-Pb isotopic characteristics of PM2.5 transported on the East-Asian continental outflows	183
240.	The hourly characteristics of aerosol chemical compositions under fog and high particle pollution events in Kinmen	183
241.	A modelling study of assessment of the effectiveness of combining foreign and local emission control strategies	184
242.	Biomass burning in the northern peninsular Southeast Asia: Aerosol chemical profile and potential exposure	185
243.	Nocturnal fine particulate nitrate formation by N <sub>2</sub> O <sub>5</sub> heterogeneous chemistry in Seoul Metropolitan Area, Korea	186
244.	Gaseous and speciated particulate emissions from the open burning of wastes from tree pruning	186
245.	Air quality during and after festivals: Aerosol concentrations, composition and health effects	187
246.	Characterization of particle size distributions during winter haze episodes in urban air	188
247.	Synoptic circulation pattern and boundary layer structure associated with PM2.5 during wintertime haze pollution episodes in Shanghai	189
248.	Evolution of the vertical structure of air pollutants during winter heavy pollution episodes: The role of regional transport and potential sources	190
249.	Polycyclic aromatic hydrocarbons in atmospheric PM2.5 and PM10 in the semi-arid city of Xi'an, Northwest China: Seasonal variations, sources, health risks, and relationships with meteorological factors	191
250.	Changes in concentrations of fine and coarse particles under the CO <sub>2</sub> -induced global warming	192
<b>5.</b>	<b>Environmental Science and pollution Research</b>	
251.	Short-term effects of ambient air pollution and cardiovascular events in Shiraz, Iran, 2009 to 2015	192
252.	Impact of air pollution on hospital admissions with a focus on respiratory	193

	diseases: a time-series multi-city analysis	
253.	Association between particulate matter air pollution and cardiovascular disease mortality in Lanzhou, China	194
254.	Short-term effects of ambient fine particulate air pollution on inpatient visits for myocardial infarction in Beijing, China	195
255.	Effect of O <sub>3</sub> , PM <sub>10</sub> and PM <sub>2.5</sub> on cardiovascular and respiratory diseases in cities of France, Iran and Italy	196
256.	Characterization of aerosol particles during the most polluted season (winter) in urban Chengdu (China) by single-particle analysis	196
257.	Levels and health risk assessments of particulate matters (PM <sub>2.5</sub> and PM <sub>10</sub> ) in indoor/outdoor air of waterpipe cafés in Tehran, Iran	197
258.	Field assessment of the effects of land-cover type and pattern on PM <sub>10</sub> and PM <sub>2.5</sub> concentrations in a microscale environment	198
259.	Characterization of chemical components and cytotoxicity effects of indoor and outdoor fine particulate matter (PM <sub>2.5</sub> ) in Xi'an, China	199
260.	Spatial and temporal variations of PM <sub>2.5</sub> mass closure and inorganic PM <sub>2.5</sub> in the Southeastern U.S.	199
<b>6.</b>	<b>Science of Total Environment- 4.9</b>	
261.	Effects of wood moisture on emission factors for PM <sub>2.5</sub> , particle numbers and particulate-phase PAHs from Eucalyptus globulus combustion using a controlled combustion chamber for emissions	200
262.	Temporal variation of oxidative potential of water soluble components of ambient PM <sub>2.5</sub> measured by dithiothreitol (DTT) assay	201
263.	Chemical source profiles of urban fugitive dust PM <sub>2.5</sub> samples from 21 cities across China	202
264.	PM <sub>2.5</sub> source apportionment for the port city of Thessaloniki, Greece	202
265.	Removal of PM <sub>2.5</sub> and secondary inorganic aerosols in the North China Plain by dry deposition	203
266.	PM <sub>2.5</sub> concentration and composition in the urban air of Nanjing, China: Effects of emission control measures applied during the 2014 Youth Olympic Games	204
267.	Factors controlling the long-term (2009–2015) trend of PM <sub>2.5</sub> and black carbon aerosols at eastern Himalaya, India	205
268.	Chemical composition and source apportionment of PM <sub>1</sub> and PM <sub>2.5</sub> in a national coal chemical industrial base of the Golden Energy Triangle, Northwest China	205
269.	Temporal variations of PM <sub>2.5</sub> -bound organophosphate flame retardants in different microenvironments in Beijing, China, and implications for human exposure	206
270.	Impacts of the near-surface urban boundary layer structure on PM <sub>2.5</sub> concentrations in Beijing during winter	207
271.	Differences in concentration and source apportionment of PM <sub>2.5</sub> between 2006 and 2015 over the PRD region in southern China	208



272.	Ground-level PM2.5 estimation over urban agglomerations in China with high spatiotemporal resolution based on Himawari-8	208
273.	Characteristics of chemical composition and seasonal variations of PM2.5 in Shijiazhuang, China: Impact of primary emissions and secondary formation	209
274.	In-vehicle PM2.5 personal concentrations in winter during long distance road travel in India	210
275.	PM2.5 vertical variation during a fog episode in a rural area of the Yangtze River Delta, China	211
276.	Characterization of polycyclic aromatic hydrocarbon (PAHs) source profiles in urban PM2.5 fugitive dust: A large-scale study for 20 Chinese cities	211
277.	Characteristics and human inhalation exposure of ionic per- and polyfluoroalkyl substances (PFASs) in PM10 of cities around the Bohai Sea: Diurnal variation and effects of heating activity	212
278.	Short-term and long-term effects of PM2.5 on acute nasopharyngitis in 10 communities of Guangdong, China	213
279.	Molecular characterization of dissolved organic matters in winter atmospheric fine particulate matters (PM2.5) from a coastal city of northeast China	214
280.	PM2.5 generated during rapid failure of fiber-reinforced concrete induces TNF-alpha response in macrophages	214
281.	Approaches for identifying PM2.5 source types and source areas at a remote background site of South China in spring	215
282.	Energy and emission pathways towards PM2.5 air quality attainment in the Beijing-Tianjin-Hebei region by 2030	216
283.	Particulate air pollution and ischemic stroke hospitalization: How the associations vary by constituents in Shanghai, China	217
284.	Characteristics and health effects of PM2.5 emissions from various sources in Gwangju, South Korea	218
285.	Short-term effects of real-time personal PM2.5 exposure on ambulatory blood pressure: A panel study in young adults	218

## 1. Aerosol and Air Quality research

### **Aerosol Climate Change Connection (AC3) Special Issue: An Overview**

**Abhijit Chatterjee<sup>1</sup>, Panuganti C.S. Devara<sup>2</sup>, Rajasekhar Balasubramanian<sup>3</sup>, Daniel**

**Source :** Aerosol and Air Quality research, Volume: 19 | Issue: 1 | Pages: 1-4  
;DOI: 10.4209/aaqr.2018.11.0435

Bose Institute, a premiere scientific research organization under Ministry of Science and Technology, Govt of India organized an international conference on “Aerosol Climate Change Connection (AC3)” held in Darjeeling, India during 25–27 April, 2017. AAQR is publishing a special issue on AC3 based on the major themes of the conference covering optical, radiative and chemical properties of composite and carbonaceous aerosols and the ground-based and remote sensing of aerosols. The papers accepted in this special issue are of good scientific merits and are useful for the scientific community working in the field of aerosol science and technology.

**Keywords:** AC3 ; Aerosol; Climate change ; Himalaya

---

### **Aerosol Characteristics over the Northwestern Indo-Gangetic Plain: Clear-Sky Radiative Forcing of Composite and Black Carbon Aerosol**

**Onam Bansal, Atinderpal Singh, Darshan Singh**

**Source:** Aerosol and Air Quality research, Volume: 19 | Issue: 1 | Pages: 5-14  
;DOI: 10.4209/aaqr.2017.09.0339

The present study examines the aerosol characteristics over Patiala in northwestern India from October 2013 to June 2014. The average mass concentration of the total suspended particulates (TSP) varied from 117 to 301  $\mu\text{g m}^{-3}$ , with  $\text{PM}_{10}$  accounting for ~63–83% from October to February (P1) and decreasing to less than ~40% from March to June (P2). The aerosol optical depth ( $\text{AOD}_{500}$ ) exhibited its highest values during October (0.818) and its lowest during April (0.332), with the wavelength dependence differing significantly on a temporal scale. The Ångström exponent ( $\alpha_{380-870}$ ) values indicated a relatively high quantity of fine-mode particles over the study region during P1 as compared to P2, which is consistent with the PM measurements. The average monthly mass concentration of the climate forcing agent black carbon (BC) varied from 2.4 to 12  $\mu\text{g m}^{-3}$ , with the highest mass concentration in December and the lowest in June. The average monthly single scattering albedo ( $\text{SSA}_{500}$ ) derived from the OPAC (Optical Properties of Aerosols and Clouds) model varied from 0.890 to 0.947, with lower values during P1 than P2. The average monthly clear-sky direct atmospheric aerosol radiative forcing (ATM ARF) estimated by the

SBDART (Santa Barbara DISORT Atmospheric Radiative Transfer) model ranged between +12 and +36  $\text{Wm}^{-2}$  over the study region. Even though the mass fraction of BC averaged over the study period was only 2.4% of the total mass of the composite aerosol, its contribution to net ATM ARF was found to be significant (> 60%), indicating that BC contributes significantly to warming on a regional scale. These results improve our understanding of the impact of BC and composite aerosol on the earth's radiation budget and hence on regional climate.

**Keywords** : Biomass burning emission; Particulates; Aerosol optical depth ;Single scattering albedo ;Aerosol radiative forcin

---

## Surface $\text{PM}_{2.5}$ Estimate Using Satellite-Derived Aerosol Optical Depth over India

Rama K. Krishna<sup>1</sup>, Sachin D. Ghude <sup>1</sup>, Rajesh Kumar<sup>2</sup>, Gufran Beig<sup>1</sup>, Rachana Kulkarni<sup>1</sup>, Sandip Nivdange<sup>3</sup>, Dilip Chate<sup>1</sup>

**Source:** Aerosol and Air Quality research, Volume: 19 | Issue: 1 | Pages: 25-37  
;DOI: 10.4209/aaqr.2017.12.0568

Concentrations of fine particulate matter ( $\text{PM}_{2.5}$ ) that exceed air quality standards affect human health and have an impact on the earth's radiation budget. The lack of round the clock ground-based observations from a dense network of air quality stations inhibits the understanding of  $\text{PM}_{2.5}$ 's spatio-temporal variability and the assessment of its health and climate effects. Aerosol optical depth (AOD) values retrieved from satellite based instruments can be used to derive surface  $\text{PM}_{2.5}$  concentrations. This study integrates Moderate Resolution Imaging Spectroradiometer (MODIS) AOD retrievals and simulations from the Weather Research and Forecasting Model coupled with Chemistry (WRF-Chem) to determine the ground-level  $\text{PM}_{2.5}$  concentrations at a 36 km resolution across India. WRF-Chem simulations provide the factor relating the AOD with the  $\text{PM}_{2.5}$ . Satellite-derived  $\text{PM}_{2.5}$  mass concentrations are compared with the available ground-based observations across India for the year of 2011. The results show a correlation between the satellite-derived monthly  $\text{PM}_{2.5}$  estimates and the ground-based observations for 15 stations in India with coefficients of 77% and diurnal scale coefficients varying from 0.45 to 0.75. The best estimations of  $\text{PM}_{2.5}$  mass concentrations on a spatio-temporal scale across India address various environmental issues.

Keywords: AOD;  $\text{PM}_{2.5}$ ; Spatio-temporal variability of  $\text{PM}_{2.5}$  ; Impact assessment

## **Two-Way Relationship between Aerosols and Fog: A Case Study at IGI Airport, New Delhi**

**Pramod Digambar Safai<sup>1</sup>, Sachin Ghude<sup>1</sup>, Prakash Pithani<sup>1</sup>, Somnath Varpe<sup>1</sup>, Rachana Kulkarni<sup>1</sup>, Kiran Todekar<sup>1</sup>, Suresh Tiwari<sup>1</sup>, Dilip Motiram Chate<sup>1</sup>, Thara Prabhakaran<sup>1</sup>, Rajendra Kumar Jenamani<sup>2</sup>, Madhavan Nair Rajeevan<sup>3</sup>**

**Source:** Aerosol and Air Quality research, Volume: 19 | Issue: 1 | Pages: 71-79  
DOI: 10.4209/aaqr.2017.11.0542

The frequency and intensity of fog episodes during the winter season has been increasing during the past decade over the megacity of Delhi due to the high pollution load. The role of atmospheric aerosols is very important in the life cycle of fog in the urban areas. This paper presents the results on the variation in aerosol optical properties (scattering and absorption coefficients) and the black carbon (BC) mass concentration during the foggy period in winter (December 2015 to February 2016) at the Indira Gandhi International (IGI) Airport, New Delhi. The interaction between scattering and absorbing aerosols, and fog before, during and after the foggy period has been studied as a typical case. The BC mass concentration, along with the aerosol scattering and absorption coefficients, increased before and during the initial phase of the dense foggy period. However, there was a steep decrease in them after the sustained period of dense fog, which suggests possible scavenging by fog droplets. Also, it was observed that the decrease in ambient temperature and depression temperature (DT) and the increase in relative humidity (RH) played a major role in sustaining the dense fog despite the reduction in aerosol load. The single-scattering albedo (SSA) decreased during the dense fog due to a higher reduction of the scattering aerosols than the absorbing ones. Both the scattering and the absorption coefficients showed a significant correlation with cloud condensation nuclei (CCN).

**Keywords:** New Delhi Airport , Winter fog , Scattering and absorption coefficients , Black carbon , Visibility.

---

## **Quantification of Carbonaceous Aerosol Emissions from Cookstoves in Senegal**

**Candela de la Sota<sup>1</sup>, Mar Viana<sup>2</sup>, Moustapha Kane<sup>3</sup>, Issakha Youm<sup>3</sup>, Omar Masera<sup>4</sup>, Julio Lumbreras<sup>1</sup>**

**Source :** Aerosol and Air Quality research, Volume: 19 | Issue: 1 | Pages: 80-91  
;DOI: 10.4209/aaqr.2017.11.0540

In some regions of the world, cooking with solid biomass fuels in open fires constitutes the largest source of elemental and organic carbon emissions. However, cooking-related carbonaceous aerosols are still poorly characterized. This paper presents an innovative characterization of elemental and organic carbon (EC and OC) emissions from cookstoves in West Africa. Four stove types (three-stone fire, rocket stove, basic ceramic stove, and

gasifier) using two wood species (dimb and filao) were analyzed on a laboratory scale. The EC and OC emission factors based on fuel energy (EFs) when burning dimb were higher for all stoves, highlighting the need to account for the fuel type when reporting cookstove EFs. The highest EC EF was found for the rocket stove ( $0.18 \pm 0.06 \text{ g MJ}^{-1}$  and  $0.06 \pm 0.01 \text{ g MJ}^{-1}$  for dimb and filao, respectively). The other tested stoves exhibited the same EC EF when burning dimb ( $0.09 \pm 0.02 \text{ g MJ}^{-1}$ ) and EC EFs ranging between  $0.04 \pm 0.01$  and  $0.05 \pm 0.01 \text{ g MJ}^{-1}$  when burning filao. The OC EF was highest, on average, for the gasifier ( $0.08 \pm 0.01 \text{ g MJ}^{-1}$ ), followed by those for the three-stone fire ( $0.18 \pm 0.03 \text{ g MJ}^{-1}$ ) and the basic ceramic stove ( $0.21 \pm 0.08 \text{ g MJ}^{-1}$ ). However, the results from testing the rocket stove and the three-stone fire under real cooking conditions using dimb wood indicate that the laboratory-scale tests overestimate the actual EC EFs. Also, the rocket stove did not show a reduction in wood use compared to the three-stone fire, suggesting that the carbonaceous aerosol emissions from the former produce more warming than those from the latter. Therefore, the total EC and OC stove emissions, in addition to the EFs, must be reported. As the impacts of carbonaceous aerosol highly depend on the location of emission, this study contributes valuable data to emission inventories and climate prediction models at national and regional levels.

**Keywords :** Emission factor; Rocket stove ; Traditional stove; West Africa

---

## **Identification of Sources from Chemical Characterization of Fine Particulate Matter and Assessment of Ambient Air Quality in Dhaka, Bangladesh**

**Bilkis A. Begum<sup>1</sup>, Philip K. Hopke**

**Source :** Aerosol and Air Quality research, Volume: 19 | Issue: 1 | Pages: 118-128  
;DOI: 10.4209/aaqr.2017.12.0604

Air pollution in Dhaka has drawn the attention of the government and the public over the past several decades, especially upon the discovery of Pb in the air. As a result, several policy interventions have been implemented to improve the air quality. Sampling for fine airborne particulate matter (PM<sub>2.5</sub>, PM with an aerodynamic diameter < 2.5  $\mu\text{m}$ ) has been conducted at a semi-residential site (AECD) in Dhaka since December 1996 using a GENT sampler. The retrieved samples were analyzed for their mass, black carbon (BC), and elemental compositions, and the resulting data set was analyzed for source identification via the Positive Matrix Factorization (PMF) technique. The identified sources are wood burning, soil dust, brick kilns, fugitive Pb, road dust, Zn sources, motor vehicles, and sea salt. The Government of Bangladesh is considering various interventions to reduce the emissions from these sources by promoting the replacement of diesel/petrol automobiles with CNG vehicles, increasing traffic speed in the city, and introducing green technologies for brick production. However, reducing the effect of transboundary contributions on the local air quality will necessitate regional measures as well.

**Keywords:** PM; Positive Matrix Factorization ; BC ,Traffic ;Compressed natural gas

---

## **Aerosol Chemical Characterization and Contribution of Biomass Burning to Particulate Matter at a Residential Site in Islamabad, Pakistan**

**Imran Shahid 1,2, Magdalena Kistler<sup>1</sup>, Muhammad Zeeshaan Shahid<sup>3</sup>, Hans Puxbaum<sup>1</sup>**

**Source :** Aerosol and Air Quality research, Volume: 19 | Issue: 1 | Pages: 148-162  
DOI: 10.4209/aaqr.2017.12.0573

Air pollution creates a very serious problem in developing countries, and scarce information is available about the nature of pollutants. This study describes the chemical composition of particulate matter (TSP and PM<sub>10</sub>), including marker compounds pointing to pollution sources, and estimates the contribution of biomass smoke to organic carbon (OC) and particulate matter (PM) at a residential site in Islamabad during the winter period in December 2007. Levoglucosan and its relationship with other anhydrosaccharides were used to estimate the biomass burning contribution, and polyols and primary and secondary saccharides were investigated regarding biological aerosol. Polyols and primary saccharides contribute a small fraction of the total PM<sub>10</sub> and TSP mass, whereas anhydrosaccharides contribute more than 90% in both the PM<sub>10</sub> and TSP. A significant contribution from biomass smoke has also been found in Islamabad, forming 10% of the TSP and 18% of the PM<sub>10</sub> mass. The analysis of the distributions of saccharide concentrations between the TSP and PM<sub>10</sub> fractions shows that anhydrosaccharides, viz., levoglucosan, mannosan and galactosan, all of which are directly related to the combustion of biomass, are mainly present in the PM<sub>10</sub>. The concentration of TSP varied from 218  $\mu\text{g m}^{-3}$  to 468  $\mu\text{g m}^{-3}$  (mean: 343  $\mu\text{g m}^{-3}$ ), and PM<sub>10</sub> concentrations were in the range of 89–304  $\mu\text{g m}^{-3}$  (mean: 194  $\mu\text{g m}^{-3}$ ). A good correlation was observed between PM<sub>10</sub>, TSP and Ca<sup>2+</sup>, which implies that mineral/road dust may be a major contributor to the PM in Islamabad.

**Keywords:** Particulate matter , Urban air pollution , Biomass burning aerosol, Saccharides.

---

# Aerosol Chamber Characterization for Commercial Particulate Matter (PM) Sensor Evaluation

Dian Ahmad Hapidin<sup>1,3</sup>, Casmika Saputra<sup>1,3</sup>, Dian Syah Maulana<sup>1,3</sup>, Muhammad Miftahul Munir<sup>1,2,3</sup>, Khairurrijal Khairurrijal<sup>1,2,3</sup>

**Source :** Aerosol and Air Quality research, Volume: 19 | Issue: 1 | Pages: 181-194  
DOI: 10.4209/aaqr.2017.12.0611

The negative impact of PM<sub>2.5</sub> exposure has encouraged the development of scattering-based PM sensors for monitoring the PM level spatially and temporally. These PM sensors excel in terms of cost, operating power, and compactness, but the performance of each model needs to be evaluated individually. The evaluation of a PM sensor can be conducted inside an aerosol chamber by measuring the PM concentration in time series using both the sensor and reference monitors. However, earlier experimental processes were time-consuming, as a long time was needed to decrease the PM concentration by loss mechanisms. We designed an aerosol chamber by introducing an output airflow rate to decay the PM concentration more quickly. The characterization of the chamber yielded an empirical equation to describe the PM concentration decay profile, which can be used to predict the measurement time and the number of data points. The chamber was then utilized to evaluate three PM sensors (Sharp GP2Y1010AU0F, Winsen ZH03A, and Novafitness SDS011). A condensation particle counter (TSI, 3025A) and particle sensor (Honeywell, HPMA115S0-XXX) were employed as reference monitors. The evaluation determined the linearity, calibration curve, and precision of the PM sensors. The evaluated models showed excellent linearity, with R<sup>2</sup> values above 0.956. The least square and RMA correlation of the evaluated PM sensors demonstrated the best linearity achieved at a low PM measurement range (0–400 µg m<sup>-3</sup>). As the Winsen ZH03A and Novafitness SDS011 sensors had coefficients of variation below 10%, both of the sensors have an acceptable precision according to the EPA standard.

**Keywords:** Aerosol chamber , Air pollution, Particulate matter, PM<sub>2.5</sub> monitor , PM sensor.

---



# **Impacts of New Particle Formation on Short-term Meteorology and Air Quality as Determined by the NPF-explicit WRF-Chem in the Midwestern United States**

**Can Dong<sup>1</sup>, Hitoshi Matsui<sup>2</sup>, Scott Spak<sup>3</sup>, Alicia Kalafut-Pettibone<sup>4</sup>, Charles Stanier<sup>1</sup>**

**Source :** Aerosol and Air Quality research, Volume: 19 | Issue: 2 | Pages: 204-220

DOI: 10.4209/aaqr.2018.05.0163

New particle formation (NPF) from nucleation and subsequent nuclei growth, which is frequently observed in the troposphere, is critical to aerosol-cloud interactions yet difficult to simulate. In this work, regional simulations with the fully coupled NPF-explicit WRF-Chem model link NPF to cloud properties and to changes in both meteorology and air quality in the U.S. Midwest during summer 2008. Simulations that include NPF have higher concentrations of condensation nuclei, as anticipated from the particle production associated with nucleation, leading to enhanced concentrations of cloud condensation nuclei (CCN) at high supersaturations. However, the online-coupled model develops a number of unexpected features that can be traced to a feedback loop involving aqueous (in-cloud) oxidation of sulfur combined with boundary layer NPF. Simulations with NPF (relative to simulations without) exhibit reduced PM<sub>2.5</sub> sulfate mass, cloud dimming (reductions in the cloud frequency, CCN concentration at a low supersaturation, cloud optical depth, and cloud droplet number concentration), and enhanced surface-reaching shortwave radiation. This effect of NPF on the PM<sub>2.5</sub> mass is mostly absent for other constituents of PM<sub>2.5</sub>. The implications of this feedback loop, which is not considered in most climate and air quality modeling, are discussed.

**Keywords:** New particle formation , Meteorology , Air quality , Sulfate, WRF-Chem, Aerosol cloud Interaction , Indirect climate effect.

---

## **Chemical Composition of Particulate Matter from Traffic Emissions in a Road Tunnel in Xi'an, China**

**Yanzhao Hao<sup>1</sup>, Shunxi Deng<sup>2,4</sup>, Yan Yang<sup>3,4</sup>, Wenbin Song<sup>5</sup>, Hui Tong<sup>4</sup>, Zhaowen Qiu<sup>1</sup>**

**Source :** Aerosol and Air Quality research, Volume: 19 | Issue: 2 | Pages: 234-246

DOI: 10.4209/aaqr.2018.04.0131

Chemical compositions of particulate matter (PM) from traffic emissions vary by region and with time. Therefore, it is necessary to obtain local mobile source profiles of PM to support regional researches for vehicle emission control policy, source apportionment modeling, etc. In this study, PM<sub>2.5</sub> and PM<sub>10</sub> samples were collected from a highway tunnel in Xi'an in northwestern China. The chemical composition, specifically, the OC, EC, water-soluble ions, and elements, was analyzed in detail to (1) provide local PM profiles for a



mixed vehicle fleet, (2) identify the origins of different elements in the tunnel environment, and (3) determine the associated factors influencing the profiles. The PM<sub>2.5</sub> profiles in the tunnel were identified as OC (34.10%), EC (11.96%), water-soluble ions (18.22%), and elements (27.73%), while the PM<sub>10</sub> profiles included OC (28.48%), EC (8.59%), water-soluble ions (14.17%), and elements (33.36%), respectively. The origins of the elements in the tunnel were classified into three categories by the receptor modeling approach: resuspended road dust and brake wear, vehicle exhaust and tire wear, and tailpipe emissions from diesel vehicles (DV). The mass fractions of OC, EC, and elements originating from resuspended road dust and brake wear were mainly affected by vehicle driving conditions (i.e., uphill/downhill and speed), whereas the mass content of bromine (Br) was influenced by the proportion of DV in the fleet.

**Keywords:** Traffic emissions PM<sub>2.5</sub> PM<sub>10</sub> Source profile Road tunnel

---

## **Pollution Characterization, Source Identification, and Health Risks of Atmospheric-Particle-Bound Heavy Metals in PM<sub>10</sub> and PM<sub>2.5</sub> at Multiple Sites in an Emerging Megacity in the Central Region of China**

**Nan Jiang , Xiaohan Liu, Shanshan Wang, Xue Yu, Shasha Yin, Shiguang Duan, Shenbo Wang, Ruiqin Zhang , Shengli Li**

**Source :** Aerosol and Air Quality research, Volume: 19 | Issue: 2 | Pages: 247-271  
;DOI: 10.4209/aaqr.2018.07.0275

A total of 588 daily PM filters were collected at five sites in Zhengzhou, and the mass concentrations and sources of the elements were analyzed. The health risks and source regions of the particles and toxic elements were also estimated. The results indicated severe PM<sub>2.5</sub> and PM<sub>10</sub> pollution, especially at traffic sites. Additionally, the PM<sub>10</sub>-bound As far exceeded the Chinese standards. Although the total elemental levels were relatively low at the rural site, they were high at the GY site. High levels of crustal elements were also observed at the SSQ and HKG sites. Seasonal-variation analysis revealed that the crustal elements, more abundant in the PM<sub>10</sub>, occurred at high levels in spring; the combustion-source elements, more abundant in the PM<sub>2.5</sub>, caused significant pollution in winter; and the elemental concentrations were low in summer. The coefficients of divergence for the PM<sub>2.5</sub> were slightly higher than those for the PM<sub>10</sub>. Vehicles, industry, coal combustion, oil fuel, dust, and biomass burning were important sources of the PM-bound elements. Although the ZM site was characterized by low traffic and high contributions from biomass burning and dust emission, the HKG site featured a high proportion of emissions from traffic sources, and the SSQ site was also highly affected by vehicular pollution. Whereas elements in the PM<sub>2.5</sub> largely originated in combustion sources, those in the PM<sub>10</sub> received greater contributions from dust sources. The levels of As and Ni posed intolerable carcinogenic risks (CR) and, along with that of Pb, also demonstrated significant non-CR risks. Children were more sensitive than adults to these risks, and the daily intake pathway demonstrated the highest CR and hazard index (HI) values. Obvious differences in the CR

and HI values were detected between the various sites, suggesting the necessity of multiple-site studies for health risk assessment. Jiyuan, Jiaozuo, Xuchang, and Zhoukou; Pingdingshan and Nanyang; and Jiyuan, Jiaozuo, Xinxiang, Anyang, and Kaifeng were the main potential sources of PM<sub>2.5</sub>, PM<sub>10</sub>, and As, respectively.

**Keywords:** Toxic elements, Coefficient of divergence, Enrichment factors, Principal component analysis, Carcinogenic risks, Potential source contribution function

---

## **Airborne Particulate Pollution Measured in Bangladesh from 2014 to 2017**

**Ashraf Mahmood<sup>1</sup>, Yongguang Hu<sup>1</sup>, Sabera Nasreen<sup>2</sup>, Philip K. Hopke<sup>3,4</sup>**

**Source :** Aerosol and Air Quality research, Volume: 19 | Issue: 2 | Pages: 272-281  
; DOI: 10.4209/aaqr.2018.08.0284

Recently, the World Health Organization ranked Narayanganj, Chittagong, and Dhaka among the top 25, 40, and 45 cities, respectively, for high ambient PM<sub>2.5</sub> concentrations. Bangladesh has instituted an air quality monitoring system operated by the Department of Environment. PM<sub>2.5</sub> and PM<sub>10</sub> were measured hourly from January 2014 through December 2017 in Dhaka, Gazipur, Narayanganj, Chittagong, Sylhet, and Barisal. All sites registered concentrations for both pollutants that exceeded the 24-h Bangladesh National Ambient Air Quality Standards. The particulate matter (PM) concentrations varied significantly seasonally and with different diel patterns from city to city. The highest concentrations were observed during the winter, typically when wind speeds and mixed layer heights are low and pollutant concentrations are increased by transport from the northwest. The PM<sub>2.5</sub> concentrations from the 1<sup>st</sup> quarters of 2014 and 2015 were compared to assess whether political unrest that appeared to reduce vehicular moment to very low levels affected the observed values. However, the PM<sub>2.5</sub> concentrations were statistically similar at the Dhaka, Narayanganj, and Sylhet sites and different for the Gazipur, Chittagong, and Barisal locations. Thus, the PM<sub>2.5</sub> concentrations during the political unrest in the 1<sup>st</sup> quarter of 2015 were not consistently lower across the measurement sites. These results indicate that vehicular emission contributions to PM<sub>2.5</sub> concentrations are smaller than in the past, which agrees with recent source apportionment studies showing that brick kilns have become the dominant source of PM.

**Keywords :** Air quality, PM<sub>2.5</sub>, PM<sub>10</sub>, Temporal patterns, Meteorology

---

# Characterization of the Air Quality Index for Urumqi and Turfan Cities, China

Zhiming Yin<sup>1</sup>, Kangping Cui <sup>1</sup>, Shida Chen<sup>1</sup>, Yixiu Zhao<sup>1</sup>, How-Ran Chao <sup>2</sup>, Guo-Ping Chang-Chien<sup>3,4</sup>

**Source:** Aerosol and Air Quality research, Volume: 19 | Issue: 2 | Pages: 282-306  
DOI: 10.4209/aaqr.2018.11.0410

This study investigated the atmospheric PM<sub>2.5</sub>, PM<sub>10</sub>, SO<sub>2</sub>, NO<sub>2</sub>, CO, and O<sub>3</sub> in Urumqi and Turfan cities from 2015 to 2017. In addition, six AQI categories and AQI values and seasonal changes in the major pollutants in Urumqi and Turpan were studied. In the three-year (2015–2017) study, in Urumqi, the average proportion of grades I, II, III, IV, V, and VI in spring were 16.3%, 59.7%, 16.0%, 5.33%, 2.67%, and 0%, respectively, were 12.0%, 82.7%, 5.33%, 0%, 0%, and 0% in summer; were 13.3%, 65.7%, 16.3%, 3.33%, 1.33%, and 0% in fall, and were 0.667%, 14.3%, 22.3%, 15.3%, 33.7%, and 13.7% in winter. In the Turpan region, the mean proportion of Grade I, II, III, IV, V, and VI pollutants were 0%, 61%, 21.3%, 8.00%, 2.33%, and 7.33% in spring, respectively; were 0.67%, 74.7%, 20.0%, 2.00%, 0.67%, and 2.00% in summer, were 1.33%, 59.7%, 42.3%, 7.67%, 0.33%, and 2.00% in fall, and were 0%, 11.0%, 35.3%, 29.3%, 20.3%, and 4.00% in winter. In the three-year (2015–2017) study, based on the results of the survey, it was determined that two cities have the best air quality in summer and the worst air quality in winter. In Urumqi, when the AQI was between 101–150, the main air pollutants in 2015 were PM<sub>2.5</sub> and PM<sub>10</sub>. In 2016, the main air pollutant was PM<sub>2.5</sub>, and in 2017, the main air pollutants were PM<sub>2.5</sub> and PM<sub>10</sub>. In Turpan, the main air pollutants in 2015 were PM<sub>2.5</sub> and PM<sub>10</sub>, were PM<sub>2.5</sub>, PM<sub>10</sub>, and O<sub>3</sub> in 2016, and was PM<sub>10</sub> in 2017. When the AQI was between 151 and 200, in Urumqi, the main atmospheric pollutant in the three-year period was PM<sub>2.5</sub>. In Turpan, the main atmospheric pollutants in the three-year period were PM<sub>2.5</sub> and PM<sub>10</sub>. When the AQI was between 201 and 300 in Urumqi, PM<sub>2.5</sub> was the main atmospheric pollutant from 2015–2017. In Turpan, the main atmospheric pollutants in the three-year period were PM<sub>2.5</sub> and PM<sub>10</sub>. To summarize, in both Urumqi and Turpan, PM<sub>2.5</sub> and PM<sub>10</sub> were the most predominant air pollutants causing high AQI values. More attention should thus be paid to the sources and reduction of these pollutants.

**Keywords:** AQI , PM<sub>10</sub> , PM<sub>2.5</sub>, SO<sub>2</sub> , NO<sub>x</sub> , CO , O<sub>3</sub>.

## **Air Pollution Profiles and Health Risk Assessment of Ambient Volatile Organic Compounds above a Municipal Wastewater Treatment Plant, Taiwan**

**Dika Rahayu Widiana<sup>1,2</sup>, Ya-Fen Wang<sup>2</sup>, Sheng-Jie You<sup>2</sup>, Hsi-Hsien Yang<sup>3</sup>, Lin-Chi Wang<sup>4,5,6</sup>, Jung-Hsuan Tsai<sup>2</sup>, Home-Ming Chen<sup>2,7</sup>**

**Source :** Aerosol and Air Quality research ,Volume: 19 | Issue: 2 | Pages: 375-382  
;DOI: 10.4209/aaqr.2018.11.0408

Municipal wastewater treatment processes have the function of removing harmful pollutants in the wastewater. However, there are probably several problems of air emissions related to these processes, especially for residents who live near a wastewater treatment plant. Volatile organic compounds exposure increases the risk of cancer. Thus, the health risk of residents to ambient volatile organic compounds exposure is essential to be conducted. One hundred and three volatile organic compounds (VOCs), total volatile organic compounds (TVOCs), and some prominent air pollutants (CO, CO<sub>2</sub>, NH<sub>3</sub>, H<sub>2</sub>S, PM<sub>1</sub>, PM<sub>2.5</sub>, PM<sub>7</sub>, PM<sub>10</sub>, TSP) were investigated at the surface of an underground wastewater treatment plant in Taipei City during four different seasons. Twenty four VOCs were identified, some of which were categorized as carcinogenic to humans (Group 1) and possibly carcinogenic to humans (Group 2B) according to the International Agency for Research on Cancer. The mean values of CO, CO<sub>2</sub>, PM<sub>1</sub>, PM<sub>2.5</sub>, PM<sub>7</sub>, PM<sub>10</sub> and TSP were found to be 0.64 ppm, 293.68 ppm, 1.37 µg m<sup>-3</sup>, 3.20 µg m<sup>-3</sup>, 10.74 µg m<sup>-3</sup>, 13.48 µg m<sup>-3</sup>, and 16.90 µg m<sup>-3</sup>, respectively. NH<sub>3</sub> and H<sub>2</sub>S were not detected in the present study. The health risk for residents was estimated following the method from United States Environmental Protection Agency (U.S. EPA). The cumulative of carcinogenic risk was 3.48 × 10<sup>-5</sup> and categorized as a possible risk. In addition, the result was also possibly affected by traffic nearby. The magnitude for non-carcinogenic risk index was less than 1.

**Keywords:** Air pollutant, Wastewater treatment plant, Volatile organic compound, Cancer risk

---

## **Health Benefit Assessment of China's National Action Plan on Air Pollution in the Beijing-Tianjin-Hebei Area**

**Wenkai Bi, Kui Chen, Zhimei Xiao, Miao Tang, Naiyuan Zheng, Ning Yang, Jingyun Gao, Yuan Li, Jun Kong, Hong Xu**

**Source :** Aerosol and Air Quality research, Volume: 19 | Issue: 2 | Pages: 383-389  
DOI: 10.4209/aaqr.2018.08.0297

To evaluate the effect of China's National Action Plan on Air Pollution (NAPAP), we assessed the health benefits of PM<sub>2.5</sub> remediation under the NAPAP from 2013 to 2017 in the Beijing-Tianjin-Hebei (BTH) area using a relative risk model with real PM<sub>2.5</sub> monitoring data and recent statistical research data. The results revealed that the PM<sub>2.5</sub> concentration in the BTH area decreased by 36  $\mu\text{g m}^{-3}$  (34.0%) under the NAPAP. PM<sub>2.5</sub>-related mortality resulting from all causes, cardiovascular disease, respiratory disease and lung cancer decreased to 58.1–65.2% of that in 2013; 102,133 PM<sub>2.5</sub>-related deaths were avoided, indicating a greater efficacy than the U.S. Cross-State Air Pollution Rule. These results demonstrated that the NAPAP is effective and can be used by other countries as a reference in enacting similar statutes.

**Keywords:** Health benefit assessment, PM<sub>2.5</sub>, National Action Plan on Air Pollution, Beijing-Tianjin-Hebei area

---

## **On the Contribution of Particulate Matter (PM<sub>2.5</sub>) to Direct Radiative Forcing over Two Urban Environments in India**

**Rama K. Krishna, Abhilash S. Panicker, Aslam M. Yusuf, Beig G. Ullah**

**Source :** Aerosol and Air Quality research, Volume: 19 | Issue: 2 | Pages: 399-410  
DOI: 10.4209/aaqr.2018.04.0128

Radiative forcing by particulate matter (PM<sub>2.5</sub>) has been estimated for a period of one year (January–December 2015) over Delhi and Pune (polluted urban metro cities in India). In situ observations of PM<sub>2.5</sub> and black carbon (BC) over both the cities were obtained from the ground-based System of Air Quality Forecasting and Research (SAFAR) network of stations. Observations have shown that PM concentrations over Pune had a strong diurnal cycle as compared to Delhi in all the seasons. Also, comparisons of the mode values and seasonal frequency distributions (FDs) over Pune and Delhi showed that pollution levels over Delhi were consistently above National Ambient Air Quality Standards (NAAQS). The mean monthly PM<sub>2.5</sub> values ranged from 61.5 to 162.9 over Delhi and from 17.4 to 74.05 over Pune. The BC mass contribution to PM<sub>2.5</sub> was found to be 10% to 25% over Pune. However, the contribution of BC to PM<sub>2.5</sub> was up to 35% over Delhi. Radiative forcing due to PM<sub>2.5</sub> (PRF) over both the sites was estimated using the Optical Properties of Aerosols and Clouds (OPAC) model along with the Santa Barbara DISORT Atmospheric Radiative Transfer (SBDART) model. The PRF in the atmosphere was between +7.73  $\text{Wm}^{-2}$  and +14.51  $\text{Wm}^{-2}$  over Delhi and between +3.12  $\text{Wm}^{-2}$  and +12.15  $\text{Wm}^{-2}$  over Pune. Sensitivity experiments showed that the impact of the increase in the hygroscopicity of the aerosols on the PRF was overshadowed by the net changes in albedo.

**Keywords:** PM<sub>2.5</sub>, AOD, Albedo, Radiative forcing.

---

## **Emission Characteristics of Regulated and Unregulated Air Pollutants from Heavy Duty Diesel Trucks and Buses**

**Sungwoon Jung<sup>1</sup>, Sunhee Mun<sup>1</sup>, Taekho Chung<sup>1</sup>, Sunmoon Kim<sup>1</sup>, Seokjun Seo<sup>1</sup>, Ingu Kim<sup>1</sup>, Heekyoung Hong<sup>1</sup>, Hwansoo Chong<sup>1</sup>, Kijae Sung<sup>2</sup>, Jounghwa Kim<sup>1</sup>, Youdeog Hong<sup>1</sup>**

**Source :** Aerosol and Air Quality research, Volume: 19 | Issue: 2 | Pages: 431-442  
DOI: 10.4209/aaqr.2018.05.0195

Due to the common stop-and-go driving style, the low temperature of vehicular exhaust gas in the urban driving cycle is a major cause of air pollution in the Seoul Metropolitan Area. We herein investigate the characteristics of regulated (NO<sub>x</sub>, PM, CO, and non-methane hydrocarbons (NMHC)) and unregulated (volatile organic compounds (VOCs), aldehydes, and polycyclic aromatic hydrocarbons (PAHs)) air pollutants emitted from heavy duty diesel trucks and buses equipped with different after-treatment systems (diesel particulate filter (DPF) + exhaust gas recirculation (EGR) and selective catalytic reduction (SCR) in urban conditions. NO<sub>x</sub> emissions depended on the combustion and working temperature of the SCR catalysts, and PM emissions were low. Alkanes dominated the non-methane volatile organic compound (NMVOC) emissions, 43–59% of which resulted from the low efficiency of the oxidation catalyst for alkane. The after-treatment system and the engine start conditions influenced the chemical components of the NMVOC emissions due to incomplete combustion and the evaporation of liquid fuel. Formaldehyde comprised the largest portion of the aldehydes, whereas PAH emissions remained largely undetected. Furthermore, formaldehyde was the largest contributor to the NMHCs, forming 14–29%. The results of this study will aid in establishing a system for calculating hazardous air pollutants emitted by vehicles in Korea.

**Keywords:** Volatile organic compounds , Aldehydes, Polycyclic aromatic hydrocarbons, Heavy duty diesel trucks and buses , After-treatment systems.

---

## **Construction and Characterization of an Indoor Smog Chamber for Measuring the Optical and Physicochemical Properties of Aging Biomass Burning Aerosols**

**Damon M. Smith<sup>1</sup>, Marc N. Fiddler<sup>2</sup>, Kenneth G. Sexton<sup>3</sup>, Solomon Bililign<sup>2,4</sup>**

**Source :** Aerosol and Air Quality research, Volume: 19 | Issue: 3 | Pages: 467-483  
DOI: 10.4209/aaqr.2018.06.0243

We describe here the construction and characterization of a new combustion-chamber system (the NCAT chamber) for studying the optical and physicochemical properties of biomass burning (BB) aerosols. This system is composed of a ~9 m<sup>3</sup> fluorinated ethylene propylene (FEP) film reactor placed in a temperature-controlled room that uses a tube furnace to combust biomass fuel samples under controlled conditions. The optical



properties are measured using a cavity ring-down spectrometer and nephelometer. Aerosol number density and size classification used condensation particle counter, and differential mobility analyzer. Other analytical instruments, used include NO<sub>x</sub>, O<sub>3</sub>, CO, and CO<sub>2</sub> analyzers, a gas chromatograph, and particle filter samples for determining the physicochemical and morphological properties. The construction details and characterization experiments are described, including measurements of the BB particulate size distribution and deposition rate, gas wall loss rates, dilution rate, light intensity, mixing speed, temperature and humidity variations, and air purification method. The wall loss rates for NO, NO<sub>2</sub>, and O<sub>3</sub> were found to be  $(7.40 \pm 0.01) \times 10^{-4}$ ,  $(3.47 \pm 0.01) \times 10^{-4}$ , and  $(5.90 \pm 0.08) \times 10^{-4} \text{ min}^{-1}$ , respectively. The NO<sub>2</sub> photolysis rate constant was  $0.165 \pm 0.005 \text{ min}^{-1}$ , which corresponds to a flux of  $(7.72 \pm 0.25) \times 10^{17} \text{ photons nm cm}^{-2} \text{ s}^{-1}$  for 296.0–516.8 nm, and the particle deposition rate was  $(9.46 \pm 0.18) \times 10^{-3} \text{ min}^{-1}$  for 100 nm mobility diameter BB particles from pine. Preliminary results of the single scattering albedo of fresh and aged BB aerosols are also reported.

**Keywords:** Biomass burning aerosols , Optical properties of aerosols , Smog chamber , Single scattering albedo, Fresh and aged aerosols.

---

## **Monitoring of Emission of Particulate Matter and Air Pollution using Lidar in Belgorod, Russia**

**Fedor Lisetskii , Andrei Borovlev**

**Source:** Aerosol and Air Quality research, Volume: 19 | Issue: 3 | Pages: 504-515  
;DOI: 10.4209/aaqr.2017.12.0593

Fine suspended particulate matter with an aerodynamic diameter smaller than 10 (PM<sub>10</sub>) or 2.5 μm (PM<sub>2.5</sub>) can be a dangerous air pollutant necessitating operational monitoring. Of the 1113 major Russian cities, however, only a few monitor industrial emissions of PM<sub>10</sub> and PM<sub>2.5</sub>. Here, we develop an approach to using mobile multi-wave (1064, 532, and 355 nm) lidar to estimate the concentration of PM<sub>10</sub> and PM<sub>2.5</sub>. This approach was implemented for Belgorod, where 1378 sources of air pollution with anthropogenic dust, primarily of carbonate composition, were registered. We have developed algorithms with seven stages of assessing the spatial distribution and monitoring of PM<sub>10</sub> and PM<sub>2.5</sub>, which made it possible to establish that fine-mode particles from tall sources of cement and construction material production (pipes with a height of ≥ 50 m) contributed 39% of the total particulate matter emissions. Using GIS to map the fields of the total suspended particulate matter (TSP) and determining the ratios of PM<sub>10</sub>/TSP and PM<sub>2.5</sub>/TSP, excesses in PM<sub>10</sub> and PM<sub>2.5</sub> up to 2.5 and 2.8 times greater, respectively, than the maximum threshold limit were observed. Tall sources' contribution to emissions increased in proportion to the distance from the source, resulting in 40–85% of the PM<sub>10</sub> and 43–91% of

the PM<sub>2.5</sub>. We demonstrate how lidar can be applied to optimize a particulate matter emissions monitoring network for environmental policy making.

**Keywords :** Particulate matters , Urban air pollution , Tall sources , Lidar measurements

---

## **Spatial and Temporal Variations of Gaseous and Particulate Pollutants in Six Sites in Tibet, China, during 2016–2017**

**Pengfei Chen<sup>1</sup>, Shichang Kang <sup>1,2</sup>, Junhua Yang<sup>1</sup>, Tao Pu<sup>1</sup>, Chaoliu Li<sup>2,3</sup>, Junming Guo<sup>1</sup>, Lekhendra Tripathee<sup>1</sup>**

**Source:** Aerosol and Air Quality research, Volume: 19 | Issue: 3 | Pages: 516-527  
DOI: 10.4209/aaqr.2018.10.0360

Long-term air quality data with high temporal and spatial resolutions are necessary to understand some processes influencing air quality and corresponding environmental and health effects. In this study, spatiotemporal variations of PM<sub>2.5</sub>, PM<sub>10</sub>, SO<sub>2</sub>, NO<sub>2</sub>, CO, and O<sub>3</sub> were investigated over a one-year period (June 2016–May 2017) at six sites of the Tibetan Plateau (TP). The annual mean concentrations of PM<sub>2.5</sub> in all cities except Nagchu were below the Grade II standard (35 µg m<sup>-3</sup>), and the values in Nagri and Nyingchi were even less than the Grade I standard (15 µg m<sup>-3</sup>). PM<sub>10</sub> concentrations showed similar distribution pattern with PM<sub>2.5</sub>. Evident seasonal variations of PM<sub>2.5</sub>, PM<sub>10</sub>, SO<sub>2</sub>, NO<sub>2</sub>, and CO concentrations were observed, with the highest seasonal average value being in winter followed by fall, spring, and summer, in descending order. By contrast, the 8-h O<sub>3</sub> concentration showed an opposite seasonal variation because the O<sub>3</sub> depended on lots of factors such as stratospheric incursions, weather conditions, and intensity of solar radiation. The diurnal trends of PM<sub>2.5</sub>, PM<sub>10</sub>, SO<sub>2</sub>, NO<sub>2</sub>, and CO concentrations in study region generally showed a flat “W” shape with two peaks occurring around noon (10:00–12:00) and midnight (21:00–23:00); these peaks were found to be affected by emission sources and weather conditions. However, the O<sub>3</sub> concentration trends did not significantly differ among the six regions, with the maximum concentration being in the afternoon. In sum, cities on the TP showed slightly higher pollution levels in regions affected by anthropogenic activities such as Lhasa and Nagchu, whereas other cities showed good air quality. Beside long-range transport pollutants from surrounding regions, local emissions (e.g., biomass burning, religious activities) also contributed much to the atmospheric pollutants. This study provides a basis for the formulation of future urban air pollution control measures on the TP.

**Keywords :** PM<sub>2.5</sub> , Ozone , Air pollution , Distribution , Tibetan Plateau.

---



## Particulate Matter Source Contributions for Raipur-Durg-Bhilai Region of Chhattisgarh, India

Sarath K. Guttikunda<sup>1,2</sup>, Pallavi Pant<sup>3</sup>, K.A. Nishadh<sup>1</sup>, Puja Jawahar<sup>1</sup>

**Source:** Aerosol and Air Quality research ,Volume: 19 | Issue: 3 | Pages: 528-540  
;DOI: 10.4209/aaqr.2018.06.0237

In Chhattisgarh, Raipur-Durg-Bhilai (RDB) tri-city area hosts the new administrative capital of the state, interconnected by an expressway forming the industrial corridor and is one of the largest steel manufacturing hubs in India. Between 1998 and 2016, the satellite and global model data derived concentrations show a 50% increase in the overall PM<sub>2.5</sub> pollution in the region. The average PM<sub>10</sub> concentration measured at commercial, industrial, and residential monitoring stations is  $125 \pm 52 \mu\text{g m}^{-3}$  in 2015. None of the stations currently measure PM<sub>2.5</sub>. The annual average PM<sub>10</sub> concentrations in 2011 is  $175 \pm 110 \mu\text{g m}^{-3}$ , which translates to 28% improvement in 5 years. A multiple pollutant emissions inventory was established for this urban airshed (extending 60 km × 30 km), with annual estimates of 41,500 tons of PM<sub>2.5</sub>, 59,650 tons of PM<sub>10</sub>, 7,600 tons of SO<sub>2</sub>, 67,000 tons of NO<sub>x</sub>, 163,300 tons of CO, 118,150 tons of NMVOCs, and 3.1 million tons of CO<sub>2</sub> for 2015, and further projected to 2030 under business as usual conditions. The ambient source contributions were calculated using WRF-CAMx chemical transport modeling system, highlighting the heavy industries (mostly steel) (23%), followed by transport (including on road dust) (29%), domestic cooking and heating (12%), open waste burning (6%), as the key air pollution sources in the urban area. The city has an estimated 26% of the ambient annual PM<sub>2.5</sub> pollution originating outside the urban airshed - this contribution is mostly coming from the coal-fired power plants, large (metal and non-metal processing) industries, and brick kilns located outside the urban airshed and seasonal open biomass fires.

**Keywords :** PM<sub>2.5</sub> , Particulate pollution , Raipur , Durg-Bhilai , India , WRF-CAMx , Emissions inventory , Dispersion modeling , Source apportionment

---

## Measurement of Black Carbon Concentration and Comparison with PM<sub>10</sub> and PM<sub>2.5</sub> Concentrations Monitored in Chungcheong Province, Korea

Youngbum Cha, Shihyoung Lee, Jeonghoon Lee

**Source:** Aerosol and Air Quality research, Volume: 19 | Issue: 3 | Pages: 541-547  
;DOI: 10.4209/aaqr.2018.08.0325

Black carbon concentrations are closely related to global warming. To characterize the atmospheric aerosols in Chungcheong Province, Korea, we measured the concentrations of black carbon for about eight months (September 2015–April 2016) and compared them with PM<sub>10</sub> and PM<sub>2.5</sub> concentrations as well as various meteorological parameters (e.g., wind velocity and wind direction). We used a multi-angle absorption photometer to measure the black carbon; the PM<sub>10</sub> and PM<sub>2.5</sub> concentrations, wind velocity, and wind direction were obtained from local monitoring stations. The highest and lowest PM<sub>10</sub>, PM<sub>2.5</sub>, and BC concentrations were observed in spring and fall, respectively. The high concentrations in spring and winter were likely due to the dominance of westerly winds, which transported pollutants, whereas the low concentrations in fall were likely due to increased wind variations, which drove turbulent mixing. Overall, although BC concentrations exhibited directly proportional correlations with PM<sub>10</sub> and PM<sub>2.5</sub>, the correlations were relatively low, probably because of differences between the sources of these three atmospheric pollutants. These results help clarify the characteristics of BC concentrations over the Korean Peninsula.

**Keywords:** Black carbon , MAAP , PM10 , PM2.5

---

## **The Geological Availability and Emissions of Sulfur and SO<sub>2</sub> from the Typical Coal of China**

**Rahib Hussain<sup>1,2</sup>, Kunli Luo <sup>1</sup>**

**Source:** Aerosol and Air Quality research, Volume: 19 | Issue: 3 | Pages: 559-570  
DOI: 10.4209/aaqr.2018.08.0281

This study aimed to assess the natural availability of sulfur and SO<sub>2</sub> in coal typical of the Jurassic, Permo-Carboniferous, and Cambrian strata in Shaanxi, China, and their emission rates. A total of 93 samples (39 Binxian Jurassic, 37 Permo-Carboniferous, and 17 Langao Cambrian) were collected and analyzed via the Eschka method (GB/T 214-1996). The results show that the average sulfur content was 2.40%, 2.85%, and 0.92% in the Binxian coal gangue, raw coal, and coal slime, respectively; 1.48%, 2.41%, and 1.5% in the Hancheng Permo-Carboniferous coal gangue, raw coal, and coal slime, respectively; and 0.84% and 2.44% in the Langao Cambrian stone-like coal and black shale rock, respectively. The annual sulfur emissions from the Binxian urban and rural areas totaled 1.5 kt and 9.3 kt (Kilotons), respectively, which contributed 1.4% of the overall SO<sub>2</sub> emitted into the atmosphere. The sulfur emissions from Hancheng urban and rural areas totaled 1.8 kt and 11.9 kt, respectively, which contributed 1.8% of the overall SO<sub>2</sub>. The sulfur emissions from Langao urban and rural areas was 0.4 kt and 2.8 kt, respectively, which contributed 0.43% of the overall SO<sub>2</sub>. Coal-waste consumption from 1991 to 2015 increased by 23% and 10% in urban and rural areas, respectively, in China, ultimately reducing the debris from coal waste. Raw-coal consumption from 1991 to 2015 decreased

from 96% to 73% and from 97% to 87% in urban and rural areas, respectively. SO<sub>2</sub> emissions since 2006 have decreased due to effective desulfurizing technology. According to the results of this study, China has been continuously reducing the emission of SO<sub>2</sub> by adopting a green economy. The study recommends installing desulfurizing equipment in power plants to further reduce the SO<sub>2</sub> emissions.

**Keywords:** Cambrian, Coal, Jurassic, Shaanxi, Sulfur, SO<sub>2</sub>.

---

## **Study on Influencing Mechanism of Outdoor Plant-related Particles on Indoor Environment and its Control Measures during Transitional Period in Nanjing**

**Bin Zhou<sup>1</sup>, Lu Feng<sup>1</sup>, Angus Shiue<sup>2</sup>, Shih-Cheng Hu<sup>2</sup>, Yu Wang<sup>1</sup>, Fei Li<sup>1</sup>, Ti Lin<sup>2</sup>, Hui-Fang Liu<sup>1</sup>, Peng Wei<sup>1</sup>, Yang Xu<sup>1</sup>**

**Source:** Aerosol and Air Quality research, Volume: 19 | Issue: 3 | Pages: 571-586  
DOI: 10.4209/aaqr.2018.01.0027

Most city trees in Nanjing are *Platanus acerifolia* and *Populus nigra*, which generate many whirling willow catkins in the air during the transitional season, yet little attention has been paid to the health risks, including itchy skin and respiratory infections, on occupants of roadside buildings. Since the air quality of these indoor spaces cannot meet WHO guidelines during the transitional season due to the influence of plant pollutants, a suitable ventilation scheme, together with air filtration measures, is urgently needed. Hence, four ventilation schemes were compared: natural ventilation, no ventilation with the door and windows closed, recirculating ventilation with a ceiling cassette fan-coil unit but no air filter, and recirculating ventilation with a ceiling cassette fan-coil unit and F7 filter. The performance of these modes was evaluated by comparing the effects of outdoor particulate matter on the indoor air quality. The results showed that the larger the particle size, the lower the I/O ratio. Furthermore, the influence of the occupants' activities on indoor particle concentrations cannot be ignored, particularly for large particles, which varied more than small particles according to indoor human activity. Therefore, we suggest operating the ceiling cassette fan-coil unit with an air filter for this application, which can reduce the indoor particle concentration to an acceptable level and decrease the potential health risk posed by plant pollutants.

**Keywords:** Plant pollutants, Transition season, Infiltration air, Ventilation modes, Indoor air quality.

---

## Sources of High Sulfate Aerosol Concentration Observed at Cape Hedo in Spring 2012

Syuichi Itahashi<sup>1,2</sup>, Shiro Hatakeyama<sup>3,4,5</sup>, Kojiro Shimada<sup>6</sup>, Akinori Takami<sup>7</sup>

**Source:** Aerosol and Air Quality research, Volume: 19 | Issue: 3 | Pages: 587-600  
DOI: 10.4209/aaqr.2018.09.0350

Intensive observation campaigns approximately 1 week long were conducted periodically from March 2010 to November 2015 at Cape Hedo, Okinawa, Japan. The maximum daily mean sulfate aerosol (SO<sub>4</sub><sup>2-</sup>) concentrations surpassed 15 µg m<sup>-3</sup> in spring 2012. In this study, source apportionment for these high concentrations was conducted using an air quality model with the tagged tracer method, and the main source was identified as volcanoes in March and as anthropogenic emissions from China in April. In March, the prevailing northerly wind transported a volcanic SO<sub>2</sub> plume with a low conversion ratio to Cape Hedo. The impacts of 15 volcanoes in Japan were estimated, and a substantial impact from Sakurajima, which accounted for more SO<sub>2</sub> than anthropogenic emissions from Japan, was found. Because the model had difficulty capturing the highest concentration, three sensitivity simulations were performed to consider the uncertainty of the volcanic SO<sub>2</sub> emission amounts and injection heights, revealing the importance of the injection height in addition to the SO<sub>2</sub> emission amount. Throughout April, contributions from anthropogenic emissions from China were found; hence, this source was further divided into 31 provincial scales. Shandong and Jiangsu Provinces, which are the first and seventh largest emission sources in China, respectively, were identified as significant sources at Cape Hedo. These sources showed day-to-day variation in their contributions, and the highest contribution from Shandong Province occurred on April 23, whereas that from Jiangsu Province occurred on April 22.

**Keywords:** Air quality model ,Source apportionment , Tagged tracer method , East Asia, Cape Hedo Atmosphere and Aerosol Monitoring Station (CHAAMS).

---

## Various Sources of PM<sub>2.5</sub> and their Impact on the Air Quality in Tainan City, Taiwan

Hung-Yi Lu<sup>1</sup>, Yee-Lin Wu<sup>1</sup>, Justus Kavita Mutuku<sup>1</sup>, Ken-Hui Chang<sup>2</sup>

**Source:** Aerosol and Air Quality research, Volume: 19 | Issue: 3 | Pages: 601-619  
DOI: 10.4209/aaqr.2019.01.0024

The recent deterioration of Taiwan's air quality is partly due to fine particulate matter (PM<sub>2.5</sub>). With several studies pointing out a direct link between PM<sub>2.5</sub> and the global disease burden, plans are underway to reach the standard of an annual average PM<sub>2.5</sub> concentration of 15 µg m<sup>-3</sup> in Taiwan by 2020. Subsequently, environmental protection bureaus in all cities should assess PM<sub>2.5</sub> emission sources and implement control

strategies. This study focuses on analysis of PM<sub>2.5</sub> sources within Tainan City in an effort to establish the contribution of large-scale pollution sources within the city as well as those from neighboring counties and cities. During this study, the top nine largest emission sources in Tainan City were investigated: (1) the Chemical manufacturing industry, (2) the iron and steel industry, (3) the power industry, (4) manufacturing of coal-based products, (5) diesel vehicles, (6) two-stroke scooters, (7) catering, (8) construction/road dust, and (9) open burning. Three important pollution sources in the central region of Taiwan were investigated as well, including: (1) the Taichung Power Plant, (2) the Formosa Petrochemical Corporation (FPCC) Sixth Naphtha Cracking Industry, and (3) the Dragon Steel Company in Taichung City, Changhua County, and Yunlin County, respectively, all of which are located on the windward side of Tainan City. The Community Multiscale Air Quality Model (CMAQ) was used to simulate the impact of the mentioned sources on Tainan's air quality. The results for the monthly contributions from the different sources averaged over a one year period indicated that diesel vehicles are the largest source, emitting up to 1.06  $\mu\text{g m}^{-3}$ , followed by the Taichung Power Plant, which had 0.87  $\mu\text{g m}^{-3}$ , the construction industry and road dust emissions, with 0.80  $\mu\text{g m}^{-3}$ , and with open burning of waste having the lowest contribution. These results can be applied to facilitate the development of follow-up air quality control strategies.

**Keywords:** Emission source , Different pollution sources , Tainan City , Air quality model (CMAQ) , PM<sub>2.5</sub>

---

## **Comparison of Discharging Electrodes for the Electrostatic Precipitator as an Air Filtration System in Air Handling Units**

**Dong Ho Shin, Chang Gyu Woo, Hak-Joon Kim, Yong-Jin Kim, Bangwoo Han**

**Source:** Aerosol and Air Quality research, Volume: 19 | Issue: 3 | Pages: 671-676  
DOI: 10.4209/aaqr.2018.10.0367

The quality of indoor air is of increasing concern because it is closely related to human health. An air handling unit (AHU) can be used to control the quality of indoor air with respect to particulate matter and CO<sub>2</sub>, as well as providing air conditioning by regulating the temperature and the humidity. Electrostatic precipitators have high collection efficiencies and low pressure drops. However, their chargers can generate ozone, which is a drawback of applying them to indoor air control. In this study, we compared four discharging electrodes: a 50- $\mu\text{m}$  tungsten wire, a 100- $\mu\text{m}$  tungsten wire, 16- $\mu\text{m}$  aluminum (Al) foil, and carbon fabric composed of 5–10- $\mu\text{m}$  fibers. The carbon-fabric electrode exhibited superior particle collection efficiency and lower ozone generation for a given power consumption compared to the 50- and 100- $\mu\text{m}$  tungsten wires, or the Al foil electrode. This low-ozone-generating, micro-sized electrode can be applied as an electrostatic precipitator in AHUs for indoor air control.

**Keywords:** Air handling unit , Carbon fabric , Discharge electrode, Ozone.

---

## **Development and Validation of a Novel Particle Source for Nano-sized Test Aerosols**

**Christian Monsé 1, Christian Monz2, Burkhard Stahlmecke3, Birger Jettkant1, Jürgen Büniger1, Thomas Brüning1, Volker Neumann2, Dirk Dahmann2**

**Source:** Aerosol and Air Quality research, Volume: 19 | Issue: 4 | Pages: 677-687  
DOI: 10.4209/aaqr.2018.06.0219

In the EU, there is an increasing need for regulatory agencies to establish health-based threshold limits for airborne particles. A prerequisite for such projects is the validation and comparison of existing and newly developed particle analyzers. Corresponding proficiency tests have often been conducted with the help of inter-laboratory tests using test aerosols. Although test aerosols in the micro- and the nanoscale range were produced with different generator systems at the technical center of the Institute for the Research on Hazardous Substances (IGF) in Dortmund, a stable and reproducible method of producing a low number concentration for nano-sized particles was not achieved. Inspired by a method of monodisperse droplet generation, we coupled a flame generator with a droplet generator and examined the concentration and the diameter of the formed particles as a consequence of the precursor concentration and the droplet frequency. In addition, the reproducibility of the method was tested daily, and the nanoparticles were collected and characterized microscopically. Finally, the measurements of the particle size distribution were mathematically examined. The resulting fits enable the prediction of the median particle diameter as a function of the precursor concentration and the frequency of the droplets. Overall, the performed experiments confirm that this system meets all the requirements with regard to a low number concentration and long-term stability and reproducibility and should therefore be suitable for further inter-laboratory round robin tests.

**Keywords:** Nanoparticles , Test aerosol, Flame generator, Droplet generator.

---

## **Spatial and Temporal Variations of PM<sub>2.5</sub> in North Carolina**

**Bin Cheng, Lingjuan Wang-Li**

**Source:** Aerosol and Atmospheric Chemistry, Volume: 19 | Issue: 4 | Pages: 698-710  
DOI: 10.4209/aaqr.2018.03.0111

Studies have indicated that the adverse effects on human health and the decrease in visibility caused by fine particulate matter (PM<sub>2.5</sub>) exhibit spatial heterogeneity. Moreover, the environmental effects produced by different chemical compositions of PM<sub>2.5</sub> vary on a regional scale. Therefore, understanding the spatiotemporal variations and chemical

compositions of PM<sub>2.5</sub> is necessary for assessing the regional impacts. Secondary inorganic PM<sub>2.5</sub> (iPM<sub>2.5</sub>) is formed through chemical reactions between the base gas NH<sub>3</sub> and acidic gas pollutants (e.g., NO<sub>2</sub> or SO<sub>2</sub>). The major components of iPM<sub>2.5</sub> include NH<sub>4</sub><sup>+</sup>, SO<sub>4</sub><sup>2-</sup>, and NO<sub>3</sub><sup>-</sup>. To fully comprehend the regional impacts of PM<sub>2.5</sub>, this research quantifies the spatiotemporal variations of iPM<sub>2.5</sub> with the aim of evaluating the contributions from iPM<sub>2.5</sub> to PM<sub>2.5</sub> in North Carolina (NC). The concentrations (at 34 sites) and chemical components (at 7 sites) of PM<sub>2.5</sub> from 2005 to 2014 were extracted from the EPA's AirData, with the highest concentrations measured in the urban areas of central NC. Notably, PM<sub>2.5</sub> concentrations have been significantly reduced over the past 10 years, with a concurrent decreasing trend in iPM<sub>2.5</sub>. Seasonal variation analysis indicates that PM<sub>2.5</sub> concentrations were higher in summer and lower in winter; however, significant variation occurred only between 2005 and 2011. Although iPM<sub>2.5</sub> formed the largest mass fraction of PM<sub>2.5</sub> for 2005–2011, organic carbon matter (OCM) contributed the dominant share for 2012–2014. Significant seasonal variations in the iPM<sub>2.5</sub> mass fractions were also observed, with NO<sub>3</sub><sup>-</sup> and SO<sub>4</sub><sup>2-</sup> exhibiting inverse variations. This study links the ambient PM<sub>2.5</sub> to various sources by revealing the spatiotemporal variations of PM<sub>2.5</sub> and their associated chemical compositions in NC, thereby enabling the development of effective control and mitigation strategies.

**Keywords:** Chemical compositions , Inorganic PM2.5 , Spatiotemporal variations

---

## **Source Apportionment and Macro Tracer: Integration of Independent Methods for Quantification of Woody Biomass Burning Contribution to PM10**

**Milena Stracquadano, Ettore Petralia , Massimo Berico, Teresa M.G. La Torretta, Antonella Malaguti, Mihaela Mircea, Maurizio Gualtieri, Luisella Ciancarella**

**Source:** Aerosol and Atmospheric Chemistry, Volume: 19 | Issue: 4 | Pages: 711-723  
DOI: 10.4209/aaqr.2018.05.0186

During the last few years, the rise in woody biomass burning (BB) for household heating has caused an increase in PM mass concentrations, particularly for the fine fraction, in Europe, as reported by the European Environmental Agency. Estimating the contribution from biomass combustion to airborne particulate matter is therefore an important issue in air quality governance, due to its potential health and environmental impacts.

Wood burning's contribution to PM10 was estimated in winter at a rural site in southern Italy by means of two independent methods: source apportionment analysis with Positive Matrix Factorization (BBPMF) and the macro tracer approach, based on levoglucosan concentrations (BBLevo). PM10 and PM2.5 samples were collected every 24 h and every 8 h, respectively, and analyzed to determine the organic and elemental carbon, levoglucosan, inorganic ions and elements.



The results obtained via these methods showed good agreement ( $r = 0.85$ ), with a linear correlation slope of about 1, and provide a reliable assessment of the BB contribution.

Woody biomass combustion contributed significantly to the PM<sub>10</sub> (on average, slightly less than 30% of the total mass) during winter. The combination of the independent methods proposed here may be used as a methodology for refining the BB contribution to air pollution.

**Keywords:** Biomass combustion , Particulate matter, Levoglucosan, PMF ,Emission sources.

---

## **Differential Probability Functions for Investigating Long-term Changes in Local and Regional Air Pollution Sources**

**Mauro Masiol<sup>1</sup>, Stefania Squizzato<sup>1</sup>, Meng-Dawn Cheng<sup>2</sup>, David Q. Rich<sup>1,3,4</sup>, Philip K. Hopke<sup>1,5</sup>**

**Source:** Aerosol and Atmospheric Chemistry, Volume: 19 | Issue: 4 | Pages: 724-736  
DOI: 10.4209/aaqr.2018.09.0327

Conditional probability functions are commonly used for source identification purposes in air pollution studies. CBPF (conditional bivariate probability function) categorizes the probability of high concentrations being observed at a location by wind direction/speed and investigate the directionality of local sources. PSCF (potential source contribution function), a trajectory-ensemble method, identifies the source regions most likely to be associated with high measured concentrations. However, these techniques do not allow the direct identification of areas where changes in emissions have occurred. This study presents an extension of conditional probability methods in which the differences between conditional probability values for temporally different sets of data can be used to explore changes in emissions from source locations. The differential CBPF and differential PSCF were tested using a long-term series of air quality data (12 years; 2005/2016) collected in Rochester, NY. The probability functions were computed for each of 4 periods that represent known changes in emissions. Correlation analyses were also performed on the results to find pollutants undergoing similar changes in local and regional sources. The differential probability functions permitted the identification of major changes in local and regional emission location. In Rochester, changes in local air pollution were related to the shutdown of a large coal power plant (SO<sub>2</sub>) and to the abatement measures applied to road and off-road traffic (primary pollutants). The concurrent effects of these changes in local emissions were also linked to reduced concentrations of nucleation mode particles. Changes in regional source areas were related to the decreases in secondary inorganic aerosol and organic carbon. The differential probabilities for sulfate, nitrate, and organic aerosol were consistent with differences in the available National Emission Inventory annual emission values. Changes in the source areas of black carbon and PM<sub>2.5</sub> mass concentrations were highly correlated.



**Keywords:** Differential probability functions , Long-term trends ,Air pollution.

---

## **Variation in Airborne Particulate Levels at a Newly Opened Underground Railway Station**

**Yingying Cha 1, Minghui Tu1, Max Elmgren2, Sanna Silvergren2, Ulf Olofsson1**

**Source:** Aerosol and Atmospheric Chemistry, Volume: 19 | Issue: 4 | Pages: 737-748  
DOI: 10.4209/aaqr.2018.06.0225

The construction of a new railway tunnel for commuter trains in Stockholm was completed in 2017. It included two modern stations (Odenplan and Stockholm City) with platform screen doors (PSD) and one old station (Stockholm Södra) without PSDs. This study evaluates the concentrations of airborne particulates at the new Odenplan station, focusing on the effects of traffic operation, system age and train movement. For comparison, the other two stations in the tunnel and an above-ground railway station (Solna) were also investigated. The new platform was clean prior to opening for traffic (the average concentration of PM<sub>10</sub> and PM<sub>2.5</sub> was 12 and 2  $\mu\text{g m}^{-3}$ , respectively). Substantial increases in the PM<sub>10</sub> and PM<sub>2.5</sub> levels were observed after it came into service, with the average concentrations increasing to 120 and 30  $\mu\text{g m}^{-3}$  after 1 week and then to 175 and 35  $\mu\text{g m}^{-3}$  after 3 months of operation. The train movement factor (traffic frequency and train stopping period) was found to have a strong effect on the coarse-sized particle concentrations (0.3–10  $\mu\text{m}$ ). Comparable levels of PM<sub>10</sub> and PM<sub>2.5</sub> were measured at both the new Odenplan station and the old station, where the amount of traffic was similar. For the other new station, Stockholm City, where traffic was only half as frequent, the PM<sub>10</sub> and PM<sub>2.5</sub> levels were substantially lower.

**Keywords:** Platform air quality , Railway tunnel , New railway station , Particulate matter, Platform screen door.

---

## **Characterization of the Air Quality Index in Southwestern Taiwan**

**Yen-Yi Lee<sup>1</sup>, Yen-Kung Hsieh <sup>2</sup>, Guo-Ping Chang-Chien <sup>3,4</sup>, Weiwei Wang<sup>5</sup>**

**Source:** Urban Air Quality ,Volume: 19 | Issue: 4 | Pages: 749-785  
DOI: 10.4209/aaqr.2019.02.0080

This study provides an investigation of atmospheric PM<sub>2.5</sub>, PM<sub>10</sub>, SO<sub>2</sub>, NO<sub>2</sub>, CO, and O<sub>3</sub> in the period from 2015–2017 in the southwestern and central part of Taiwan. In addition, the seasonal distribution of six AQI classes and corresponding primary pollutants were further analyzed. The daily AQIs were 15–194 in 2015, 17–213 in 2016, and 16–184 in 2017, respectively. During the three year period, in the studied area, the mean proportions of levels with Grade I, II, III, IV, V, and VI were 3%–31%, 30%–57%, 17%–46%, 0%–12%, 0%–1% and 0% in spring; were 38%–76%, 21%–57%, 0%–10%, 0%–2%, 0% and 0% in

summer; were 2%–45%, 34%–77%, 13%–36%, 0%–18%, 0% and 0% in fall, and were 0%–12%, 38%–67%, 24%–41%, 1%–22%, 0% and 0% in winter. Generally, it was found that summer has the best air quality and that winter has the worst, where spring and fall are similar in terms of air quality. PM<sub>2.5</sub> was the typical primary air pollutant when the AQI classes were 51–200, followed by O<sub>3</sub> in summer, spring and fall, and PM<sub>10</sub> in winter. As for class 201–300, the primary air pollutant was O<sub>3</sub> and the 300–500 class did not occur.

**Keywords:** AQI , PM2.5 , PM10 , SO2 , NO2 , CO , O3

---

## **Ambient Endotoxin and Chemical Pollutant (PM<sub>10</sub>, PM<sub>2.5</sub>, and O<sub>3</sub>) Levels in South Korea**

**Sung Ho Hwang<sup>1</sup>, Dong Uk Park<sup>2</sup>**

**Source:** Urban Air Quality, Volume: 19 | Issue: 4 | Pages: 786-793

DOI: 10.4209/aaqr.2018.06.0235

We measured the levels of airborne endotoxins in South Korea and compared them to PM<sub>10</sub>, PM<sub>2.5</sub>, and O<sub>3</sub> levels in ambient environments; environmental factors affecting these levels were also analyzed. A total of 81 air samples were collected and analyzed using the kinetic Limulus Amebocyte Lysate (LAL) assay. The geometric mean was determined for the levels of endotoxin (0.132 EU m<sup>-3</sup>), PM<sub>10</sub> (51.9 μg m<sup>-3</sup>), PM<sub>2.5</sub> (22.6 μg m<sup>-3</sup>), and O<sub>3</sub> (0.018 ppm). The endotoxin levels were significantly higher in fall and winter than in summer. The levels of PM<sub>10</sub> and PM<sub>2.5</sub> were significantly higher, and the level of O<sub>3</sub> was by far its highest, in spring. Negative correlations were found between the endotoxin and O<sub>3</sub> levels ( $r = -0.491$ ) and between the endotoxin levels and temperature ( $r = -0.302$ ). The PM<sub>10</sub> levels were also negatively associated with the O<sub>3</sub> levels and temperature but positively associated with the PM<sub>2.5</sub> levels. Given the negative relationship between airborne endotoxins and O<sub>3</sub> determined here, further studies with larger sample sizes are needed to identify the responsible mechanisms.

**Keywords:** Endotoxins , Particulate matter , Ozone , Ambient conditions , Seasons

---

## **Black Carbon Aerosol in the Industrial City of Xuzhou, China: Temporal Characteristics and Source Appointment**

**Wei Chen<sup>1</sup>, Huimin Tian<sup>1</sup>, Kai Qin<sup>2</sup>**

**Source:** Urban Air Quality, Volume: 19 | Issue: 4 | Pages: 794-811

DOI: 10.4209/aaqr.2018.07.0245

Black carbon (BC) aerosol in urban environments potentially affects the local environment, the regional climate cycle, and even human health. A two-year field

measurement (May 2014 to July 2016) of BC and particulate matter in Xuzhou, a large industrial city and the economic center of Huaihai Economic Zone in central China, was conducted. The average annual concentrations of BC, PM<sub>1.0</sub>, PM<sub>2.5</sub>, and PM<sub>10</sub> were 2.44 μg m<sup>-3</sup>, 56.6 μg m<sup>-3</sup>, 61.8 μg m<sup>-3</sup>, and 75.8 μg m<sup>-3</sup>, respectively. The highest daily average for the BC concentrations was 11.6 μg m<sup>-3</sup>, and more than 10% of the hourly BC measurements had concentrations above 5 μg m<sup>-3</sup>. All of the BC and PM concentrations displayed two diurnal peaks (during rush hours in the morning and in the evening) and one valley (in the afternoon). The overall BC concentrations, and the BC fractions in the PM were higher in winter and spring, whereas the overall PM concentrations were higher in winter and autumn. The backward trajectory analysis indicated that most of the high BC concentrations in Xuzhou were associated with north and northwest winds, and the potential source contribution function (PSCF) model proved that the provinces of central China were the most likely source regions. Our findings can be used to set appropriate atmospheric pollution control measures for these central provinces and to increase the accuracy of air quality forecasting.

**Keywords:** Black carbon , Particulate matter , PM2.5 , Air pollution

---

## **Evaluation of Indoor Air Pollution during Decorating Process and Inhalation Health Risks in Xi'an, China: A Case Study**

**Tian Chang<sup>1</sup>, Jinhui Wang<sup>2</sup>, Jiaqi Lu<sup>1</sup>, Zhenxing Shen <sup>1</sup>, Yu Huang<sup>3</sup>, Jian Sun<sup>1</sup>,  
Hongmei Xu<sup>1</sup>, Xin Wang<sup>4</sup>, Dongxiao Ren<sup>1</sup>, Junji Cao<sup>3</sup>**

**Source:** Aerosol and Atmospheric Chemistry, Volume: 19 | Issue: 4 | Pages: 854-864  
DOI: 10.4209/aaqr.2018.07.0261

PM<sub>2.5</sub>, formaldehyde, and 8 volatile organic compounds (VOCs) were observed in 6 newly decorated apartment units to evaluate the effects of the decorating process on the indoor air quality in Xi'an, China. The comparison of indoor and outdoor formaldehyde and VOCs concentrations showed that the outdoor PM<sub>2.5</sub> concentration exceeded the indoor one during the monitoring process, whereas the indoor formaldehyde and VOCs concentrations exceeded the outdoor ones. The levels of formaldehyde and VOCs in different rooms were investigated, and the concentrations in the bedroom were found to be the highest. Furthermore, the formaldehyde and VOCs concentrations were measured in 200 other rooms decorated within a 2-year period in Xi'an, and the results indicated that wallpapering, wooden flooring, and furniture were the major decorating processes emitting these compounds. In addition, a health risk assessment of the monitored formaldehyde and VOCs in the rooms 1 year after decorating showed that benzene posed the greatest health risk among the assessed VOCs.

**Keywords:** Indoor air quality, Decorating process, Inhalation health risks, Xi'an.

---

## Characteristics of PM<sub>2.5</sub>-bound PAHs at an Urban Site and a Suburban Site in Jinan in North China Plain

Yan Zhang<sup>1</sup>, Lingxiao Yang<sup>1,2</sup>, Xiongfei Zhang<sup>1</sup>, Jingshu Li<sup>1</sup>, Tong Zhao<sup>1</sup>, Ying Gao<sup>1</sup>, Pan Jiang<sup>1</sup>, Yanyan Li<sup>1</sup>, Xiangfeng Chen<sup>3</sup>, Wenxing Wang<sup>1</sup>

**Source:** Air Pollution and Health Effects Volume: 19 | Issue: 4 | Pages: 871-884

DOI: 10.4209/aaqr.2018.09.0353

The PM<sub>2.5</sub> samples at an urban site (JN) and a suburban site (QXT) were simultaneously collected in a heavily polluted city in North China Plain (Jinan) from March to December in 2016, and eighteen polycyclic aromatic hydrocarbons (PAHs) were analyzed. The annual average  $\sum$ PAHs concentrations were  $39.8 \pm 36.6$  and  $23.6 \pm 14.0$  ng m<sup>-3</sup> at JN and QXT, respectively, with the highest concentrations observed during winter. PHE and CHY were the two most abundant PAHs, accounting for 31.1% at JN and 34.2% at QXT. Source apportionment analyses from the results of Principal Component Analysis (PCA) revealed that coal/biomass combustion and vehicle emission were the major PAH sources in PM<sub>2.5</sub>. The ratio of LMW + MMW (LMW: low molecular weight; MMW: middle molecular weight) PAHs to  $\sum$ PAHs at JN was significantly lower ( $p < 0.001$ ) than that at QXT, indicating coal/biomass burning made more significant contribution to suburban area than that to urban area. Conversely, vehicle emission worked more effectively to urban area. The total benzo[a]pyrene (BaP) equivalent concentration (BaP<sub>eq</sub>) of PAHs (gas + particle phases) was 9.66 times higher than the standard value (1.00 ng m<sup>-3</sup>) and mainly originated from PAHs in particles (93.1%) with the highest contributor of Benzo(a)pyrene (BaP, 60.8%) at the urban site of Jinan in winter. The total incremental lifetime cancer risk (ILCR) assessment suggested that all age groups may have potential health risk at JN in winter except for infant. The Concentration Weighted Trajectory (CWT) model indicated that local emission and short-distance transport were the main sources of PAHs during spring and winter, and long-range transport played a key role on PAH concentrations in summer and autumn.

**Keywords:** Seasonal variation , Diurnal variation , PCA , Health risk assessment , CWT

---

## Effects of Surface Properties of Vertical Textiles Indoors on Particle Deposition: A Small-scale Chamber Study

Yan Wang<sup>1</sup>, Angui Li<sup>1</sup>, Xiaowei Fan<sup>2</sup>, Shiyan Lu<sup>3</sup>, Liangyue Shang<sup>3</sup>

**Source:** Aerosol and Atmospheric Chemistry, Volume: 19 | Issue: 4 | Pages: 885-895

DOI: 10.4209/aaqr.2018.08.0321

The present study aims to further understand the effect of surface properties of vertical textiles indoors on the particle deposition. A 512 L cubic aluminum experimental chamber was built to obtain the deposition loss rate coefficients for 0.37, 0.54, 0.75, 0.9, 1.3, and 1.6

$\mu\text{m}$  particles under three different airflow conditions. Eight curtain fabrics—four window voile fabrics and four curtain cloths—were selected as the deposition surfaces in investigating the effect of fabric porosity on particle deposition. The total fabric porosity can be roughly divided into inter-yarn porosity and inter-fiber porosity. The experimental results reveal that both the near-surface airflow velocity and the particle size affect the deposition loss rate coefficient. The trend of the deposition loss rate coefficient with increasing inter-yarn porosity differs from that with increasing inter-fiber porosity.

**Keywords:** Deposition loss rate coefficient , Curtain, Fine particle, Fabric, Porosity.

---

## **Trends of Fog and Visibility in Taiwan: Climate Change or Air Quality Improvement?**

**Maylin Maurer 1, Otto Klemm 1, Hanna L. Lokys1, Neng-Huei Lin2**

**Source:** Aerosol and Atmospheric Chemistry, Volume: 19 | Issue: 4 | Pages: 896-910  
DOI: 10.4209/aaqr.2018.04.0152

This study provides insight into how the visibility in Taiwan has varied over time and what the main drivers of these visibility changes are. From 1985 to 2016, urban inland sites showed increases in visibility and decreases in the frequency of hazy and/or foggy days, whereas urbanized and rural coastal regions either showed no clear trend or even an overall decrease in visibility. Over the most recent 5 to 10 years, a consistent increase in the visibility and decrease in the haze frequency has been found for most of the stations, except for the rural to suburban regions.

In general, visibility is driven by the relative humidity (rH) and the mass concentration of aerosol particles (PM). On the one hand, the combination of climate change and urbanization, resulting in a rise in temperature (on average,  $+0.035^{\circ}\text{C y}^{-1}$ ) and an associated overall decrease in rH (on average,  $-0.125\% \text{ y}^{-1}$ ), has had a positive influence on long-term visibility in the cities of Taiwan. On the other hand, improvements in air quality supported the increase in visibility during the late 2000s and early 2010s. Our results show an almost exponential relationship between visibility and PM10. At lower PM10 levels, the visibility is more sensitive to changes in the PM10. Thus, the influence of the long-term PM10 on visibility becomes weaker at high PM10 levels. Consequently, over the long term, the PM10 more strongly influenced the visibility trends at the northern urban stations, which had lower PM10 concentrations to begin with. At the southern urban stations, the PM10 concentrations were generally higher and hence were less of a factor in variations in visibility. Therefore, the visibility trends at these sites were more related to changes in rH until about 2011, at which time these regions reached a lower level of pollution.

**Keywords:** Visibility trends , Fog , Haze, PM10, Relative humidity.

---

## Characteristics of Air Pollutants and Greenhouse Gases at a Regional Background Station in Southwestern China

Linjun Cheng<sup>1</sup>, Dongsheng Ji<sup>2,3</sup>, Jun He<sup>4</sup>, Liang Li<sup>1</sup>, Li Du<sup>1</sup>, Yang Cui<sup>2,5</sup>, Hongliang Zhang<sup>6</sup>, Luxi Zhou<sup>7</sup>, Zhiqing Li<sup>8</sup>, Yingxin Zhou<sup>9</sup>, Shengyuan Miao<sup>9</sup>, Zhengyu Gong<sup>1</sup>, Yuesi Wang<sup>2,3</sup>

**Source:** Aerosol and Atmospheric Chemistry, Volume: 19 | Issue: 5 | Pages: 1007-1023  
DOI: 10.4209/aaqr.2018.11.0397

The characteristics of air pollutants and greenhouse gases at regional background sites are critical to assessing the impact of anthropogenic emissions on the atmospheric environment, ecosystems and climate change. However, observational studies are still scarce at such background sites. In this study, continuous hourly observations of air pollutants (O<sub>3</sub>, CO, SO<sub>2</sub>, NO<sub>x</sub>, PM<sub>2.5</sub> and PM<sub>10</sub>) and greenhouse gases (CO<sub>2</sub>, CH<sub>4</sub> and N<sub>2</sub>O) were performed for one year (from January 1 to December 31, 2017) at the Gongga Mountain background station (GGs; 101°97'E, 29°55'N; elevation: 3541 m) in southwestern China. The concentrations and variations of these air pollutants and greenhouse gases were determined, and the effect of transboundary atmospheric transport on the air pollution at the study site was investigated. The results showed that the average annual concentrations (mixing ratios) of the O<sub>3</sub>, CO, SO<sub>2</sub>, NO<sub>2</sub>, CO<sub>2</sub>, CH<sub>4</sub>, N<sub>2</sub>O, PM<sub>2.5</sub> and PM<sub>10</sub> were 74.7 ± 22.0 μg m<sup>-3</sup>, 0.3 ± 0.2 mg m<sup>-3</sup>, 0.5 ± 0.6 μg m<sup>-3</sup>, 1.7 ± 1.3 μg m<sup>-3</sup>, 406.1 ± 9.5 ppm, 1.941 ± 0.071 ppm, 324.5 ± 14.8 ppb, 6.5 ± 6.2 μg m<sup>-3</sup> and 10.6 ± 11.2 μg m<sup>-3</sup>, respectively. The concentrations (mixing ratios) of the abovementioned substances at the GGs are comparable to those at other background sites in China and around the world. The slight differences among concentrations at different sites may be mainly attributable to the impacts of anthropogenic emissions near the background sites and meteorological conditions. High values of O<sub>3</sub> were observed in spring and summer, while SO<sub>2</sub> and PM<sub>2.5</sub> showed higher concentrations in summer than in autumn. Relatively high CO, NO<sub>2</sub> and PM<sub>10</sub> values were mostly observed in spring and winter. Relatively low CO<sub>2</sub> concentrations were observed in summer due to the vigorous summertime photosynthesis of vegetation. The lowest concentrations for CH<sub>4</sub> were recorded in summer, whereas the levels in the other three seasons were similar to each other; by contrast, the highest N<sub>2</sub>O concentrations were observed in summer due to enhanced microbial activity resulting from high ambient summer temperatures. A diurnal variation in O<sub>3</sub> was observed, with early morning minima and afternoon maxima. CO and NO<sub>2</sub> displayed higher concentrations in the daytime than in the nighttime. A slight increase in both PM<sub>2.5</sub> and PM<sub>10</sub> concentrations was also recorded in the daytime. These patterns were closely related to scattered anthropogenic emissions and regional atmospheric transport. Nevertheless, CO<sub>2</sub> exhibited lower concentrations in the daytime than in the nighttime, although CH<sub>4</sub> showed no obvious diurnal variation. The N<sub>2</sub>O concentration peaked between 10:00 and 12:00 (local time), which can be ascribed to the enhancement of microbial activity due to the increased soil temperature. The results based on the relationship between the wind and the concentrations of air pollutants and greenhouse gases were almost consistent with those based on the potential contribution source function. It appears that O<sub>3</sub> and its precursors in parts of Inner Mongolia and Gansu, Ningxia, Sichuan, Chongqing and Hubei

Provinces as well as adjacent areas of Hunan, Guizhou and Guangxi Provinces contributed to the increase in O<sub>3</sub> at the study site. The potential source areas for CO and SO<sub>2</sub> were similar and mainly distributed in India and Pakistan and areas of Inner Mongolia and Gansu and Guizhou Provinces in China. Potential source areas for NO<sub>2</sub>, PM<sub>2.5</sub> and PM<sub>10</sub> were found in neighboring countries of South Asia in addition to domestic regions, including Inner Mongolia, Gansu Province and the Cheng-Yu economic region. Furthermore, parts of Yunnan Province (China) as well as India and Pakistan were potential source areas for CO<sub>2</sub>, CH<sub>4</sub> and N<sub>2</sub>O.

**Keywords:** Air pollutants , Greenhouse gases , Background station , Southwestern China

---

## **Applicability of Optical and Diffusion Charging-Based Particulate Matter Sensors to Urban Air Quality Measurements**

**Joel Kuula 1, Heino Kuuluvainen<sup>2</sup>, Topi Rönkkö<sup>2</sup>, Jarkko V. Niemi<sup>3</sup>, Erkka Saukko<sup>4</sup>, Harri Portin<sup>3</sup>, Minna Aurela<sup>1</sup>, Sanna Saarikoski<sup>1</sup>, Antti Rostedt<sup>2</sup>, Risto Hillamo<sup>1</sup>, Hilikka Timonen<sup>1</sup>**

**Source:** Aerosol and Atmospheric Chemistry, Volume: 19 | Issue: 5 | Pages: 1024-1039  
DOI: 10.4209/aaqr.2018.04.0143

High spatial resolution particulate matter measurements are necessary to accurately characterize urban air quality issues. This study investigates how sensors can be used in an urban area to complement existing air quality measurements. A measurement campaign was conducted during winter in Helsinki, Finland, where the performance of a custom-built optical instrument—the Prototype Aerosol Sensor (PAS; uses Shinyei PPD60PV and PPD42NS sensor modules)—and three commercial diffusion charging-based sensors (Pegasor AQ Urban, DiSCmini and Partector) was evaluated against reference instruments. The results showed that the PAS was able to measure the coarse (PM<sub>2.5-10</sub>; range: 0–400 µg m<sup>-3</sup>) and fine (PM<sub>2.5</sub>; range: 0–50 µg m<sup>-3</sup>) fractions with reasonably high correlations (R<sup>2</sup> = 0.87 and 0.77) when compared to a gravimetric monitor. Likewise, the lung deposited surface area (LDSA) concentrations delivered by the three diffusion charging sensors indicated good performance (R<sup>2</sup>: 0.92–0.97) when compared to LDSA concentrations calculated from the size distribution data of the differential mobility particle sizer. A clear correlation (R<sup>2</sup> = 0.77) between the black carbon and Pegasor-measured LDSA concentrations, as well as similar diurnal cycles, was observed, suggesting a common source. The optical sensors were useful for measuring the mass concentrations of coarse local particles. By contrast, the diffusion charging sensors were applicable in urban environments, where ultrafine particles from traffic or other local combustion sources affect air quality.

**Keywords:** Urban air quality, Low-cost sensor, Optical, Diffusion charging, PM<sub>2.5</sub>.

---

# **Aerosol Impacts on Meteorological Elements and Surface Energy Budget over an Urban Cluster Region in the Yangtze River Delta**

**Xiaolu Ling 1,2, Xiaomen Han1**

**Source:** Aerosol and Atmospheric Chemistry, Volume: 19 | Issue: 5 | Pages: 1040-1055  
DOI: 10.4209/aaqr.2017.12.0602

The Yangtze River Delta (YRD) is a typical example of regions that are dramatically influenced by both human activity and a monsoonal climate. Data on the near-surface micro-meteorology, radiation, and energy fluxes were collected and analyzed at the Lishui field observation site in the suburb of Nanjing to investigate aerosol impacts on the radiation budget and land surface-atmosphere heat, water, and mass exchanges. Cluster analysis, composite analysis, and case study were applied to selected typical polluted/non-polluted days. The results indicate that the mean daily surface pressure is 6.6 hPa lower on polluted than non-polluted days in Nanjing. Northeasterly winds often prevail on the polluted days, with wind speeds being 60% lower than on non-polluted days. Aerosols directly reduce the net radiation flux at the surface, with a maximum reduction of 180 W m<sup>-2</sup>. During the early stage of air pollution events, the surface pressure is lower, and wind speeds rapidly decrease, whereas during the peak of pollution, low surface pressure and wind speeds linger, effectively preventing the dispersion of air pollutants. Meanwhile, the temperature often decreases, and the relative humidity subsequently increases. As the wind speed and surface pressure increase, the AQI gradually decreases, and the air pollution event ends.

**Keywords:** Urban cluster region , Meteorological elements , Surface energy budget.

---

## **Fine Particulate Matter-induced Toxic Effects in an Animal Model of *Caenorhabditis elegans***

**Meng-Ching Chung<sup>1</sup>, Ming-Hsien Tsai<sup>2</sup>, Danielle E. Que<sup>3</sup>, Sayre J. Bongo<sup>4</sup>, Wen-Li Hsu<sup>1,5</sup>, Lemmuel L. Tayo<sup>4</sup>, Yi-Hsien Lin<sup>6</sup>, Sheng-Lun Lin<sup>7,8,9</sup>, Yan-You Gou<sup>1</sup>, Yi-Chyun Hsu<sup>10</sup>, Wen-Che Hou<sup>3</sup>, Kuo-Lin Huang<sup>1</sup>, How-Ran Chao <sup>1,11</sup>**

**Source:** Aerosol and Atmospheric Chemistry, Volume: 19 | Issue: 5 | Pages: 1068-1078  
DOI: 10.4209/aaqr.2019.03.0127

Research has been focused on the health hazards of ambient PM<sub>2.5</sub> related to humans. Many PM<sub>2.5</sub> toxicity assessments using in vitro studies have focused on PM<sub>2.5</sub>-bounded hazardous pollutants. However, PM<sub>2.5</sub> toxicity assessment by in vivo studies allow for better observation of the overall effects of PM<sub>2.5</sub> exposure on entire organisms, making in vivo PM<sub>2.5</sub> toxicity assessment relevant. The toxic effects of outdoor PM<sub>2.5</sub>, collected from National Pingtung University of Science and Technology (NPUST) and Linluo Junior High School (LJHS), Pingtung, Taiwan, on nematode *Caenorhabditis elegans* (*C. elegans*) were



investigated. PM<sub>2.5</sub> from NPUST and LJHS were found to be 4.5 and 2.5  $\mu\text{g Nm}^{-3}$ , respectively, which did not meet the standard. This levels of PM<sub>2.5</sub> in Taiwan. For acute toxicity, no significant PM<sub>2.5</sub> lethality on *C. elegans* was observed between NPUST and LJHS. PM<sub>2.5</sub> from NPUST exhibited greater toxicity to lifespan (ageing), locomotion (head thrash), and reproduction (brood size) in the *C. elegans* animal models than that from LJHS; therefore, adverse effects could be correlated with PM<sub>2.5</sub> concentrations. Prolonged exposure to PM<sub>2.5</sub> led to more severe toxicity in nematodes as compared to acute exposure. In conclusion, this study suggests that the long-term adverse effects of ambient PM<sub>2.5</sub> on environmental organisms should be carefully considered even when PM<sub>2.5</sub> is at low levels. *C. elegans* is a sensitive animal model for the evaluation of PM<sub>2.5</sub> ecotoxicity.

**Keywords:** *C. elegans* , PM<sub>2.5</sub>, Lifespan , Locomotion , Reproduction Ageing.

---

## **Bioaerosol Concentrations and Size Distributions during the Autumn and Winter Seasons in an Industrial City of Central China**

**Ting Liu<sup>1</sup>, L.-W. Antony Chen <sup>2</sup>, Mi Zhang<sup>3</sup>, John G. Watson<sup>3</sup>, Judith C. Chow<sup>3</sup>, Junji Cao<sup>4</sup>, Hongyu Chen<sup>1</sup>, Wei Wang<sup>1</sup>, Jiaquan Zhang<sup>1</sup>, Changlin Zhan<sup>1</sup>, Hongxia Liu<sup>1</sup>, Jingru Zheng<sup>1</sup>, Naiwen Chen<sup>5</sup>, Ruizhen Yao<sup>1</sup>, Wensheng Xiao<sup>1</sup>**

**Source:** Aerosol and Atmospheric Chemistry, Volume: 19 | Issue: 5 | Pages: 1095-1104  
DOI: 10.4209/aaqr.2018.11.0422

The ambient bioaerosols were measured in PM<sub>2.5</sub> and PM<sub>10</sub> samples taken in Huangshi City, Hubei Province, China, during autumn and winter from November 2017 to February 2018. Both the bioaerosol number concentration and size distribution (0.37–16  $\mu\text{m}$ ) were obtained by direct fluorescent staining coupled with microscopic imaging. The bioaerosol number concentrations ranged from 0.05 to 3.4 #  $\text{cm}^{-3}$  for PM<sub>2.5</sub> and from 0.17 to 5.7 #  $\text{cm}^{-3}$  for PM<sub>10</sub>, with averages of 0.90 #  $\text{cm}^{-3}$  and 1.9 #  $\text{cm}^{-3}$ , respectively. In terms of particle number, the bioaerosols were dominated by fine particles (0.37–2.5  $\mu\text{m}$  in diameter), with a larger proportion of submicron than supermicron particles. Assuming a unit density of 1  $\text{g cm}^{-3}$  and a spherical shape for the particles, the mass abundances of the bioaerosols were estimated to be  $2.4 \pm 1.9\%$  and  $4.8 \pm 3.2\%$  of the PM<sub>2.5</sub> and PM<sub>10</sub>, respectively, as measured by a nearby compliance monitor. Higher bioaerosol concentrations were observed in winter than autumn and on polluted than non-polluted days. During heavily polluted conditions, bioaerosols in the PM<sub>2.5</sub> and PM<sub>10</sub> were enriched by 6 and 3.7 times, respectively, compared to non-polluted days and contributed up to 15% of the PM<sub>10</sub> mass. Rainfall and snowfall appeared to lower the bioaerosol levels. As enhanced emission controls on combustion and dust sources decrease PM levels in China, the bioaerosol fraction in measured PM concentrations will likely increase.

**Keywords:** Primary biological aerosol particles (PBAP), PM<sub>2.5</sub>, PM<sub>10</sub>, Size distribution , Air quality ,Fluorescence microscopy.

---

## **The Effect of Sampling Inlet Direction and Distance on Particle Source Measurements for Dispersion Modelling**

**Alexander Christian Østerskov Jensen 1, Mikko Poikkimäki<sup>2</sup>, Anders Brostrøm<sup>3</sup>, Miikka Dal Maso<sup>2</sup>, Ole John Nielsen<sup>4</sup>, Thomas Rosenørn<sup>5</sup>, Andrew Butcher<sup>5</sup>, Ismo Kalevi Koponen<sup>6</sup>, Antti Joonas Koivisto<sup>1</sup>**

**Source:** Aerosol and Atmospheric Chemistry, Volume: 19 | Issue: 5 | Pages: 1114-1125  
DOI: 10.4209/aaqr.2018.08.0322

The source rate is the single most critical input parameter in dispersion models. Determining accurate source rates from workplace processes can be challenging due to interference with work operation and poorly known dilution between the outlet of the particle generator and the measurement point. In this work, we measured the aerosol source rate in a chamber with a steady release of TiO<sub>2</sub> particles generated by an aerosol brush generator. The number concentrations measured directly from the particle generator and in the source position near the source spanned three orders of magnitude depending on the relative location and orientation to the source. Moreover, a dispersion factor was calculated based on a single mode fit of the obtained source rates. The dispersion factor takes into account the dispersion and dilution occurring between the measurement point and the source outlet for subsequent modelling. The particle emission rates were implemented in a previously published multi-box aerosol dispersion model using a one-box layout. The modelled concentrations were compared with concentrations measured in three locations in the chamber. We found that using a dispersion factor of one, meaning that at-source dilution or dispersion was not accounted for, the modelled concentrations were 1 to 3 orders of magnitude lower than measured concentrations for all source rates except the source rates measured directly from the aerosol generator. When applying the calculated dispersion factor, thereby correcting the source rate for initial dilution and dispersion, the concentrations were within 0.5 to 2 times the measured concentrations suggesting the use of such a factor to correctly estimate the source rate, and hence the occupational exposure.

**Keywords:** Source measurements, Dispersion modeling, Chamber studies, Aerosol dispersion, Occupational health.

---

## **Responses of Secondary Inorganic PM<sub>2.5</sub> to Precursor Gases in an Ammonia Abundant Area In North Carolina**

**Bin Cheng, Lingjuan Wang-Li**

**Source:** Air Pollution Modeling, Volume: 19 | Issue: 5 | Pages: 1126-1138  
DOI: 10.4209/aaqr.2018.10.0384

Secondary inorganic fine particulate matter (iPM<sub>2.5</sub>) constitutes a significant amount of the atmospheric PM<sub>2.5</sub>. The formation of secondary iPM<sub>2.5</sub> is characterized by thermodynamic equilibrium gas-particle partitioning of gaseous ammonia (NH<sub>3</sub>) and aerosol ammonium (NH<sub>4</sub><sup>+</sup>). To develop effective strategies for controlling atmospheric PM<sub>2.5</sub>, it is essential to understand the responses of secondary iPM<sub>2.5</sub> to different precursor gases. In southeastern North Carolina, the amount of NH<sub>3</sub> is in excess to fully neutralize acidic gases (i.e., NH<sub>3</sub>-rich conditions). NH<sub>3</sub>-rich conditions are mainly attributed to the significant NH<sub>3</sub> emissions in the region, especially from the large amounts of animal feeding operation (AFO). To gain a better understanding of the impact of NH<sub>3</sub> on the formation of secondary iPM<sub>2.5</sub> in this area, the responses of iPM<sub>2.5</sub> to precursor gases under different ambient conditions were investigated based upon three-year monitoring data of the chemical components in iPM<sub>2.5</sub>, gaseous pollutants, and meteorological conditions. The gas ratio (GR) was used to assess the degree of neutralization via NH<sub>3</sub>, and ISORROPIA II model simulation was used to examine the responses of iPM<sub>2.5</sub> to changes in the total NH<sub>3</sub>, the total sulfuric acid (H<sub>2</sub>SO<sub>4</sub>), and the total nitric acid (HNO<sub>3</sub>). It was discovered that under different ambient temperature and humidity conditions, the responses of iPM<sub>2.5</sub> to precursor gases vary. In general, iPM<sub>2.5</sub> responds nonlinearly to the total NH<sub>3</sub> but linearly to the total H<sub>2</sub>SO<sub>4</sub> and the total HNO<sub>3</sub>. In NH<sub>3</sub>-rich regions, iPM<sub>2.5</sub> is not sensitive to changes in the total NH<sub>3</sub>, but it is very sensitive to changes in the total H<sub>2</sub>SO<sub>4</sub> and/or the total HNO<sub>3</sub>. Reducing the total H<sub>2</sub>SO<sub>4</sub>, as opposed to the total HNO<sub>3</sub> or the total NH<sub>3</sub>, leads to a significant reduction in iPM<sub>2.5</sub> and is thus a more effective strategy for decreasing the concentration of iPM<sub>2.5</sub>. This research provides insight into controlling and regulating PM<sub>2.5</sub> in NH<sub>3</sub>-rich regions.

**Keywords:** Ammonia , Inorganic PM2.5 , Thermodynamic equilibrium modeling , ISORROPIA II , Animal feeding operations

---

## Synoptic Weather Patterns and Associated Air Pollution in Taiwan

Chia-Hua Hsu, Fang-Yi Cheng

**Source:** Aerosol and Atmospheric Chemistry, Volume: 19 | Issue: 5 | Pages: 1139-1151  
DOI: 10.4209/aaqr.2018.09.0348

In this study, cluster analysis is applied to the daily averaged wind fields and sea-level pressure observed at surface weather stations in Taiwan from January 2013 to March 2018 to classify the synoptic weather patterns and study the characteristics of corresponding air pollutants, including fine particulate matter (PM<sub>2.5</sub>), coarse particulate matter (PM<sub>10</sub>), and ozone (O<sub>3</sub>). The classification identified six weather types: Clusters 1, 2, and 3 (C1–C3), which are typical winter weather types and associated with high air pollutant concentrations—C3, in particular, influenced by weak synoptic weather, is associated with the lowest wind speeds and the highest PM<sub>2.5</sub> and PM<sub>10</sub> concentrations and represents the most prevalent weather type that is prone to the occurrence of PM<sub>2.5</sub> events; C4, which occurs mostly during seasonal transition months and is associated with the highest O<sub>3</sub>

concentrations; and C5 and C6, which are summer weather types with low air pollutant concentrations.

Further analysis of the local wind flow using the 0.3° ERA5 reanalysis dataset and surface-observed wind data indicates that in western Taiwan, the land-sea breeze is embedded within the synoptic weather type of C3, which is favorable to air pollutant accumulation. However, when the prevailing northeasterly wind is obstructed by the Central Mountain Range, southwestern Taiwan, being situated on the leeward side of the mountains, often exhibits the worst air pollution due to stagnant wind conditions.

**Keywords:** Synoptic weather classification , Cluster analysis , PM2.5 ,Ozone ,Stagnant wind.

---

## **Effects of Wind Direction on the Airflow and Pollutant Dispersion inside a Long Street Canyon**

**Yuan-Dong Huang<sup>1</sup>, Ren-Wei Hou<sup>1</sup>, Ze-Yu Liu<sup>1</sup>, Ye Song<sup>1</sup>, Peng-Yi Cui<sup>1</sup>, Chang-Nyung Kim<sup>2</sup>**

**Source:** Aerosol and Atmospheric Chemistry, Volume: 19 | Issue: 5 | Pages: 1152-1171  
DOI: 10.4209/aaqr.2018.09.0344

This study investigates the effects of wind direction on the airflow and pollutant dispersion inside a long street canyon using computational fluid dynamics (CFD). A 3D CFD model for predicting the flow and dispersion in a canyon is first developed using the FLUENT code and then validated against wind tunnel experiments. Then, the airflow and traffic pollutant dispersion in an isolated canyon with a street-length-to-building-height ratio of 10 are numerically simulated for seven wind directions ( $\alpha = 0^\circ, 15^\circ, 30^\circ, 45^\circ, 60^\circ, 75^\circ$  and  $90^\circ$ , where  $\alpha$  is the angle between the approaching flow and street axis). The results demonstrate that the mean ( $\bar{u}$ ) and turbulent ( $ACH'$ ) air exchange rates (ACHs) for the canyon are close when  $\alpha = 0^\circ, 15^\circ, 30^\circ, 45^\circ$  and  $60^\circ$ , whereas the magnitude of  $ACH'$  is significantly greater than that of  $\bar{u}$  when  $\alpha = 75^\circ$  and  $90^\circ$ . Additionally, the ACH reaches its maximum and minimum values when  $\alpha = 30^\circ$  and  $90^\circ$ , respectively. The computed velocity and concentration fields clearly reveal the variation in the in-canyon flow pattern and pollutant distributions on the canyon walls and footpaths due to the wind direction. Evaluating the maximum, minimum and average concentrations on the canyon walls and footpaths for each of the seven wind directions, we determine: On the leeward-oriented wall, the wall-averaged concentration increases greatly with  $\alpha$ , and the values of the wall-maximum are highest when  $\alpha = 75^\circ$  and lowest when  $\alpha = 0^\circ$ . By contrast, on the windward-oriented wall, both the wall-averaged and wall-maximum concentrations are highest when  $\alpha = 0^\circ$ . Finally, at the human respiration height, the highest concentration on the footpath next to the leeward-oriented wall occurs when  $\alpha = 75^\circ$ , whereas the highest concentration on the footpath close to the windward-oriented wall is observed when  $\alpha = 0^\circ$ .

**Keywords:** Wind direction, Airflow, Pollutant dispersion, Street canyon, CFD.

---

## **Effect of Large-scale Biomass Burning on Aerosol Optical Properties at the GAW Regional Station Pha Din, Vietnam**

**Nicolas Bukowiecki<sup>1</sup>, Martin Steinbacher<sup>2</sup>, Stephan Henne<sup>2</sup>, Nhat Anh Nguyen<sup>3</sup>, Xuan Anh Nguyen<sup>4</sup>, Anh Le Hoang<sup>5</sup>, Dac Loc Nguyen<sup>4</sup>, Hoang Long Duong<sup>3</sup>, Guenter Engling<sup>6</sup>, Günther Wehrle<sup>1</sup>, Martin Gysel-Beer<sup>1</sup>, Urs Baltensperger**

**Source:** Optical/Radiative Properties and Remote Sensing Volume: 19 | Issue: 5 | Pages: 1172-1187 DOI: 10.4209/aaqr.2018.11.0406

In 2014, Pha Din (1466 m a.s.l.) was established as a Global Atmosphere Watch (GAW) regional station for aerosol and trace gas measurements in northwestern Vietnam. This study presents a five-year climatology of aerosol optical properties derived from nephelometer and aethalometer measurements and a comparison with ground-based remote sensing measurements at the nearby AERONET station Son La. The annual variations of the aerosol measurements at Pha Din are clearly dominated by annually recurring periods with high biomass burning activity in northern Southeast Asia (February–May). During these periods, the majority of air masses arriving at Pha Din originate from the southwest (northern Thailand, Laos and Myanmar). Both the meteorological conditions and the aerosol optical properties are very similar during the individual high biomass burning periods (increased temperature: > 20°C; moderate ambient relative humidity: 60–70%; decreased single scattering albedo: 0.8–0.9; increased absorption Ångström exponent: 1.6–2.0; and scattering Ångström exponent significantly larger than 1). Prior to the biomass burning season (October–January), the meteorological conditions at Pha Din are influenced by the SE Asian monsoon, leading to a frequent transport of air masses from SW China with moderate aerosol loadings. The lowest pollution levels are observed from June to September, which represents the wet season.

**Keywords:** Aerosol optical properties, Biomass burning, Black carbon, Long-term measurements, Global Atmosphere Watch

---

## **Impact of Biomass Burning in South and Southeast Asia on Background Aerosol in Southwest China**

**Yuanxin Liang<sup>1</sup>, Huizheng Che<sup>1</sup>, Ke Gui<sup>1</sup>, Yu Zheng<sup>1</sup>, Xianyi Yang<sup>1,2</sup>, Xiaopan Li<sup>1,2</sup>, Chao Liu<sup>1,3</sup>, Zhizhong Sheng<sup>1,2</sup>, Tianze Sun<sup>1</sup>, Xiaoye Zhang<sup>1</sup>**

**Source:** Optical/Radiative Properties and Remote Sensing Volume: 19 | Issue: 5 | Pages: 1188-1204 DOI: 10.4209/aaqr.2018.08.0324

Biomass burning (BB) in Southeast Asia is particularly pronounced during the dry season. However, the complex topography and long-range transport inherent to Southeast Asia have limited local research on pollution resulting from BB. In this study, the monthly variation in aerosol optical properties at six sites in Southeast Asia (Chiang Mai, Mukdahan, Bac-Lieu, Penang, Singapore, and Bandung) and the fire-point distribution have been analyzed in detail. The Hybrid Single Particle Lagrangian Integrated Trajectory (HYSPLIT) model was used to simulate the 72-hour back-trajectory from the Shangri-La atmospheric background station in Yunnan Province, China. Our results showed that BB was more common on the Indochinese Peninsula from March to May, whereas it was more common on the Malay Archipelago from August to October due to the latitudinal difference and crop harvest season. Significant BB activity on the Indochinese Peninsula in March resulted in a high surge in extinction ( $AOD_{t440nm} = 1.32 \pm 0.69$ ,  $AOD_{f440nm} = 1.24 \pm 0.59$ ) by particles with a smaller diameter ( $AE = 1.68 \pm 0.13$ ) in Chiang Mai. Mapping the long-range transport of BB aerosols reveals that Shangri-La's pollution was primarily affected by emissions from northern-central India (accounting for 45.2%), and Bangladesh and northern Myanmar (accounting for 38.7%), which indicates that the aerosol pollution on the Yunnan-Guizhou Plateau in springtime could have originated on the southern periphery of the Tibetan Plateau. The results also indicate that BB emission in Southeast Asia had a limited impact on pollution in Southwest China but a relatively large effect on local areas. This study is the first to analyze the trend of aerosols produced from BB in Southeast Asia via ground-based observation, which deepens our understanding of the potential effects of BB aerosols transported long-range from outside Southwest China.

**Keywords:** Aerosol optical properties, Biomass burning, Southeast Asia, Yunnan-Guizhou plateau

---

## **Climatology and Chemistry of Surface Ozone and Aerosol under Alpine Conditions in East Siberia**

**Vladimir L. Potemkin, Lydmila P. Golobokova, Tamara V. Khodzher**

**Source:** Special Session: Atmospheric Chemistry and Physics at Mountain Sites 2017

Volume: 19 | Issue: 6 | Pages: 1214-1225 DOI: 10.4209/aaqr.2018.05.0172

We present the results of synchronous observations of the ozone and gaseous impurity concentrations, chemical composition of the aerosol and meteorological parameters with a high temporal resolution (of minutes) at the background site Mondy, which is located in the highland area of East Siberia. We also analyzed the seasonal dynamics exhibited by the ozone, gaseous impurities of sulfur and nitrogen, and ionic composition of the aerosol over the long term (1998–2016). Ozone variability in the boundary layer depended on complicated relief and dynamic processes occurring in the atmosphere. The concentration of ions in the aerosol decreased by 2 times for the period of 2010–2015 compared to the beginning of the new millennium. Furthermore, sulfate, nitrate, chloride, potassium and sodium became the dominant ions in the aerosol. Due to the remote location of the site, the

absence of anthropogenic pollution sources and the large series of data with different parameters obtained via on-line monitoring, this site may be regarded as a representative global background site for the vast region of Central Asia.

**Keywords:** East Sayan , Climatic parameters , Ozone , Aerosol , Troposphere

---

## **Evaluation of WRF-Chem Model Forecasts of a Prolonged Saharan Dust Episode over the Eastern Alps**

**Kathrin Baumann-Stanzer 1, Marion Greilinger1, Anne Kasper-Giebl2, Claudia Flandorfer1, Alexander Hieden1, Christoph Lotteraner1, Martin Ortner3, Johannes Vergeiner4, Gerhard Schauer5, Martin Piringer1**

**Source:** Aerosol and Atmospheric Chemistry, Volume: 19 | Issue: 6 | Pages: 1226-1240  
DOI: 10.4209/aaqr.2018.03.0116

Transported Saharan dust creates a substantial natural background to particulate matter concentrations in Central Europe. The contributions by Saharan dust are especially detectable at Alpine mountain sites, where many other sources have little impact. The ability of a chemical weather forecasting model to simulate dust transport is of vital interest, as serious health effects due to this phenomenon, similar in scale to those resulting from nuclear or industrial accidents, wildfires, pollen, etc., may require countermeasures. Thus, we investigate whether the WRF-Chem model set-up, which is run operationally for air quality forecasts in Austria, can accurately predict the transport of the Saharan dust cloud towards Central Europe in April 2016. WRF-Chem simulations with and without desert dust emissions reveal that whenever PM concentrations were high during the three periods of this event, 60–70% of the dust arriving at the Eastern Alps originated in the desert. The measurements and model results deliver a detailed picture of the course of this extraordinary dust event, with successive peaks over the Eastern Alpine region. Using this long-lasting Saharan dust event as an example, a structured step-wise approach is proposed to investigate peak dust episodes based on data analysis of representative background sites, source area analysis by means of Lagrangian dispersion modelling, and coupled meteorological and chemical modelling.

**Keywords:** Saharan dust, Long-range transport, WRF-Chem model, FLEXPART model ,Source-receptor sensitivity , Ceilometer.

---

# Aerosol Optical Properties over Gurushikhar, Mt. Abu: A High Altitude Mountain Site in India

Thazhathakal A. Rajesh<sup>1,2</sup>, Srikanthan Ramachandran<sup>1</sup>

**Source:** Special Session: Atmospheric Chemistry and Physics at Mountain Sites 2017  
Volume: 19 | Issue: 6 | Pages: 1259-1271 DOI: 10.4209/aaqr.2018.05.0177

Continuous and simultaneous measurements of aerosol optical properties (the scattering and absorption coefficients) were conducted, for the first time, at a mountain site, Gurushikhar, Mt. Abu, in the Aravalli Range in western India from January 2015 to December 2016. The aerosol scattering and absorption coefficients were higher in the afternoon than during the forenoon and night because of atmospheric boundary layer dynamics that, when accompanied by strong thermal convection, promote an upward movement of pollutants to the observational site from the surrounding foothills. The aerosol scattering and absorption coefficients exhibited a strong seasonal variability. The average scattering coefficients during the winter, premonsoon, monsoon and postmonsoon seasons were  $78.5 \pm 22.9$ ,  $61.8 \pm 12.2$ ,  $49.9 \pm 25.1$  and  $121.8 \pm 47.4$   $\text{Mm}^{-1}$ , respectively, and the corresponding absorption coefficients were  $14.9 \pm 3.1$ ,  $9.1 \pm 2.9$ ,  $5.1 \pm 3.2$  and  $20.2 \pm 10.2$   $\text{Mm}^{-1}$ . The single scattering albedo also exhibited a significant seasonal variation, with the maximum occurring during the monsoon season (0.91) and the minimum during winter (0.83). The mean annual  $\beta_{\text{sca}}$ ,  $\beta_{\text{abs}}$  and SSA at 550 nm were  $74 \pm 34$   $\text{Mm}^{-1}$ ,  $12 \pm 7$   $\text{Mm}^{-1}$  and  $0.87 \pm 0.04$ . These results indicate that Gurushikhar, a remote high altitude site, is influenced by local and long-range transported aerosols through convection and advection processes. However, the aerosol properties at this pristine location are governed by transported emissions rather than local anthropogenic sources and also display low inter-annual variability. Thus, Gurushikhar can be considered a background site for the nearby source regions in western India.

**Keywords:** Aerosol scattering coefficient , Aerosol absorption coefficient , Single scattering albedo , Mountain site , Inter-annual variability

---

## Variability of Aerosol Optical Properties Observed at a Polluted Marine (Gosan, Korea) and a High-altitude Mountain (Lulin, Taiwan) Site in the Asian Continental Outflow

Soojin Park<sup>1</sup>, Sang-Woo Kim<sup>1</sup>, Neng-Huei Lin<sup>2</sup>, Shantanu Kumar Pani<sup>2</sup>, Patrick J. Sheridan<sup>3</sup>, Elisabeth Andrews<sup>3</sup>

**Source:** Aerosol and Atmospheric Chemistry, Volume: 19 | Issue: 6 | Pages: 1272-1283  
DOI: 10.4209/aaqr.2018.11.0416

We investigated the variability of in-situ and columnar aerosol optical properties (AOPs) at two regional background sites in the Asian continental outflow from 2012 to 2014. The



monthly variability of the AOPs at each site is described in terms of its relationship with regional-scale atmospheric circulation patterns and the resulting changes in air mass sources. The median aerosol scattering and absorption coefficient values for sub-10  $\mu\text{m}$  particles ( $\sigma_{\text{sp}10 \mu\text{m}}$  and  $\sigma_{\text{ap}10 \mu\text{m}}$ ) were larger at the polluted marine site, Gosan (GSN;  $\sigma_{\text{sp}10 \mu\text{m}}$ : 59.94  $\text{Mm}^{-1}$ ,  $\sigma_{\text{ap}10 \mu\text{m}}$ : 4.73  $\text{Mm}^{-1}$ ), than at the high-altitude mountain site, Lulin (LLN;  $\sigma_{\text{sp}10 \mu\text{m}}$ : 17.07  $\text{Mm}^{-1}$ ,  $\sigma_{\text{ap}10 \mu\text{m}}$ : 1.72  $\text{Mm}^{-1}$ ). Elevated  $\sigma_{\text{sp}10 \mu\text{m}}$  and  $\sigma_{\text{ap}10 \mu\text{m}}$  at GSN in May and June can be explained by the accumulation of locally emitted aerosols along with long-range transported aerosols during conditions of stagnant synoptic patterns, enhanced particle formation and subsequent growth. The significant peaks of  $\sigma_{\text{sp}10 \mu\text{m}}$  and  $\sigma_{\text{ap}10 \mu\text{m}}$ , with median values of 50.76  $\text{Mm}^{-1}$  and 5.92  $\text{Mm}^{-1}$ , at LLN during March and April are attributable to biomass burning aerosols transported from northern Indochina and southern China. The LLN site was mostly influenced by clean free troposphere air and maritime air masses during the other months, showing medians of  $14.65 \pm 19.81 \text{ Mm}^{-1}$  and  $1.46 \pm 1.86 \text{ Mm}^{-1}$  for  $\sigma_{\text{sp}10 \mu\text{m}}$  and  $\sigma_{\text{ap}10 \mu\text{m}}$ , respectively. Lower median sub-micron to sub-10  $\mu\text{m}$  ratios for the aerosol scattering and absorption coefficients at GSN (0.60 and 0.81, respectively) than at LLN (0.81 and 0.91, respectively) are indicative of the larger proportion of coarse aerosols, such as sea salt and dust, at GSN. The single-scattering albedo for sub-10  $\mu\text{m}$  particles showed similar median values at both sites (GSN:  $0.93 \pm 0.02$ , LLN:  $0.91 \pm 0.03$ ).

**Keywords:** Aerosol, Aerosol scattering coefficient, Aerosol absorption coefficient, Gosan, Luli.

---

## Characteristics and Formation Mechanisms of Sulfate and Nitrate in Size-segregated Atmospheric Particles from Urban Guangzhou, China

Feng Jiang<sup>1,2</sup>, Fengxian Liu<sup>1,2</sup>, Qin hao Lin<sup>1</sup>, Yuzhen Fu<sup>1,2</sup>, Yuxiang Yang<sup>1,2</sup>, Long Peng<sup>1,2</sup>, Xiufeng Lian<sup>1,2</sup>, Guohua Zhang<sup>1</sup>, Xinhui Bi<sup>1</sup>, Xinming Wang<sup>1</sup>, Guoying Sheng<sup>1</sup>

**Source:** Aerosol and Atmospheric Chemistry, Volume: 19 | Issue: 6 | Pages: 1284-1293  
DOI: 10.4209/aaqr.2018.07.0251

Various water-soluble inorganic compounds, including  $\text{Na}^+$ ,  $\text{NH}_4^+$ ,  $\text{K}^+$ ,  $\text{Ca}^{2+}$ ,  $\text{Mg}^{2+}$ ,  $\text{Cl}^-$ ,  $\text{NO}_3^-$ ,  $\text{PO}_4^{3-}$  and  $\text{SO}_4^{2-}$ , were analyzed in 130 sets of size-segregated (< 0.49, 0.49–0.95, 0.95–1.5, 1.5–3.0, 3.0–7.2 and 7.2–10.0  $\mu\text{m}$ ) aerosol samples collected from March 2013 to April 2014 in Guangzhou, China.  $\text{SO}_4^{2-}$  was unimodally distributed and peaked during a typical droplet mode (0.49–0.95  $\mu\text{m}$ ). However, the distribution of  $\text{NO}_3^-$  significantly varied across the four seasons. It was unimodally distributed in summer and autumn, peaking in the coarse mode (3.0–7.2  $\mu\text{m}$ ), and bimodally distributed in winter and spring, peaking in the size ranges of 0.49–0.95  $\mu\text{m}$  and 3.0–7.2  $\mu\text{m}$ , respectively. The coarse-mode  $\text{NO}_3^-$  was mainly related to the influence of soil/dust. The additional mode during winter and spring was attributable to the formation of ammonium nitrate. Compared to clean days, polluted days favored the formation of  $\text{SO}_4^{2-}$  in summer and autumn and  $\text{NO}_3^-$  in winter and spring. The sulfur oxidation ratios (SORs) for < 0.49, 0.49–0.95 and 0.95–1.5  $\mu\text{m}$  particles were negatively correlated with the relative humidity (RH) in spring, summer and

autumn, respectively. However, the SORs for 0.49–3.0  $\mu\text{m}$  particles were positively correlated with the RH in winter, implying an important contribution from the aqueous oxidation of  $\text{SO}_2$ . Further analysis shows that the  $\text{SO}_4^{2-}$  in  $< 0.49 \mu\text{m}$  particles was formed primarily through gas-phase photochemical oxidation of  $\text{SO}_2$  during all four seasons. The formation of  $\text{NO}_3^-$  was mainly attributable to heterogeneous reactions for 1.5–3.0  $\mu\text{m}$  particles year-round and homogeneous gas-phase reactions for  $< 0.49 \mu\text{m}$  particles in winter. Correlation analysis also indicates a positive influence from biomass burning on the formation of nitrate and sulfate. The average pH of  $\text{PM}_3$  was calculated to be 2.6–5.6. Thus, the aqueous oxidation of  $\text{SO}_2$  by  $\text{NO}_2$  plays a limited role in the formation of sulfate in the atmosphere of Guangzhou.

**Keywords:** Water-soluble inorganic compounds, Sulfate Nitrate, Sulfur oxidation ratio, Nitrogen oxidation ratio, Guangzhou.

---

## Aerosol Pollution Characterization before Chinese New Year in Zhengzhou in 2014

Xiuli Wei 1, Huaqiao Gui<sup>1,3</sup>, Jianguo Liu<sup>1,3</sup>, Jie Zhang<sup>2</sup>, James Schwab<sup>2</sup>, Minguang Gao<sup>1</sup>

**Source:** Aerosol and Atmospheric Chemistry, Volume: 19 | Issue: 6 | Pages: 1294-1306  
DOI: 10.4209/aaqr.2018.06.0226

Fourier-transform infrared (FTIR) spectroscopy is a useful and nondestructive method for measuring the current atmospheric concentrations of inorganic compounds (sulfate, nitrate, and ammonium) and has been extensively used for environmental monitoring since the 1980s. In this study, we used FTIR spectroscopy to measure the inorganic compounds in particulate matter with a diameter of less than 2.5  $\mu\text{m}$  and combined the data of gaseous pollutants ( $\text{NO}_2$  and  $\text{SO}_2$ ) to analyze the inorganic compounds in  $\text{PM}_{2.5}$  from January 24 to January 31, 2014, in Zhengzhou. The measurement period was divided into three pollution stages. During Stage 1 (January 24–26), the low-pollution stage, wind from the east of Zhengzhou caused the pollutants to rapidly disperse and the haze to clear. During Stage 2 (January 26 to the noon of January 30), transported emissions were the main contributor to the high sulfate concentration, as indicated by the poor correlation between the sulfur oxidation ratio (SOR) and the  $\text{SO}_4^{2-}$  concentration ( $R^2 = 0.45$ ). Nitrate was formed through homogeneous gas-phase reactions of  $\text{NO}_2$  with OH or  $\text{O}_3$ , resulting in  $\text{HNO}_3$  in the  $\text{PM}_{2.5}$ , as indicated by the good correlation between the nitrogen oxidation ratio (NOR) and the  $\text{NO}_3^-$  concentration ( $R^2 = 0.91$ ). During Stage 3 (the afternoon of January 30 to January 31), the average concentration of the  $\text{PM}_{2.5}$  increased from approximately 140  $\mu\text{g m}^{-3}$  to 260  $\mu\text{g m}^{-3}$ , and the concentrations of sulfate, nitrate, and ammonium decreased from 37.62  $\mu\text{g m}^{-3}$ , 56.63  $\mu\text{g m}^{-3}$ , and 34.63  $\mu\text{g m}^{-3}$  to 32.14  $\mu\text{g m}^{-3}$ , 31.14  $\mu\text{g m}^{-3}$ , and 26.35  $\mu\text{g m}^{-3}$ , respectively. The high levels of  $\text{PM}_{2.5}$  during this stage may have been caused primarily by the hygroscopic growth of particles.

**Keywords:** FTIR, Inorganic compounds, PM2.5, Hygroscopic growth.

---

## **Impact of Extreme Meteorological Events on Ozone in the Pearl River Delta, China**

**Xiaohua Lin, Zibing Yuan , Leifeng Yang, Huihong Luo, Wenshi Li**

**Source:** Urban Air Quality Volume: 19 | Issue: 6 | Pages: 1307-1324

DOI: 10.4209/aaqr.2019.01.0027

Along with rapid economic development in the Pearl River Delta (PRD) region of China for the past two decades, ozone ( $O_3$ ) pollution has deteriorated significantly. Extreme meteorological events (EMEs), including heat wave (HW), atmospheric stagnation (AS), and temperature inversion (TI), exert significant impacts on  $O_3$ . Base on observational  $O_3$  data and meteorological reanalysis data, we analyze the impact of EMEs on  $O_3$  during  $O_3$  season of April–October in 2006–2017 over the PRD. Statistical analysis indicates significant but spatially heterogeneous sensitivities of  $O_3$  to EMEs. AS poses the largest impact on  $O_3$  concentration over the PRD, resulting in 58% increase compared with normal days, while the increases by HW and TI are 28% and 14%, respectively.  $O_3$  pollution events are largely initiated by HW and AS which favor formation and build-up of  $O_3$ , while  $O_3$  pollution events are maintained mostly by persistent AS and TI. HW poses higher impacts on northern and eastern PRD, while AS impacts more on central and western PRD. The effect of AS on  $O_3$  concentration is similar as 10 K temperature increase during non-AS days, while the effect of AS and TI on  $O_3$  exceedance is comparable with 6 K temperature increase during non-EMEs condition.  $O_3$  concentrations under different synoptic patterns are largely associated with the occurrence of AS, and Siberian high and the approaching of a tropical cyclone are the dominant synoptic patterns for EMEs impact on  $O_3$  and largely determines the long-term increasing trend of  $O_3$  concentration over the PRD. This study highlights the importance of establishing a location-specific  $O_3$  control strategy targeting on normal conditions and  $O_3$  pollution events separately. This study also provides scientific support to use EMEs forecast as an indicator to implement contingency  $O_3$  control in advance so as to maximize peak  $O_3$  reduction over the PRD.

**Keywords:** Extreme meteorological events ,  $O_3$  , Synoptic patterns , Spatial heterogeneity , Pearl River Delta

---

## **Chemical Characteristics and Source Apportionment of PM<sub>2.5</sub> during Winter in the Southern Part of Urumqi, China**

**Yusan Turap<sup>1</sup>, Suwubinuer Rekefu<sup>1</sup>, Guo Wang<sup>1</sup>, Dilinuer Talifu<sup>1</sup>, Bo Gao<sup>2</sup>, Tuergong Aierken<sup>1</sup>, Shen Hao<sup>1</sup>, Xinming Wang<sup>3</sup>, Yalkunjan Tursun<sup>1</sup>, Mailikezhati Maihemuti<sup>1</sup>, Ailijiang Nuerla<sup>4</sup>**

**Source:** Aerosol and Atmospheric Chemistry, Volume: 19 | Issue: 6 | Pages: 1325-1337  
DOI: 10.4209/aaqr.2018.12.0454

Urumqi, the administrative center of Xinjiang, suffers from severe atmospheric aerosol pollution; however, no study has comprehensively analyzed the local constituents and sources of fine particulate matter (PM<sub>2.5</sub>). The characteristics of PM<sub>2.5</sub> in Urumqi were observed the first winter (2012–2013) after natural gas replaced coal as an energy source. Enrichment factors, backward trajectories, the potential source contribution function (PSCF) model, and positive matrix factorization (PMF) were used to identify the source area and categories. The results showed a mean concentration of 197.40  $\mu\text{g m}^{-3}$  for the PM<sub>2.5</sub>, which significantly decreased after the conversion from coal to natural gas. Although the concentration of NO<sub>3</sub><sup>-</sup> increased post-conversion, the SO<sub>4</sub><sup>2-</sup> and Cl<sup>-</sup> decreased by 42.54% and 32.93%, respectively. The water-soluble ions (WSIs) mainly consisted of NH<sub>4</sub>HSO<sub>4</sub>, CaSO<sub>4</sub>, MgSO<sub>4</sub>, Ca(NO<sub>3</sub>)<sub>2</sub>, Mg(NO<sub>3</sub>)<sub>2</sub>, and KCl. Elements such as Pb, Cr, and As decreased following the fuel switch. The organic carbon and elemental carbon were strongly correlated, and the mean concentration of the secondary organic carbon was 18.90  $\mu\text{g m}^{-3}$ . Pyr, Chr, BbF, BkF, IcdP, and BghiP were the most prevalent individual polycyclic aromatic hydrocarbons, and BaP exceeded health-based guidelines. The results from trajectory clustering and PSCF modeling suggested that emissions from both the city and its surroundings, as well as the valley-and-basin topography, may be responsible for the heavy PM<sub>2.5</sub> pollution in southern Urumqi. PMF identified five primary sources: secondary formation, biomass and waste burning, vehicle emissions, crustal minerals, and industrial pollution and coal combustion.

**Keywords:** Fine particulate matter, Chemical composition, Source apportionment, Urumqi.

---

## **Heavy Particulate Matter Pollution during the 2014–2015 Winter in Tianjin, China**

**Zhenli Sun<sup>1</sup>, Fengkui Duan<sup>1</sup>, Yongliang Ma<sup>1,2</sup>, Kebin He<sup>1,2</sup>, Lidan Zhu<sup>1</sup>, Tao Ma<sup>1</sup>**

**Source:** Urban Air Quality Volume: 19 | Issue: 6 | Pages: 1338-1345  
DOI: 10.4209/aaqr.2018.04.0121

Tianjin, a city located in North China, is heavily polluted with frequent haze, particularly in winter. In this study, continuous online field observations of the sulfate, nitrate, ammonium, PM<sub>2.5</sub>, and gaseous pollutant concentrations in addition to the meteorological parameters were conducted in Tianjin during the 2014–2015 winter (December–January–February). The PM<sub>2.5</sub> concentrations ranged from 5.6 to 495.6  $\mu\text{g m}^{-3}$ , with an average value of  $112.2 \pm 96.1 \mu\text{g m}^{-3}$ . The worst pollution was observed in January, when levels on 10% of the days exceeded 250  $\mu\text{g m}^{-3}$ , qualifying as severely polluted, and four haze episodes, each lasting 5–7 days, occurred in rapid succession (separated by ~1-day intervals). Back-trajectory and chemical composition analysis suggested that elevated levels of secondary ionic aerosol species were a primary cause of these episodes. Regional transport of PM<sub>2.5</sub> also played a large role in the formation of haze. CO was selected as an inactive chemical tracer in studying the chemical process of PM<sub>2.5</sub> formation. The results indicated that when high concentrations of PM<sub>2.5</sub> were present, the formation of secondary PM<sub>2.5</sub> increased while the photochemical production of O<sub>3</sub> ceased. The sulfur oxidation ratio [SOR =  $n\text{SO}_4^{2-}/(n\text{SO}_4^{2-} + n\text{SO}_2)$ ; n refers to the molar concentration] and nitrate oxidation ratio [NOR =  $n\text{NO}_3^-/(n\text{NO}_3^- + n\text{NO}_2)$ ] increased with the PM<sub>2.5</sub> level, and heterogeneous processes on the surfaces of fine particles rather than photochemistry drove the haze events. This research elucidates haze formation mechanisms, which must be understood in order to create effective control policies in Tianjin.

**Keywords:** Aerosols , PM<sub>2.5</sub>, Secondary formation, Tianjin , Winter haze

---

## **Effects of Retarding Fuel Injection Timing on Toxic Organic Pollutant Emissions from Diesel Engines**

**Yixiu Zhao<sup>1</sup>, Kangping Cui <sup>1</sup>, Jingning Zhu<sup>1</sup>, Shida Chen<sup>1</sup>, Lin-Chi Wang <sup>2,3,4</sup>,  
Nicholas Kiprotich Cheruiyot<sup>5</sup>, Justus Kavita Mutuku<sup>5</sup>**

**Source:** Aerosol and Atmospheric Chemistry, Volume: 19 | Issue: 6 | Pages: 1346-1354  
DOI: 10.4209/aaqr.2019.03.0112

Retarding the fuel injection timing is an effective strategy for controlling NO<sub>x</sub> emissions from diesel engines. However, the influence of retarding the fuel injection timing on polycyclic aromatic hydrocarbon (PAH) and persistent organic pollutant (POP) emissions has not yet been investigated. In this study, the diesel engine was tested using four of the existing thirteen European steady state cycle (ESC) modes. The fuel injection timing was retarded from  $-8^\circ$  to  $-6^\circ$  and the diesel exhaust gas samples were analyzed for PAH and POP emissions. The NO<sub>x</sub> emission factor reduced by ~25% when the fuel injection timing was retarded. However, the strategy had a negative effect on combustion efficiency. The carbon monoxide (CO) and particulate matter (PM) emissions were 1.4 and 1.2 times higher for the  $-6^\circ$  scenario, respectively. The emission factors of all the toxic organic pollutants increased drastically when the fuel injection timing was retarded. For instance, the emission factors of PAH and polychlorinated dibenzo-p-dioxin/dibenzofuran (PCDD/F) for the  $-6^\circ$  scenario, based on BaP<sub>eq</sub> and WHO-TEQ, were 22 and 10 times higher than for

the  $-8^\circ$  scenario. The retardation had more influence on these pollutants in the particle-phase than in gas-phase. The resultant negative impact on combustion increased the emissions of products of incomplete combustion, enhancing the potential of POP formation via de novo synthesis. The study concludes that although retarding the fuel injection timing leads to a decrease in NO<sub>x</sub> emissions from diesel engines, it also results in an increase in PAH and POP emissions.

**Keywords:** Diesel engine, Injection timing , POPs, Emission , Organic toxic pollutants, PCDD/Fs.

---

## **Inhalation Health Risk Assessment for the Human Tracheobronchial Tree under PM Exposure in a Bus Stop Scene**

**Xiaoyu Xu<sup>1,2,3</sup>, Yidan Shang<sup>2</sup>, Lin Tian <sup>2</sup>, Wenguo Weng<sup>1</sup>, Jiyuan Tu <sup>2,3,4</sup>**

**Source:** Aerosol and Atmospheric Chemistry, Volume: 19 | Issue: 6 | Pages: 1365-1376  
DOI: 10.4209/aaqr.2018.09.0343

Inhalation exposure to airborne particulate matter (PM) can induce respiratory/cardiovascular disease and lung cancer in humans. Determining the specific particle deposition distribution in the human tracheobronchial tree is crucial to evaluating the health risk. Thus, an integrated human nasal-oral-tracheobronchial airway model was employed to study the particle deposition, and empirical equations for calculating the lung lobe risk contribution fractions were developed. The risk contribution of each lobe to non-carcinogenesis and carcinogenesis was predicted using prior experimental data collected at a bus stop. The regional inhalation health risk was analyzed by evaluating the hazard quotient (HQ) and excess lifetime cancer risk (ELCR) of selected non-carcinogenic and carcinogenic elements (viz., Cr, Mn, and Ni). Fine particles (10 nm–1 μm) contributed the highest risk fractions for the lung lobes, inducing higher potential health consequences in the lungs than coarser particles. Cr posed carcinogenic lung risks to people who commuted by public transport, with the ELCR to every lobe exceeding the recommended limit. The non-carcinogenic and carcinogenic risks were 1.5 times greater for the right lung than for the left lung. Of the lung lobes, the RLL incurred the highest risk, followed by the LLL, RUL, LUL, and RML. Inhalation exposure to Cr posed a much higher risk to the lungs than exposure to Ni and Mn. However, compared to the other two elements, Mn potentially induced a higher chance of developing upper respiratory disease.

**Keywords:** Tracheobronchial airway, Particulate matter, Chemical composition ,Inhalation assessment, Lung lobe deposition.

---

## **Evaluation of Different Machine Learning Approaches to Forecasting PM2.5 Mass Concentrations**

**Hamed Karimian<sup>1,2</sup>, Qi Li<sup>2</sup>, Chunlin Wu<sup>2</sup>, Yanlin Qi<sup>2</sup>, Yuqin Mo<sup>2</sup>, Gong Chen<sup>2,4</sup>, Xianfeng Zhang<sup>2</sup>, Sonali Sachdeva<sup>3</sup>**

**Source:** Aerosol and Atmospheric Chemistry, Volume: 19 | Issue: 6 | Pages: 1400-1410  
DOI: 10.4209/aaqr.2018.12.0450

With the rapid growth in the availability of data and computational technologies, multiple machine learning frameworks have been proposed for forecasting air pollution. However, the feasibility of these complex approaches has seldom been verified in developing countries, which generally suffer from heavy air pollution. To forecast PM<sub>2.5</sub> concentrations over different time intervals, we implemented three machine learning approaches: multiple additive regression trees (MART), a deep feedforward neural network (DFNN) and a new hybrid model based on long short-term memory (LSTM). By capturing temporal dependencies in the time series data, the LSTM model achieved the best results, with RMSE = 8.91  $\mu\text{g m}^{-3}$  and MAE = 6.21  $\mu\text{g m}^{-3}$ . It also explained 80% of the variability ( $R^2 = 0.8$ ) in the PM<sub>2.5</sub> concentrations and predicted 75% of the pollution levels, proving that this methodology can be effective for forecasting and controlling air pollution.

**Keywords:** Air pollution, Machine learning, Neural networks, Deep learning, Prediction.

---

## **Chemical Characterization of Fine Particulate Matter in Gasoline and Diesel Vehicle Exhaust**

**Hsi-Hsien Yang<sup>1,2</sup>, Narayan Babu Dhital<sup>1,2,3</sup>, Lin-Chi Wang<sup>4,5</sup>, Yueh-Shu Hsieh<sup>1</sup>, Kuei-Ting Lee<sup>1</sup>, Ya-Tin Hsu<sup>1</sup>, Shi-Cheng Huang<sup>1</sup>**

**Source:** Aerosol and Atmospheric Chemistry, Volume: 19 | Issue: 6 | Pages: 1439-1449  
DOI: 10.4209/aaqr.2019.04.0191

This study investigated the chemical composition (carbonaceous species, water-soluble ions and metal elements) of fine particulate matter (PM<sub>2.5</sub>) emitted by gasoline and diesel vehicles. The emission factors of PM<sub>2.5</sub>, total hydrocarbons (THC), carbon monoxide (CO) and oxides of nitrogen (NO<sub>x</sub>) were also determined. The emission measurements were performed for four gasoline and four diesel vehicles on a dynamometer with a constant volume sampling system. Vehicles having larger engines and higher accumulated mileages had higher emission factors of gaseous pollutants. Moreover, the average emission factor of NO<sub>x</sub> was about 30 times higher for diesel vehicles than for gasoline vehicles. The average PM<sub>2.5</sub> emission factors for gasoline and diesel vehicles were 1.57 mg km<sup>-1</sup> and 57.8 mg km<sup>-1</sup>, respectively. The ratio of organic carbon to elemental carbon (OC/EC) was found to be a good indicator of gasoline vehicle emissions (OC/EC > 1) and diesel vehicle emissions (OC/EC < 1). Among water-soluble ions, Ca<sup>2+</sup> and SO<sub>4</sub><sup>2-</sup> had the highest contribution to

PM<sub>2.5</sub> emitted by gasoline vehicles, while NO<sub>3</sub><sup>-</sup>, SO<sub>4</sub><sup>2-</sup> and Ca<sup>2+</sup> had the highest contribution to PM<sub>2.5</sub> emitted by diesel vehicles. Na, Ca, Fe and Zn were the top four metal elements in terms of their contributions to PM<sub>2.5</sub> mass for both types of the vehicles, while Cd, Cr, Pb and Sb were some of the toxic metal elements detected in PM<sub>2.5</sub>.

**Keywords:** Emission factor, Elemental carbon, Organic carbon, Water-soluble ion, Metal element.

---

## **Analysis of Chemical Composition, Source and Processing Characteristics of Submicron Aerosol during the Summer in Beijing, China**

**Qi Jiang<sup>1</sup>, Fei Wang<sup>2</sup>, Yele Sun<sup>3</sup>**

**Source:** Aerosol and Atmospheric Chemistry, Volume: 19 | Issue: 6 | Pages: 1450-1462  
DOI: 10.4209/aaqr.2018.12.0480

In this study, an aerosol chemical speciation monitor (ACSM) and various collocated instruments are used to observe and analyze the chemical compositions, sources and extinction characteristics of submicron aerosol (PM<sub>1</sub>; aerodynamic diameter < 1 μm) in Beijing from July to September 2012. The results show that the average mass concentration of the PM<sub>1</sub> for the entire observation period is 53.8 μg m<sup>-3</sup>, accounting for 70–85% on average of the PM<sub>2.5</sub>, and the average mass concentration of the non-refractory submicron aerosol (NR-PM<sub>1</sub>) declines monthly from July to September as the fraction of organic aerosol (OA) in it increases. During clean days, OA forms the largest mass fraction of the PM<sub>1</sub>, and the fraction of inorganics shows a significant increasing trend as pollutants accumulate. The effects of meteorology on PM pollution and aerosol processing are also explored. In particular, the SOR increases significantly during periods of elevated relative humidity (RH), suggesting that SO<sub>2</sub> is more efficiently converted to SO<sub>4</sub><sup>2-</sup> during pollution episodes via aqueous-phase oxidation than gas-phase oxidation. In addition, the effect of wind speed is significantly weaker on primary species (PPM) than secondary species (SPM). Furthermore, the mass concentration of the SPM (or organics) is more sensitive than that of the PPM (or inorganics) to changes in wind speed. The proportion of oxygenated OA (OOA) is significantly higher than that of hydrocarbon-like OA (HOA) in the OA, and as the proportion of OA in the PM<sub>1</sub> increases, the mass fraction of OOA in the OA gradually decreases. Moreover, the aerosol acidity in Beijing is essentially neutral during the observation period. The total extinction coefficient of the particulate matter (PM) correlates well with the mass concentration of the PM<sub>1</sub> ( $r^2 = 0.72$ ), and the extinction efficiency of the secondary particulate matter (SPM) ( $r^2 = 0.92$ ) is significantly higher than that of the primary particulate matter (PPM) ( $r^2 = 0.58$ ). Meanwhile, the correlation is weaker between the OA and the extinction coefficient ( $r^2 = 0.56$ ) than between the inorganic aerosol and the extinction coefficient ( $r^2 = 0.86$ ).

**Keywords:** ACSM, NR-PM<sub>1</sub>, SPM, Extinction coefficient.

---



## **Coarse and Fine Particulate Matter Components of Wildland Fire Smoke at Devils Postpile National Monument, California, USA**

**Donald Schweizer**<sup>1,2</sup>, **Ricardo Cisneros**<sup>2</sup>, **Monica Buhler**<sup>3</sup>

**Source:** Aerosol and Atmospheric Chemistry, Volume: 19 | Issue: 7 | Pages: 1463-1470  
DOI: 10.4209/aaqr.2019.04.0219

Fine (PM<sub>2.5</sub>) and coarse (PM<sub>10</sub>) particulate matter were monitored during the summer and fall of 2018 at Devils Postpile National Monument, California, USA. This remote site, located in the Sierra Nevada, was downwind of a number of wildland fires that were burning in California. The coarse (PM<sub>2.5-10</sub>) and the fine (PM<sub>2.5</sub>) fractions of the PM in the wildland fire smoke showed median PM<sub>2.5-10</sub>/PM<sub>2.5</sub> ratios of .47 and 1.37 during periods with and without smoke, respectively. The concentrations at ground level were significantly ( $p < 0.001$ ) higher during the periods with smoke for both the PM<sub>2.5-10</sub> (10.3  $\mu\text{g m}^{-3}$ ) and the PM<sub>2.5</sub> (35.3  $\mu\text{g m}^{-3}$ ), although the PM<sub>2.5</sub> contributed most of the increase. These concentrations suggest that the fire size and intensity along with the distance and transport of smoke determine the exposure risk to humans. Current exposure estimates obtained via modeling and emission estimates may misrepresent ground-level concentrations due to a lack of understanding of the aerosol distribution in an aging wildland fire smoke plume.

**Keywords:** PM2.5 , PM10, Wilderness air quality, Emission characterization

---

## **Investigating the Role of Meteorological Factors in the Vertical Variation in PM2.5 by Unmanned Aerial Vehicle Measurement**

**Si-Jia Lu**<sup>1</sup>, **Dongsheng Wang**<sup>1</sup>, **Zhanyong Wang**<sup>2</sup>, **Bai Li**<sup>1</sup>, **Zhong-Ren Peng**<sup>1,3,4</sup>, **Xiao-Bing Li**<sup>1</sup>, **Ya Gao**<sup>1</sup>

**Source:** Aerosol and Atmospheric Chemistry, Volume: 19 | Issue: 7 | Pages: 1493-1507  
DOI: 10.4209/aaqr.2018.07.0266

Clarifying the effects of meteorology on the vertical variation in PM<sub>2.5</sub> is critical to understanding the formation of haze. We investigated the PM<sub>2.5</sub> and synchronous meteorological variations in a three-dimensional space by measuring them with a lightweight unmanned aerial vehicle (UAV) equipped with portable monitors. Our field campaign was conducted on 5 separate days selected between August 2014 and February 2015 at altitudes  $\leq 1000$  m above a  $4 \times 4$  km<sup>2</sup> area in Lin'an, China. The UAV measurement was performed 4 times on each of the selected days, and every flight followed a designed spiral route from ground level up to an altitude of 1000 m. The PM<sub>2.5</sub> mass concentration and meteorological factors, viz., the air temperature, relative humidity, dew point temperature and air pressure, were sampled at three-dimensional spatial locations during each flight. The measurements indicate that the PM<sub>2.5</sub> distribution is more homogeneous horizontally than vertically. The PM<sub>2.5</sub> concentration also decreases as the height

increases; furthermore, it exhibits obvious stratification in the morning but more homogeneity in the afternoon. The concentrations above 500 m slightly rise in the afternoon, especially on days that display more stratification. The vertical gradient of the concentrations shows a decrease from the morning to the afternoon, which is smaller during winter than summer and autumn. Meteorologically induced changes in the planetary boundary layer height and inversion layer also significantly affect the PM<sub>2.5</sub> variation in the lower troposphere. Our results serve as a reference for analyzing and forecasting PM<sub>2.5</sub> pollution and provide a basis for smarter and more targeted air pollution management and governance.

**Keywords:** PM<sub>2.5</sub>, Spatio-temporal variation, Vertical distribution, Meteorology, UAV.

---

## **Biological and Chemical Air Pollutants in an Urban Area of Central Europe: Co-exposure Assessment**

**Łukasz Grewling<sup>1</sup>, Agata Frątczak<sup>2</sup>, Łukasz Kostecki<sup>1</sup>, Małgorzata Nowak<sup>1</sup>, Agata Szymańska<sup>1</sup>, Paweł Bogawski<sup>3</sup>**

**Source:** Aerosol and Atmospheric Chemistry, Volume: 19 | Issue: 7 | Pages: 1526-1537  
DOI: 10.4209/aaqr.2018.10.0365

Synergistic interactions between biological and chemical air pollutants, enhanced by the effect of meteorological factors, may increase the risk of respiratory disease. Therefore, to accurately evaluate the impact of air pollution on human health, the concomitant behaviors of various air pollutants should be investigated. In this study, the peculiarities of the temporal co-existence of allergenic pollen (alder, birch, grass, and mugwort), fungal spores (*Alternaria* and *Cladosporium*), and hazardous air pollutants (ground-level ozone and particulate matter, PM<sub>10</sub>) collected in Poznań (western Poland) from 2005 to 2016 were analyzed with particular attention to their relation with air temperature. The results of the statistical analysis showed that the daily concentrations of certain airborne particles (pollen, fungal spores, and ozone) significantly increased on days with high mean temperatures. However, high temperatures occurring during earlier stages of development for grass and mugwort, prior to pollen release, decreased the overall quantity of pollen produced and released during the season. Furthermore, the daily concentration of PM<sub>10</sub> decreased with increasing temperature. As a result, the co-exposure of alder pollen and PM<sub>10</sub> was limited to a narrow temperature range (4–10°C) and mainly recorded during February and March. In most cases, a characteristic pattern was observed: The co-occurrence of air pollutants increased with the temperature. When birch and grass pollen co-occurred with other air pollutants, the temperature was significantly higher (by 2.0 to 8.0°C) than when only pollen grains were observed. In general, high temperatures favored the simultaneous occurrence of pollen grains, fungal spores, and ozone, which was most pronounced during hot days in June and August. Such conditions should therefore be considered the most hazardous for people suffering from allergic airway diseases.

**Keywords:** Bioaerosols , Allergens, Ozone , PM10, Respiratory health.

---

## **Emissions of PM2.5-bound Polycyclic Aromatic Hydrocarbons and Metals from a Diesel Generator Fueled with Biodiesel Converted from Used Cooking Oil**

**Jen-Hsiung Tsai<sup>1</sup>, Shui-Jen Chen <sup>1</sup>, Sheng-Lun Lin<sup>2,3,4</sup>, Kuo-Lin Huang<sup>1</sup>, Cheng-Kai Hsueh<sup>1</sup>, Chih-Chung Lin<sup>1</sup>, Po-Min Li<sup>5</sup>**

**Source:** Aerosol and Atmospheric Chemistry, Volume: 19 | Issue: 7 | Pages: 1555-1565  
DOI: 10.4209/aaqr.2019.04.0204

To elucidate the characteristics of fine particulate matter pollutant emitted from a diesel engine, a fossil-based diesel fuel (D100) and two blended fuels consisting of D100 and waste cooking oil (WCO) converted biodiesel (W) are tested with a diesel engine generator at loads of 1.5 kW and 3.0 kW. The blended fuels contain 20% and 40% W and are referred to as W20 and W40, respectively. The PM<sub>2.5</sub> emissions and their polycyclic aromatic hydrocarbon (PAH) and metallic components are investigated. Experimental results show that higher concentrations of PM<sub>2.5</sub>, PM<sub>2.5</sub>-bound  $\Sigma$ PAHs and  $\Sigma$ metals, and  $\Sigma$ BaP<sub>eq</sub> are generated at the 3.0 kW load, with its greater fuel consumption (FC), than the 1.5 kW load. Additionally, of the three fuels, using W20 emits the lowest concentrations of PM<sub>2.5</sub>, PM<sub>2.5</sub>-bound  $\Sigma$ PAHs, and  $\Sigma$ BaP<sub>eq</sub>. Specifically, the reduction in  $\Sigma$ BaP<sub>eq</sub> mainly results from the effective inhibition of HMW-BaP<sub>eq</sub>. Conversely, when using W40, the PM<sub>2.5</sub>-bound  $\Sigma$ metals significantly decreases, and its composition is strongly affected by the metallic content in the fuel. Although W20 and W40 exhibit higher FC (3.0% more) and brake-specific fuel consumption (BSFC; 3.1% more) than D100, they generate lower concentrations of PM<sub>2.5</sub> (18.1% less), PM<sub>2.5</sub>-bound  $\Sigma$ PAHs (22.8% less) and  $\Sigma$ metals (22.0% less), and  $\Sigma$ BaP<sub>eq</sub> (35.0% less) at both engine loads. The emission factors of these pollutants in the engine exhaust are also reduced, particularly at the higher load (3.0 kW). Accordingly, WCO-based biodiesel additives may decrease the PM<sub>2.5</sub>, PAHs, and metals exhausted by diesel engines, thus reducing the BaP<sub>eq</sub> of these emissions.

**Keywords:** PM2.5, Biodiesel, PAHs, Metals, Generator.

---

## **Emission of Carbonyl Compounds from Cooking Oil Fumes in the Night Market Areas**

**Danielle E. Que<sup>1</sup>, How-Ran Chao <sup>2,3</sup>, Yi-Chyun Hsu <sup>4</sup>, Kangping Cui<sup>5</sup>, Shida Chen<sup>5</sup>, Lemmuel L. Tayo<sup>6</sup>, Rachele D. Arcega<sup>6</sup>, Ying-I Tsai<sup>7</sup>, I-Cheng Lu<sup>2</sup>, Lin-Chi Wang<sup>8,9,10</sup>, Li-Hao Young<sup>11</sup>, Kwong-Leung J. Yu<sup>12</sup>, Chane-Yu Lai<sup>13</sup>, Wen-Che Hou<sup>1</sup>, Sheng-Lun Lin<sup>8,9,10</sup>**

**Source:** Air Toxics Volume: 19 | Issue: 7 | Pages: 1566-1578  
DOI: 10.4209/aaqr.2019.06.0289

Cooking oil fumes (CF) coming from night market stalls exhaust contain substantial amounts of air pollutants such as carbonyl compounds that may contribute to outdoor air pollution and may have adverse health effects on the Taiwanese population. Carbonyl emission characteristics depend on several factors, which include but are not limited to, the cooking style and food material being used. The current study evaluated carbonyl compound emissions from two scenarios: a standard kitchen cooking classroom with a stack gas tunnel and night market food stalls. The different cooking styles and food types cooked using a liquefied petroleum gas (LPG) stove, such as grilled chicken with (GCS) and without sauce (GC), mixed barbecue with sauce (MBS), grilled vegetables with sauce (GVS), stir-fried oyster omelet (OM), fried Taiwanese chicken nuggets (FN) in the kitchen cooking classroom, and grilled chicken with (GCS) and without sauce (GC), stir-fried oyster omelet (OM), grilled vegetables with sauce (GVS), and fried steak (FS) in the night market were evaluated for carbonyl carbon emissions. OM from the kitchen classroom and GCS from the night market showed the highest mean total carbonyl compound concentrations ( $1850 \pm 682$  ppb and  $1840$  ppb). Formaldehyde was found to be the most predominant carbonyl compound, with contribution percentages ranging from 70.9–99.58% of the total carbonyl emission factors in CFs. Grilled vegetables with sauce had the highest emission factor magnitude of  $274 \mu\text{g kg}^{-1}$  wt. Factors such as the addition of sauce and grilling were also observed to increase carbonyl compound emissions. Corresponding health risks of carbonyl compounds in CFs for the night market vendors were also assessed. All values for cancer risk (R) were above the standard R value for workplace exposure, and HQ values were all greater than 1, suggesting a high risk for adverse health effects. Although our reported values were relatively high due to our sampling conditions, our study was first to be conducted in Taiwan and holds an important contribution to the global existing data of carbonyl compound emissions.

**Keywords:** Cooking oil fumes , Carbonyl compounds , Health risks , Air pollutants , Night market

---

## **Dominant Factors Influencing the Concentrations of Particulate Matters inside Train Carriages Traveling in Different Environments in the Taipei Mass Rapid Transit System**

**Yu-Hsiang Cheng 1,2, Xuan-Huy Ninh1, Shu-Lun Yeh1**

**Source:** Aerosol and Atmospheric Chemistry, Volume: 19 | Issue: 7 | Pages: 1579-1592  
DOI: 10.4209/aaqr.2018.09.0335

Air quality inside metro systems is a critical issue for commuters and metro employees because of the considerable time they spend traveling or working in such systems. This study measured the PM<sub>10</sub>, PM<sub>2.5</sub>, particle number (PN), and CO<sub>2</sub> levels and particle mass size distributions inside operating trains to reveal the factors influencing the concentrations and size distributions of particulate matter (PM) inside metro train carriages traveling in different environments. The measurement results demonstrated that

the CO<sub>2</sub> level was associated with ridership and that the PM levels and particle mass size distributions were highly affected by the immediate surroundings of the train, such as whether it was journeying through underground tunnels or on ground-level tracks as well as its direction of travel. Furthermore, the particle mass size distributions inside the metro train carriages exhibited a clear triple-mode pattern, whereas those for the ground-level and underground routes differed considerably due to different particle sources.

**Keywords:** Train carriage , Train carriage, Particle mass size distribution, Particle mass size distribution, Journey, Underground tunnel.

---

## **Regional Air Quality Forecast Using a Machine Learning Method and the WRF Model over the Yangtze River Delta, East China**

**Mengwei Jia<sup>1,3</sup>, Xinghong Cheng<sup>2</sup>, Tianliang Zhao<sup>3</sup>, Chongzhi Yin<sup>3</sup>, Xiangzhi Zhang<sup>4</sup>, Xianghua Wu<sup>5</sup>, Liming Wang<sup>5</sup>, Renjian Zhang<sup>6</sup>**

**Source:** Aerosol and Atmospheric Chemistry, Volume: 19 | Issue: 7 | Pages: 1602-1613  
DOI: 10.4209/aaqr.2019.05.0275

A statistical forecasting method of air quality based on meteorological elements with high spatiotemporal resolution simulated by the Weather Research and Forecasting (WRF) model and a back-propagation (BP) neural network was established to predict 72 h PM<sub>2.5</sub> mass concentrations over the Yangtze River Delta (YRD) region of eastern China. Short-term statistical forecasting of air quality in 25 major cities in the YRD region was conducted and the PM<sub>2.5</sub> forecast was validated using the corresponding surface PM<sub>2.5</sub> observational data in this study. Results indicate that the short-term air quality forecasting system has a ability to accurately forecast PM<sub>2.5</sub> concentration in the major cities in the YRD region. The average index of agreement (IA) between PM<sub>2.5</sub> forecasts and observations in the four seasons ranges from 74% to 77%, and the root mean square error (RMSE) fall between 15.2  $\mu\text{g m}^{-3}$  and 33.0  $\mu\text{g m}^{-3}$ . The data with PM<sub>2.5</sub> concentration greater than 115  $\mu\text{g m}^{-3}$  are selected to establish the EXP-Polluted model and then used to predict PM<sub>2.5</sub> concentration during heavy haze periods in 2017. The RMSEs of PM<sub>2.5</sub> forecasts during severe haze periods are improved by 44.1%, which compared to predictions using the EXP-All Time model constructed by the full-year data.

**Keywords:** Regional air quality forecast, BP Network, WRF model, Heavy haze, Yangtze River Delta.

---

## **Black Carbon Emissions from Light-duty Passenger Vehicles Using Ethanol Blended Gasoline Fuels**

**Xuan Zheng<sup>1,2</sup>, Xian Wu<sup>2</sup>, Liqiang He<sup>2</sup>, Xin Guo<sup>3</sup>, Ye Wu<sup>2,4</sup>**

**Source:** Technical Note Volume: 19 | Issue: 7 | Pages: 1645-1654

DOI: 10.4209/aaqr.2019.02.0095

Vehicular emissions of soot vary with the driving conditions and fuel properties. In 2017, China's central government released a policy to promote ethanol blended gasoline fuels, and this policy will be rolled out nationwide in 2020. It is necessary to characterize the emission differences between traditional vehicular fuels used in China and ethanol blended fuels. In this study, black carbon (BC) emissions from three gasoline light-duty passenger vehicles (LDPVs) were measured using the New European Driving Cycle (NEDC) and the Worldwide harmonized Light vehicles Test Cycle (WLTC). This study utilized three fuels, namely, two E10 fuels and a traditional gasoline (E0). The experimental results showed that the use of E10 blends (gasoline containing 10% ethanol) reduced BC emissions by 7–38%. Based on phase-separated analysis, BC emissions in the initial driving phase and the high-speed phase (e.g., the 1<sup>st</sup> ECE-15 phase in the NEDC and the extra-high speed phase in the WLTC) represented the majority (86–96%) of the total BC emissions, and the emission factors during the 1<sup>st</sup> ECE-15 phase (NEDC) and the low-speed phase (WLTC) were 0.36 mg km<sup>-1</sup> and 0.37 mg km<sup>-1</sup> lower, respectively, for the ethanol-blended fuels than the ethanol-free fuel. Furthermore, we found that using ethanol-blended fuels could reduce the mass concentration of the BC emitted during cold starts, which lasted 53–95 s for the tested vehicles, by 4.28 ± 4.19 mg km<sup>-1</sup> and 2.06 ± 0.17 mg km<sup>-1</sup> in the NEDC and the WLTC, respectively.

**Keywords:** Black carbon emissions , Light duty passenger vehicles , Ethanol blended fuels , Driving conditions , Cold start

---

## **Testing of an Indoor Air Cleaner for Particulate Pollutants under Realistic Conditions in an Office Room**

**Miriam Küpper, Christof Asbach , Ute Schneiderwind, Hartmut Finger, Daniel Spiegelhoff, Stefan Schumacher**

**Source:** Indoor Air Volume: 19 | Issue: 8 | Pages: 1655-1665

DOI: 10.4209/aaqr.2019.01.0029

Mobile air cleaners have been gaining popularity as potentially effective tools for improving indoor air quality. Usually, the efficacy of an air cleaner is quantified by determination of the clean air delivery rate (CADR) under strictly defined conditions within test chambers lacking furniture and featuring adequate and homogeneous mixing of the test aerosol. By contrast, real-world scenarios may considerably differ from these

conditions, resulting in adverse consequences, as a less homogeneous distribution of the cleaned air may produce spatial differences in the CADR and lead to lower overall efficacy for the air cleaner.

Therefore, in this study, the spatial variance of a mobile air purifier's cleaning efficacy across several positions in a furnished and in-use office room was investigated for four different scenarios, in each of which the air cleaner was placed in a different position inside the room. Ambient outdoor air was supplied as target aerosol by opening a window prior to the measurements, and the local CADR was calculated based on the decay rate of the lung-deposited surface area (LDSA) concentration. It was found that the relative decay of the LDSA concentration was almost identical for all of the measuring points throughout the room, hinting at a homogeneous distribution of the cleaned air. Varying the position of the air cleaner in the room resulted in only minor differences, except when the device was placed in an intentionally unfavourable location under a desk, which significantly reduced the cleaning efficacy. Despite the high spatial homogeneity, the CADR in the office room was significantly lower than the one determined according to the Chinese standard GB/T 18801-2015 in a standardized test chamber, which is presumably mainly attributable to the differing size distributions of the realistic and the standard test aerosol.

**Keywords:** Indoor air quality , Mobile air cleaners , Spatial variance of CADR , Ultrafine particles , Lung deposited surface area concentration

---

## Elemental Composition, Morphology and Sources of Fine Particulates (PM<sub>2.5</sub>) in Hefei City, China

Huaqin Xue<sup>1,2</sup>, Guijian Liu <sup>1,2</sup>, Hong Zhang<sup>1,3</sup>, Ruoyu Hu<sup>1</sup>, Xin Wang<sup>1</sup>

**Source:** Aerosol and Atmospheric Chemistry, Volume: 19 | Issue: 8 | Pages: 1688-1696  
DOI: 10.4209/aaqr.2018.09.0341

Elemental composition and morphology were studied for atmospheric fine particles (PM<sub>2.5</sub>) collected from a fast developing city, Hefei, with an aim of tracing the potential emission sources. The sampling was conducted every month at two urban sites between June 2014 and December 2015. We used X-ray fluorescence (XRF) to determine the elemental composition, and scanning electronic microscopy (SEM) and transmission electron microscope (TEM) to characterize the particles in morphology.

Our results showed that PM<sub>2.5</sub> contained large fractions of particles likely derived from fuel burning, construction and automobile emissions and was highly enriched in sulfur. Aggregations of particles suggested a strong secondary reaction under high SO<sub>2</sub> levels. Some discrepancies in elemental composition at the two sampling sites were observed, which were attributed to the difference in traffic density and construction fugitive dust emissions. A negative correlation existed between the polluted elements in PM<sub>2.5</sub> and the

ambient temperature and a positive correlation existed with the pressure, likely caused by a reduction in the height of the terrestrial boundary layer and reaction rates of pollutants.

**Keywords:** PM2.5, Elemental composition, Morphology, Sources identification

---

## **Characteristics of Single Aerosol Particles during Pollution in Winter in an Urban Area of Ningbo, China**

**Meng-Rong Yang<sup>1,2,3</sup>, Jun Zhou<sup>4</sup>, Xiao-Rong Dai<sup>1,3</sup>, Dominik van Pinxteren<sup>5</sup>, Ming-Yang Cao<sup>6</sup>, Mei Li<sup>7</sup>, Hang Xiao<sup>1,3</sup>**

**Source:** Aerosol and Atmospheric Chemistry, Volume: 19 | Issue: 8 | Pages: 1697-1707  
DOI: 10.4209/aaqr.2019.01.0038

The size and composition of individual atmospheric particles were assessed using a single particle aerosol mass spectrometer in Ningbo, China, from 30 December 2016 to 12 January 2017. The particles were primarily carbonaceous and inorganic, with the majority (60%) being carbonaceous. All of the major particle types contained internally mixed secondary species, such as nitrate and sulfate. The temporal trends of the particle number concentrations and PM<sub>2.5</sub> (particulate matter with an aerodynamic diameter < 2.5 μm) mass concentrations indicated that secondary formation in Ningbo severely affected the air quality. The sampling period was divided into three subperiods according to the PM<sub>2.5</sub> mass concentration. During Period I, local emission and secondary formation were the primary contributors of the pollution, and during Periods II and III, the abundance of particles occurring with high-speed winds indicated that regional transport was a primary factor in these two pollution processes. Additionally, high PM<sub>2.5</sub> mass concentrations were often observed at night during high relative humidity and low temperatures across the entire sampling period. These results demonstrate that stagnant meteorological conditions increase pollution during winter. Overall, this study enhances our understanding of particulate pollution in the southern Yangtze River Delta region and provides useful information on the formation and growth of atmospheric aerosols.

**Keywords:** Particulate matter, Mixing state, Mass spectral characteristics, Size distribution.

---



# A Big Data Analysis of PM<sub>2.5</sub> and PM<sub>10</sub> from Low Cost Air Quality Sensors near Traffic Areas

Shida Chen<sup>1</sup>, Kangping Cui<sup>1</sup>, Tai-Yi Yu<sup>2</sup>, How-Ran Chao<sup>3,4,5</sup>, Yi-Chyun Hsu<sup>6</sup>, I-Cheng Lu<sup>3</sup>, Rachele D. Arcega<sup>3</sup>, Ming-Hsien Tsai<sup>7</sup>, Sheng-Lun Lin<sup>8,9,10</sup>, Wan-Chun Chao<sup>11</sup>, Chunneng Chen<sup>11</sup>, Kwong-Leung J. Yu<sup>12</sup>

**Source:** Urban Air Quality Volume: 19 | Issue: 8 | Pages: 1721-1733

DOI: 10.4209/aaqr.2019.06.0328

Particulate matter (PM) pollution (including PM<sub>2.5</sub> and PM<sub>10</sub>), which is reportedly caused primarily by industrial and vehicular emissions, has become a major global health concern. In this study, we aimed to reveal spatiotemporal characteristics and diurnal patterns of PM<sub>2.5</sub> and PM<sub>10</sub> data obtained from 50 air quality sensors situated in public bike sites in Kaohsiung City on June and November 2018 using principal component analysis (PCA). Results showed that PM concentrations in the study were above the standard World Health Organization criteria and were found to be associated, although complicated, with relative humidity. Specifically, the relationship between PM concentrations and relative humidity suggest a clear association at lower PM concentrations. Temporal analysis revealed that PM<sub>2.5</sub> and PM<sub>10</sub> occurred at higher concentrations in winter than in summer, which could be explained by the long-range transport of pollutants brought about by the northeast monsoon during the winter season. Both PM fractions displayed similar spatial distribution, wherein PM<sub>2.5</sub> and PM<sub>10</sub> were found to be concentrated in the heavily industrialized areas of the city, such as near petrochemical factories in Nanzih and Zuoying districts in north Kaohsiung and near the shipbuilding and steel manufacturing factories in Xiaogang district in south Kaohsiung. A pronounced diurnal variation was found for PM<sub>2.5</sub>, which generally displayed higher peaks during the daytime than in the nighttime. Peaks generally occurred at 7:00–9:00 a.m., noontime, and 5:00–7:00 p.m., while minima generally appeared at nighttime. The diurnal pattern of PM was greatly influenced by a greater number of industrial and human transportation activities during the day than at night. Overall, a number of factors such as relative humidity and type of season, transboundary pollution from neighboring countries, and human activities, such as industrial operations and vehicle use, affects the PM quality in Kaohsiung City, Taiwan.

**Keywords:** Particulate matter , Public bike sites , Principal component analysis , Internet of things , Low-cost air sensor

## **Characteristics and Formation Mechanism of Surface Ozone in a Coastal Island of Southeast China: Influence of Sea-land Breezes and Regional Transport**

**Baoye Hu<sup>1,2,3</sup>, Taotao Liu<sup>1,2,3</sup>, Yuxiang Yang<sup>4</sup>, Youwei Hong<sup>1,2</sup>, Mengren Li<sup>1,2</sup>,  
Lingling Xu<sup>1,2</sup>, Hong Wang<sup>5</sup>, Naihua Chen<sup>4</sup>, Xin Wu<sup>1,2,3</sup>, Jinsheng Chen<sup>1,2</sup>**

**Source:** Aerosol and Atmospheric Chemistry, Volume: 19 | Issue: 8 | Pages: 1734-1748  
DOI: 10.4209/aaqr.2019.04.0193

The ozone (O<sub>3</sub>) concentrations in island cities are low due to the relatively low concentrations of O<sub>3</sub> precursors. However, Pingtan, a typical island city along the southeast coast of China, suffers from frequent O<sub>3</sub> pollution. In this study, one year of hourly O<sub>3</sub> concentration data collected from three sites (rural, suburban, and urban) on Pingtan were used to investigate the characteristics and formation mechanism of O<sub>3</sub> pollution. The results showed that the minimum O<sub>3</sub> concentrations measured at the three sites were larger than 55.53 μg m<sup>-3</sup>, which was likely caused by low NO titration over Pingtan. The O<sub>3</sub> concentrations in summer were low because of the East Asian monsoon. The daily maximum O<sub>3</sub> concentrations with sea and land breezes (SLBs) were higher than those without SLBs at all three sites (8.52, 9.84, and 14.30 μg m<sup>-3</sup> at the rural, suburban, and urban sites, respectively). In addition, SLBs amplified the diurnal variation in O<sub>3</sub> concentrations. Cluster analysis and the analysis of an episode of high O<sub>3</sub> concentration indicated that the developed Yangtze River Delta is the main source of O<sub>3</sub> in Pingtan. This study helps reveal the characteristics and formation mechanism of O<sub>3</sub> pollution in island cities.

**Keywords:** Ozone (O<sub>3</sub>) , Spatiotemporal variation, Transport, Sea and land breezes ,Island.

---

## **Emission Factors of NO<sub>x</sub>, SO<sub>2</sub>, PM and VOCs in Pharmaceuticals, Brick and Food Industries in Shanxi, China**

**Yao Hu<sup>1</sup>, Zhiyong Li<sup>1,2</sup>, Lei Wang<sup>1</sup>, Hongtao Zhu<sup>3</sup>, Lan Chen<sup>1,2</sup>, Xiaobiao Guo<sup>1,2</sup>, Caixiu An<sup>3</sup>, Yunjun Jiang<sup>3</sup>, Aiqin Liu<sup>3</sup>**

**Source:** Air Toxics Volume: 19 | Issue: 8 | Pages: 1785-1797  
DOI: 10.4209/aaqr.2019.06.0304

The acquisition of accurate emission factors (EFs) of pollutants is an inevitable step to the establishment of emission inventories for development of pollution control policies. The current studies were focused on large-scale industries (LSIs) although tremendous pollutants emitted from the small-scale industries (SSIs) with small coal-fired boilers (SCFBs) ascribe to the deficiency of pollutant removal facilities (RFs). A systematic field sampling and measurements conducted in 51 enterprises involving production of

pharmaceuticals, brick and food to obtain the EFs of SO<sub>2</sub>, NO<sub>x</sub>, PM, and VOCs (SNPV) associated with coal consumption (EF<sub>I</sub>), industrial output (EF<sub>II</sub>), and product yield (EF<sub>III</sub>). Among them, PM-RFs were all equipped except for 3 brick factories, no NO<sub>x</sub>- and VOCs-RFs were installed, and SO<sub>2</sub>-RFs were installed in part. Obvious fluctuations existed in EF<sub>I</sub> and EF<sub>II</sub> values among 51 companies owing to the differences of pollutant removal efficiencies, coal compositions, annual outputs, production processes, and products. Co-burning of coal and coal gangue (raw material) in brick production weakened the correlation between sulfur contents in coal and SO<sub>2</sub> EF<sub>I</sub> values. The using of organic solvents in drug making process promoted the emission of VOCs. SO<sub>2</sub> EFs in factories with RFs were much lower than those factories without RFs. SO<sub>2</sub> EFs dominated over those of PM and NO<sub>x</sub> among three kinds of enterprises, especially in brick companies. For EF<sub>I</sub> (in kg t<sup>-1</sup>), food industry possessed highest value for SO<sub>2</sub>, PM, and NO<sub>x</sub>, while the maximum value for VOCs occurred at pharmaceuticals industry. Due to the low output values of brick companies, their SNPV possessed the highest EF<sub>II</sub> compared to the other two kinds of factories. NO<sub>x</sub> EFs experienced lessen fluctuations than other pollutants among all the factories due to the different formation mechanism and no installation of NO<sub>x</sub> RFs. EF<sub>III</sub> showed various fluctuations due to the different product types.

**Keywords:** Emission factor , NO<sub>x</sub> , SO<sub>x</sub> , VOCs , Pharmaceutical industry ,Brick industry

---

## **Effects of Ambient PM<sub>2.5</sub> Collected Using Cyclonic Separator from Asian Cities on Human Airway Epithelial Cells**

**Pratiti H. Chowdhury<sup>1</sup>, Akiko Honda <sup>1</sup>, Sho Ito<sup>1</sup>, Hitoshi Okano<sup>1</sup>, Toshinori Onishi<sup>1,2</sup>, Makoto Higashihara<sup>1</sup>, Tomoaki Okuda<sup>3</sup>, Toshio Tanaka<sup>4</sup>, Seitarou Hirai<sup>4</sup>, Hirohisa Takano<sup>1</sup>**

**Source:** Air Pollution and Health Effects, Volume: 19 | Issue: 8 | Pages: 1808-1819

DOI: 10.4209/aaqr.2019.01.0016

Recent studies have shown that air pollution is intense and hazardous in Asia compared to other parts of the world due to the late and poor implementation of updated technology in automobiles and industry as well as to the high population density. Respiratory disease, including asthma, is exacerbated by air pollution. However, the effects of PM<sub>2.5</sub>, especially on respiratory allergies in Asian cities, have not yet been examined in detail. In this study, airway epithelial cells were exposed to crude PM<sub>2.5</sub> particles collected by cyclonic separation from three different Asian cities, namely, Sakai, Bangkok, and Taipei. We compared the cytotoxicity and inflammatory potential of the PM<sub>2.5</sub> from these cities by measuring IL-6 and IL-8. The samples from Sakai and Bangkok caused cytotoxic effects at a dose of 75 µg mL<sup>-1</sup> and, moreover, induced the release of IL-6 and IL-8 even at low doses. The release of these two interleukins was highly associated with fluoranthene derivatives, microbial factors (endotoxin and β-glucan), metals (e.g., Ti), and organic (OC2 and OC3) and elemental carbon (EC1) in the PM<sub>2.5</sub>. Thus, these components potentially contribute to

cellular damage and a pro-inflammatory response in the airway epithelial cells, and the effect depends on PM<sub>2.5</sub> sources in the locations.

**Keywords:** Crude PM<sub>2.5</sub> , Cyclone sampler , Cytotoxicity , Pro-inflammatory response

---

## **Speciated PM Composition and Gas and Particle Emission Factors for Diesel Construction Machinery in China**

**Qingyao Hu<sup>1</sup>, Cheng Huang <sup>1</sup>, Liping Qiao<sup>1</sup>, Yingge Ma<sup>1</sup>, Qiang Yang<sup>2</sup>, Wei Tang<sup>2</sup>, Min Zhou<sup>1</sup>, Shuhui Zhu<sup>1</sup>, Shengrong Lou<sup>1</sup>, Shikang Tao<sup>1</sup>, Yun Chen<sup>3</sup>, Li Li <sup>1</sup>**

**Source:** Aerosol and Atmospheric Chemistry, Volume: 19 | Issue: 8 | Pages: 1820-1833  
DOI: 10.4209/aaqr.2018.07.0272

On-board emission measurements were performed on nine diesel construction machines operated under real-world conditions in China. The emission factors (EFs) for NO<sub>x</sub>, CO, the total hydrocarbons, PM, and the particle number concentration were determined under actual operating conditions, i.e., during idling, moving, and working. To investigate the chemical composition of PM from diesel machinery, organic carbon (OC), containing particulate organic matter (POM); elemental carbon (EC); water-soluble ions (WSIs); and elements were also analyzed herein. OC was the most abundant component (contributing  $39.3 \pm 11\%$  of the mass), followed by EC ( $37.7 \pm 13\%$ ). POM species, including n-alkanes, hopanes, polycyclic aromatic hydrocarbons (PAHs), and n-fatty acids, contributed approximately 2.4–6.4% of the total PM mass. Compounds with 3 or 4 aromatic rings, including pyrene, phenanthrene, and fluoranthene, dominated the particulate PAHs, accounting for 62% of the total mass. These results are consistent with those of previous studies and can

**Keywords:** Non-road machinery, Emission factors, PM components, PAH emissions , Diesel emissions.

---

## **Meteorological Parameters and Gaseous Pollutant Concentrations as Predictors of Ground-level PM<sub>2.5</sub> Concentrations in the Beijing-Tianjin-Hebei Region, China**

**Xinpeng Wang , Wenbin Sun, Zhen Wang, Yahui Wang, Hongkang Ren**

**Source:** Aerosol and Atmospheric Chemistry, Volume: 19 | Issue: 8 | Pages: 1844-1855  
DOI: 10.4209/aaqr.2018.12.0449

Ground-level PM<sub>2.5</sub> concentrations—especially those during episodes of heavy pollution—are severely underestimated by mixed-effects models that ignore the effects of primary pollutant emissions and secondary pollutant conversion. In this work, meteorological

parameters and NO<sub>2</sub>, SO<sub>2</sub>, CO, and O<sub>3</sub> concentrations are introduced as predictors to a mixed-effects model to improve the estimated concentration of PM<sub>2.5</sub>, which is based on the Moderate Resolution Imaging Spectroradiometer (MODIS) aerosol optical depth (AOD). The Beijing-Tianjin-Hebei (JingJinJi) region is used as the study area. The model provides an overall cross-validation (CV) R<sup>2</sup> of 0.84 and root-mean-square prediction error (RMSE) of 33.91 μg m<sup>-3</sup>. The CV R<sup>2</sup> and RMSE of the proposed model are higher by 0.11 and lower by 9.16 μg m<sup>-3</sup>, respectively, than those of a model lacking gaseous pollutants as predictors. The R<sup>2</sup> and RMSE of the proposed model increases and decreases by 0.14 and 13.37 μg m<sup>-3</sup>, respectively, when PM<sub>2.5</sub> concentrations exceed 75 μg m<sup>-3</sup>. The high values predicted for the PM<sub>2.5</sub> concentration indicate a drastic improvement in the estimation, and the spatial distribution generated by the model for periods of heavy pollution is highly consistent with that inferred from monitoring data. Thus, the proposed model can be used to generate highly accurate maps of the PM<sub>2.5</sub> distribution for long-term and short-term exposure studies and to correctly classify exposure in heavily polluted areas.

**Keywords:** PM<sub>2.5</sub>, Aerosol optical depth, Gaseous pollutant, Heavy pollution, Mixed-effects model.

---

## Characteristics of Carbon Dioxide Emissions from a Seismically Active Fault

Duoxing Yang<sup>1</sup>, Qi Li<sup>2</sup>, Lianzhong Zhang<sup>3</sup>

**Source:** Control Techniques and Strategy Volume: 19 | Issue: 8 | Pages: 1911-1919

DOI: 10.4209/aaqr.2019.06.0282

Seismically active faults are key features of the earth, and earthquake-induced carbon dioxide released from natural faults has been detected. But the link between active fault deformation and amounts of carbon dioxide emission remains poorly understood. In this paper we monitor progressive carbon dioxide levels and strain signals from the boreholes in a seismically active fault, and show that the carbon dioxide variations are sensitive to the fault deformation over the same time scale of the observations. Therefore, we preliminarily propose a mass-wave propagation model (e.g., interaction of shock waves with advection-diffusion of mass, namely the gas hammer effect) to physically interpret carbon dioxide variations due to dilation or compaction of fluid paths in the natural fault. Of particular interest is that the penetration of shock waves into the natural fault mechanically influences carbon dioxide migration.

**Keywords:** Natural fault, Carbon dioxide emission, Shockwaves, Carbon dioxide capture and geological storage

---

## **Review of Effluents and Health Effects of Cooking and the Performance of Kitchen Ventilation**

**Yujiao Zhao 1,2, Lang Liu 1,2, Pengfei Tao<sup>3</sup>, Bo Zhang<sup>1,2</sup>, Chao Huan<sup>1,2</sup>, Xiaoyan Zhang<sup>1,2</sup>, Mei Wang<sup>1,2</sup>**

**Source:** Aerosol and Atmospheric Chemistry, Volume: 19 | Issue: 8 | Pages: 1937-1959  
DOI: 10.4209/aaqr.2019.04.0198

Cooking effluents are one of the most important sources of pollution in the indoor and outdoor environment. Exposure to cooking oil fumes (COFs) can increase the risk of many diseases. A healthy indoor environment and an energy-efficient ventilation system in kitchens are urgently demanded. This review is concerned with the current knowledge of the physical and chemical compositions of aerosols generated from typical cooking processes as reported in the literature. It is focused on the effects of cooking fuel, cooking oil, cooking temperature, cooking method, cooking style and other factors on the characteristics of cooking particles. The improvement measures in kitchen ventilation, supply air strategy and evaluation index for the kitchen environmental protection are also reviewed. It was found that the cooking process emits high concentrations of particulate matter (PM), and inhalable particles account for a high proportion, which may cause serious harm to human body. Coupled with various factors affecting the particle concentrations and particle size distribution, as well as the main chemical components groups used to characterize the cooking particles, include PAHs, fatty acids, dicarboxylic acids, n-alkanes, sterols, monosaccharide anhydrides, metals and ions. Using an appropriate ventilation system and some auxiliary measures can effectively reduce cooking oil fumes pollution.

**Keywords:** Cooking particles, Indoor air quality, Health effect, Kitchen ventilation.

---

## **Characteristics, Formation Mechanisms and Potential Transport Pathways of PM<sub>2.5</sub> at a Rural Background Site in Chongqing, Southwest China**

**Chao Peng<sup>1,2</sup>, Mi Tian <sup>1,7</sup>, Yang Chen<sup>1</sup>, Huanbo Wang<sup>1</sup>, Leiming Zhang<sup>3</sup>, Guangming Shi<sup>1,4</sup>, Yuan Liu<sup>1</sup>, Fumo Yang <sup>1,4,5</sup>, Chongzhi Zhai<sup>6</sup>**

**Source:** Aerosol and Atmospheric Chemistry, Volume: 19 | Issue: 9 | Pages: 1980-1992  
DOI: 10.4209/aaqr.2019.01.0010

Daily PM<sub>2.5</sub> samples were collected at a rural background station (JinYun) located in Chongqing across four consecutive seasons from October 2014 to July 2015. The major water-soluble inorganic ions (WSIIs), organic carbon (OC) and elemental carbon (EC) were analyzed, and their chemical characteristics, transport pathways and potential source regions were investigated. The average annual PM<sub>2.5</sub> concentration was  $56.2 \pm 31.0 \mu\text{g m}^{-3}$ .

3, of which secondary inorganic aerosol (SNA) and carbonaceous aerosols composed 41.0% and 29.4%, respectively. Higher concentrations of and contributions from SO<sub>4</sub><sup>2-</sup>, which were likely caused by the secondary transformation of SO<sub>2</sub> into SO<sub>4</sub><sup>2-</sup>, were observed in summer than in autumn and spring. Additionally, transportation from the urban area of Chongqing (Yubei) played an important role in elevating the SO<sub>4</sub><sup>2-</sup> during this season. Although the accumulation of PM<sub>2.5</sub> during pollution episodes in winter was also due to aqueous-phase reactions, based on the entire year, NO<sub>3</sub><sup>-</sup> formation may have been primarily driven by homogeneous gas-phase reactions. Furthermore, the aerosol environment was ammonium-rich, and NH<sub>4</sub><sup>+</sup> formation promoted the production of NO<sub>3</sub><sup>-</sup> at lower temperatures. The carbonaceous component, which consisted of 81.0–84.6% OC, exhibited higher concentrations in winter than in the other seasons; 50.0–77.2% of the total OC, in turn, was contributed by primary organic carbon (POC). Potential source contribution function (PSCF) analysis suggests that the site was mainly affected by regional pollution originating in the southwestern and northern areas of Chongqing.

**Keywords:** PM<sub>2.5</sub>, Rural background site, Chemical transformation, Potential transport pathways.

---

## **Spatial Distribution and Multiscale Transport Characteristics of PM<sub>2.5</sub> in China**

**Qing Wang, Kun Luo, Jianren Fan, Xiang Gao, Kefa Cen**

**Source:** Aerosol and Atmospheric Chemistry, Volume: 19 | Issue: 9 | Pages: 1993-2007  
DOI: 10.4209/aaqr.2019.04.0202

The Weather Research and Forecasting (WRF) model coupled with the Community Multiscale Air Quality (CMAQ) model was used to simulate the temporal and spatial distribution and the multiscale transport patterns of PM<sub>2.5</sub> in 2 large regions (“NORTH” and “SOUTH”), 7 small regions (“North,” “Northeast,” “East,” “Center,” “South,” “Southwest,” and “Northwest”) and 31 provinces in China during January and July of 2015. The simulated PM<sub>2.5</sub> concentrations were compared with the observed values to assess the accuracy of WRF-CMAQ. During January and July, local emissions contributed the majority of the PM<sub>2.5</sub>, with their percentage exceeding 60% in 7 of the regions. External transport was the dominant source of PM<sub>2.5</sub> in some of the provinces, such as Shanghai and Qinghai, whereas local emission was the main contributor in others, such as Hebei and Xinjiang. We also identified the primary PM<sub>2.5</sub> source in each region, the results of which indicated distinctly different regional transport patterns among the provinces and regions of China.

**Keywords:** Particulate Matter, Regional transport, WRF-CMAQ model, Multiscale regions.

---

## Source Apportionment of PM<sub>2.5</sub> at Urban and Suburban Sites in a Port City of Southeastern China

Shui-Ping Wu <sup>1,2</sup>, Chao Xu<sup>1</sup>, Lu-Hong Dai<sup>1</sup>, Ning Zhang<sup>1</sup>, Ya Wei<sup>1</sup>, Yang Gao<sup>1</sup>, Jin-Pei Yan<sup>3</sup>, James J. Schwab<sup>4</sup>

**Source:** Aerosol and Atmospheric Chemistry, Volume: 19 | Issue: 9 | Pages: 2017-2031  
DOI: 10.4209/aaqr.2019.01.0007

Shipping emissions potentially contribute to the degradation of air quality in port cities. In this study, PM<sub>2.5</sub> samples were collected from two sites at different distances from the shipping channel of Xiamen Port in southeastern China between November 2015 and May 2018 and analyzed for their chemical compositions, which included water-soluble ions, carbonaceous species, and elements. The average annual PM<sub>2.5</sub> mass concentrations were  $55.8 \pm 22.7 \mu\text{g m}^{-3}$  and  $56.5 \pm 24.5 \mu\text{g m}^{-3}$  at the urban and suburban sites, respectively, with the lowest values in summer and the highest in winter/spring. Significantly higher values for vanadium (V) and nickel (Ni) were found at the urban site due to the shorter distance between this location and the shipping channel. Using a PMF model, six source factors were identified: sulfate and shipping emissions (16.6–20.9%), secondary nitrate and chloride (14.7–17.3%), fugitive dust (16.9–23.0%), industrial emissions (5.5–7.0%), primary organic aerosol (14.1–14.8%), and traffic emissions and biomass burning (23.8–24.6%). Potential source contribution function analysis indicated that air masses from the South China Sea contributed significantly to the shipping emissions. The PMF-based method did not distinguish primary shipping emissions from secondary sulfate. When a V-based method was used, the primary PM<sub>2.5</sub> from shipping emissions plus its associated secondary sulfate was shown to contribute 5.5–8.9% of the ambient PM<sub>2.5</sub> on average. The results from the V-based method exhibited strong positive correlations with those of the PMF-based method. Considering the potential negative effect on air quality and the expanding international maritime trade in the long term, our research indicates that policies and regulations for controlling shipping emissions are necessary in all major port cities, including those outside the domestic emission control areas of China.

**Keywords:** Shipping emissions, PM<sub>2.5</sub>, Source apportionment, PMF, Vanadium.

---

## Emissions of NO<sub>x</sub>, PM, SO<sub>2</sub>, and VOCs from Coal-fired Boilers Related to Coal Washing, Iron-steel Production, and Lime and Gypsum Making in Shanxi, China

Zhiyong Li <sup>1,2</sup>, Yutong Wang<sup>1</sup>, Yao Hu<sup>1</sup>, Lan Chen<sup>1,2</sup>, Hongtao Zhu<sup>1,2</sup>

**Source:** Air Toxics Volume: 19 | Issue: 9 | Pages: 2056-2069  
DOI: 10.4209/aaqr.2019.07.0363



The accurate pollutant inventories are important for the development of pollution control policies, which further rely on detailed emission factors (EFs) to some extent. However, detailed air pollutant EFs for coal-fired boilers (CFBs) associated with coal washing (CW), iron-steel production (IS), and lime and gypsum manufacturing (LG) are lacking in China at present. CFBs of 91 enterprises involving CW, IS, and LG were investigated to obtain their pollutant EFs associated with coal consumption (EFI, kg t<sup>-1</sup>), outputs (EFII, kg MY<sup>-1</sup>), and product yields (EFIII, kg t<sup>-1</sup>) through field investigation and sampling. The weak correlation between EFs of 4 air pollutants vs. corresponding removal efficiencies (REs), and EFs vs. coal compositions among three industries implied the impact of actual combustion conditions and operating status of removal facilities (RFs). EFs of VOCs from small-scale CW enterprises (SSEs) were much higher than those of large- and medium-scale enterprises (LSEs and MSEs) owing to the incomplete combustion of coal. Also the SO<sub>2</sub> and NO<sub>x</sub> EFs of CW increased with decreasing enterprise scale, while the maximum PM occurred at MSEs. The mean EFI values of LG for the 4 air pollutants was PM > NO<sub>x</sub> > VOCs > SO<sub>2</sub>, differed from PM > SO<sub>2</sub> > NO<sub>x</sub> for the IS, VOCs > PM > NO<sub>x</sub> > SO<sub>2</sub> for the CW LSEs and MSEs, and VOCs > NO<sub>x</sub> > PM > SO<sub>2</sub> for the CW SSEs, which suggested the influence of combined factors including coal composition, production processes, combustion conditions, and pollutant removal technologies and removal efficiencies. EFI values for the 8 IS factories followed the order PM > SO<sub>2</sub> > NO<sub>x</sub>, while they were PM > NO<sub>x</sub> > SO<sub>2</sub> for EFII values due to their output fluctuation. For the EFII and EFIII values of SO<sub>2</sub>, NO<sub>x</sub>, and PM, LG dominated within the 3 industries, while the corresponding maximum VOCs occurred at the CW industry.

**Keywords:** Emission factor , Coal washing , Lime-gypsum making , SO<sub>2</sub> , NO<sub>x</sub> , VOCs

---

## Seasonal Variations, Source Apportionment, and Health Risk Assessment of Heavy Metals in PM<sub>2.5</sub> in Ningbo, China

Yue Wu<sup>1</sup>, Beibei Lu<sup>2</sup>, Xinlei Zhu<sup>3</sup>, Aihong Wang<sup>2</sup>, Meng Yang<sup>4</sup>, Shaohua Gu<sup>2</sup>, Xiaoxia Wang<sup>5</sup>, Pengbo Leng<sup>2</sup>, Kristina M. Zierold<sup>6</sup>, Xiaohai Li<sup>2</sup>, Ke Kerri Tang<sup>6</sup>, Lanyun Fang<sup>2</sup>, Ruixue Huang<sup>1</sup>, Guozhang Xu<sup>2</sup>, Lv Chen<sup>1</sup>

**Source:** Air Pollution and Health Effects, Volume: 19 | Issue: 9 | Pages: 2083-2092

DOI: 10.4209/aaqr.2018.12.0452

In order to assess the seasonal variations, potential sources, and health risks of heavy metals in fine particulate matter (PM<sub>2.5</sub>), PM<sub>2.5</sub> samples (n = 96) were collected between March 2015 and February 2016 in Ningbo, China. Twelve heavy metals (Sb, As, Cd, Cr, Pb, Mn, Ni, Se, Tl, Al, Be, and Hg) found in the PM<sub>2.5</sub> were analyzed by inductively coupled plasma mass spectrometry (ICP-MS). We used enrichment factors and principal component analysis/absolute principal component scores (PCA/APCS) to determine the sources of these heavy metals, and models from the United States Environmental Protection Agency (EPA) to assess both the carcinogenic and non-carcinogenic risks to adults and children. Results showed that the average annual mass concentration of the PM<sub>2.5</sub> was 62.7 μg m<sup>-3</sup>, which exceeded the limit specified in the Chinese

National Ambient Air Quality Standards (NAAQS). The average annual concentrations of the Pb, Cd, and As were  $57.2 \text{ ng m}^{-3}$ ,  $1.5 \text{ ng m}^{-3}$ , and  $4.7 \text{ ng m}^{-3}$ , respectively, which were below the NAAQS limits. The highest total concentrations for the heavy metals occurred in winter, whereas the lowest concentrations were observed in summer. Enrichment factor analysis indicated that the Sb, Cd, Pb, Se, As, and Tl were mainly from anthropogenic sources. Additionally, source apportionment by PCA/APCS identified four major sources for the studied metals: coal combustion and motor vehicles (46.3%), soil and construction dust (37.1%), steelworks (6.9%), and other smelting industries (6.8%). The carcinogenic risk of heavy metals in Ningbo fell within the safe level of exposure for both children and adults. However, the total non-carcinogenic risk exceeded the safe level ( $HI = 1.38$ ), which warrants further research on sources of air pollution and measures for controlling pollutants in Ningbo, China.

**Keywords:** PM2.5 , Heavy metal , Enrichment factor, Principal component analysis/absolute principal component scores , Health risk assessment.

---

## **Is Morning or Evening Better for Outdoor Exercise? An Evaluation Based on Nationwide PM2.5 Data in China**

**Xiu-Feng Ni<sup>1</sup>, Shu-Chuan Peng<sup>1</sup>, Ji-Zhong Wang<sup>2,3</sup>**

**Source:** Aerosol and Atmospheric Chemistry, Volume: 19 | Issue: 9 | Pages: 2093-2099  
DOI: 10.4209/aaqr.2019.07.0362

Proper sports exercise is important to health, both physically and mentally. However, the benefits from outdoor exercise may be impaired by potential health risks due to air pollution. As air pollution varies spatially and temporally within a day and a season, it is important to know the proper time for outdoor exercise in order to avoid or minimize potential health risks from inhalation of atmospheric particulate matter such as PM2.5 (i.e., particulate matter having a diameter less than  $2.5 \mu\text{m}$ ). The present study determined the increment of inhalation exposure (referred to as  $\Delta F_{in}$ ) to PM2.5 during outdoor exercise due to differences in PM2.5 concentrations between indoor and outdoor environments. Based on PM2.5 data collected by a total of 1505 air quality monitoring stations across 367 Chinese cities in 2014, we investigated the variation of  $\Delta F_{in}$  between morning (6–8 AM) and evening (6–8 PM) periods in different provinces or districts across China as well as seasonal variations of  $\Delta F_{in}$ . The results revealed an overall decreasing gradient in  $\Delta F_{in}$  from the morning to evening periods in most Chinese regions, suggesting that outdoor exercise in the evening leads to less inhalation exposure to PM2.5 and should be given preference over morning exercise. However, the patterns also varied seasonally and geographically, leading to different health advisories on the choice of exercise time.

**Keywords:** PM2.5, Inhalation exposure, Morning exercise, Evening exercise.

---

## Multifractal Cascade Analysis on the Nature of Air Pollutants Concentration Time Series over China

Xin Gao , Xuan Wang, Hongbin Shi

**Source:** Aerosol and Atmospheric Chemistry, Volume: 19 | Issue: 9 | Pages: 2100-2114  
DOI: 10.4209/aaqr.2018.10.0364

This study investigates the temporal multifractal cascade behaviors of air pollution in major cities of China by using 1-year data of the hourly time series of six pollutants (PM<sub>2.5</sub>, PM<sub>10</sub>, CO, NO<sub>2</sub>, O<sub>3</sub>, and SO<sub>2</sub>) and the air quality index (AQI) as model inputs. Given that the air pollution time series generally exhibit positive skewness with a heavy tail, a stable distribution with four parameters, such as Levy  $\alpha$ -stable distribution, reasonably fits the frequency distributions of the data over the entire range. The periodicity and nonstationarity shared by the series are also spectrally analyzed, and all of the pollutants display a daily and semi-daily cycle as well as two dynamical regimes with a cut-off scale around 11 days. Using universal multifractal analysis, the two parameters ( $\alpha$  and C1) in an air pollution system are measured, and their underlying significance is also addressed via analogues of the Monte Carlo simulation data. Moreover, self-organizing criticality analysis on the data of the air pollution index (API) indicates first-order multifractal phase transitions, with an estimated interval of the order of the moment ( $qD$ ) that varies between 1.95 and 2.98. Finally, downscaled performances of multifractal cascade models are numerically evaluated, demonstrating that log-normal and log-Poisson models, but not  $\alpha$ ,  $\beta$ , binomial, and uniform models, can effectively recover extreme values.

**Keywords:** Cascade, Multifractal, Air pollutant, Time series, Downscaling.

---

## Performance Evaluation of a Very-low-volume Sampler for Atmospheric Particulate Matter

Maria Catrambone<sup>1</sup>, Silvia Canepari<sup>2</sup>, Marina Cerasa<sup>1</sup>, Tiziana Sargolini<sup>1</sup>, Cinzia Perrino<sup>1</sup>

**Source:** Aerosol and Atmospheric Chemistry, Volume: 19 | Issue: 10 | Pages: 2160-2172  
DOI: 10.4209/aaqr.2019.04.0195

A cheap and small device for sampling atmospheric particulate matter (PM) has been recently developed. It works at a very low flow rate (0.5 L min<sup>-1</sup>) and is able to collect the atmospheric aerosol on filters, allowing subsequent chemical analyses. The samplings have a long duration (1–2 months), and the devices can be used to make cheap networks over a territory. These very-low-volume samplers (VLVS) can be used to trace long-term concentration variations and to draw up concentration maps of PM and its chemical components.

The performance of the VLVS was evaluated in terms of measurement repeatability and of agreement with the results obtained when using a 2.3 m<sup>3</sup> h<sup>-1</sup> reference sampler (REF). The study period was 1 year. The considered PM components were ions, polycyclic aromatic hydrocarbons (PAHs), levoglucosan and elements.

The repeatability of the measurements was very good for all the examined PM components: the standard deviation of 3 replicates (co-located samplers) over 9 measurement periods was in the range 2.0–5.5% for ions, 10–17% for PAH, 5.2% for levoglucosan and 5.6–16% for elements. It was 8.2% for the PM mass concentration. This satisfactory performance indicates that the VLVSs can be reliably used to evaluate the spatial variability and to draw concentration maps of PM and PM components.

A very good agreement with the reference sampler was obtained for ions, with the only exception of ammonium nitrate and ammonium chloride (VLVS values were up to 10–20% lower than the reference values), levoglucosan and elements. In the case of PAH, instead, the ratio VLVS/REF was in the range 1.2–1.6 for 4-ring congeners and 0.4–0.8 for 5- and 6-ring congeners. For all the congeners, anyway, these typical ratios were kept, with small variations, during the whole study period.

**Keywords:** Validation, Sampling artifacts, Sampling duration, Spatial distribution, Concentration maps.

---

## On the Performance Parameters of PM<sub>2.5</sub> and PM<sub>1</sub> Size Separators for Ambient Aerosol Monitoring

Xinghua Li <sup>1</sup>, Bing Ruan<sup>1</sup>, Philip K. Hopke<sup>2,3</sup>, Tariq Mehmood<sup>1</sup>

**Source:** Aerosol and Atmospheric Chemistry, Volume: 19 | Issue: 10 | Pages: 2173-2184  
DOI: 10.4209/aaqr.2019.03.0103

The performance of particle size separators that are characterized by their cutpoint ( $d_{50}$ ) and the steepness of their penetration curves ( $\sigma_g$ ) is a critical feature of measurement methods for ambient PM<sub>2.5</sub> and PM<sub>1</sub> monitoring. The parameters  $d_{50}$  and  $\sigma_g$  for PM<sub>2.5</sub> size separators are regulated in the official measurement methods of many countries and regions. However, those parameters for PM<sub>1</sub> size separators have not been previously specified. The interaction of particle size distributions (PSDs) and the particle size separator performance characteristics has significant influence on the PM sampling results. Atmospheric PSDs for each of the four seasons covering a range of particulate pollution concentrations were measured in urban Beijing. The relative differences (RD) between estimated PM<sub>2.5</sub>/PM<sub>1</sub> sampler concentrations and actual concentrations associated with the interaction between performance characteristics of size separator and actually measured urban PSDs, as well as for three idealized ambient PSDs, have been systematically investigated. For the PM<sub>2.5</sub> size separator, when tolerance of cutpoint is  $2.5 \pm 0.2 \mu\text{m}$  and  $\sigma_g$  is no greater than 1.3, RD values for most typical urban atmospheric aerosol conditions were within the permissible error range ( $\pm 5\%$ ). For the PM<sub>1</sub> size

separator, when tolerance of cutpoint and sharpness is  $1.00 \pm 0.02 \mu\text{m}$  and  $\sigma$  no greater than 1.2, respectively, the RD values for typical urban atmospheric aerosol conditions are within the permissible range. Those parameters could also meet the requirements for sampling of the idealized ambient aerosol distribution.

**Keywords:** PM2.5, PM1, Size separator, Cutpoint, Sharpness, Particle size distribution.

---

## **Chemical Characteristics, Sources Apportionment, and Risk Assessment of PM2.5 in Different Functional Areas of an Emerging Megacity in China**

**Xiaohan Liu, Nan Jiang, Xue Yu, Ruiqin Zhang, Shengli Li, Qiang Li, Panru Kang**

**Source:** Aerosol and Atmospheric Chemistry, Volume: 19 | Issue: 10 | Pages: 2222-2238  
DOI: 10.4209/aaqr.2019.02.0076

The mass concentration, chemical composition, and source apportionment of PM2.5 in the urban, industrial, scenic, traffic, and rural sites of Zhengzhou were studied from February to December of 2016. The average annual concentration of PM2.5 in these five sites was  $119 \mu\text{g m}^{-3}$ , which was lower than the annual average between 2013 and 2015. However, PM2.5 pollution remains serious in Zhengzhou. PM2.5, elemental carbon (EC), organic carbon (OC), and water-soluble inorganic ions (WSIIs)—with the exception of  $\text{F}^-$ ,  $\text{Ca}^{2+}$ , and  $\text{Mg}^{2+}$ —showed a relatively homogeneous spatial distribution in this area. Among these pollutants, WSIIs, carbonaceous species (EC and OC), and elements accounted for 47.7%, 14.4%, and 9.6% of PM2.5 concentration in Zhengzhou, respectively. The annual OC/EC ratio in Zhengzhou was 8.3, which indicates the possible presence of a secondary organic carbon. Six main sources of PM2.5 in Zhengzhou, namely, soil dust (15.1%), coal combustion (17.6%), secondary aerosol (35.1%), vehicle traffic (17.3%), industry (7.3%), and biomass burning (7.7%), were identified by using a positive matrix factorization model. The results of the back trajectory and potential source contribution function analysis revealed that the air mass from regions of the Shandong and Hubei Provinces aggravated the pollution in Zhengzhou, and Puyang, Hebi, Xinxiang, and Kaifeng were the main potential sources of PM2.5, respectively. The carcinogenic risks of As to children through the ingestion pathway exceeded the acceptable level. The findings of this work can provide an in-depth understanding of the PM2.5 pollution in Zhengzhou.

**Keywords:** PM2.5, Spatial distribution, Positive matrix factorization, Coefficients of divergence, Health risk assessment.

---

## **Current Status of Fine Particulate Matter (PM<sub>2.5</sub>) in Vietnam's Most Populous City, Ho Chi Minh City**

**To Thi Hien 1, Nguyen Doan Thien Chi<sup>1</sup>, Nguyen Thao Nguyen<sup>1</sup>, Le Xuan Vinh<sup>1</sup>, Norimichi Takenaka<sup>2</sup>, Duong Huu Huy<sup>3</sup>**

**Source:** Aerosol and Atmospheric Chemistry, Volume: 19 | Issue: 10 | Pages: 2239-2251  
DOI: 10.4209/aaqr.2018.12.0471

This paper provides insights into fine particulate matter pollution in the urban atmosphere of Ho Chi Minh City (HCMC), the most populous city in Vietnam. Fine particulate matter (PM<sub>2.5</sub>) samples were collected daily at five exposed sites from March 2017 to March 2018. PM<sub>10</sub> data (daily) and real-time PM<sub>2.5</sub> (hourly) data were recorded concurrently at a roadside site. Daily particulate pollutant levels (i.e., PM<sub>2.5</sub> and PM<sub>10</sub>) were determined using the gravimetric method using an impact sampler, and real-time PM<sub>2.5</sub> data were measured using a continuous monitor. The measured PM<sub>2.5</sub> concentrations varied from 10.4 to 110.8  $\mu\text{g m}^{-3}$ , with an annual mean of  $36.3 \pm 13.7 \mu\text{g m}^{-3}$ . All annual mean concentrations at the exposed sites exceeded the value limits of the Vietnamese standard (25  $\mu\text{g m}^{-3}$ ) and World Health Organization air quality guideline (10  $\mu\text{g m}^{-3}$ ), indicating high health risk at these sites. Although the sampling sites varied in their exposure levels, they exhibited very strong correlations and low differences in PM<sub>2.5</sub> levels. Diurnal variation with a pronounced peak 2 hours after the morning rush hour was observed. This peak is likely attributable to not only primary sources (e.g., traffic-related sources) but also secondary aerosol formation. The urban atmosphere of HCMC was affected by strong local emission sources, as evidenced by the pronounced peak during morning rush hour as well as the significant negative correlation between PM<sub>2.5</sub> and wind speed. In addition, monthly PM<sub>2.5</sub> levels exhibited remarkable seasonal variability, with the lowest and highest levels observed during the rainy and dry seasons, respectively. However, elevated PM<sub>2.5</sub> levels were observed during the months with heavy rains, highlighting the influence of strong emission sources, likely the biomass burning of rice straw residues in the Mekong Delta area.

**Keywords:** Ho Chi Minh City, PM<sub>2.5</sub>, Urban air pollution, Tropical climate.

---

## **Chemical Composition and Health Risk of PM<sub>2.5</sub> from Near-ground Firecracker Burning in Micro Region of Eastern Taiwan**

**Huazhen Shen<sup>1,2</sup>, Chung-Shin Yuan<sup>2</sup>, Chun-Chung Lu<sup>2</sup>, Yubo Jiang<sup>2</sup>, Guohua Jing<sup>1</sup>, Gongren Hu<sup>1</sup>, Ruilian Yu<sup>1</sup>**

**Source:** Aerosol and Atmospheric Chemistry, Volume: 19 | Issue: 10 | Pages: 2252-2266  
DOI: 10.4209/aaqr.2019.08.0410



The randomness of firecracker-burning site and the overlapping impact of multi-sources makes the source apportionment of PM<sub>2.5</sub> during the firecracker burning events more difficult. To investigate the influences of the downwind distance to the firecracker-burning site on the temporospatial distribution of PM<sub>2.5</sub> and public health risk, PM<sub>2.5</sub> were sampled at three sites adjacent to a fixed firecracker-burning route accompanied with annual pilgrimage activity during the Lantern Festival in Taitung, Taiwan, which had a low background PM<sub>2.5</sub> concentration. The metallic elements, water-soluble ions, carbonaceous contents were analyzed. The potential sources were identified using positive matrix factorization. Finally, the health risks were assessed by calculating the hazard quotient and incremental lifetime carcinogenic risk, respectively. The results showed that the average concentration of PM<sub>2.5</sub> on the event days increased by approximately five-fold compared to the non-event days. The increase of chemical components varied significantly from the distance to the burning site. The concentrations of K, Fe, Al, Mg, K<sup>+</sup>, Cl<sup>-</sup> and OC rose by 6–14 times at one site close to a site with intensive firecracker burning, while increased by 2–6 times at one site far away from the firecracker burning sites. The PM<sub>2.5</sub> increment on the event days was mostly attributed to firecracker burning, kitchen fumes, and mobile sources. The health risk assessment results showed that the hazard index differed between the sampling sites. Furthermore, the cancer risk of one site close to the firecracker burning site was over the threshold, while that far away from the site was below the threshold.

**Keywords:** PM<sub>2.5</sub>, Firecracker burning, Chemical composition, PMF, Health risk.

---

## **Molecular Compositions and Sources of Organic Aerosols from Urban Atmosphere in the North China Plain during the Wintertime of 2017**

**Xiaodi Liu<sup>1</sup>, Jingjing Meng<sup>1,2</sup>, Zhanfang Hou<sup>1,2</sup>, Li Yan<sup>3</sup>, Gehui Wang<sup>2,4</sup>, Yanan Yi<sup>1</sup>, Benjie Wei<sup>1</sup>, Mengxuan Fu<sup>1</sup>, Jianjun Li<sup>2</sup>, Junji Cao<sup>2</sup>**

**Source:** Aerosol and Atmospheric Chemistry, Volume: 19 | Issue: 10 | Pages: 2267-2280  
DOI: 10.4209/aaqr.2019.08.0418

PM<sub>2.5</sub> samples were collected from Liaocheng, a typical city in the North China Plain, during a winter haze episode around 2017 Chinese Spring Festival (Lunar New Year, LNY) to investigate the impact of firework on organic aerosols. A comparison of PM<sub>2.5</sub> concentrations during different periods, with different air mass origins, and under different pollution situations was done. Organic compounds including normal alkanes (n-alkanes), polycyclic aromatic hydrocarbons (PAHs), saccharides, and organic acids in PM<sub>2.5</sub> aerosols were determined by GC/MS. Sources were analyzed by diagnostics ratios and principal component analysis/multiple linear regression (PCA/MLR) model. The results showed that fireworks burning has significant impacts on fine particle pollution. During the haze period, a sharp increase in n-alkanes, PAHs, saccharides, and fatty acids were observed, but the influence of fireworks burning on n-alkanes concentration is minor. The concentrations of carcinogenic PAHs during haze and LNY periods were more than three times higher than those in the clean period, indicating that PAHs were more carcinogenic during the two periods. In addition, the estimated ILCR for children and adults were both about three

times higher than those in the clean periods, suggesting a moderate potential carcinogenic risk in Liaocheng. The higher concentration and the dominance of levoglucosan in the total saccharides suggested that the biomass burning is the predominance source of saccharides. Both the ratios of C18:1/C18:0 and BaP/BeP were the highest during the haze period, indicating that aerosols in the haze period were more oxidized. According to the source precise molecular tracers and the PCA-MLR model, coal combustion, biomass burning, and vehicle emissions were the major sources of organic compounds in PM<sub>2.5</sub> aerosols during the winter in Liaocheng, cooking activity and firework burning had impact on organic aerosols obviously during LNY. Our data provided first analysis of the molecular distributions and sources of organic aerosols during Chinese Spring Festival in Liaocheng and their potential effects on human health.

**Keywords:** Organic compounds, PM<sub>2.5</sub>, Fireworks burning, Source identification, Health risk.

---

## **Comparative Study of PAHs in PM<sub>1</sub> and PM<sub>2.5</sub> at a Background Site in the North China Plain**

**Yan Zhang<sup>1</sup>, Lingxiao Yang<sup>1,2</sup>, Ying Gao<sup>1</sup>, Jianmin Chen<sup>1,2</sup>, Yanyan Li<sup>1</sup>, Pan Jiang<sup>1</sup>, Junmei Zhang<sup>1</sup>, Hao Yu<sup>3</sup>, Wenxing Wang<sup>1</sup>**

**Source:** Aerosol and Atmospheric Chemistry, Volume: 19 | Issue: 10 | Pages: 2281-2293  
DOI: 10.4209/aaqr.2018.12.0462

Polycyclic aromatic hydrocarbons (PAHs) are carcinogenic and mutagenic. They bounded in atmospheric fine (PM<sub>2.5</sub>) and submicron (PM<sub>1</sub>) particles severely affect human health. To characterize 18 PAHs at a background site (Mount Tai) in the heavily polluted North China Plain (NCP), PM<sub>1</sub> and PM<sub>2.5</sub> samples were collected in the autumn of 2014. The sampling periods were classified into clean conditions and polluted conditions according to PM<sub>2.5</sub> concentration. Biomass burning condition was selected from polluted conditions to clarify the impact of biomass burning to PAHs concentrations. The concentrations of  $\Sigma$ 18 PAHs were 14.5 and 24.5 ng m<sup>-3</sup> and the contents were 515 and 607  $\mu$ g g<sup>-1</sup> in PM<sub>1</sub> and PM<sub>2.5</sub>, respectively. Three-ring PAHs were the primary contributors to the total PAHs. The major PAHs sources at Mount Tai were pyrogenic and traffic emission. Diesel combustion played more significant role to the emission of PM<sub>1</sub>-bound PAHs, while wood burning source was more obvious for PM<sub>2.5</sub>-bound PAHs. PAHs concentrations and cancer risks were the highest during biomass burning condition compared with those during polluted and clean conditions. The lifetime accumulated cancer risk of PM<sub>1</sub>-bound PAHs was considered to be acceptable, whereas it elevated to “potential risk” (10<sup>-6</sup>) for adults (30–70 years old) exposed to PM<sub>2.5</sub>-bound PAHs. The Concentration-weighted trajectory (CWT) model indicated long-distance transport from Northwest China was the major source of PM<sub>1</sub>-bound PAHs under the clean conditions. Compare with clean conditions, PAHs were more strongly influenced by short-distance transported air masses from the South of Shandong Province under the polluted conditions.



**Keywords:** Polycyclic aromatic hydrocarbon, Biomass burning, Health risk assessment, Source identification, CWT model.

---

## **Analysis of PAHs Associated with PM10 and PM2.5 from Different Districts in Nanjing**

**Xiansheng Liu<sup>1,2,3</sup>, Jürgen Schnelle-Kreis<sup>2</sup>, Brigitte Schloter-Hai<sup>2</sup>, Lili Ma<sup>1</sup>, Pengfei Tai<sup>4</sup>, Xin Cao<sup>2,3</sup>, Cencen Yu<sup>1</sup>, Thomas Adam<sup>2,5</sup>, Ralf Zimmermann<sup>2,3</sup>**

**Source:** Aerosol and Atmospheric Chemistry, Volume: 19 | Issue: 10 | Pages: 2294-2307  
DOI: 10.4209/aaqr.2019.06.0301

Nanjing has areas with different degrees of pollution and is therefore predestined for the analysis of particle phase polycyclic aromatic hydrocarbons (P-PAHs) in different functional areas and their correlation with the latter. The functional sites include a background area (BGA), an industrial area (IDA), a traffic area (TFA), a business area (BNA) and a residential area (RDA), where parameters such as PAH composition, content, carcinogenic and mutagenic potencies were analyzed. The results revealed increasing P-PAH contents (PM2.5, PM10) in the following order: BGA (14.02 ng m<sup>-3</sup>, 38.45 ng m<sup>-3</sup>) < BNA (16.33 ng m<sup>-3</sup>, 44.13 ng m<sup>-3</sup>) < TFA (17.13 ng m<sup>-3</sup>, 48.31 ng m<sup>-3</sup>) < RDA (21.11 ng m<sup>-3</sup>, 61.03 ng m<sup>-3</sup>) < IDA (50.00 ng m<sup>-3</sup>, 93.08 ng m<sup>-3</sup>). Thereby, the P-PAH content in the industrial area was significantly higher than in the other functional zones ( $P < 0.01$ ). Furthermore, the gas phase PAH concentrations were also estimated by the G/P partitioning model and the total PAH toxicity was assessed applying toxicity equivalent factors ( $\sum\text{BaPTEF}$ ) and mutagenicity equivalent factors ( $\sum\text{BaPMEF}$ ). Finally, the incremental lifetime cancer risk (ILCR) value of children and adolescents in Nanjing was higher than that of adults.

**Keywords:** Particle phase, PAHs, Different functional areas, Toxicity assessment, Incremental lifetime cancer risk.

---

## **Fine Particulate Matter and Ozone Pollution in the 18 Cities of the Sichuan Basin in Southwestern China: Model Performance and Characteristics**

**Xue Qiao<sup>1,2,3</sup>, Hao Guo<sup>3</sup>, Pengfei Wang<sup>3</sup>, Ya Tang<sup>4</sup>, Qi Ying<sup>5</sup>, Xing Zhao<sup>6</sup>, Wenye Deng<sup>7</sup>, Hongliang Zhang<sup>3,8</sup>**

**Source:** Aerosol and Atmospheric Chemistry, Volume: 19 | Issue: 10 | Pages: 2308-2319  
DOI: 10.4209/aaqr.2019.05.0235

The Sichuan Basin (SCB) is located in southwestern China and has a total population of 108.1 million across 18 cities, including the 2 largest in western China (Chengdu and

Chongqing). As most air quality monitoring stations are located in urban areas, we simulated the PM<sub>2.5</sub> (i.e., particulate matter with an aerodynamic diameter < 2.5 μm) and ozone (O<sub>3</sub>) in the entire SCB during winter (December 2014–February 2015) and summer (June–August 2015) by using the Weather Research and Forecasting (WRF) and the Community Multi-scale Air Quality (CMAQ) models. The simulated concentrations of 24-h PM<sub>2.5</sub> and its major components generally agree with observations during both seasons, but the simulated 1-h and 8-h O<sub>3</sub> are acceptable only for summer. Increasing in severity from the rim of the SCB to its inner areas, the PM<sub>2.5</sub>, as well as its major components, exhibits hotspots near the central urban areas of Chongqing and Chengdu, with concentrations of 150–200 μg m<sup>-3</sup> and 40–60 μg m<sup>-3</sup> during winter and summer, respectively. The 1-h and 8-h O<sub>3</sub> exhibit no hotspots in the urban centers of Chongqing and Chengdu but show elevated levels in some rural and suburban areas (55–70 ppb and 65–80 ppb, respectively), including those on the western and southwestern rim of the SCB, and downwind of the urban center of Chongqing. Despite the great spatial variations in the PM<sub>2.5</sub> and O<sub>3</sub> concentrations, the vast majority of the basin fails to meet the WHO guidelines for 24-h PM<sub>2.5</sub> (25 μg m<sup>-3</sup>) and 8-h O<sub>3</sub> (~47 ppb) on > 70% of the days during winter and > 40% of the days during summer, respectively. Based on the aforementioned spatial patterns of the PM<sub>2.5</sub> and O<sub>3</sub> concentrations, and the wind directions within the basin, strictly controlling emissions originating in the SCB may greatly reduce PM<sub>2.5</sub> and O<sub>3</sub> concentrations within the basin.

**Keywords:** Chengdu Chongqing, Spatio-temporal variations, Air pollution.

---

## **A Novel Method of Collecting and Chemically Characterizing Milligram Quantities of Indoor Airborne Particulate Matter**

**Gavin J. Parker<sup>1</sup>, Chun H. Ong<sup>2</sup>, Robert B. Manges<sup>3</sup>, Emma M. Stapleton<sup>3</sup>, Alejandro P. Comellas<sup>3</sup>, Thomas M. Peters <sup>2</sup>, Elizabeth A. Stone <sup>2</sup>**

**Source:** Aerosol and Atmospheric Chemistry, Volume: 19 | Issue: 11 | Pages: 2387-2395  
DOI: 10.4209/aaqr.2019.04.0182

Because people spend the majority of the day indoors, it is important to evaluate indoor air, especially airborne particulate matter (PM), for its potential health effects. However, collecting milligram-sized samples of indoor PM, which are necessary for detailed chemical and biological assays, remains challenging because of the noise, power requirements, and size of traditional PM samplers. Therefore, we developed a novel method of collection using an electrostatic precipitator (ESP). Laboratory experiments were conducted to characterize the ESP collection efficiency (41–65%) and PM recovery (50–95%) for three aerosol types. After characterization, the ESPs were deployed in 21 homes in eastern Iowa for 30 days, during which they collected 6–87 mg of indoor PM. The samples were acid digested and subsequently analyzed by inductively coupled plasma mass spectrometry for their magnesium, aluminum, vanadium, manganese, iron, nickel, copper, zinc, arsenic, and lead content. Crustal metals (magnesium, iron, and aluminum), ranging from 3,000 to 25,000 ng mg<sup>-1</sup> in concentration, contributed the largest mass fractions of the PM. The relative

abundances of the metals were similar between homes, although the PM mass fractions were highly variable. This ESP sampling method can be applied in future studies to collect milligram-sized quantities of indoor PM, enabling a detailed analysis of its composition and potential health effects.

**Keywords:** Indoor air, Particulate matter, Electrostatic precipitation, Metals.

---

## **Characterization and Source Analysis of Water-soluble Ions in Atmospheric Particles in Jinzhong, China**

**Ling Mu , Lirong Zheng, Meisheng Liang , Mei Tian, Xuemei Li, Danhua Jing**

**Source:** Aerosol and Atmospheric Chemistry, Volume: 19 | Issue: 11 | Pages: 2396-2409  
DOI: 10.4209/aaqr.2019.03.0109

Size-segregated samples (< 2.5, 2.5–5, 5–10, and 10–100  $\mu\text{m}$ ) and PM<sub>2.5</sub> samples were collected to analyze the water-soluble inorganic ions (WSIs, including F<sup>-</sup>, Cl<sup>-</sup>, NO<sub>3</sub><sup>-</sup>, SO<sub>4</sub><sup>2-</sup>, Na<sup>+</sup>, NH<sub>4</sub><sup>+</sup>, K<sup>+</sup>, Mg<sup>2+</sup>, and Ca<sup>2+</sup>), through ion chromatography from January to October in 2017 in Jinzhong. The median concentration of the total WSIs in PM<sub>2.5</sub> was 37  $\mu\text{g m}^{-3}$ , thereby accounting for 31% of the PM<sub>2.5</sub>, with the lowest level in spring and the highest in autumn. SO<sub>4</sub><sup>2-</sup>, NO<sub>3</sub><sup>-</sup>, and NH<sub>4</sub><sup>+</sup> were the most abundant substances and were primarily on the fine particles (0–2.5  $\mu\text{m}$ ), whereas Ca<sup>2+</sup>, Mg<sup>2+</sup>, and F<sup>-</sup> were concentrated on the coarse particles (2.5–100  $\mu\text{m}$ ). The results of the correlation analysis led to the conclusions that (NH<sub>4</sub>)<sub>2</sub>SO<sub>4</sub>, NH<sub>4</sub>Cl and K<sub>2</sub>SO<sub>4</sub> were the primary compounds on the fine particles, MgSO<sub>4</sub> and CaSO<sub>4</sub> were the major chemical forms of WSIs on the coarse particles, thus indicating that the formation mechanisms of these compounds were different; however, NH<sub>4</sub>NO<sub>3</sub> and KNO<sub>3</sub> were present in both the types of particles. The particles that were observed in Jinzhong were alkaline during the study period, and their acidity was negligible. The ratio analysis showed that the highest ratio of Cl<sup>-</sup>/K<sup>+</sup> was found in winter in both fine and coarse particles; however, no obvious distinction has been made between Mg<sup>2+</sup>/Ca<sup>2+</sup> during the four seasons. The NO<sub>3</sub><sup>-</sup>/SO<sub>4</sub><sup>2-</sup> ratio in coarse particles was observed to be significantly higher than that in fine particles, particularly in summer, thus indicating that the heterogeneous reaction on particles plays a vital role in the formation of NO<sub>3</sub><sup>-</sup> in coarse particles. The PCA analysis showed that the primary factors of WSIs, which were secondary formation, coal combustion, biomass burning, dust particles, and industrial emission. The coal combustion and biomass burning have been considered as the leading emission sources to be controlled for improving air quality in Jinzhong.

**Keywords:** Fine particles, Coarse particles , WSIs, Size distribution, Source factors.

---

# Vertical Distribution of Particulate Matter and its Relationship with Planetary Boundary Layer Structure in Shenyang, Northeast China

Xiaolan Li 1, Yanjun Ma 1, Yangfeng Wang<sup>1</sup>, Wei Wei<sup>2</sup>, Yunhai Zhang<sup>1</sup>, Ningwei Liu<sup>1</sup>,  
Ye Hong<sup>1</sup>

**Source:** Aerosol and Atmospheric Chemistry, Volume: 19 | Issue: 11 | Pages: 2464-2476  
DOI: 10.4209/aaqr.2019.06.0311

The impact of the planetary boundary layer (PBL) structure on the vertical distribution of aerosols in Northeast China, which experiences air pollution frequently in autumn and winter, is not well understood. We investigated the characteristics of the vertical distribution of particulate matter (PM<sub>1</sub>, PM<sub>2.5</sub>, and PM<sub>10</sub>) mass concentrations and their relationships with PBL structures in Shenyang, a provincial capital city in Northeast China, using balloon sounding data collected during an intensive observation period in November 2018. Aerosols typically decreased with increases in height and were mostly distributed below 400 m at night and reached higher altitudes (~800 m) in the daytime due to convective turbulence. The concentration ratios of PM<sub>1</sub>/PM<sub>2.5</sub> and PM<sub>2.5</sub>/PM<sub>10</sub> measured about 0.6 and 0.8, respectively, below 0.6–1.0 km during the daytime, and below 0.5 km at nighttime. On average, stronger atmospheric stability resulted in greater vertical gradients and higher PM concentrations near the surface. During four air pollution episodes (November 1–4, 7–10, 14–15, and 25–27), when atmospheric stability was strong at night, aerosols tended to remain in a shallow stable surface layer (< 300 m) and at the bottom of a residual layer (250–500 m) due to weak vertical mixing. After sunrise, these aerosols were mixed uniformly in the PBL (the depth increasing from 200 m to more than 1 km), subsequently affecting surface air quality. In addition, strong wind speeds and wind shears caused by nocturnal low-level jets and cold front systems influenced the formation and evolution of air pollution episodes. These processes controlled aerosol transport/dispersion processes and can modify atmospheric stability and PBL height. These results have important implications for understanding the vertical distribution of aerosols, and the crucial roles that PBL structures play in modulating aerosol pollution in Shenyang.

**Keywords:** Vertical distribution, Particulate matter, Planetary boundary layer structure , Air pollution, Northeast China.

---

## **PM2.5 Associated PAHs and Inorganic Elements from Combustion of Biomass, Cable Wrapping, Domestic Waste, and Garbage for Power Generation**

**Zhiyong Li 1,2, Yutong Wang1, Songtao Guo1, Zhenxin Li1, Yiran Xing1, Guoqing Liu1, Rui Fang1, Yao Hu1, Hongtao Zhu1, Yulong Yan 2**

**Source:** Aerosol and Atmospheric Chemistry, Volume: 19 | Issue: 11 | Pages: 2502-2517  
DOI: 10.4209/aaqr.2019.10.0495

PM2.5 fractions were collected by re-suspension of the ashes derived from the incineration processes of peanut straw (PS), wheat straw (WS), garbage-fired power plant (GFPP), domestic garbage for volume reduction (DG), and workshop of cable combustion for metal reclamation (WCC) for the analysis of 16 PAHs and 26 elements to obtain the information about their composition profiles, toxicity of PAHs, and exposure risks posed by heavy metals (HMs) and As. GFPP possessed the highest  $\Sigma 16\text{PAHs}$ , while the lowest value occurred at DG. HMW-PAHs dominated in GFPP, while LMW-PAHs were predominant in PS and WS. BaP was the top PAH in GFPP and GFPP possessed the highest TEQ values based on the 2,3,7,8-tetrachlorodibenzodioxin (TCDD) and BaP associated TEFs, and followed by WCC > DG > WS > PS. Except for DG vs. WCC, the PAH-, and HM vs. As-profiles between any 2 out of 5 sources were different based on higher coefficients of divergence than 0.3. The sum of 10 HMs and As ( $\Sigma 11\text{IEs}$ ) dominated in WCC due to high contents of Cu, Zn, and Pb, and followed by GFPP > DG > WS > PS. The most enriched HMs were Sb, Cu, and Pb for WCC, Sn for GFPP, and Cd for both GFPP and DG. The integrated carcinogenic risks (CRs) for children posed by both dermal adsorption (Derm) and ingestion (ING) were higher than those for adults. The CRs for children from all the 5 sources exceeded the acceptable level of  $1 \times 10^{-4}$ . The non-carcinogenic risks (NCRs) for children posed by both ING and DERM for 5 sources were much higher than those for adults. The NCRs for children posed by ING significantly exceeded 1, which were 63.8, 10.9, 4.11, 3.58, and 2.19 for WCC, GFPP, WS, DG, and PS.

**Keywords:** PAHs, Heavy metals, Cable wrapping, Garbage-fired power plant, Domestic garbag.

---

## **Source Identification on High PM2.5 Days Using SEM/EDS, XRF, Raman, and Windblown Dust Modeling**

**Jeff Wagner , Zhong-Min Wang, Sutapa Ghosal, Stephen Wall**

**Source:** Aerosol and Atmospheric Chemistry, Volume: 19 | Issue: 11 | Pages: 2518-2530  
DOI: 10.4209/aaqr.2019.05.0276

When community exposures to PM<sub>2.5</sub> are high, identification of the particle sources enables more effective control and assessment of health impacts. This study demonstrates forensic particle analysis methods that can be used when only limited, archived samples are available. Federal reference method (FRM) filters from seven high PM<sub>2.5</sub> days were analyzed using optical and electron microscopy, X-ray fluorescence, and Raman microspectroscopy to determine individual particle morphology and composition, together with supplemental wind roses, GIS mapping, FRM inlet penetration calculations, and windblown dust modeling. This approach identified three distinct sources of high PM<sub>2.5</sub> measurements: 1) local, wind-blown dust from an atypical direction, consistent with modeling predictions for a normally operating PM<sub>2.5</sub> inlet challenged with a high concentration of windblown dust particles, potentially enhanced by re-entrainment of particles from within the inlet, 2) wintertime, regional, hygroscopic, nitrogen- and sulfur-rich salts, consistent with ammonium nitrate and ammonium sulfate, and 3) sampling or documentation error. This approach can be used in any location in which regulatory PM filters and other air quality data are available.

**Keywords:** Air quality, Area sources, Mineral dust, Measurement techniques, PM<sub>2.5</sub>, Secondary aerosol, Source apportionment.

---

## **A Dynamic Dust Emission Allocation Method and Holiday Profiles Applied to Emission Processing for Improving Air Quality Model Performance**

**Guanglin Jia<sup>1</sup>, Zhijiong Huang<sup>2</sup>, Yuanqian Xu<sup>1</sup>, Zhuangmin Zhong<sup>2</sup>, Qinge Sha<sup>1</sup>, Xiaobo Huang<sup>1</sup>, Jing Yang<sup>1</sup>, Junyu Zheng<sup>1,2</sup>**

**Source:** Aerosol and Atmospheric Chemistry, Volume: 19 | Issue: 11 | Pages: 2531-2542  
DOI: 10.4209/aaqr.2019.01.0021

An accurate depiction of temporal and spatial variations in emissions is critical in simulating air quality with atmospheric chemical transport models. Most emission processing systems typically use prescribed profiles to allocate anthropogenic emissions based on the assumptions that the temporal variance is periodical and spatial variance is time-independent. However, these assumptions are not applicable to emission sources heavily influenced by meteorology and holiday activity. In this study, we improved the temporal and spatial allocation of anthropogenic emissions by, first of all, developing a dynamic allocation method for fugitive dust that uses the negative correlation between dust emissions and precipitation, based on hourly rainfall data generated by the Weather Research and Forecasting model. Second, we employed holiday-specific profiles that were established using continuous emission monitoring system and traffic flow monitoring data to allocate power plant and on-road mobile emissions during the Spring Festival period, when human activity differs considerably from that of non-holiday periods. The new dynamic allocation method and holiday-specific profiles were applied to emissions in the Pearl River Delta region as a demonstration. Validated using a chemical transport model,

this method obviously improved the model performance for periods with rainfall, with the normalized mean bias (NMB) decreasing by 6.27% for PM<sub>10</sub> (particulate matter with a diameter of  $\leq 10 \mu\text{m}$ ) and 4.33% for PM<sub>2.5</sub> (particulate matter with a diameter of  $\leq 2.5 \mu\text{m}$ ). The holiday simulations revealed that the holiday-specific profiles mitigated overestimations of NO<sub>2</sub>, SO<sub>2</sub>, and PM<sub>10</sub> for the Spring Festival period, with the NMBs decreasing by 37.95%, 18.56%, and 20.83%, respectively. Hence, refining the allocation of emissions improved model simulation and air quality forecasting.

**Keywords:** Fugitive dust, Dynamic allocation, Holiday profile, Emission process.

---

## **Simulation-based Design of Regional Emission Control Experiments with Simultaneous Pollution of O<sub>3</sub> and PM<sub>2.5</sub> in Jinan, China**

**Haoyue Wang<sup>1</sup>, Wenxuan Sui<sup>1,2</sup>, Xiao Tang<sup>2,6</sup>, Miaomiao Lu<sup>2,3</sup>, Huangjian Wu<sup>2</sup>, Lei Kong<sup>2,4</sup>, Lina Han<sup>5</sup>, Lin Wu<sup>2</sup>, Weiguo Wang<sup>1</sup>, Zifa Wang<sup>2,4,6</sup>**

**Source:** Aerosol and Atmospheric Chemistry, Volume: 19 | Issue: 11 | Pages: 2543-2556  
DOI: 10.4209/aaqr.2019.03.0125

High O<sub>3</sub> and PM<sub>2.5</sub> concentrations were frequently observed in Jinan during June 2015 and simultaneously occurred on 8 days, with a maximum 8-hour-averaged O<sub>3</sub> concentration of 255  $\mu\text{g m}^{-3}$  and a maximum daily averaged PM<sub>2.5</sub> concentration of 111  $\mu\text{g m}^{-3}$ . In order to investigate simultaneously controlling these two air pollutants, two simulation-based regional emission control experiments were designed using a nested air quality prediction model system (NAQPMS). One emission control scenario ("Conventional Control") implemented the strictest control measures in Jinan and surrounding areas and resulted in a 15.7% reduction of O<sub>3</sub> and a 21.3% reduction of PM<sub>2.5</sub> on days polluted by O<sub>3</sub> and PM<sub>2.5</sub>, respectively. The other emission control scenario ("Source-tagging Control"), by contrast, used online source-tagging modeling results from NAQPMS to select emission reduction regions based on their source contributions to the O<sub>3</sub> and the PM<sub>2.5</sub> in Jinan and resulted in a 16.2% reduction of O<sub>3</sub> and a 22.8% reduction of PM<sub>2.5</sub> on days polluted by O<sub>3</sub> and PM<sub>2.5</sub>, respectively. Compared to Conventional Control, this scheme produced smaller reductions in emissions from areas with low contributions to the O<sub>3</sub> and PM<sub>2.5</sub> concentrations in Jinan as well as in the total emissions of primary pollutants (the reduced emissions was only 61% of that needed by Conventional Control), and the area and the population affected by these reductions decreased by 12% and 31%, respectively. However, this study demonstrates that Source-tagging Control is more efficient than Conventional Control in reducing simultaneous pollution by O<sub>3</sub> and PM<sub>2.5</sub> through regional measures.

**Keywords:** Emission control, Source tagging method, Simultaneous pollution, O<sub>3</sub>, PM<sub>2.5</sub>.

---



## **Sources and Characteristics of Particulate Matter at Five Locations in an Underground Mine**

**Sanna Saarikoski 1, Laura Salo<sup>2</sup>, Matthew Bloss<sup>1</sup>, Jenni Alanen<sup>2</sup>, Kimmo Teinilä<sup>1</sup>, Felipe Reyes<sup>3</sup>, Yeanice Vázquez<sup>3</sup>, Jorma Keskinen<sup>2</sup>, Pedro Oyola<sup>3</sup>, Topi Rönkkö<sup>2</sup>, Hilikka Timonen<sup>1</sup>**

**Source:** Aerosol and Atmospheric Chemistry, Volume: 19 | Issue: 12 | Pages: 2613-2624  
DOI: 10.4209/aaqr.2019.03.0118

The sources and characteristics of particulate matter (PM) were determined in a modern underground chrome mine in Finland. Measurements were conducted at five locations in the mine: the maintenance area, blasting area, ore pit dumping area, crushing station and conveyor belt. The measurement set-up consisted of a Soot Particle Aerosol Mass Spectrometer (SP-AMS) for the particles' chemical composition; an Electrical Low Pressure Impactor, Nano Scanning Mobility Particle Sizer and Optical Particle Counter for the particle number and mass size distribution; and an Aethalometer for black carbon (BC). The particle number and mass concentration depended strongly on the measurement location and period. The PM<sub>10</sub> and the total number concentrations varied from 22 to 1100  $\mu\text{g m}^{-3}$  and  $1.7 \times 10^3$  to  $2.3 \times 10^5 \text{ # cm}^{-3}$ , respectively, in the mine. In terms of the composition, the sub-micrometer particles (PM<sub>1</sub>) consisted mostly of organic matter and BC, but at the blasting site, the fraction of sulfate was also significant. The SP-AMS data was analyzed with Positive Matrix Factorization (PMF) to identify and quantify the main sources of PM<sub>1</sub> in the mine. Based on the PMF analysis, the PM<sub>1</sub> originated mostly from diesel engines (35–84%) and blasting (7–60%). The impact of blasting on air quality in mines may become more pronounced in the future as the emissions from diesel engines decrease due to alternative fuels and better engine and after-treatment technologies.

**Keywords:** Chemical composition, Aerosol mass spectrometer, Source apportionment.

---

## **High Loadings of Water-Soluble Oxalic Acid and Related Compounds in PM<sub>2.5</sub> Aerosols in Eastern Central India: Influence of Biomass Burning and Photochemical Processing**

**Dhananjay K. Deshmukh<sup>1</sup>, Kimitaka Kawamura<sup>1</sup>, Tarun Gupta<sup>2</sup>, Md. Mozammel Haque<sup>3</sup>, Yan-Lin Zhang<sup>3</sup>, Dharmendra K. Singh<sup>1,4</sup>, Ying I. Tsai<sup>5</sup>**

**Source:** Aerosol and Atmospheric Chemistry, Volume: 19 | Issue: 12 | Pages: 2625-2644  
DOI: 10.4209/aaqr.2019.10.0543

Water-soluble organic compounds are important constituents of atmospheric aerosols and have been recognized as unique fingerprints to identify atmospheric processes. Fine aerosol samples (PM<sub>2.5</sub>) were collected at Ambikapur (23.1°N and 83.2°E) in eastern central India from March to June 2017. The samples were analyzed for water-soluble dicarboxylic acids (C<sub>2</sub>–C<sub>12</sub>), glyoxylic acid ( $\omega$ C<sub>2</sub>), glyoxal (Gly), methylglyoxal (MeGly),



organic carbon (OC), elemental carbon (EC) and water-soluble OC (WSOC). Oxalic acid (C2) was detected as the most abundant species, followed by succinic (C4) and malonic (C3) acids. Temporal variation in concentrations of C2 diacid and related compounds was pronounced from early to late April when biomass burning (BB) was dominant in eastern central India. Strong positive correlations of C2 diacid and related compounds with levoglucosan ( $r = 0.83-0.99$ ) further demonstrate that organic aerosols (OAs) were affected by BB in eastern central India. Strong positive correlations of C2 with saturated diacids (C3-C9:  $r = 0.78-0.97$ ),  $\omega$ C2 ( $r = 0.98$ ), Gly ( $r = 0.96$ ) and MeGly ( $r = 0.84$ ) suggest that their sources and formation processes were similar and oxalic acid might be produced via the photochemical degradation of precursor compounds. The relatively high ratios of WSOC to OC (avg. 0.69) and C3 to C4 diacid (avg. 0.95) suggest that water-soluble OAs were photochemically processed during the campaign. The total water-soluble organic compounds detected in Ambikapur PM<sub>2.5</sub> samples accounted for an average of 1.9% (1.1–3.1%) of OC. Our results demonstrate that BB and photochemical processing caused high levels of water-soluble organic compounds over eastern central India.

**Keywords:** Water-soluble organic aerosols, Dicarboxylic acids, Secondary formation, Photochemical production, Biomass burning emission.

---

## **Inter-correlation of Chemical Compositions, Transport Routes, and Source Apportionment Results of Atmospheric PM<sub>2.5</sub> in Southern Taiwan and the Northern Philippines**

**Yu-Lun Tseng<sup>1</sup>, Chung-Shin Yuan <sup>1</sup>, Gerry Bagtasa<sup>2</sup>, Hsueh-Lung Chuang<sup>1</sup>, Tsung-Chang Li<sup>1</sup>**

**Source:** Aerosol and Atmospheric Chemistry, Volume: 19 | Issue: 12 | Pages: 2645-2661  
DOI: 10.4209/aaqr.2019.10.0526

This study investigated the inter-correlation of atmospheric PM<sub>2.5</sub> between southern Taiwan and the northern Philippines. 24-hour samples of PM<sub>2.5</sub> were simultaneously collected at two remote sites, Checheng (Taiwan) and Laoag (Philippines), during all four seasons. The water-soluble ions, metallic elements, carbonaceous content, and anhydrosugars in the PM<sub>2.5</sub> were then analyzed to characterize the chemical fingerprint. Furthermore, principal component analysis, chemical mass balance (CMB) receptor modeling, and backward trajectory simulation were applied to resolve the source apportionment of PM<sub>2.5</sub> at both of the sites.

The results showed that Checheng and Laoag were highly influenced by polluted air masses transported long-range from the north, producing elevated PM<sub>2.5</sub> concentrations during winter and spring. The water-soluble ions (WSIs) were abundant in secondary inorganic aerosols (SO<sub>4</sub><sup>2-</sup>, NO<sub>3</sub><sup>-</sup>, and NH<sub>4</sub><sup>+</sup>), which accounted for 34.1–76.0%. Crustal elements dominated the metallic content in the PM<sub>2.5</sub>, but the concentrations of trace elements originating from anthropogenic sources increased during the northwestern monsoon

periods. More organic carbon (OC) than elemental carbon (EC) was found, with secondary OC (SOC) contributing approximately 23.9–38.9% to the former. Moreover, the level of levoglucosan highly correlated with those of K<sup>+</sup> and OC, confirming that these three substances are key indicators of biomass burning.

The two sites exhibited similar chemical compositions for PM<sub>2.5</sub>, indicating the possibility of transport between Checheng and Laoag, and a paired t-test obtained a p-value of 0.030 ( $p < 0.05$ ), implying a potential inter-correlation for PM<sub>2.5</sub> between southern Taiwan and the northern Philippines. The major sources of the PM<sub>2.5</sub> were soil dust, mobile sources, sea salt, and biomass burning along the northerly transport routes during winter and spring. The contribution of anthropogenic sources (i.e., industrial boilers, waste incinerators, and secondary aerosols) to the PM<sub>2.5</sub> frequently increased during winter and spring, unlike during summer, suggesting that the northerly transport of PM<sub>2.5</sub> highly affected particulate air pollution at both of the sites.

**Keywords:** Inter-correlation of remote sites , Atmospheric fine particles (PM<sub>2.5</sub>), Chemical fingerprints , Transport routes , Source apportionment.

---

## **Relieved Air Pollution Enhanced Urban Heat Island Intensity in the Yangtze River Delta, China**

**Hao Wu<sup>1,2</sup>, Tijian Wang<sup>2</sup>, Qin'geng Wang<sup>1</sup>, Nicole Riemer<sup>3</sup>, Yang Cao<sup>4</sup>, Chong Liu<sup>2</sup>,  
Chaoqun Ma<sup>2</sup>, Xiaodong Xie<sup>2</sup>**

**Source:** Aerosol and Atmospheric Chemistry, Volume: 19 | Issue: 12 | Pages: 2683-2696  
DOI: 10.4209/aaqr.2019.02.0100

The National Air Pollution Control Plan implemented by China in 2013 reduced the concentrations of air pollutants, especially PM<sub>2.5</sub> (aerosol particles with an aerodynamic diameter equal to or less than 2.5  $\mu\text{m}$ ), between 2014 and 2017. This reduction in PM<sub>2.5</sub> potentially affected the intensity of urban heat islands (UHIs), as the presence of fine particles can influence the energy balance of the earth-atmosphere system. In this study, the effect of the pollution control plan on the UHI intensity in the Yangtze River Delta, China, was investigated via observational analysis and numerical modeling. According to the observational data, the PM<sub>2.5</sub> concentrations in the megacities of the Yangtze River Delta, viz., Shanghai, Nanjing, Hangzhou and Hefei, in 2017 were  $\sim 35 \mu\text{g m}^{-3}$ , showing decreases of approximately 48.36%, 28.25%, 29.41% and 32.5%, respectively, compared to 2014. Furthermore, these reductions in the PM<sub>2.5</sub> concentration correlated well with the strengthened diurnal intensity (increasing by up to 1 K) and the weakened nocturnal intensity (decreasing by up to 1 K) of the UHIs. Numerical simulations confirmed that this “seesaw effect” on the UHI intensity was due to the decrease in PM<sub>2.5</sub> and the consequent increase in the downward surface shortwave radiation and the outgoing top-of-the-atmosphere longwave radiation. Thus, the Air Pollution Control Plan noticeably affected

the UHI intensity by reducing PM2.5—a factor which should be considered in future studies on urban climate and environmental planning.

**Keywords:** PM2.5, Urban heat island , WRF-Chem, Yangtze River Delta.

---

## **Climate Impacts of the Biomass Burning in Indochina on Atmospheric Conditions over Southern China**

**Lina Huang<sup>1</sup>, Wenshi Lin <sup>1,2</sup>, Fangzhou Li<sup>3</sup>, Yuan Wang<sup>4</sup>, Baolin Jiang<sup>3</sup>**

**Source:** Aerosol and Atmospheric Chemistry, Volume: 19 | Issue: 12 | Pages: 2707-2720  
DOI: 10.4209/aaqr.2019.01.0028

Substantial biomass burning (BB) activities in Indochina during March and April of each year generate aerosols that are transported via westerly winds to southern China. These BB aerosols have both radiative (direct and semi-direct) and indirect effects on the climate. This study evaluates impacts of BB in Indochina during April 2013 on atmospheric conditions in southern China using WRF-Chem sensitivity simulations. We show that the atmosphere becomes drier and hotter under the aerosol radiative effect in southern China, while the changes linked to the indirect effect are opposite. The former (the latter) rises (reduces) surface temperature 0.13°C (0.19°C) and decrease (increase) water vapor mixing ratios 0.23 g kg<sup>-1</sup> (0.40 g kg<sup>-1</sup>) at 700 hPa. Atmospheric responses to aerosols in turn affect aerosol dissipation. Specifically, BB aerosols absorb solar radiation and heat the local atmosphere, which inhibits the formation of clouds (reducing low-level cloud about 7%) related to the aerosol semi-direct effect. Less cloud enhances surface solar radiation flux and temperature. Otherwise, northeasterly winds linked to radiative effect suppress water vapor transport. In this case, precipitation reduces 1.09 mm day<sup>-1</sup>, diminishing wet removal and westward transport of aerosols. Under the indirect effect, greater cloud coverage is formed, which reduces surface solar radiation flux and increases local latent heat release. This extra heating promotes air convection and diffusion of pollution. Regional mean precipitation increases 0.49 mm d<sup>-1</sup>, facilitating wet pollution removal. Under indirect effect, aerosol extinction coefficient reduces 0.011 km<sup>-1</sup> at 2-km height over southern China. However, it increases around 0.002 km<sup>-1</sup> at 3-km height over southernmost China related to radiative effect. Therefore, atmospheric changes linked to indirect effect play a greater role in removing pollutants from the atmosphere than radiative effect over southern China.

**Keywords:** Aerosol radiative effect , Aerosol indirect effect, Cloud cover, WRF-Chem ,Latent heat.

---

## **Characteristics of PM<sub>10</sub> Levels Monitored for More than a Decade in Subway Stations in South Korea**

**Sangjun Choi<sup>1</sup>, Ju-Hyun Park<sup>2</sup>, Seo-Yeon Bae<sup>3</sup>, So-Yeon Kim<sup>3</sup>, Hyeajeong Byun<sup>4</sup>, Hyunseok Kwak<sup>5</sup>, Sungho Hwang<sup>6</sup>, Jihoon Park<sup>7</sup>, Hyunhee Park<sup>8</sup>, Kyong-Hui Lee<sup>9</sup>, Won Kim<sup>10</sup>, Dong-Uk Park<sup>3</sup>**

**Source:** Aerosol and Atmospheric Chemistry, Volume: 19 | Issue: 12 | Pages: 2746-2756  
DOI: 10.4209/aaqr.2019.05.0263

This study aimed to evaluate the variation in PM<sub>10</sub> concentration and identify the factors influencing it in Korean subways during the past decade. The PM<sub>10</sub> measured internally by subway companies according to legal requirements was categorized by the subway's characteristics, which were statistically examined using a mixed effects model to identify the relevant parameters. The average levels monitored near or on the platforms and in the waiting rooms ranged from 53.9 to 92.4  $\mu\text{g m}^{-3}$ , remaining below the Indoor Air Quality Control Act regulatory standard of 150  $\mu\text{g m}^{-3}$ . However, the levels monitored on the platforms far exceeded the average yearly atmospheric environmental standard (50  $\mu\text{g m}^{-3}$ ). Based on both univariate and multiple analyses, several subway characteristics, including the presence of a platform screen door (PSD), were found to significantly correlate with the concentration, although slight differences in the significant factors were detected between the cities. Particularly, the absence of transfer lines and the presence of a PSD reduced the platform concentration, except at Busan and during specific years.

**Keywords:** Subway, PM<sub>10</sub>, Platform screen door (PSD), Indoor air quality.

---

## **Air Pollution Characteristics and Meteorological Correlates in Lin'an, Hangzhou, China**

**Xintao Lin, Jian Chen, Ting Lu, Dongming Huang, Jing Zhang**

**Source:** Aerosol and Atmospheric Chemistry, Volume: 19 | Issue: 12 | Pages: 2770-2780  
DOI: 10.4209/aaqr.2019.03.0104

The concentration and distribution of atmospheric particulate matter depend primarily on the meteorological conditions associated with a fixed pollution source. The effects of meteorological factors on particulate matter have been analyzed on the meteorological seasonal scale, but few researchers have considered the climatic season, which is divided based on the distribution feature of climatic factors. In addition, the hysteresis effect of meteorological factors is easily neglected. Here, we reviewed the characteristics and influential factors of particle pollution based on particle concentration and meteorological data from January 2013 through December 2013. Results from nonparametric tests and Spearman's nonparametric correlation coefficient showed that particle pollution exhibited a statistically significant seasonal trend. The pollution on workdays was slightly less than

that on holidays, but no significant difference was found. The air pressure 1–2 days earlier showed a higher positive correlation with the current particle concentrations (except in winter), and the temperature 2–3 days earlier in summer and fall showed a stronger negative correlation with the particle concentration. Lower moisture and frequent precipitation would significantly reduce the pollution on the current day and the next day (except in summer). The variation of particulate matter concentration in summer exhibited a high-low-high variation, caused mainly by temperature and precipitation; the air quality during the plum rain period was significantly better than that in the period before the plum rain. The fine particle pollution level during the high-temperature and heat wave days was the lowest, after which the concentration increased.

**Keywords:** Particulate matter, Meteorological factors, Climatic season, Hysteresis effect, Temporal variation.

---

## **Effects of Blending Ethanol with Gasoline on the Performance of Motorcycle Catalysts and Airborne Pollutant Emissions**

**Jiun-Horng Tsai<sup>1,2</sup>, Ya-Li Ko<sup>1</sup>, Ci-Min Huang<sup>1</sup>, Hung-Lung Chiang<sup>3</sup>**

**Source:** Aerosol and Atmospheric Chemistry, Volume: 19 | Issue: 12 | Pages: 2781-2792  
DOI: 10.4209/aaqr.2019.10.0539

This study investigated the effects of blending ethanol with gasoline on the exhaust emissions of fuel-injected motorcycles. Regulated gasoline (RF), and 15 (E15) and 30 (E30) vol% ethanol fuel were used as test fuels. Measurements of several air pollutants (CO, HC, and NO<sub>x</sub>) and organic air pollutant groups were conducted for two new fuel-injected four-stroke motorcycles. In addition, various catalysts were inserted into the motorcycles' tailpipes to determine the characteristics and performance of the catalysts in treating the exhaust.

Compared to using RF, we found that using blended fuel potentially reduced the CO and HC emissions by 30–37% and 19–28%, respectively. New catalytic systems, in conjunction with using different fuels, reduced CO, HC, and NO<sub>x</sub> emissions in the tailpipe exhaust by 12–61%, 32–39%, and 81–85%, respectively. The CO and HC emissions were directly proportional in quantity to the running mileage of the catalyst, but the NO<sub>x</sub> emissions were unaffected by this mileage, although they increased as the catalyst aged.

We also discovered that at identical running mileages for a catalyst, the fuel consumption increased by –1.7–6.5% and 4.1–15% when using E15 and E30 fuel instead of RF. Furthermore, the specific surface area and pore volume of the catalyst decreased with the aged catalyst the phosphorus and sulfur content in the catalyst increased with the catalyst's running mileage; adding ethanol to the fuel decreased emissions of paraffins, olefins, and aromatics but increased those of carbonyls; and the ozone formation potential of volatile

organic compounds (VOCs) in the tailpipe exhaust was 16.7–17.2% for paraffins, 22–33% for olefins, 26–45% for aromatics, and 4.9–25% for carbonyls.

**Keywords:** Criteria air pollutant, Fuel consumption, VOC species, Catalyst.

---

## **Infants' Neurodevelopmental Effects of PM<sub>2.5</sub> and Persistent Organohalogen Pollutants Exposure in Southern Taiwan**

**Cheng-Chih Kao<sup>1,2</sup>, Chih-Cheng Chen<sup>3</sup>, Japheth L. Avelino<sup>4</sup>, Mariene-syne P. Cortez<sup>4</sup>, Lemmuel L. Tayo<sup>4</sup>, Yi-Hsien Lin<sup>5</sup>, Ming-Hsieh Tsai<sup>6</sup>, Chu-Wen Lin<sup>6</sup>, Yi-Chyun Hsu<sup>7</sup>, Lien-Te Hsieh<sup>1</sup>, Chieh Lin<sup>1</sup>, Lin-Chi Wang<sup>8,9,10</sup>, Kwong-Leung J. Yu<sup>2</sup>, How-Ran Chao<sup>1,11,12</sup>**

**Source:** Aerosol and Atmospheric Chemistry, Volume: 19 | Issue: 12 | Pages: 2793-2803  
DOI: 10.4209/aaqr.2019.10.0550

Several studies have stated the harmful effects of PM<sub>2.5</sub> to population health, including disruption of neurological development. However, the mechanism behind the neurodevelopmental effects of ambient PM<sub>2.5</sub> and postnatal PBDEs and OCPs exposure is still unknown. Our goal was to determine influence of breastmilk residues, polybrominated diphenyl ethers (PBDEs) and organochlorine pesticides (OCPs), to the infants' neurodevelopment with respect to high and low PM<sub>2.5</sub> exposure areas. The participants were recruited from high PM<sub>2.5</sub> exposure areas (n = 32) and low PM<sub>2.5</sub> exposure areas (n = 23) of southern Taiwan. The extracted 14 PBDEs and 20 OCPs compounds were analyzed using gas chromatography coupled with mass spectrometer. The infants, aging from 8-12 months, were examined by Bayley Scales of Infants and Toddlers Development, Third Edition (Bayley-III) for neurodevelopment. Results showed that high PM<sub>2.5</sub> exposure caused reduced head circumference and had significant effects on the motor skill and social emotional development. For breastmilk PBDEs, a positive correlation between BDE-196 and social emotion, after multivariate analysis with adjustment of confounders, was observed while BDE-99, 196, 197, and 207 showed higher magnitudes in low PM<sub>2.5</sub> areas than in high PM<sub>2.5</sub> areas. For OCPs, only  $\gamma$ -hexachlorocyclohexanes ( $\gamma$ -HCH) presented the significant difference between high and low PM<sub>2.5</sub> exposure areas. Most breastmilk OCPs residues, including 4,4'-dichlorodiphenyltrichloroethane (4,4'-DDT),  $\gamma$ -HCH, endrin, and heptachlor epoxide showed negative impact on the Bayley-III scores after multivariate analysis. In conclusion, infants' neurodevelopment was significantly correlated with the location of PM<sub>2.5</sub> exposure and breastmilk intake of certain PBDEs and OCPs. Breastmilk OCPs might obviously affect infants' neurodevelopment more compared to breastmilk PBDEs based on our finding. Moreover, this study further employs awareness about viable effects of PM<sub>2.5</sub> in infants' neurodevelopment.

**Keywords:** PM<sub>2.5</sub>, Organochlorine pesticide, PBDEs, Infant neurodevelopment, Bayley-III.

---



# Identifying Leading Nodes of PM2.5 Monitoring Network in Taiwan with Big Data-oriented Social Network Analysis

I-Cheng Chang

**Source:** Aerosol and Atmospheric Chemistry, Volume: 19 | Issue: 12 | Pages: 2844-2864  
DOI: 10.4209/aaqr.2019.11.0554

TEPA (Taiwan Environmental Protection Administration) currently has regulated six types of air pollutants based on the AQI. Among these, the three items most prone to exceeding the standard are PM2.5, PM10, and O3, in that order. PM2.5 pollution episodes in Taiwan mainly occur in winter and spring when the northeast monsoon prevails. In addition to local pollution sources, transboundary air pollution affects Taiwan. Obviously, the existing AQ monitoring data analyzed by the BD-oriented perspective not only simplifies the simulation calculation and verification resources of the AQ model but also assists in real-time insight into the causal relationships between the AQ and important parameters of meteorology, pollution sources, and regions. This study integrates the BD-oriented Social Network Analysis (SNA) approach and data visualization tools to analyze the event co-occurrence and spatial correlation characteristics of two pollution scenarios for AQ monitoring stations based on two severe PM2.5 pollution conditions: (1) the Z-value of PM2.5 daily average concentration is higher than 1.65 (Scenario I), and (2) the daily average concentration of PM2.5 exceeds TEPA's regulation on the AQ standard (Scenario II), to identify the regional leading nodes suitable for different pollution scenarios. Furthermore, Principal Component Analysis (PCA) and time series data are employed to verify the spatial-temporal representation of these leading nodes, which can be regarded as means to the real-time AQ management decision-making as well as instant transboundary pollution precaution in the future. This study contributes to the application of the discrete data-driven approach (SNA) and the continuous data-driven approach (PCA) in an ambient AQ monitoring network, which can clearly explain and analyze the regional high pollution characteristics of PM2.5 in Scenarios I and II. The results of this study are consistent with previously relevant findings in Taiwan.

**Keywords:** PM2.5, pollution scenarios, Transboundary air pollution episodes, Social Network Analysis, Betweenness centrality.

---

## 2. Atmosphere Chemistry and Physics

### Characterization of black carbon-containing fine particles in Beijing during wintertime

Junfeng Wang<sup>1</sup>, Dantong Liu<sup>2</sup>, Xinlei Ge<sup>1</sup>, Yangzhou Wu<sup>1</sup>, Fuzhen Shen<sup>1</sup>, Mindong Chen<sup>1</sup>, Jian Zhao<sup>3,4</sup>, Conghui Xie<sup>3,4</sup>, Qingqing Wang<sup>3</sup>, Weiqi Xu<sup>3,4</sup>, Jie Zhang<sup>5</sup>, Jianlin Hu<sup>1</sup>, James Allan<sup>2,6</sup>, Rutambhara Joshi<sup>2</sup>, Pingqing Fu<sup>3</sup>, Hugh Coe<sup>2</sup>, and Yele Sun<sup>3,4</sup>

Source : Atmos. Chem. Phys.,19, 447–458, 2019 <https://doi.org/10.5194/acp-19-447-2019>

Refractory black carbon (BC) is a product of incomplete combustion of fossil fuel, biomass and biofuel, etc. By mixing with other species, BC can play significant roles in climate change, visibility impairment and human health. Such BC-containing particles in densely populated megacities like Beijing may have specific sources and properties that are important to haze formation and air quality. In this work, we exclusively characterized the BC-containing particles in urban Beijing by using a laser-only Aerodyne soot particle aerosol mass spectrometer (SP-AMS), as part of the Atmospheric Pollution & Human Health (APHH) 2016 winter campaign. The average mass ratio of coating to BC core ( $R_{BC}$ ) was found to be  $\sim 5.0$ . Positive matrix factorization shows the presence of significant primary fossil fuel and biomass-burning organics (64 % of total organics). Yet secondary species, including sulfate, nitrate and oxygenated organic aerosol (OA) species, could have significant impacts on the properties of BC-containing particles, especially for ones with larger BC core sizes and thicker coatings. Analyses of sources and diurnal cycles of organic coating reveal significant afternoon photochemical production of secondary OA (SOA), as well as nighttime aqueous production of a portion of highly oxygenated OA. Besides SOA, photochemical production of nitrate, not sulfate, appeared to be important. Further investigations on BC-containing particles during different periods show that, on average, more polluted periods would have more contributions from secondary species and more thickly coated BC tended to associate with more secondary species, indicating the important role of chemical aging to the pollution of BC-containing particles in urban Beijing during wintertime. However, for individual pollution events, primary species (fossil fuel, coal and biomass-burning emissions) could also play a dominant role, as revealed by the compositions of BC-containing particles in two polluted episodes during the sampling period.



# Vertical characterization of aerosol optical properties and brown carbon in winter in urban Beijing, China

Conghui Xie<sup>1,2</sup>, Weiqi Xu<sup>1,2</sup>, Junfeng Wang<sup>4</sup>, Qingqing Wang<sup>1</sup>, Dantong Liu<sup>5</sup>, Guiqian Tang<sup>1</sup>, Ping Chen<sup>6</sup>, Wei Du<sup>1,2</sup>, Jian Zhao<sup>1,2</sup>, Yingjie Zhang<sup>1</sup>, Wei Zhou<sup>1,2</sup>, Tingting Han<sup>1</sup>, Qingyun Bian<sup>2,7</sup>, Jie Li<sup>1</sup>, Pingqing Fu<sup>1,2</sup>, Zifa Wang<sup>1,2,3</sup>, Xinlei Ge<sup>4</sup>, James Allan<sup>5,8</sup>, Hugh Coe<sup>5</sup>, and Yele Sun<sup>1,2,3</sup>

**Source** : Atmos. Chem. Phys., 19, 165–179, 2019 <https://doi.org/10.5194/acp-19-165-2019>

Aerosol particles are of importance in the Earth's radiation budget since they scatter and absorb sunlight. While extensive studies of aerosol optical properties have been conducted at ground sites, vertical measurements and characterization are very limited in megacities. In this work, we present simultaneous real-time online measurements of aerosol optical properties at ground level and at 260 m on a meteorological tower from 16 November to 13 December in 2016 in Beijing along with measurements of continuous vertical profiles during two haze episodes. The average ( $\pm 1\sigma$ ) scattering and absorption coefficients ( $b_{\text{sca}}$  and  $b_{\text{abs}}$ ;  $\lambda=630$  nm) were  $337.6 (\pm 356.0)$  and  $36.6 (\pm 33.9)$   $\text{Mm}^{-1}$  at 260 m, which were 26.5 % and 22.5 % lower than those at ground level. Single scattering albedo (SSA), however, was comparable between the two heights, with slightly higher values at ground level ( $0.89 \pm 0.04$ ). Although  $b_{\text{sca}}$  and  $b_{\text{abs}}$  showed overall similar temporal variations between ground level and 260 m, the ratios of 260 m to ground varied substantially from less than 0.4 during the clean stages of haze episodes to  $> 0.8$  in the late afternoon. A more detailed analysis indicates that vertical profiles of  $b_{\text{sca}}$ ,  $b_{\text{abs}}$ , and SSA in the low atmosphere were closely related to the changes in meteorological conditions and mixing layer height. The mass absorption cross section (MAC) of equivalent black carbon (eBC,  $\lambda=630$  nm) varied substantially from 9.5 to  $13.2 \text{ m}^2 \text{ g}^{-1}$  in winter in Beijing, and it was strongly associated with the mass ratio of coating materials on refractory BC (rBC) to rBC ( $M_{\text{R}}$ ), and also the oxidation degree of organics in rBC-containing particles. Our results show that the increases in MAC of eBC in winter were mainly caused by photochemically produced secondary materials. Light absorption of organic carbon (brown carbon, BrC) was also important in winter, which on average accounted for 46 ( $\pm 8.5$ ) % and 48 ( $\pm 9.3$ ) % of the total absorption at 370 nm at ground level and 260 m, respectively. A linear regression model combined with positive matrix factorization analysis was used to show that coal combustion was the dominant source contribution of BrC (48 %–55 %) followed by biomass burning (17 %) and photochemically processed secondary organic aerosol ( $\sim 20$  %) in winter in Beijing.

# **Devastating Californian wildfires in November 2018 observed from space: the carbon monoxide perspective**

**Oliver Schneising, Michael Buchwitz, Maximilian Reuter, Heinrich Bovensmann, and John P. Burrows**

**Source :** <https://doi.org/10.5194/acp-2019-5>

Due to proceeding climate change, some regions such as California are becoming warmer and drier entailing the risk that destructive wildfires and associated air pollution episodes continue to increase. November 2018 has turned into one of the most disastrous months in Californian history with two particularly destructive wildfires raging concurrently through the North and the South of the state leaving about 1000 km<sup>2</sup> of land burnt to cinders. Both fires ignited at the wildland-urban interface causing at least 88 civilian fatalities and forcing the total evacuation of several cities and communities.

Here we demonstrate that the inherent carbon monoxide CO emissions of the wildfires and subsequent transport can be observed from space by analysing radiance measurements of the TROPOspheric Monitoring Instrument (TROPOMI) onboard the Sentinel-5 Precursor satellite in the shortwave infrared spectral range. From the determined CO distribution we assess the corresponding air quality burden in Californian major cities caused by the fires. As a result of the prevailing wind conditions, the largest CO load during the first days of the fires is found in Sacramento and San Francisco with city area averages exceeding boundary layer concentrations of 6 mg m<sup>-3</sup> and 4 mg m<sup>-3</sup>, respectively. For some neighbourhoods in the northwest of Sacramento national ambient air quality standards (10 mg m<sup>-3</sup> with 8-hour averaging time) are likely exceeded.

---

## **On what scales can GOSAT flux inversions constrain anomalies in terrestrial ecosystems?**

**Brendan Byrne<sup>1</sup>, Dylan B. A. Jones<sup>1,2</sup>, Kimberly Strong<sup>1</sup>, Saroja M. Polavarapu<sup>3</sup>, Anna B. Harper<sup>4</sup>, David F. Baker<sup>5,6</sup>, and Shamil Maksyutov<sup>7</sup>**

**Source :** <https://doi.org/10.5194/acp-2018-909>

Interannual variations in temperature and precipitation impact the carbon balance of terrestrial ecosystems, leaving an imprint in atmospheric CO<sub>2</sub>. Quantifying the impact of climate anomalies on the net ecosystem exchange (NEE) of terrestrial ecosystems can

provide a constraint to evaluate terrestrial biosphere models against, and may provide an emergent constraint on the response of terrestrial ecosystems to climate change. We investigate the spatial scales over which interannual variability in NEE can be constrained using atmospheric CO<sub>2</sub> observations from the Greenhouse Gases Observing Satellite (GOSAT). NEE anomalies are calculated by performing a series of inversion analyses using the GEOS-Chem model to assimilate GOSAT observations. Monthly NEE anomalies are compared to proxies, variables which are associated with anomalies in the terrestrial carbon cycle, and to upscaled NEE estimates from FLUXCOM. Strong agreement is found in the timing of anomalies in the GOSAT flux inversions with soil temperature and FLUXCOM. Strong correlations are obtained ( $P < 0.05$ ,  $R > R_{\text{NINO3.4}}$ ) in the tropics on continental and larger scales, and in the northern extratropics on sub-continental scales during the summer ( $R^2 \geq 0.49$ ). These results, in addition to a series of observing system simulation experiments that were conducted, provide evidence that GOSAT flux inversions can isolate anomalies in NEE on continental and larger scales. However, in both the tropics and northern extratropics, the agreement between the inversions and the proxies/FLUXCOM is sensitive to the flux inversion configuration. Our results suggest that regional scales are likely the minimum scales that can be resolved in the tropics using GOSAT observations, but obtaining robust NEE anomaly estimates on these scales may be difficult.

---

## **Tropical Pacific Climate Variability under Solar Geoengineering: Impacts on ENSO Extremes**

**Abdul Malik<sup>1,2</sup>, Peer J. Nowack<sup>1,3,4</sup>, Joanna D. Haigh<sup>1,3</sup>, Long Cao<sup>5</sup>, Luqman Atique<sup>5</sup>, and Yves Plancherel<sup>1</sup>**

**Source :** <https://doi.org/10.5194/acp-2018-1312>

Many modelling studies suggest that the El Niño Southern Oscillation (ENSO), in interaction with the tropical Pacific background climate, will change under rising atmospheric greenhouse gas concentrations. Solar geoengineering (reducing the solar flux from outer space) has been proposed as a means to counteract anthropogenic greenhouse-induced changes in climate. Effectiveness of solar geoengineering is uncertain. Robust results are particularly difficult to obtain for ENSO because existing geoengineering simulations are too short (typically ~ 50 years) to detect statistically significant changes in the highly variable tropical Pacific background climate. We here present results from a 1000-year sunshade geoengineering simulation, G1, carried out with the coupled atmosphere-ocean general circulation model HadCM3L. In agreement with previous studies, reducing the shortwave solar flux more than compensates the warming in the

tropical Pacific that develops in the  $4\times\text{CO}_2$  scenario: we observe an overcooling of  $0.3\text{ }^\circ\text{C}$  (5 %) and  $0.23\text{-mm day}^{-1}$  (5 %) reduction in mean rainfall relative to preindustrial conditions in the G1 simulation. This is due to the different latitudinal distributions of the shortwave (solar) and longwave ( $\text{CO}_2$ ) forcings. The location of the Intertropical Convergence Zone (ITCZ) located north of equator in the tropical Pacific, which moved  $7.5^\circ$  southwards under  $4\times\text{CO}_2$ , is also restored to its preindustrial location. However, other aspects of the tropical Pacific mean climate are not reset as effectively. Relative to preindustrial conditions, in G1 the zonal wind stress, zonal sea surface temperature (SST) gradient, and meridional SST gradient are reduced by 10 %, 11 %, and 9 %, respectively, and the Pacific Walker Circulation (PWC) is consistently weakened. The overall amplitude of ENSO strengthens by 5–8 %, but there is a 65 % reduction in the asymmetry between cold and warm events: cold events intensify more than warm events. Importantly, the frequency of extreme El Niño and La Niña events increases by 44 % and 32 %, respectively, while the total number of El Niño events increases by 12 %. Paradoxically, while the number of total and extreme events increase, the most extreme El Niño events also become weaker relative to preindustrial state while the La Niña events become stronger. That is, extreme El Niño events in G1 become less extreme than in preindustrial conditions, but extreme El Niño events become more frequent. In contrast, extreme La Niña events become stronger in G1. This is in agreement with the general overcooling of the tropical Pacific in G1 relative to preindustrial conditions, which depict a shift towards generally more La Niña-like conditions.

---

## **Seasonal and diurnal variability in $\text{O}_3$ , black carbon, and CO measured at the Rwanda Climate Observatory**

**H. Langley DeWitt<sup>1</sup>, Jimmy Gasore<sup>1,3,4</sup>, Maheswar Rupakheti<sup>2</sup>, Katherine E. Potter<sup>1</sup>, Ronald G. Prinn<sup>1</sup>, Jean de Dieu Ndikubwimana<sup>3</sup>, Julius Nkusi<sup>3</sup>, and Bonfils Safari<sup>4</sup>**

**Source** : Atmos. Chem. Phys., 19, 2063–2078, 2019  
<https://doi.org/10.5194/acp-19-2063-2019>

Air pollution is understudied in sub-Saharan Africa, resulting in a gap in the scientific understanding of emissions, atmospheric processes, and impacts of air pollutants in this region. The Rwanda Climate Observatory, a joint partnership between MIT and the government of Rwanda, has been measuring ambient concentrations of key long-lived greenhouse gases and the short-lived climate-forcing pollutants  $\text{CO}_2$ , CO,  $\text{CH}_4$ , black carbon (BC), and  $\text{O}_3$  with state-of-the-art instruments on the summit of Mt. Mugogo ( $1.586^\circ\text{S}$ ,

29.566° E; 2590 m above sea level) since May 2015. Rwanda is a small, mountainous, and densely populated country in equatorial East Africa, currently undergoing rapid development but still at less than 20 % urbanization. Black carbon concentrations during Rwanda's two dry seasons (December–January–February, DJF, and June–July–August, JJA), which coincide with the two regional biomass burning seasons, are higher at Mt. Mugogo than in major European cities with daily values (24 h) during the dry season of around  $5 \mu\text{g m}^{-3}$  (daily average concentrations ranging from less than 0.1 to over  $17 \mu\text{g m}^{-3}$  for the entire measurement period). BC baseline concentrations during biomass burning seasons are loosely correlated with fire radiative power data for the region acquired with a MODIS satellite instrument. The position and meteorology of Rwanda is such that the emissions transported from both the northern and southern African biomass burning seasons affect BC, CO, and O<sub>3</sub> concentrations in Rwanda. Spectral aerosol absorption measured with a dual-spot Aethalometer varies seasonally due to changes in types of fuel burned and the direction of pollution transport to the site. Ozone concentrations peaked during Rwanda's dry seasons (daily measured maximum of 70 ppbv). The understanding and quantification of the percent contributions of regional and local (beyond large-scale biomass) emissions is essential to guide policy in the region. During the rainy seasons, local emitting activities (e.g., cooking, transportation, trash burning) remain steady, regional biomass burning is low, and transport distances are shorter as rainout of pollution occurs regularly. Thus, local pollution at Mugogo can be estimated during this time period and was found to account for up to 35 % of annual average BC measured. Our measurements indicate that air pollution is a current and growing problem in equatorial East Africa.

---

## Direct radiative effect of dust–pollution interactions

Klaus Klingmüller<sup>1</sup>, Jos Lelieveld<sup>1,2</sup>, Vlassis A. Karydis<sup>1,3</sup>, and Georgiy L. Stenchikov<sup>4</sup>

Source : Atmos. Chem. Phys., 19, 7397–7408, 2019

<https://doi.org/10.5194/acp-19-7397-2019>

The chemical ageing of aeolian dust, through interactions with air pollution, affects the optical and hygroscopic properties of the mineral particles and hence their atmospheric residence time and climate forcing. Conversely, the chemical composition of the dust particles and their role as coagulation partners impact the abundance of particulate air pollution. This results in a change in the aerosol direct radiative effect that we interpret as an anthropogenic radiative forcing associated with mineral dust–pollution interactions. Using the ECHAM/MESSy atmospheric chemistry climate model (EMAC), which combines the Modular Earth Submodel System (MESSy) with the European Centre Hamburg (ECHAM) climate model, including a detailed parametrisation of ageing processes and an

emission scheme accounting for the chemical composition of desert soils, we study the direct radiative forcing globally and regionally, considering solar and terrestrial radiation. Our results indicate positive and negative forcings, depending on the region. The predominantly negative forcing at the top of the atmosphere over large parts of the dust belt, from West Africa to East Asia, attains a maximum of about  $-2 \text{ W m}^{-2}$  south of the Sahel, in contrast to a positive forcing over India. Globally averaged, these forcings partially counterbalance, resulting in a net negative forcing of  $-0.05 \text{ W m}^{-2}$ , which nevertheless represents a considerable fraction (40 %) of the total dust forcing.

---

## **Future climatic drivers and their effect on PM<sub>10</sub> components in Europe and the Mediterranean Sea**

**Arineh Cholakian<sup>1,2,a</sup>, Augustin Colette<sup>2</sup>, Isabelle Coll<sup>1</sup>, Giancarlo Ciarelli<sup>1,b</sup>, and Matthias Beekmann<sup>1</sup>**

**Source :** Atmos. Chem. Phys., 19, 4459–4484, 2019

<https://doi.org/10.5194/acp-19-4459-2019>

Multiple CMIP5 (Coupled Model Intercomparison Project phase 5) future scenarios run with the CHIMERE chemistry transport model (CTM) are compared to historic simulations in order to study some of the drivers governing air pollution. Here, the focus is on regional climate, anthropogenic emissions and long-range transport. Two major subdomains are explored – the European region and the Mediterranean Basin – with both areas showing high sensitivity to climate change. The Mediterranean area is explored in the context of the ChArMEx (the Chemistry Aerosol Mediterranean Experiment) project, which examines the current and future meteorological and chemical conditions of the Mediterranean area. This climate impact study covers the period from 2031 to 2100 and considers possible future scenarios in comparison with 1976 to 2005 historic simulations using three Representative Concentration Pathways (RCPs; RCP2.6, RCP4.5 and RCP8.5). A detailed analysis of total PM<sub>10</sub> (particulate matter with a diameter smaller than  $10 \mu\text{m}$ ) concentrations is carried out, including the evolution of PM<sub>10</sub> and changes to its composition. The individual effects of meteorological conditions on PM<sub>10</sub> components are explored in these scenarios in an effort to pinpoint the meteorological parameter(s) governing each component. The anthropogenic emission impact study covers the period from 2046 to 2055 using current legislation (CLE) and maximum feasible reduction (MFR) anthropogenic emissions for the year 2050 compared with historic simulations covering the period from 1996 to 2005 and utilizing CLE2010 emissions data. Long-range transport is explored by changing the boundary conditions in the chemistry transport model over the same period as the

emission impact studies. Finally, a cumulative effect analysis of these drivers is performed, and the impact of each driver on PM<sub>10</sub> and its components is estimated. The results show that regional climate change causes a decrease in the PM<sub>10</sub> concentrations in our scenarios (in both the European and Mediterranean subdomains), as a result of a decrease in nitrate, sulfate, ammonium and dust atmospheric concentrations in most scenarios. On the contrary, BSOA (biogenic secondary organic aerosol) displays an important increase in all scenarios, showing more pronounced concentrations for the European subdomain compared with the Mediterranean region. Regarding the relationship of different meteorological parameters to concentrations of different species, nitrate and BSOA show a strong temperature dependence, whereas sulfate is most strongly correlated with relative humidity. The temperature-dependent behavior of BSOA changes when looking at the Mediterranean subdomain, where it displays more dependence on wind speed, due to the transported nature of BSOA existing in this subdomain. A cumulative look at all drivers shows that anthropogenic emission changes overshadow changes caused by climate and long-range transport for both of the subdomains explored, with the exception of dust particles for which long-range transport changes are more influential, especially in the Mediterranean Basin. For certain species (such as sulfates and BSOA), in most of the subdomains explored, the changes caused by anthropogenic emissions are (to a certain extent) reduced by the boundary conditions and regional climate changes.

---

## **Anthropogenic aerosol forcing under the Shared Socioeconomic Pathways**

**Marianne T. Lund, Gunnar Myhre, and Bjørn H. Samset**

**Source :** <https://doi.org/10.5194/acp-2019-606>

Emissions of anthropogenic aerosols are expected to change drastically over the coming decades, with potentially significant climate implications. Using the most recent generation of harmonized emission scenarios, the Shared Socioeconomic Pathways (SSPs) as input to a global chemistry transport and radiative transfer model, we provide estimates of the projected future global and regional burdens and radiative forcing of anthropogenic aerosols under three different levels of air pollution control: strong (SSP1), medium (SSP2) and weak (SSP3). We find that the broader range of future air pollution emission trajectories spanned by the SSPs compared to previous scenarios translates into total aerosol forcing estimates in 2100 relative to 1750 ranging from  $-0.04 \text{ W m}^{-2}$  in SSP1-1.9 to  $-0.51 \text{ W m}^{-2}$  in SSP3-7.0. Compared to our 1750–2015 estimate of  $-0.61 \text{ W m}^{-2}$ , this shows that depending on the success of air pollution policies over the coming decades, aerosol

radiative forcing may weaken by nearly 95 % or remain close to the pre-industrial to present-day level. In all three scenarios there is a positive forcing in 2100 relative to 2015, from  $0.51 \text{ W m}^{-2}$  in SSP1-1.9 to  $0.04 \text{ W m}^{-2}$  in SSP3-7.0. Results also demonstrate significant differences across regions and scenarios, especially in South Asia and Africa. While rapid weakening of the negative aerosol forcing following effective air quality policies will unmask more of the greenhouse gas-induced global warming, slow progress on mitigating air pollution will significantly enhance the atmospheric aerosol levels and risk to human health. In either case, the resulting impacts on regional and global climate can be significant.

---

## Effective densities of soot particles and their relationships with the mixing state at an urban site of the Beijing mega-city in the winter of 2018

Hang Liu<sup>1,2</sup>, Xiaole Pan<sup>1</sup>, Yu Wu<sup>3</sup>, Dawei Wang<sup>1</sup>, Yu Tian<sup>1,2</sup>, Xiaoyong Liu<sup>1,4</sup>, Lu Lei<sup>1,2</sup>, Yele Sun<sup>1,2,4</sup>, Pingqing Fu<sup>5</sup>, and Zifa Wang<sup>1,2,4</sup>

Source : <https://doi.org/10.5194/acp-2019-526>

The effective density ( $\rho_{\text{eff}}$ ) of refractory black carbon (rBC) is a key parameter relevant to their mixing state that imposes great uncertainty when evaluating the direct radiation forcing effect. In this study, a novel tandem DMA-CPMA-SP2 system was used to investigate the relationship between the effective density ( $\rho_{\text{eff}}$ ) and the mixing state of rBC particles during the winter of 2018 in the Beijing mega-city. During the experiment, aerosols with a known mobility diameter ( $D_{\text{mob}}$ ) and known  $\rho_{\text{eff}}$  values (0.8, 1.0, 1.2, 1.4, 1.6, and  $1.8 \text{ g/cm}^3$ ) were selected and measured by the SP2 to obtain their corresponding mixing states. The results showed that the  $\rho_{\text{eff}}$  well represented the morphological variation in rBC-containing particles. The rBC-containing particles changed from an irregular and loose structure to a compact spherical structure with the increase in  $\rho_{\text{eff}}$ . A  $\rho_{\text{eff}}$  value of  $1.4 \text{ g/cm}^3$  was the morphological transition point. The morphology and  $\rho_{\text{eff}}$  value of the rBC-containing particles were intrinsically related to the mass ratio of non-refractory matter to rBC ( $M_{\text{R}}$ ). As the  $\rho_{\text{eff}}$  values of the rBC-containing particles increased from 0.8 to  $1.8 \text{ g/cm}^3$ , the  $M_{\text{R}}$  of the rBC-containing particles significantly increased from 2 up to 6–8, indicating that atmospheric aging processes were likely to lead to the reconstruction of more compact and regular particle shapes. During the observation period, the  $\rho_{\text{eff}}$  of most rBC-containing particles was lower than the morphology transition point independent of the pollution conditions, suggesting that the major rBC-containing particles did not have a spherical structure. Simulation based on an aggregate model considering the morphological



information of the particles demonstrated that absorption enhancement of rBC-containing particles could be overestimated by  $\sim 17\%$  by using a core-shell model. This study highlights the strong dependence of the morphology of ambient rBC-containing particles on  $\rho_{\text{eff}}$  and will be helpful for elucidating the micro physical characteristics of rBC and reducing uncertainty in the evaluation of rBC climate effects and health risks.

---

## **Quantifying snow darkening and atmospheric radiative effects of black carbon and dust on the South Asian monsoon and hydrological cycle: experiments using variable-resolution CESM**

**Stefan Rahimi<sup>1</sup>, Xiaohong Liu<sup>1</sup>, Chenglai Wu<sup>1,2</sup>, William K. Lau<sup>3</sup>, Hunter Brown<sup>1</sup>, Mingxuan Wu<sup>1</sup>, and Yun Qian<sup>4</sup>**

**Source** : Atmos. Chem. Phys., 19, 12025–12049, 2019  
<https://doi.org/10.5194/acp-19-12025-2019>

Black carbon (BC) and dust impart significant effects on the South Asian monsoon (SAM), which is responsible for  $\sim 80\%$  of the region's annual precipitation. This study implements a variable-resolution (VR) version of the Community Earth System Model (CESM) to quantify two radiative effects of absorbing BC and dust on the SAM. Specifically, this study focuses on the snow darkening effect (SDE), as well as how these aerosols interact with incoming and outgoing radiation to facilitate an atmospheric response (i.e., aerosol–radiation interactions, ARIs). By running sensitivity experiments, the individual effects of SDE and ARI are quantified, and a theoretical framework is applied to assess these aerosols' impacts on the SAM. It is found that ARIs of absorbing aerosols warm the atmospheric column in a belt coincident with the May–June averaged location of the subtropical jet, bringing forth anomalous upper-tropospheric (lower-tropospheric) anticyclogenesis (cyclogenesis) and divergence (convergence). This anomalous arrangement in the mass fields brings forth enhanced rising vertical motion across South Asia and a stronger westerly low-level jet, the latter of which furnishes the Indian subcontinent with enhanced Arabian Gulf moisture. Precipitation increases of  $2 \text{ mm d}^{-1}$  or more (a  $60\%$  increase in June) result across much of northern India from May through August, with larger anomalies ( $+5$  to  $+10 \text{ mm d}^{-1}$ ) in the western Indian mountains and southern Tibetan Plateau (TP) mountain ranges due to orographic and anabatic enhancement. Across the Tibetan Plateau foothills, SDE by BC aerosols drives large precipitation anomalies of  $> 6 \text{ mm d}^{-1}$  (a  $21\%$ – $26\%$  increase in May and June), comparable to ARI of absorbing aerosols from April through August. Runoff changes accompany BC SDE-induced snow changes across Tibet, while runoff changes across India result

predominantly from dust ARI. Finally, there are large differences in the simulated SDE between the VR and traditional 1° simulations, the latter of which simulates a much stronger SDE and more effectively modifies the regional circulation.

---

## Estimating global surface ammonia concentrations inferred from satellite retrievals

Lei Liu<sup>1,2,3</sup>, Xiuying Zhang<sup>2</sup>, Anthony Y. H. Wong<sup>3</sup>, Wen Xu<sup>4</sup>, Xuejun Liu<sup>4</sup>, Yi Li<sup>5</sup>, Huan Mi<sup>3,6</sup>, Xuehe Lu<sup>2</sup>, Limin Zhao<sup>2</sup>, Zhen Wang<sup>2</sup>, Xiaodi Wu<sup>2,7</sup>, and Jing Wei<sup>8</sup>

Source : Atmos. Chem. Phys., 19, 12051–12066, 2019

<https://doi.org/10.5194/acp-19-12051-2019>

Ammonia (NH<sub>3</sub>), as an alkaline gas in the atmosphere, can cause direct or indirect effects on the air quality, soil acidification, climate change and human health. Estimating surface NH<sub>3</sub> concentrations is critically important for modeling the dry deposition of NH<sub>3</sub> and for modeling the formation of ammonium nitrate, which have important impacts on the natural environment. However, sparse monitoring sites make it challenging and difficult to understand the global distribution of surface NH<sub>3</sub> concentrations in both time and space. We estimated the global surface NH<sub>3</sub> concentrations for the years of 2008–2016 using satellite NH<sub>3</sub> retrievals combining vertical profiles from GEOS-Chem. The accuracy assessment indicates that the satellite-based approach has achieved a high predictive power for annual surface NH<sub>3</sub> concentrations compared with the measurements of all sites in China, the US and Europe ( $R^2=0.76$  and  $RMSE = 1.50 \mu\text{g N m}^{-3}$ ). The satellite-derived surface NH<sub>3</sub> concentrations had higher consistency with the ground-based measurements in China ( $R^2=0.71$  and  $RMSE = 2.6 \mu\text{g N m}^{-3}$ ) than the US ( $R^2=0.45$  and  $RMSE = 0.76 \mu\text{g N m}^{-3}$ ) and Europe ( $R^2=0.45$  and  $RMSE = 0.86 \mu\text{g N m}^{-3}$ ) at a yearly scale. Annual surface NH<sub>3</sub> concentrations higher than  $6 \mu\text{g N m}^{-3}$  are mainly concentrated in the North China Plain of China and northern India, followed by  $2\text{--}6 \mu\text{g N m}^{-3}$  mainly in southern and northeastern China, India, western Europe, and the eastern United States (US). High surface NH<sub>3</sub> concentrations were found in the croplands in China, the US and Europe, and surface NH<sub>3</sub> concentrations in the croplands in China were approximately double those in the croplands in the US and Europe. The linear trend analysis shows that an increase rate of surface NH<sub>3</sub> concentrations ( $> 0.2 \mu\text{g N m}^{-3} \text{ yr}^{-1}$ ) appeared in eastern China during 2008–2016, and a middle increase rate ( $0.1\text{--}0.2 \mu\text{g N m}^{-3} \text{ yr}^{-1}$ ) occurred in northern Xinjiang over China. NH<sub>3</sub> increase was also found in agricultural regions in the central and eastern US with an annual increase rate of lower than  $0.10 \mu\text{g N m}^{-3} \text{ yr}^{-1}$ . The satellite-derived

surface NH<sub>3</sub> concentrations help us to determine the NH<sub>3</sub> pollution status in the areas without monitoring sites and to estimate the dry deposition of NH<sub>3</sub> in the future.

---

### 3. Atmospheric Environment - 3.629

#### **Investigating horizontal and vertical pollution gradients in the atmosphere associated with an urban location in complex terrain, Reno, Nevada, USA**

**Ashley M. Pierce<sup>a</sup>, S. Marcela Loría-Salazar<sup>b</sup>, Heather, A. Holmes<sup>b</sup>, Mae S. Gustin<sup>a</sup>**

**Source :** Atmospheric Environment, Volume:196, January 2019, Pages 103-117

A new statistical method, the quadrant method, was used to aid in identifying different conditions affecting the relationship between columnar aerosol optical depth ( $\tau_{\text{ext}}$ ) and surface concentrations of particulate matter ( $<2.5 \mu\text{g m}^{-3}$  in aerodynamic diameter, PM<sub>2.5</sub>). The main goal of this study was to identify air pollution sources and atmospheric processes affecting gradients of atmospheric pollutants observed at two valley sites (~1370 m) and a high elevation site (2515 m) located in and adjacent to Reno, Nevada, USA. The two valley sites were used to investigate the horizontal gradient of pollutants associated with mobile sources from high volume highways. Results indicated statistically significant differences in concentrations of criteria air pollutants between the two valley sites, located 0.03 km and  $>1$  km from major highways. Vertical gradients were impacted by air pollution sources, including local and long-range transport, and atmospheric boundary layer stability. During periods when  $\tau_{\text{ext}}$  and surface PM<sub>2.5</sub> concentrations were associated (i.e. both increase), emissions from wildfires and local pollutants in a well-mixed boundary layer dominated the relationship. During periods of no association, stable boundary layer conditions and pollution aloft created vertical heterogeneity of PM<sub>2.5</sub> concentrations. Results showed that the quadrant method, developed for hourly data, can be used with 24 h PM<sub>2.5</sub> and gaseous data and that it is a useful tool for identifying air pollution sources and atmospheric physics driving pollution gradients.

**Keywords :** Quadrant method; Aerosol optical depth; PM<sub>2.5</sub>; Atmospheric stability; Vertical heterogeneity; Near-road pollution gradients.

---

## **A modelling study of the terrain effects on haze pollution in the Sichuan Basin**

**LeiZhang<sup>ab</sup>, XiaomeiGuo<sup>bcd</sup>, TianliangZhao<sup>ab</sup>, SunlingGong<sup>e</sup>, XiangdeXu<sup>f</sup>, YueqingLi<sup>g</sup>, LeiLuo<sup>g</sup>, KeGui<sup>e</sup>, HaoliangWang<sup>ab</sup>, YuZheng<sup>ab</sup>, XiaofeiYin<sup>h</sup>**

**Source** : Atmospheric Environment, Volume:196, January2019, Pages 77- 85

The Sichuan Basin (SB), covering 260,000 km<sup>2</sup> immediately to the east of the Tibetan Plateau (TP) with a large drop exceeding 3000 m in elevation over a short horizontal distance, is a region of high haze pollution in China. The terrain effects of this unique deep basin on haze pollution have not been well investigated. During 14–19 January 2014, heavy haze pollution engulfed the SB with high PM<sub>2.5</sub> concentrations. By using the WRF-Chem model, the topographic effects on haze pollution in the SB and the underlying mechanisms were investigated by two sets of simulation with and without the basin topography. The simulation results show that the SB topography lead to an increase of 48 μg m<sup>-3</sup> in the basin-averaged surface PM<sub>2.5</sub> contributing about 44% to the PM<sub>2.5</sub> concentrations during heavy haze pollution, indicating an important role of the basin topography in worsening air pollution. The surface PM<sub>2.5</sub> level enhancements varied spatially from 0 to 30 μg m<sup>-3</sup> in the eastern basin to 60–120 μg m<sup>-3</sup> in the western basin, respectively corresponding to 0–20% and 50–70% relative to the concentrations simulated without the SB topographic condition, reflecting the stronger topographic effect of the TP in the western SB. The topographic effects intensify the haze pollution via reducing wind speed, raising air temperature and humidity in the lower troposphere, as well as dropping boundary layer height in the basin. Resulted from the impact of TP on mid-latitude westerly winds, a typical leeside vortex of immediately upstream TP over the basin was developed with accentuating PM<sub>2.5</sub> accumulations in the basin, implying a strong influence of TP on air quality in the SB.

**Keywords** : Terrain effects; Haze pollution; Sichuan Basin; WRF-Chem.

---

## **Synoptic and local circulations associated with events of high particulate pollution in Valparaiso, Chile**

**DianaPozo<sup>ad</sup>, Julio C.Marín<sup>ad</sup>, Graciela B.Raga<sup>b</sup>, orgeArévalo<sup>ae</sup>, DarrelBaumgardner<sup>c</sup>, Ana M.Córdova<sup>a</sup>, JorgeMora<sup>a</sup>**

**Source** : Atmospheric Environment, Volume:196, January2019, Pages 164- 178

This study discusses the synoptic situations associated with cases of high pollution in terms of black carbon (BC) concentrations observed at the research site during the four months of the VAMPIRE campaign that is described fully in the companion study by Marín et al. (2017). Cases in which the concentration of BC exceeded the 85<sup>th</sup> percentile were selected to evaluate composite synoptic situations, resulting in a total of fifteen cases analyzed. These fifteen cases occurred during one of the three prevalent synoptic situations identified and labeled as: i) **Coastal low**, characterized by weak easterly winds and low planetary boundary layer (PBL) height due to an enhancement of the temperature inversion before the arrival of the coastal low; ii) **Pre-frontal**, also characterized by low PBL height, with a cold front approaching from the South and the coastal low retreating northwards, also associated with pollution episodes in Santiago (Rutllant and Garreaud, 1995); and iii) **SEP anticyclone** characterized by large stability, very low gradient in the mean sea level pressure and weak westerly-southwesterly wind due to the dominance of the southeast Pacific anticyclone. **Coastal low** cases were observed not only during winter but also in all four months of the VAMPIRE field campaign, while **Pre-frontal** cases were observed only at the end of July and August 2014. All three synoptic situations are consistent with a reduced synoptic forcing, in which the mesoscale sea-land breeze predominates and advects large pollutant concentrations from local/regional emission sources to the research site. Detailed analysis is presented here for two case studies: one **Coastal low** and one **Pre-frontal**, combining the observations of pollutants as well as mesoscale modeling with the WRF model to estimate back-trajectories and evaluate the relative role of the synoptic and mesoscale forcing on the pollution episodes in Valparaíso. These synoptic conditions and their interplay with meso-scale circulations identified during VAMPIRE provide evidence and insight that will aid in future air quality forecasts for Valparaíso.

**Keywords :** Pollution episodes; Black carbon; Synoptic forcing; Land-sea breeze.

---

## **Atmospheric emission inventory of SO<sub>3</sub> from coal-fired power plants in China in the period 2009–2014**

**JialiShen, ChenghangZheng, Linjie, XuYangZhang, Yongxin, Zhang, ShaojunLiuXiangGao**

**Source :** Atmospheric Environment, Volume:197,15 January2019,Pages14 – 21

Sulfur trioxide (SO<sub>3</sub>) pollution is becoming another severe problem in coal-fired power plants after SO<sub>2</sub>, NO<sub>x</sub>, and PM, however, the characteristics of SO<sub>3</sub> emission in China remains unclear. In this paper, we established a refined activity data, and summarized the removal efficiency of different control technologies according to the literature review and field test results. An emission inventory of SO<sub>3</sub> from coal-fired power plants in China between 2009 and 2014 was developed, which indicated the SO<sub>3</sub> emission increased from 199.7 kilotons (kt) to 314.6 kt at an average annual growth rate of 9.7%. The results show that Neimenggu, Shānxi, Jiangsu, Shandong, Guangdong and Guizhou were the largest emitters, accounting for 49.7% of the total SO<sub>3</sub> emissions in 2014. We analyzed the

historical data with ArcGIS system, which allocates the emission into 36 km × 36 km grid cells. In addition, the result shows the unevenly spatial distribution. Combined with future economic development as well as implementation of policy, three different scenarios were set to project SO<sub>3</sub> emission in coal-fired power plants in 2020, which represented the potential of SO<sub>3</sub> emission reduction. Compared with scenario A, SO<sub>3</sub> emission can be reduced to 83.9 kt in scenario B, and in scenarios C, SO<sub>3</sub> emission can be reduced to 38.4 kt. Coal-fired power plants should adopt different technology routes to meet the ultra-low emission requirement and reduce the SO<sub>3</sub> emission according to the boilertype, sulfur content, and the emission standard.

**Keywords :** SO<sub>3</sub> emission; Inventory; Coal-fired power plants; Ultra-low emission; Scenario.

---

## **Urban land use regression models: can temporal deconvolution of traffic pollution measurements extend the urban LUR to suburban areas?**

**Kerolyn, K.Shairsingh<sup>a</sup>, Cheol-HeonJeong<sup>a</sup>, Jonathan M.Wang<sup>c</sup>, Jeffrey R.Brook<sup>ab</sup>, Greg J.Evans<sup>a</sup>**

**Source :** Atmospheric Environment, Volume:196,January2019,Pages – 143-151

Land use regression (LUR) models that predict intra-urban variability of traffic-related air pollution are frequently used to inform exposure assessments in epidemiological studies. Spatially extending models built in city centres to unmeasured surrounding areas could be beneficial as it increases the size of area available for exposure assessment, which can improve the statistical power of health studies. However, past studies have shown poor performance when these models were transferred to unmeasured areas. In this study, ambient concentrations of black carbon (BC), ultrafine particles (UFP), nitric oxide (NO) and nitrogen dioxide(NO<sub>2</sub>) with response times ranging from 1 s to 20 s were measured in the summer using a mobile laboratory. These ambient concentrations were temporally deconvolved into local, neighbourhood- and regional-background time-series signals. The temporally resolved signals were used to develop resolved LUR models (i.e. local, neighbourhood-background and regional-background models) while unresolved LUR models were developed from total ambient concentrations (i.e., measurements that were not temporally resolved). Both resolved and unresolved LUR models displayed modest R<sup>2</sup> values when compared to models developed from fixed sites which may be due to the mobile nature of our data. External validation of the resolved and unresolved models within the models' original geographic domain showed comparable performance for BC (R<sup>2</sup> for resolved vs. unresolved: 0.44 vs. 0.47), UFP (0.34 vs. 0.35), NO (0.18 vs. 0.19) and NO<sub>2</sub> (0.42 vs.0.40). However, the resolved models were better able to assess exposure than the unresolved models when they were spatially extended to suburban areas bordering the

urban area: UFP ( $R^2$ : 0.42 vs. 0.29),  $\text{NO}_2$  (0.36 vs 0.26), NO (0.21 vs 0.14) and BC (0.32 vs 0.30). Furthermore, the resolved models were better able to predict the observed variability in suburban areas with both similar and different land uses to the urban area.

**Keywords** : Mobile sampling; Local model; Neighbourhood background model; Ultrafine particles; Nitrogen oxides; Land use regression.

---

## **Spatio-temporal variation of wind influence on distribution of fine particulate matter and its precursor gases**

**Hamed, KarimianaQiLiab, ChengcaiLic, GongChenaYuqin, MoaChunlin, WuaJunxiangFana**

**Source** : Atmospheric Pollution Research, Volume 10, Issue 1, January 2019, Pages 53-64

Frequent occurrence of severe haze in Beijing indicates the importance of effective decisions and clear goals to reduce the concentration of particulate matter in the atmosphere. To achieve this goal, elucidation of the elements governing fine particulate matter concentrations should be considered as one of the priorities. In this paper, we proposed a statistical model based on physical understanding of the diffusion of air pollutants by wind to investigate the sensitivity of fine particulate matter and its precursor gases concentrations to wind speed and direction. By using our method, it is possible to determine the major wind directions that have large impact on air quality for a particular area. Our results showed that the influence of wind on the concentration of particulate matter and its precursor gases varies spatially over Beijing. Our method suggested that both local emission sources of fine particulate matter and its precursor gas ( $\text{NO}_2$ ) and transported  $\text{SO}_2$  from regional industries should be reduced for the remediation of severe air pollution scenarios, especially in the Beijing urban area. Our approach serves as a good complement for commonly used approaches for source apportionment analysis without exploiting complicated methods. The method shows its feasibility in identifying air pollutant emission sources based on wind patterns and can be used in other regions as an aid in air pollution controlling programs.

**Keywords** : Tropospheric aerosol, Ground level concentration, Air pollution, Statistical model, Particle transport.

---

## **Seasonal variation, sources and health risk assessment of polycyclic aromatic hydrocarbons in different particle fractions of PM<sub>2.5</sub> in Beijing, China**

**HaojunSongab, YangZhangb, MinLuoa, Jianzhong, GubMinghong, WubDiandou, XuaGangXub, LinglingMaa**

**Source :** Atmospheric Pollution Research, Volume 10, Issue 1, January 2019, Pages 105-114

The ratio of SO<sub>2</sub>/NO<sub>2</sub> together with PM<sub>2.5</sub>/CO was applied to explain the source of particulate matters (PM) pollution in Beijing. Polycyclic aromatic hydrocarbons (PAHs) bounded with ultrafine particles were investigated as well. A total of 188 graded PM in four-stage size segregated aerosol particles were collected and analyzed by GC-MS in 2016 to investigate the sources and distribution patterns of PAHs in metropolis-Beijing. A significant seasonal variation of 16 PAHs in PM<sub>2.5</sub> around in Beijing was observed with  $32.93 \pm 15.19 \text{ ng m}^{-3}$ ,  $17.77 \pm 8.08 \text{ ng m}^{-3}$ ,  $31.61 \pm 12.67 \text{ ng m}^{-3}$  and  $78.06 \pm 40.97 \text{ ng m}^{-3}$  in spring, summer, autumn and winter, respectively. The ratio of SO<sub>2</sub>/NO<sub>2</sub> demonstrated that vehicle emissions significantly contributed to air pollution. On the contrary, the lower ratio of PM<sub>2.5</sub>/CO showed high direct discharge from combustion. Seasonal distribution patterns of PM<sub>0.2</sub>/PM<sub>2.5</sub> suggested that abundant secondary aerosols were produced in the autumn and winter. The spread of pollutants was not significant in winter. Both the combustion of fuel and coal were the primary sources of PM<sub>2.5</sub>-bound PAHs. A health risk assessment was represented by benzo[a]pyrene equivalent (BaP<sub>eq</sub>) indicating potential cancer risk in Beijing. Furthermore, the lifetime excess cancer risk (ECR) was  $3.00 \times 10^{-4}$ , which was higher than the guidelines of USEPA and European Commission, indicating high carcinogenic risk of PM<sub>2.5</sub> in Beijing. Therefore, more strictly control measures should be taken to reduce PAHs emissions from coal and vehicle.

**Keywords:** Particulate matter, Fractions, Polycyclic aromatic hydrocarbons (PAHs), Sources, Health risk assessment.

---

## **Applying machine learning methods in managing urban concentrations of traffic-related particulate matter (PM<sub>10</sub> and PM<sub>2.5</sub>)**

**A.Suleimana, M.R.Tightb, A.D.Quinnb**

**Source :** Atmospheric Pollution Research, Volume 10, Issue 1, January 2019, Pages 134-144

This study presents a new method for evaluating the effectiveness of roadside PM<sub>10</sub> and PM<sub>2.5</sub> reduction scenarios using Machine Learning (ML) based models. The ML methods include Artificial Neural Networks (ANN), Boosted Regression Trees (BRT) and Support Vector Machines (SVM). Traffic, meteorological and pollutant data collected at nineteen Air Quality Monitoring (AQM) sites in London for a period between 2007 and 2012 was used.



The ML models performed very well in predicting the concentrations of PM10 and PM2.5 with around 95% of their predictions falling within the factor of two of the observed concentrations at the roadsides. The prediction errors observed were very small as indicated by the average normalised mean gross errors of 0.2. Also, the predictions of the models correlated well with the observed concentrations as shown by the average values of R (0.8) and index of agreement (0.74). Additionally, when some PM10 and PM2.5 reduction scenarios were modelled, the ML models predicted various degree of reductions in the roadside concentrations. In conclusion, well trained ANN and BRT models can be successfully applied in predictions of roadside PM10 and PM2.5 concentrations. Moreover, they can be applied in measuring the effectiveness of roadside particle reduction scenarios.

**Keywords:** Machine learning, Air quality, Particulate matter, Traffic emissions, Neural networks, Boosted regression trees

---

## **PM2.5 and its ionic components at a roadside site in Wuhan, China**

**WuGuang, Lin-JunLi, Rong-BiaoXiang**

**Source :** Atmospheric Pollution Research, Volume 10, Issue 1, January 2019, Pages 162-167

PM2.5 samples were collected at a roadside site in Wuhan, China, for one year period. Ion chromatography was used to determine the water soluble ions in PM2.5 samples. Results showed that the overall average of PM2.5 mass was  $118.1 \pm 70.3 \mu\text{g m}^{-3}$ , being slightly higher than those measured in urban sites in Wuhan, China. The major water soluble ions were  $\text{NH}_4^+$  ( $8.7 \pm 4.0 \mu\text{g m}^{-3}$ ),  $\text{NO}_3^-$  ( $12.1 \pm 9.5 \mu\text{g m}^{-3}$ ),  $\text{SO}_4^{2-}$  ( $15.2 \pm 8.2 \mu\text{g m}^{-3}$ ), accounting for 21%、29%、37% of quantified total ions, respectively.  $\text{NH}_4^+$ ,  $\text{NO}_3^-$ , and  $\text{SO}_4^{2-}$  were closely correlated, and  $(\text{NH}_4)_2\text{SO}_4$  and  $\text{NH}_4\text{NO}_3$  were possibly their main existing forms. Ion concentrations differed greatly in different seasons, with inconsistent variation pattern for individual ions. Values of NOR (nitrogen oxidation ratio) and SOR (sulfur oxidation ratio) peaked in winter and in summer, respectively.  $\text{NO}_3^-/\text{SO}_4^{2-}$  ratio revealed that emission from stationary sources was still remarkable. Significant correlation was observed between  $\text{Mg}^{2+}$  and  $\text{Ca}^{2+}$ , possibly due to their common source of soil dust. On the other hand,  $\text{Cl}^-$  linked with  $\text{K}^+$ ,  $\text{NO}_3^-$ ,  $\text{NH}_4^+$ , and  $\text{SO}_4^{2-}$ . The data reported here will provide inputs for human exposure and air pollution control studies in Wuhan, China.

**Keywords:** PM<sub>2.5</sub>, Water-soluble ions, Seasonal variation, Correlation, Roadside.

---

## **Analyses of regional pollution and transportation of PM<sub>2.5</sub> and ozone in the city clusters of Sichuan Basin, China**

**SupingZhao<sup>abc</sup>, YeYu<sup>a</sup>, DaheQin<sup>c</sup>, DaiyingYin<sup>d</sup>, LongxiangDong<sup>a</sup>, JianjunHe<sup>e</sup>**

**Source** : : Atmospheric Environment, Volume 10, Issue 2, March 2019, Pages 374-385

Regional PM<sub>2.5</sub> and ozone pollution and inter-city transportation in the city clusters of the Sichuan Basin (SB) were revealed using k-means clustering and the HYSPLIT backward trajectory model. The PSCF (potential source contribution function) and CWT (concentration-weighted trajectory) methods also were used to identify potential source regions of PM<sub>2.5</sub> and ozone in the basin. The regional PM<sub>2.5</sub> pollution was obvious with high levels at western and southern SB, while regional pollution characteristics of ozone were less significant than that of PM<sub>2.5</sub> inside the basin. Additionally, PM<sub>2.5</sub> was often transported directionally from one city to another city, while regional transportation of ozone was less significant than PM<sub>2.5</sub> inside the basin, which may be related to the fact that ozone reacted easily with primary emissions during transportation. The Tibetan Plateau (TP) also may be an important source region of high ozone in the city clusters of Sichuan Basin, especially west part of the basin. The results will provide advice to the government to take measures in improving air quality of SB.

**Keywords** : Sichuan Basin,Regional pollution,PM<sub>2.5</sub>,Ozone,HYSPLIT,Clustering analysis.

---

## **Sources of indoor air pollution at a New Zealand urban primary school; a case study**

**JulieBennett<sup>a</sup>, PerryDavy<sup>b</sup>BillTrompetter<sup>b</sup>, YuWang<sup>c</sup>, NevilPierse<sup>a</sup>, MikaelBoulic<sup>c</sup>, RobynPhipps<sup>c</sup>, PhilippaHowden-Chapman<sup>a</sup>**

**Source** : Atmospheric Environment, Volume 10, Issue 2, March 2019, Pages 418-434

Children are particularly vulnerable to the health effects of air pollution and as they spend a large proportion of time at school, this is an important environment for children's exposure to air pollution. Understanding the factors that influence indoor air quality in schools is critical for the assessment and control of indoor air pollution. This study analysed the concentration and sources of air pollution at an urban primary school (5–11 years) in Wellington, the capital of New Zealand. Over a three-week period during spring, indoor measures of particulate matter (PM<sub>2.5</sub>, PM<sub>10</sub>), temperature, humidity, carbon dioxide (CO<sub>2</sub>) and nitrogen dioxide (NO<sub>2</sub>) were taken and hourly air particulate matter samples (PM<sub>2.5</sub>, PM<sub>10-2.5</sub>) were collected inside and outside for elemental speciation analysis. Indoor PM<sub>10</sub> concentrations during the school day were significantly ( $p < 0.001$ ) higher than

outdoor concentrations 30.1 (range 10.0–75.0, SD 1.9)  $\mu\text{g m}^{-3}$  c.f. 8.9 (range <1.0–35.0, SD 6.8)  $\mu\text{g m}^{-3}$ . Elemental analysis and receptor modelling of PM samples showed that indoor  $\text{PM}_{10}$  was primarily composed of crustal matter (soil) elements, possibly brought in on children's footwear. The primary driver of indoor  $\text{PM}_{2.5}$  was from the infiltration of outdoor pollutants inside, with by-products of motor vehicle emissions the main contributor to indoor  $\text{PM}_{2.5}$ . There is a need for mitigation strategies to reduce exposure to indoor air pollution at school, such as improved cleaning methods, reducing the use of carpet in schools and improved ventilation. The findings from this study will be applicable to many other schools and public buildings with high foot traffic.

**Keywords :** Air quality, Air pollution, Schools, Children, Source apportionment.

---

## **Sources of indoor air pollution at a New Zealand urban primary school; a case study**

**Julie Bennetta, Perry Davyb, Bill Trompetterb, Yu Wangc, Nevil Piersea, Mikael Boulicc, Robyn Phippsc, Philippa, Howden-Chapmana**

**Source :** Atmospheric Pollution Research, Volume 10, Issue 2, March 2019, Pages 435-444

Children are particularly vulnerable to the health effects of air pollution and as they spend a large proportion of time at school, this is an important environment for children's exposure to air pollution. Understanding the factors that influence indoor air quality in schools is critical for the assessment and control of indoor air pollution. This study analysed the concentration and sources of air pollution at an urban primary school (5–11 years) in Wellington, the capital of New Zealand. Over a three-week period during spring, indoor measures of particulate matter ( $\text{PM}_{2.5}$ ,  $\text{PM}_{10}$ ), temperature, humidity, carbon dioxide ( $\text{CO}_2$ ) and nitrogen dioxide ( $\text{NO}_2$ ) were taken and hourly air particulate matter samples ( $\text{PM}_{2.5}$ ,  $\text{PM}_{10-2.5}$ ) were collected inside and outside for elemental speciation analysis. Indoor  $\text{PM}_{10}$  concentrations during the school day were significantly ( $p < 0.001$ ) higher than outdoor concentrations 30.1 (range 10.0–75.0, SD 1.9)  $\mu\text{g m}^{-3}$  c.f. 8.9 (range <1.0–35.0, SD 6.8)  $\mu\text{g m}^{-3}$ . Elemental analysis and receptor modelling of PM samples showed that indoor  $\text{PM}_{10}$  was primarily composed of crustal matter (soil) elements, possibly brought in on children's footwear. The primary driver of indoor  $\text{PM}_{2.5}$  was from the infiltration of outdoor pollutants inside, with by-products of motor vehicle emissions the main contributor to indoor  $\text{PM}_{2.5}$ . There is a need for mitigation strategies to reduce exposure to indoor air pollution at school, such as improved cleaning methods, reducing the use of carpet in schools and improved ventilation. The findings from this study will be applicable to many other schools and public buildings with high foot traffic.

**Keywords :** Air quality, Air pollution, Schools, Children, Source apportionment.

---

## **On-road measurements and modelling of vehicular emissions during traffic interruption and congestion events in an urban traffic corridor**

**Arti Choudhary, Sharad Gokhale**

**Source :** Atmospheric Environment, Volume 10, Issue 2, March 2019, Pages 480-492

Traffic events such as interruptions and congestions occur on urban roads causing higher vehicular emissions resulting in air-pollution hotspots. This study investigates the performances of two emission models for estimating emissions from passenger cars and auto-rickshaws of different mileages, moving with a traffic fleet during these events. The instantaneous measurements of emissions and speeds were carried out on a test route of 3.8 km by integrating the auto-gas analyser and V-Box for estimating the on-road emission factors (EFs). The measured driving profiles and acceleration/decelerations were used in the IVE emission model and the speed was averaged in the COPERT-IV emission model into 0–10 km/h; 10–25 km/h; 25–35 km/h and >35 km/h. The on-road EFs of CO, HC, CO<sub>2</sub> and NO<sub>x</sub> at peak hours (PHs) and off-peak hours (OPHs) were compared with the modelled EFs. The estimates of COPERT-IV were about 25% less for CO, HC and CO<sub>2</sub> and 26–39% more for NO<sub>x</sub> than IVE during PHs. As compared to the on-road EF, the IVE estimates for CO, HC, CO<sub>2</sub> was 5–50% less and 12–50% higher for NO<sub>x</sub> for auto-rickshaw and passenger car; and the COPERT-IV estimates for CO, HC, CO<sub>2</sub> were 30–74% less and 6–86% higher for NO<sub>x</sub>, showing that instantaneous driving profiles in emission modelling are important. The interruptions during PHs were 80% of the time, a cause of deviations in the models. Thus, the real-world emissions vary with the levels of interruptions and congestions on the roads, and hence emission models must account for these events.

**Keywords :** Traffic flow, Instantaneous driving profile, Emission model, Congestion, Traffic speed.

---

## **Bottom-up emission inventories of multiple air pollutants from open straw burning: A case study of Jiangsu province, Eastern China**

**LiLiQiuyue, ZhaoJieZhang, Huipeng, LiQianLiu, Chunyan, LiFengChen, YueZhenQiao, JunzanHan**

**Source :** Atmospheric Pollution Research, Volume 10, Issue 2, March 2019, Pages 501-507

Open straw burnings during harvest season generated large amounts of air pollutants in a short duration, resulting in significant visibility reduction, air quality deterioration and adverse impact on human health. In this study, a bottom-up approach of county level emission inventory from open straw burning was developed. A 1 km resolution inventories

for Jiangsu province, Eastern China, was established as a case study. In order to increase temporal-spatial resolution, county level, seasonal data and local parameters were preferentially used. Per capita disposable income of rural residents was used to adjust burning proportion for different cities. Emissions during summer-harvest and autumn-harvest seasons were calculated separately. The inventory was further allocated based on both MODIS fire product and land use data of cropland. Total emissions of SO<sub>2</sub>, NO<sub>x</sub>, THC, NH<sub>3</sub>, OC, BC and primary PM<sub>2.5</sub> from open straw burning in 2015 were 3.72, 15.25, 43.52, 2.65, 16.08, 2.08 and 44.70 Gg, respectively. From 2010 to 2015, provincial emissions decreased by 50.7% in average, and the difference between southern and northern Jiangsu has been even enlarged. Autumn-harvest crop straw contributed 63%–67% to NH<sub>3</sub>, OC and PM<sub>2.5</sub>, while summer-harvest crop straw contributed 60% to BC. Wheat and rice straws burning accounted for the majority of emissions at 80%–91% of the total for all 7 pollutants. Uncertainties ranged from a low of within 29% for BC to a high of within 40% for NH<sub>3</sub>. The EFs and the crop production of autumn-harvest rice and summer harvest wheat, are the key uncertainty sources.

**Keywords :** Open straw burning, Emission inventory, High resolution, MODIS, Land use.

---

## **Dust emission from crushing of hard rock aggregates**

**Marjo, Sairanen, Mikael , Rinne**

**Source :** Atmospheric Pollution Research, Volume 10, Issue 2, March 2019, Pages 656-664

Dust constitutes one of the major environmental concerns near many aggregate quarries, with crushing often being the most significant source. In this study, dust emissions and dispersion measurements were conducted under real operating conditions at six aggregate quarries in southern Finland. Five of them represent granitic rocks and one a limestone quarry.

Dust concentrations during crushing were measured at varying distances with time intervals of five seconds. The variation in dust concentration was high within all the measured distances, ranging from 10 to 200 m.

Crushing produces mainly coarse (TSP and PM<sub>10</sub>) dust particles, which settle near the dust source. The mass concentration of coarse particles in this investigation varied from few tens of µg/m<sup>3</sup> to over  $6.5 \times 10^3$  µg/m<sup>3</sup> downwind from the crusher.

The mass concentration of fine particles (PM<sub>2.5</sub> and PM<sub>1</sub>) ranged between ten µg/m<sup>3</sup> and few hundreds of µg/m<sup>3</sup> downwind from the crusher. The fine particles originated mainly from machinery used in the quarries and remote sources, such as nearby traffic.

In quarries operating with secondary crushing, the background concentrations were achieved approximately from a 350 m distance for coarse particles. Local dust sources,

such as hauling, impacted the results inside the quarry. Crushing produced more dust compared to comparable studies for drilling. The dust concentrations at the limestone quarry were approximately 50% of concentrations measured at quarries with granitic rocks.

**Keywords:** Aggregate, Crushing, Dust mass concentration, Open-pit quarry, PM<sub>10</sub>, TSP.

---

## **Simulation analysis of atmospheric SO<sub>2</sub> contributions from different regions in China**

**JieJiang<sup>a</sup>, YongZha<sup>b</sup>, LongLi<sup>b</sup>**

**Source :** Atmospheric Environment, Volume 10, Issue 3, May 2019, Pages 913-920

Sulfur dioxide (SO<sub>2</sub>) is an atmospheric pollution source that poses a threat to the environment and human health. Investigating atmospheric SO<sub>2</sub> contributions between different regions will help to reduce SO<sub>2</sub> emissions and control pollution. Using the weather research and forecasting (WRF) model and the community multiscale air quality (CMAQ) modeling system, as well as the intercontinental chemical transport experiment phase B (INTEX-B) data, we analyzed the regional contributions of atmospheric SO<sub>2</sub> in China. The results showed that SO<sub>2</sub> contributions varied significantly between regions and seasons. The atmospheric SO<sub>2</sub> levels in Central China (CTR) originated mostly from self-emissions, accounting for as much as 60% of the total emissions in January and April and up to 85% in July and October. The SO<sub>2</sub> concentrations in Northeast China (NE) were mainly affected by emissions from CTR, especially in January (39.53%). SO<sub>2</sub> concentrations in Northwest China (NW) were mainly affected by external emissions, which exceeded half of the SO<sub>2</sub> in this region. SO<sub>2</sub> concentrations in Southwest China (SW) were dominated by self-emissions, which accounted for more than 90% of the total SO<sub>2</sub>. In terms of seasons, SO<sub>2</sub> concentrations were significantly affected by external emissions in January and April and were dominated by self-emissions in July and October. Coal use, population, area, and thermal power were found to have the greatest impacts on SO<sub>2</sub> concentrations. Among these, coal consumption had the biggest impact on the national SO<sub>2</sub> concentration.

**Keywords :** Sulfur dioxide, Spatial pattern, Driving factor, CMAQ simulation.

---

## **Air quality, emissions, and source contributions analysis for the Greater Bengaluru region of India**

**SarathK.Guttikunda<sup>abc</sup>, K.A.Nishadh<sup>a</sup>, SudhirGota<sup>a</sup>, PratimaSingh<sup>c</sup>, ArijitChanda<sup>c</sup>,  
PujaJawahar<sup>a</sup>, JaiAsundi<sup>c</sup>**

**Source :** Atmospheric Environment, Volume 10, Issue 3, May 2019, Pages 941-953

Bengaluru - capital of the state of Karnataka is the original “Silicon Valley” of India. In this paper, we present a comprehensive snapshot of the state of air quality in Bengaluru, along with an emissions inventory for the pollutants necessary for chemical transport modeling at 0.01° grid resolution (approximately 1-km), for an urban airshed covering 60 × 60 grids (4300 km<sup>2</sup>). For 2015, emission estimates for the city are 31,300 tons of PM<sub>2.5</sub>, 67,100 tons of PM<sub>10</sub>, 5300 tons of SO<sub>2</sub>, 56,900 tons of NO<sub>x</sub>, 335,550 tons of CO, and 83,500 tons of NMVOCs. Overall, transport is the key emission source for Bengaluru - vehicle exhaust and on-road dust resuspension account for a combined 56% and 70% of total PM<sub>2.5</sub> and PM<sub>10</sub> emissions; followed by industries (17.8% including the brick kilns), open waste burning (11.0%), and domestic cooking, heating, and lighting (6.5%), in case of PM<sub>2.5</sub>. We conducted particulate pollution source apportionment of local and non-local sources, using WRF meteorological model and CAMx chemical transport modeling system. A comparison of range of 24-hr average modeled PM<sub>2.5</sub> concentrations (36.5 ± 9.0 µg/m<sup>3</sup>) and monitored PM<sub>2.5</sub> concentrations (32.3 ± 24.2 µg/m<sup>3</sup>) by month, shows that the model catches the quantitative ranges and qualitative trends. The modeled source contributions highlight the vehicle exhaust (28%) and dust (including on-road resuspended dust and construction activities) (23%), and open waste burning (14%), as the key air pollution sources. Unless there is an aggressive strategy to improve urban planning and public transport options, pollutant emissions under the business as usual scenario are expected to increase at least 50% in 2030 and doubling the urban area with PM<sub>2.5</sub> annual averages above the national ambient standard of 40 µg/m<sup>3</sup>.

**Keywords :** Air quality, Particulates, PM<sub>2.5</sub>, Bengaluru, Bangalore, India, Emissions inventory, Chemical transport modeling, WRF-CAMx.

---

## **PM<sub>2.5</sub> emission characteristics of coal-fired power plants in Beijing-Tianjin-Hebei region, China**

**SongtaoLiu<sup>a</sup>, ZhiboZhang<sup>ab</sup>, YuWang<sup>a</sup>, YanglinHu<sup>a</sup>, WentingLiu<sup>a</sup>, ChuanminChen<sup>a</sup>,  
YuqianMei<sup>a</sup>, HeSun<sup>b</sup>**

**Source :** Atmospheric Environment, Volume 10, Issue 3, May 2019, Pages 954-959

In this study, six typical coal-fired power plants (CFPPs) in Beijing-Tianjin-Hebei (BTH) region were selected to investigate the emission characteristic of PM<sub>2.5</sub>. A 5-stage large flow impact sampler (DGI) was applied to collect PM<sub>2.5</sub>. Five parallel samples were collected at the same sampling location and particles were divided into five parts: >2.5 μm, 1–2.5 μm, 0.5–1 μm, 0.2–0.5 μm and <0.2 μm, respectively. Inductively coupled plasma-optical emission spectrometry/inductively coupled plasma-mass spectroscopy (ICP-OES/ICP-MS) was used to analyze the element composition. The results showed that the wet flue gas desulfurization (WFGD) system removed 52.30% total suspended particulate (TSP), while concentration of PM<sub>2.5</sub> increased slightly by 3.82%. The concentration of different particle size sections in all 6 power plants occurred the trend as c (>2.5 μm) >c (<0.2 μm) >c (0.2–0.5 μm) >c (0.5–1 μm) >c (1–2.5 μm). The analysis of element revealed that Si and Al were the main elements in PM<sub>2.5</sub> before and after the desulfurization. The concentration of Ca, K, Na, Mg and As increased 56.62%, 29.24%, 98.78%, 114.27% and 195.34% in PM<sub>2.5</sub> through the WFGD system and others decreased or remained constant.

**Keywords :** Coal-fired power plant, PM<sub>2.5</sub>, Wet flue gas desulfurization, Element composition, Size distribution.

---

## **Effects of meteorology and emission reduction measures on air pollution in Beijing during heating seasons**

**Nianliang, Chengab, Bingfen, Chengab, Shanshan, LicTingzhouNingde**

**Source :** Atmospheric Pollution Research, Volume 10, Issue 3, May 2019, Pages 971-979

Beijing implemented five-year clean air plan during 2013–2017, and realized the continuous improvement of air quality in the whole city year by year. In this study, the MK (Mann-Kendall) test and KZ (Kolmogorov-Zurbenko) filtering analysis method were applied to evaluate the variations of PM<sub>2.5</sub> concentration at different sites in Beijing before and after the filtering meteorological conditions. The results showed that the averaged PM<sub>2.5</sub> concentrations in five sites decreased by 29.82% after filtering weather conditions, which was significantly lower than the average decrease rate (33.61%) of the original data. The emissions by human activities contributed about 69–94% to the decreased PM<sub>2.5</sub> concentrations during 2013–2017 at different sites in Beijing while the meteorological conditions contributed not more than 31% indicating the leading role of the emission reduction measures in the air quality improvement in Beijing. Contrary to the monthly averaged trends, the original PM<sub>2.5</sub> concentrations in heating seasons during 2013–2016 did not decrease obviously and not passed the significant test ( $\alpha = 0.1$ ) due to the unfavorable weather conditions which always aggravated degree and duration of air pollution. In order to further improve air quality, emission reduction measures such as reducing coal combustion, reducing oil consumption, controlling vehicles, emissions reduction, and cleaning dust should be continuously promoted.



**Keywords :** Air pollution, PM<sub>2.5</sub>, Emission reduction, Meteorology, Beijing, KZ filtering.

---

## **Identification of industrial point sources of airborne dust particles in an urban environment by a combined mineralogical and meteorological analyses: A case study from the Upper Silesian conurbation, Poland**

**Mariola, Jabłońska, JanuszJaneczek**

**Source :** Atmospheric Pollution Research, Volume 10, Issue 3, May 2019, Pages 980-988

Specific industrial point sources of PM<sub>10</sub> were identified by combining real-time meteorological observations and mineralogical examination (XRD, SEM-EDS, TEM-EDS) of individual particles collected during five individual week-long sampling campaigns in 2011 in the most industrialized region of Poland. Major (>20 vol%) and subordinate components of PM<sub>10</sub> (soot, quartz, gypsum, aluminosilicates, Fe-oxides, dolomite, and Pb-chloride) occur in different proportions season-depending and are of limited use in the identification of the emission point sources. Some minor components (particles of Cd- and Tl-bearing ZnS, and of iron and Cr-steel) related to meteorological conditions enabled identification of a large zinc refinery (35 km NW of the sampling site) and integrated iron and steelmaking plant located close to (10 km NE) the sampling site as the most probable emission point sources. Three other large steel plants located in the SW wind rose sector at a distance of 28, 75, and 80 km of the sampling site were typified as potential point sources based on submicron metal particles (Mn-alloyed steel, brass, hematite, magnetite, Fe-spinels). Combination of meteorological data and mineralogical investigation of airborne individual particles enabled distinguishing between sources of similar mineral tracers located in different sectors of wind rose and provided direct evidence for Zn and Cl speciation.

**Keywords :** PM<sub>10</sub>, Meteorological observations, Mineral indicators, Urban environment.

---

## **Long-term measurements of planetary boundary layer height and interactions with PM<sub>2.5</sub> in Shanghai, China**

**Liang, Panab Jianming, XuabXuexi, TieacdeXiaoqing, MaoabWeiGaoab, LuyuChangab**

**Source :** Atmospheric Pollution Research, Volume 10, Issue 3, May 2019, Pages 989-996

The planetary boundary layer (PBL) height plays important roles in modulating the local air pollution near surface, such as PM<sub>2.5</sub> (particles with diameter  $\leq 2.5 \mu\text{m}$ ) concentrations. However, it is very difficult to continuously measure a long-term PBL height. This study is the first time to analyze the long-term variability of PBL height (from 2010 to 2015) by using the continuous measurements from a micro-pulse Lidar (MPL) in Shanghai, China.

The aim of this paper is to investigate the long-term variation of PBL height and its relationship with meteorological factors and PM<sub>2.5</sub> concentration in the mega city of Shanghai, China. The results showed that there was no significant long-term trend of PBL height in Shanghai during the 6-year period with a mean value of 400 m, indicating the changes of air pollution during the same period were likely driven by other factors, e.g. wind speed or emissions. The PBL height was positively correlated with solar radiation and wind speed, while negatively correlated with vertical temperature gradient and PM<sub>2.5</sub> concentration. By comparison, the PBL height was more sensitive to solar radiation and vertical temperature gradient, indicating that the variation of PBL height was mostly driving by thermal effect. The diurnal variation of PBL height had strong impact on the diurnal cycle of PM<sub>2.5</sub> concentration. For example, the PM<sub>2.5</sub> diurnal variation presented different patterns between summer and winter. In winter the PM<sub>2.5</sub> diurnal cycle exhibited two-peaks pattern, appeared in the morning at 8:00 BJT and at night around 20:00 BJT respectively. Both peaks were well corresponding to the low PBL conditions (200–300 m). While in summer, the PM<sub>2.5</sub> peaked at noon under high PBL condition (1000 m). This noon peak was likely due to the elevation of secondary aerosol formation, which offsets the diffusion effect on PM<sub>2.5</sub> resulted from PBL developments. There was a strong interaction among the solar radiation, PBL, and PM<sub>2.5</sub> concentration. The higher PM<sub>2.5</sub> caused the reduction of solar radiation to inhibit PBL, further depressed the aerosols in a shallow layer to yield higher PM<sub>2.5</sub> concentration. As a result, PBL and PM<sub>2.5</sub> concentrations presented non-linearly anti-correlations. During the lower range of PBL (less than 400 m), the PM<sub>2.5</sub> variability was very sensitive to the changes in the PBL. On the other hand PM<sub>2.5</sub> presented substantial effects on PBL evolutions. The daytime PBL developed more fully under low PM<sub>2.5</sub> conditions compared with that under high PM<sub>2.5</sub> levels. The PBL height decreased about 100 m when PM<sub>2.5</sub> concentration increased about 30–50 µg/m<sup>3</sup> under the condition that daily PM<sub>2.5</sub> concentration was greater than 70 µg/m<sup>3</sup>. The statistical analysis showed that the mean ratios of PM<sub>2.5</sub>/PBL during 6-year period were 0.37, 0.11, 0.30, and 0.37 (µg/m<sup>4</sup>) in spring, summer, autumn, and winter respectively, suggesting that the PM<sub>2.5</sub> levels were more sensitive to PBL in spring and winter.

**Keywords :** PBL, Planetary boundary layer height, PM<sub>2.5</sub>, A long-term measurement.

---

## **Health risk assessment for highway toll station workers exposed to PM<sub>2.5</sub>-bound heavy metals**

**Peng-huiLi<sup>abc</sup>, JieYu<sup>d</sup>Cheng-liangBi<sup>bc</sup>, Jun-jieYue<sup>c</sup>Qian-qianLi<sup>e</sup>. LiWang<sup>c</sup>,  
JinpengLiu<sup>f</sup>ZhimeiXiao<sup>g</sup>, LiqiongGuo<sup>h</sup>, Bi-jieHuang<sup>a</sup>**

**Source :** Atmospheric Environment, Volume 10, Issue 4, July 2019, Pages 1024-1030

Highway toll station workers exposed to vehicle emissions during their working time, could induce excessive reactive oxygen species (ROS) generation and lead to significant health

effects. This study conducted a comprehensive exposure investigation of environmental pollutants and oxidative stress levels for highway toll station workers during March–May 2014 in Tianjin, China. PM<sub>2.5</sub> exposure samples were collected by personal monitors during worker' day-shift working time (9:00 a.m. - 5:00 p.m.), and particulate heavy metals were analyzed by ICP-MS. Urinary 8-OHdG concentrations were analyzed in pre- and post-work urine samples from selected subjects to reflect their oxidative stress (OS) level variation. Results showed that PM<sub>2.5</sub> average exposure concentration was  $230.73 \pm 142.99 \mu\text{g m}^{-3}$ . Pb, Zn and Cr were the most abundant elements of metals, accounting for over 70% of total particulate heavy metals. Values based on geoaccumulation index (Igeo) and enrichment factor (EF) analysis indicated that heavy metals including Pb, As, Cd, Cr, Ni, Cu, Zn were mainly derived from anthropogenic sources, presenting heavily pollution levels. Health assessment was conducted using integrated toxicity values and Monte Carlo simulation, and results indicated that exposure to PM<sub>2.5</sub>-bound heavy metals can trigger significant adverse non-carcinogenic and carcinogenic risk. Urinary 8-OHdG concentrations of participants elevated over 2 times after their day-shift working exposure, indicating that pollutants from vehicle emission could cause DNA damage for highway toll station workers. However, we did not find significant association between fine particle-bound heavy metals and urinary 8-OHdG levels. Much work should be conducted in the future study focusing on confounding factors.

**Keywords :** PM<sub>2.5</sub>, Heavy metal, DNA damage, Exposure, Risk assessment.

---

## **Determinants of commuter exposure to PM<sub>2.5</sub> and CO during long-haul journeys on national highways in India**

**Soma Sekhara, Rao Kollurua, Aditya KumarPatraab, PrashantKumarc**

**Source :** Atmospheric Pollution Research, Volume 10, Issue 4, July 2019, Pages 1031-1041

National Highways (NH) are the major road networks linking cities but exposure studies during long commutes on highways are limited. We assessed exposure concentrations of fine particles  $\leq 2.5 \mu\text{m}$  in diameter (PM<sub>2.5</sub>) and carbon monoxide (CO) inside bus, ac (air-conditioned) and non-ac car and on an Indian NH over 200 km length. A total of nine round journeys were made in three modes. Analysis of variance (ANOVA) and generalized linear model (GLM) were applied to quantify the contribution of determinants that may explain the variability of exposure concentrations and their association with in-vehicle temperature and relative humidity (RH). The highest and lowest exposures concentrations to PM<sub>2.5</sub> were observed in non-ac car ( $89 \pm 32 \mu\text{g m}^{-3}$ ) and the ac car ( $55 \pm 19 \mu\text{g m}^{-3}$ ). Exposures concentrations in non-ac car were higher during in-city travel ( $113 \pm 36 \mu\text{g m}^{-3}$ ). The average CO exposure concentrations were highest in ac car ( $2.0 \pm 0.9 \text{ ppm}$ ). Results of GLM analysis suggested that travel mode, highway segments (in/out-city) and the journey times are key determinants of personal exposure concentrations. Travel mode for PM<sub>2.5</sub> (15%) and NH segments for CO (21%) explained

maximum variability. Altogether, these explained 33% and 57% of the variability in PM2.5 and CO exposure concentrations, respectively. PM2.5 consists of soot, mineral and fly ash that are a proxy of fresh exhaust emissions, re-suspended road dust and industrial emissions, respectively. Additionally, EDX analyses revealed an abundance of Si, Al, Ca and Pb, confirming re-suspension, brake/tire wear and construction dust as important sources.

**Keywords :** Personal exposure concentrations, National highway, Travel mode, GLM, SEM-EDX.

---

## **Enhancing source identification of hourly PM2.5 data in Seoul based on a dataset segmentation scheme by positive matrix factorization (PMF)**

**Min-BinPark, Tae-Jung, Lee, Eun-Sun, Lee, Dong-Sool, Kim**

**Source :** Atmospheric Pollution Research, Volume 10, Issue 4, July 2019, Pages 1042-1059

Hourly PM2.5 datasets and corresponding meteorological parameters were obtained from the National Institute of Environmental Research (NIER) in Korea. Initially the datasets at the Seoul Intensive Monitoring Station (SIMS) contained 12,376 samples, each with 24 chemical variables, from Jan. 1, 2013 to Dec. 31, 2014. To identify site-specific sources, to clarify vague or unknown source types, and to develop a database containing abundance patterns for tracers for each source, three stage-by-stage positive matrix factorization (PMF) modeling tasks were performed based on a dataset segmentation scheme. In this study, the PM2.5 datasets were segmented using meteorological parameters of wind direction, wind speed, and precipitation. After performing 18 independent PMF modeling simulations, 10 and 14 sources were identified before and after use of the segmentation scheme, respectively. As the number of identified sources increased, the overall contributions from ubiquitous sources continued to show both increasing and decreasing trends. This behavior was noticeable in cases where the contribution of major sources, such as secondary aerosols and coal burning sources, were observed to decrease, and their contributions were reassigned in various burning sources, such as local secondary nitrate and oil sources. Moreover, the contributions of various waste burning sources, such as incineration and biomass burning, moved into secondary nitrate and Br-related waste burning sources. The results of this analysis demonstrated that, when using large PM2.5 datasets, segmenting tasks expands the potential ability to increase the number of specified sources using PMF analysis.

**Keywords :** PM<sub>2.5</sub>, Receptor model, PMF, Dataset segmentation scheme, Marker species, Seoul.

---

## VOC characteristics and source apportionment at a PAMS site near an industrial complex in central Taiwan

Chun-HaoChen<sup>a</sup>, Yen-ChangChuang<sup>a</sup>, Chu-ChinHsieh<sup>a</sup>, Chih-ShengLee<sup>b</sup>

**Source :** Atmospheric Environment, Volume 10, Issue 4, July 2019, Pages 1060-1074

Hourly data of volatile organic compounds (VOCs) were collected for three consecutive years from photochemical assessment monitoring stations (PAMS) in Taixi, Taiwan. Analysis of the VOC data allows for apportionment of the anthropogenic sources of VOCs. The VOC concentrations and characteristics were analyzed for temporal variations over a three-year period 2014 to 2016. Out of 54 VOCs detected, 21 VOC compounds from 55 to 99% were below the method detection level; others ranged from 100% occurrence (ethane) to 56–61% for trimethylbenzene. In order to have meaningful statistical results, this paper only used results from 33 VOCs where they were detected at least 65% of the time. This was a requirement to be able to determine statistical parameters such as means and standard deviations. The highest VOC average concentrations observed for three consecutive years, in order, for the period were toluene (3.7–4.3  $\mu\text{g m}^{-3}$ ), then propane (2.5–2.6  $\mu\text{g m}^{-3}$ ), ethane (2.2–2.5  $\mu\text{g m}^{-3}$ ), ethylene (1.1–1.5  $\mu\text{g m}^{-3}$ ) and propylene (0.8–1.1  $\mu\text{g m}^{-3}$ ). A positive matrix factorization (PMF) receptor model was used to evaluate VOC sources in the area. Six factors were identified by PMF analysis, including solvent use, vehicle exhaust, diesel exhaust, petrochemical, refinery and aged air mass. The conditional probability function indicates that the VOCs in six factors were emitted from their source locations via different wind directions. The contribution of the northwest industrial complex to the PAMS data is linked to the VOCs observed. Actually, seasonal wind directions having only north and north-northwest directions played an important role.

**Keywords :** Volatile organic compounds (VOCs), Photochemical assessment monitoring stations (PAMS), Positive matrix factorization (PMF), Conditional probability function (CPF), Ozone formation potential (OFP).

---

## Exposure to traffic-related particulate matter and deposition dose to auto rickshaw driver in Dhanbad, India

Sunil Kumar, Gupta, Suresh Pandian, Elumalai

**Source :** Atmospheric Environment, Volume 10, Issue 4, July 2019, Pages 1128-1139

Driver's exposure in vehicular systems contributes an important fraction of the daily burden of air pollutants. In this study, we examined the PM concentrations in the various microenvironments (ME's) such as in-vehicle [auto-rickshaws], outdoor and indoor. The drivers were estimated to have respiratory deposition doses (RDDs) of PM fractions

(PM<sub>10</sub>, PM<sub>2.5</sub> and PM<sub>1</sub>) in the different part of the respiratory tract (head airways (HD), tracheobronchial (TB) and alveolar (AL)) in various ME's to auto-rickshaw drivers. The results showed that average PM concentrations were 3.3 times higher inside auto-rickshaws than ambient level. The highest PM fractions concentrations were observed during congestion period (844  $\mu\text{gm}^{-3}$  for PM<sub>10</sub>, 458  $\mu\text{gm}^{-3}$  for PM<sub>2.5</sub> and 302  $\mu\text{gm}^{-3}$  for PM<sub>1</sub>) of auto-rickshaw riding. The survey reports showed that eighty percent of drivers believed they were more exposed than a non-driver. More than half of auto-rickshaws drives believed, alternative fuel like CNG was a better way to reduce the air pollution. In the health screening, about 23% and 20% of auto-rickshaws drivers complained of the 'body pain and eye irritation' and 'a headache', respectively. Overall, the total RDDs values were estimated 4.8 (PM<sub>10-2.5</sub>), 8.8 (PM<sub>2.5-1</sub>) and 10.1 (PM<sub>1</sub>) times higher compared to ambient level to auto-rickshaw drivers in an average day. Based on this result, the fine particulate matter showed in a higher risk of auto-rickshaw drivers in Dhanbad city. This study indicated that driver awareness of traffic air pollution was limited. Future studies should focus on reducing exposures and increasing awareness among auto-rickshaw drivers.

**Keywords :** Air pollution, Particulate matter, Auto-rickshaw drivers, RDDs.

---

## **The pollution characteristics of PM<sub>10</sub> and PM<sub>2.5</sub> during summer and winter in Beijing, Suning and Islamabad**

**DongLvab1, YingChenac1, TianleZhua, TongtongLid, FangxiaShena, XinghuaLia  
Tariq, Mehmooda**

**Source :** Atmospheric Pollution Research, Volume 10, Issue 4, July 2019, Pages 1159-1164

To understand the atmospheric particulate pollution characteristics of cities in different sizes and regions, PM<sub>10</sub> and PM<sub>2.5</sub> were simultaneously collected in three cities: Beijing, China, Islamabad, Pakistan and Suning, China, in summer (2016) and winter (2017), respectively. The associated species including carbonaceous, metal elements and water soluble ions were analyzed. Both PM<sub>10</sub> and PM<sub>2.5</sub> concentrations in winter are higher than those in summer in three cities. In Beijing, OM, NH<sub>4</sub>NO<sub>3</sub> and (NH<sub>4</sub>)<sub>2</sub>SO<sub>4</sub> are the main components, the PM<sub>2.5</sub>/PM<sub>10</sub> ratio is the highest among three cities, and the NO<sub>3</sub>-/SO<sub>4</sub><sup>2-</sup> ratio is lower than that in Islamabad in winter, suggesting that coal-fired process contributed more in Beijing. In Islamabad, the main components of PM<sub>10</sub> and PM<sub>2.5</sub> are crust and OM. The average concentrations of both Ca and Na in PM<sub>10</sub> are higher than those in Beijing and Suning, indicating that the soil dust may be one of main air pollution sources in Islamabad. The concentrations of OC in both PM<sub>10</sub> and PM<sub>2.5</sub> in Islamabad are in relatively high level in summer, which indicates that more secondary organic aerosols are formed in summer in Islamabad. The highest PM<sub>10</sub> and PM<sub>2.5</sub> concentrations occur in Suning and the chemical composition of PM<sub>2.5</sub> in Suning is similar to that in Beijing whether it is summer or winter, and the proportion of EC in Suning is higher than that in the other two cities in both PM<sub>10</sub> and PM<sub>2.5</sub>, which are attributed to atmospheric pollutants transport from the surrounding cities and the diesel vehicle emission.

**Keywords :** PM<sub>2.5</sub>/PM<sub>10</sub>, Summer/winter, Chemical composition, Beijing, Islamabad, Suning.

---

## **Correlations of PM10 concentrations in urban areas with vehicle fleet development, rain precipitation and diesel fuel sales**

**Giuseppe Piras<sup>a</sup>, Fabrizio Pini<sup>b</sup>, Davide Astiaso Garcia<sup>a</sup>**

**Source :** Atmospheric Environment, Volume 10, Issue 4, July 2019, Pages 1165-1179

Although in many developed countries the green transition towards sustainable mobility is going faster and faster towards low or zero emission vehicles, road traffic is so far one of the key PM10 pollution source in urban areas. This research compares and analyses correlations between PM10 pollution trends in urban areas and the following parameters: vehicles fleet, rain precipitations and diesel fuel sales. The city of Rome has been selected as pilot area, analysing data gathered by its PM10 monitoring network between 2006 and 2017. Statistical correlations have been computed between all trends giving particular regard to the replicability of methods and strategies to other cities. The obtained results showed an integrated analysis of correlations between PM10 concentrations and vehicle fleet development, rain precipitation, diesel fuel sales, highlighting in which months the rain has a higher effect on PM10 concentrations; the differences between rain precipitation amounts and the number of rainy days per month; the possibility to forecast data using the statistical correlations analysis; the effects of vehicle fleet and diesel fuel sales on the PM10 concentrations.

**Keywords :** PM10 pollution, Traffic source, Roadside measurements, Correlation analysis, Sustainable mobility.

---

## **A severe fog-haze episode in Beijing-Tianjin-Hebei region: Characteristics, sources and impacts of boundary layer structure**

**Chao Liua, Cong Huaa, Hengde Zhanga, Bihui Zhanga, Gang Wangb, Wenhui Zhucd, RanXua**

**Source :** Atmospheric Pollution Research, Volume 10, Issue 4, July 2019, Pages 1190-1202

Beijing–Tianjin–Hebei (BTH) region is recognized as one of the most polluted regions in China. In this study, characteristics, synoptic condition, boundary layer structure, and

sources of a severe fog–haze episode during the December of 2016 and January of 2017 are investigated. The results show that BTH region is controlled by the uniform pressure field and southwest wind, and the average mass concentrations of PM<sub>2.5</sub> in Beijing (BJ), Tianjin (TJ), and Shijiazhuang (SJZ) are 263.5, 192.7, and 296.1 µg/m<sup>3</sup>, respectively. Besides, the maximum hourly concentration and growth rate of PM<sub>2.5</sub> are 578.8 µg/m<sup>3</sup> and 13.1 µg/(m<sup>3</sup>·h), respectively for BJ. According to the wind profiler radar and L–band radar data, the maximum concentration of PM<sub>2.5</sub> in two stages basically coincides with the minimum ventilation index (VI) value, and the minimum VI value in stage I and stage II are 5124 m<sup>2</sup>/s and 4524 m<sup>2</sup>/s. Moreover, the two stages are accompanied by significant inversion layer in the low levels. Although the maximum temperature inversion (10.8 °C) in stage I is higher than that in stage II (8.3 °C) in the boundary layer, the maximum inversion strength in stage II (0.33 °C/hPa) is stronger than that in stage I (0.20 °C/hPa). Besides, weighted potential source contribution function (WPSCF) and conditional probability function analysis (CPF) are applied to investigate the potential source regions of PM<sub>2.5</sub>, the results show that southern BJ, as well as central and southern Hebei province (HB) are the main potential sources, and CPF values from the wind direction (180°–270°) are all over 0.3.

**Keywords :** Fog–haze episode, PM<sub>2.5</sub>, Boundary layer, Air masses trajectories, WPSCF.

---

## **Temporospatial variations and Spearman correlation analysis of ozone concentrations to nitrogen dioxide, sulfur dioxide, particulate matters and carbon monoxide in ambient air, China**

**Zongshuang Wang<sup>a</sup>, Jungang Lv<sup>b</sup>, Yufei Tan<sup>a</sup>, Min Guo<sup>a</sup>, Yanyue Gu<sup>a</sup>, Shu Xu<sup>a</sup>, Yuhua Zhou<sup>a</sup>**

**Source :** Atmospheric Environment, Volume 10, Issue 4, July 2019, Pages 1203-1210

Ozone has been an important pollutant in China since 2013. The increasing number of days with over-standard ozone (O<sub>3</sub>) has been observed in many cities. In this study, what we mainly focus on are shown as follows: sampling of ambient air in 365 days in 2017 from 338 main cities; comparing concentration levels of ozone, nitrogen dioxide, sulfur dioxide, particulate matters and carbon monoxide in ambient air; investigating air quality conditions related to monthly variations of ozone, in this study, five areas with relatively higher O<sub>3</sub>-8 h over-standard days were identified and illustrated. An inverted “V” shape curve in North and a multiple “M” shape curve in South were identified in ozone monthly changes. Furthermore, possible reasons for spatial and temporal distribution were discussed. Spearman correlation analyses of ozone to nitrogen dioxide (NO<sub>2</sub>), sulfur dioxide (SO<sub>2</sub>), particulate matters (PM) and carbon monoxide (CO) in every chosen city were performed, and the distribution patterns were illustrated in maps. The results revealed



that ozone concentrations in most north cities have negative correlations with concentrations of other pollutants in 2017, while some cities in south appeared positive correlations. As ozone pollution is not easily monitored by ordinary people without equipment, people in the cities where ozone concentrations were significantly related to PM or other pollutants, could primarily predict ozone pollution and take protective actions.

**Keywords :** Ozone, O<sub>3</sub>-8h, Temporospatial distribution, Ambient air, Spearman correlation analysis.

---

## **Particulate matter size distribution in air surface layer of Middle Ural and Arctic territories**

**E.M. Baglaevaab, A.P.Sergeevab, A.G.Buevichab, I.E.Subbotinaa, A.V.Shichkinab**

**Source :** Atmospheric Pollution Research, Volume 10, Issue 4, July 2019, Pages 1220-1226

To investigate the mass concentration, size-distribution, height stratification and season variability of atmospheric particulate matter, the data were collected at two sampling sites: residential quarters in Ekaterinburg, Russia, from March to May 2016 and Belyy Island, Yamal Peninsula, Russia, without any industrial air pollution in July of the same year. The particles size distribution in Ekaterinburg showed that most particles had diameters in the range of 0.5–2.5 µm. In Belyy Island the particles size distributions had two dominants: Land Breeze and Sea Breeze patterns, which associated with the wind direction. The first time the air dust content and the particles size distribution was studied at 73.1° North latitude.

**Keywords :** Particulate matter, Size-distribution, Height stratification, Urban territory, Dust air pollution.

---

## **Chemical speciation of water-soluble ionic components in PM<sub>2.5</sub> derived from peatland fires in Sumatra Island**

**Yusuke Fujiia, Haryono , Setiyo Huboyob Susumu, TohnocTomoaki Okudad, Syafrudinb**

**Source :** Atmospheric Pollution Research, Volume 10, Issue 4, July 2019, Pages 1260-1266

We conducted a field study to characterize water-soluble ionic species in PM<sub>2.5</sub> from peatland fires using ground-based samplings at fire sources and receptor sites in the Riau Province, Sumatra, Indonesia. We determined the concentrations of PM<sub>2.5</sub> mass, water-soluble ions, and some chemical elements. Through PM<sub>2.5</sub> field samplings at three peatland fire sources, we have shown that the mass fractions of typical peatland fire water-soluble

ionic components tend to differ between peatland fire sources. Thus, our results indicate that PM<sub>2.5</sub> source profiles of water-soluble ionic components for peatland fire must be selected with extreme caution if applied to a receptor model. From the viewpoint of ionic composition of each peatland fire sample, Cl<sup>-</sup> and NH<sub>4</sub><sup>+</sup> were consistently dominant anions and cations, respectively, for all peatland fire samples, i.e., NH<sub>4</sub>Cl was a consistently dominant component. Through field samplings of the ambient PM<sub>2.5</sub> in Pekanbaru during peatland fire-induced haze and non-haze periods, we found differences in PM<sub>2.5</sub> mass and total water-soluble ionic component concentrations between haze and non-haze samples. Four components, C<sub>20</sub>A<sub>2</sub><sup>-</sup>, NO<sub>3</sub><sup>-</sup>, SO<sub>4</sub><sup>2-</sup>, and NH<sub>4</sub><sup>+</sup>, showed highly elevated levels during haze periods. Since these four ions are recognized as the major secondarily formed aerosol components, the increased total concentrations of water-soluble ionic components during haze periods can mainly be derived from the gas-to-aerosol conversion process. The ionic compositions of haze samples at receptor sites are obviously different from those at peatland fire source samples. In particular, NH<sub>4</sub>Cl, which is characteristic of peatland fire PM<sub>2.5</sub> sources, is low at sites during haze periods.

**Keywords :** Peatland fire, Indonesia, PM<sub>2.5</sub>, Biomass burning, Source profile, Haze.

---

## **Exploring the stratospheric source of ozone pollution over China during the 2016 Group of Twenty summit**

**Zhi-Zhen Nia, KunLuoa, Xiang Gaoa, Yang Gao, bJian-RenFan a ,Joshua S.Fu c ,Chang-Hong Chend**

**Source :** Atmospheric Pollution Research, Volume 10, Issue 4, July 2019, Pages 1267-1275

The 2016 Group of Twenty (G20) Hangzhou Summit was concurrently accompanied by extratropical cyclogenesis. To investigate whether the extratropical cyclone exerts any impact on the near surface ozone concentration, the Weather Research Forecast with Chemistry (WRF-Chem) model, with stratospheric passive tracers turned on, was used to simulate the air quality from August 24 to September 06, 2016. It turns out the WRF-Chem model generally performed well when compared to the observed data from a large number of air quality monitoring sites and satellite measurements. During the period, an occurrence of stratospheric intrusion was observed, associated with tropopause fold and curved upper-level jet in East Asia. A fairly large number of stratospheric passive tracers that had quite positive correlation with O<sub>3</sub> concentrations were also found over the southeast China. Besides, observed ground surface anomaly of high O<sub>3</sub> and the accompanied low CO as well as humidity further implied the downward transport of O<sub>3</sub> from the stratosphere. These results suggest that stratospheric ozone intrusion acts as an additional source of the near surface tropospheric ozone concentration, which deteriorates the O<sub>3</sub> pollution in China. This helps to explain the difficulty of O<sub>3</sub> control during the campaign period of the G20, and provides some insights into stratosphere-to-troposphere transport of O<sub>3</sub>.

**Keywords :** Ozone pollution, Stratospheric intrusion, Tropopause fold, WRF-Chem, Extratropical cyclogenesis.

---

## **Analysis and visualization of multidimensional time series: Particulate matter (PM10) from São Carlos-SP (Brazil)**

**Eduardo Carlos Alexandrina<sup>a</sup> Evandro S.Ortigossa<sup>b</sup> Elaine SchornobayLui<sup>c</sup> José Antônio Silveira Gonçalves<sup>a</sup> Nivaldo AparecidoCorrêa<sup>d</sup> Luis GustavoNonato<sup>b</sup> Mônica LopesAguiar<sup>a</sup>**

**Source :** Atmospheric Pollution Research, Volume 10, Issue 4, July 2019, Pages 1299-1311

Data visualization techniques have been successfully used in a time series context for many years. In this work, a web-based data visualization system was developed to support the evolutionary analysis of atmospheric particulate matter (PM10) behavior, collected in the central region of São Carlos, São Paulo State, Brazil. The samples were acquired following two patterns: daily in the first stage and on alternate days in the second stage. Each measurement covered a period of 23 h and 30 min, using a large volume sampler (high-volume). To interrogate the acquired data, an interactive visualization tool was developed in JavaScript and D3 library. The tool is portable and can be used in all modern web browsers, not requiring any software installation. The values obtained from São Carlos' PM10 monitoring campaign from 2014 to 2017 clearly showed a decrease of PM10 in the city atmosphere, in comparison with past data from the 1997 to 2005 campaign. This decreasing trend in PM10 concentrations could be due to an increase in the severity of law n° 997 of 05/31/1976 and decree 54.487 of 06/26/2009, which charges the anthropogenic agents with air pollution control.

**Keywords :** Air pollution, Particulate matter (PM<sub>10</sub>), Information visualization, Time series, Air quality.

---

## **Airborne PM10 and lead concentrations at selected traffic junctions in Khyber Pakhtunkhwa, Pakistan: Implications for human health**

**IqbalAhmad<sup>a</sup>, BushraKhan<sup>a</sup>, SardarKhan<sup>a</sup>, Zia urRahman<sup>ab</sup>, Muhammad AmjadKhan<sup>a</sup>, NidaGul**

**Source :** Atmospheric Pollution Research, Volume 10, Issue 4, July 2019, Pages 1320-1325

The airborne particulates pollution is a serious concern due to its adverse health impacts. This study was carried out to assess the PM10 mass concentration and PM10-bound lead (Pb) at two major traffic junctions in Charsadda and Upper Dir Districts of Khyber

Pakhtunkhwa (KP), Pakistan. A high-volume Reference Ambient Air Sampler (RAAS) was used to collect PM10 samples (n = 30) on glass fiber filters from April 2017 to September 2017. The PM10 mass was determined by gravimetric analysis weighing each filter disc before and after sampling. The PM10-bound Pb concentrations were determined using graphite furnace atomic absorption spectroscopy after filters acid digestion. Health risks of PM10-bound Pb were evaluated numerically by hazard quotient (HQ) and hazard index (HI). The PM10 mass (24 h mean) was 4.6 times higher than the WHO guideline value for air quality. Likewise, the PM10-bound Pb was 1.3 times higher than the WHO guideline value. Mean PM10 concentrations were  $254 \pm 67 \mu\text{g}/\text{m}^3$  and  $208 \pm 85 \mu\text{g}/\text{m}^3$  and mean PM10-bound Pb concentrations were  $709 \pm 206 \text{ ng}/\text{m}^3$  and  $638 \pm 231 \text{ ng}/\text{m}^3$  at the traffic junctions in Charsadda and Upper Dir Districts respectively. The mean HI values were less than 1 for the exposed adults and children indicating that health effects are unlikely to occur in the exposed population. Measures should be taken to monitor the airborne PM10 on regular basis and reduce its emissions into the air.

**Keywords :** Air pollution, PM<sub>10</sub>, Airborne lead, Human exposure, Health risks, Khyber Pakhtunkhwa.

---

## **Trace elements bound to airborne PM10 in a heavily industrialized site nearby Athens: Seasonal patterns, emission sources, health implications**

**K.G.Koukoulakis<sup>a</sup>, E.Chrysohou<sup>a</sup>, P.G.Kanellopoulos<sup>a</sup>, S.Karavoltzos<sup>b</sup>, G.Katsouras<sup>b</sup>, M.Dassenakis<sup>b</sup>, D.Nikolelis<sup>b</sup>, E.Bakeas<sup>a</sup>**

**Source :** Atmospheric Pollution Research, Volume 10, Issue 4, July 2019, Pages 1347-1356

Trace elements in PM10 samples were studied at Elefsis city, a heavily industrialized area of Greece. Seasonal samplings were carried out from December 2015 to August 2017. Concentration levels of 18 metal (loid)s were measured by Inductively Coupled Plasma – Mass Spectrometry (ICP-MS). Al, Ba and Zn were the most abundant elements with mean concentrations ranging between 1000 and 22 000 ng m<sup>-3</sup>, Fe and Sr between 100 and 1000 ng m<sup>-3</sup>, while Cr, V, Mn, Pb, Cu, Ni, Ga, Rb were detected in traces (<50 ng m<sup>-3</sup>) and As, Co, Cd, Cs and Tl in ultratrace concentrations (<2 ng m<sup>-3</sup>). PM10, Al, Fe, Zn and Ba showed a seasonal variation, with maximum concentrations prevailing during the cold period of the year. The source apportionment tools employed, comprising use of enrichment factors analysis, wind patterns and correlation analysis, revealed that the industrial zone located at the study area constitutes a significant hotspot in terms of trace elements emission in the air (e.g. Cd, Pb), due to the presence of activities including coal and/or fossil fuel combustion, ferrous and non-ferrous production, operation of smelters and municipal solid waste incineration. An estimation of the excess lifetime cancer risk due to toxic metals exposure via inhalation, revealed that 2 people out of 30 000 in Elefsis area are at risk of cancer development.

**Keyword:** PM<sub>10</sub>, Trace elements, Industrial city, ICP-MS, PCA, Excess cancer risk.

---

## **Spatial-temporal characteristics of the air quality in the Guangdong–Hong Kong–Macau Greater Bay Area of China during 2015–2017**

**Xingqin Fang, Qi Fan, Zhiheng Liao, Jielan Xie, Xinqi Xu, Shaojia Fan**

**Source :** Atmospheric Environment, Volume 210, 1 August 2019, Pages 14-34

Spatial-temporal characteristics of the air quality including size-segregated particulate matter (PM) portions and ozone (O<sub>3</sub>) in the Guangdong–Hong Kong–Macau Greater Bay Area (GBA) of China are analyzed using daily observational data during 2015–2017. A big picture of multiple years' in situ observational air quality in GBA is provided. A collection of three neighboring cities Foshan (FS), Guangzhou (GZ), and Dongguan (DG), referred to as FGD, on average has the worst air quality in GBA, mostly due to the heavy primary emissions and high chance of secondary pollutant productions and accumulations. The air quality in FGD generally has a significant seasonal cycle which is influenced by the East Asian Monsoon and modulated by ENSO. Different cities have different prominent air quality issues and there are special multi-scale characteristics in PM<sub>2.5</sub> at FS, O<sub>3</sub> at DG, and PM<sub>2.5-10</sub> at DG. The inter-city differences of multi-scale air quality variations in FGD could be attributed to both sources and meteorology. For example, DG has extremely high O<sub>3</sub> (especially in 2015) and PM<sub>2.5</sub>/PM<sub>10</sub> but relatively low PM, and PM<sub>2.5-10</sub> at DG has strong 2–3 days' oscillation but weak seasonal oscillation. The special air quality characteristics at DG might be attributed to combined effects of the different ventilation and dilution consequences of the sea-land breeze to different air quality components which have different three-dimensional source distributions. Through a combined multi-scale lag correlation analysis of air quality, some prior air quality components (with different leading time on different scales) are identified as potential indicators for statistic air quality prediction.

**Keywords:** Spatial-temporal characteristics, Air quality, Multi-scale lag correlation analysis, Particulate matter, Ozone, Guangdong–Hong Kong–Macau greater bay area.

---

## **Role of the position of the North Atlantic jet in the variability and odds of extreme PM<sub>10</sub> in Europe**

**Carlos Ordóñez<sup>a</sup>, David Barriopedro<sup>b</sup>, Ricardo García-Herrera<sup>ab</sup>**

**Source:** Atmospheric Environment, Volume 210, 1 August 2019, Pages 35-46

We have analysed the impact of the North Atlantic jet on the winter PM10 (particulate matter with aerodynamic diameter  $\leq 10 \mu\text{m}$ ) concentrations in Europe during a 10-year period. For this purpose we have extracted the daily latitude and strength of the jet from a reanalysis dataset and surface PM10 observations from the AirBase network. We show that the detection of the jet over the eastern North Atlantic ( $0^\circ$ – $15^\circ$  W) is preferred compared to the whole North Atlantic basin as this maximises the signal on the PM10 concentrations. Four preferred jet positions have been identified over that region and season: southern (south of  $41^\circ$  N), central-southern (between  $41^\circ$  N and  $51^\circ$  N), central-northern (between  $51^\circ$  N and  $63^\circ$  N) and northern (north of  $63^\circ$  N). According to our results, the jet latitude exerts a stronger influence than the jet strength on the mean PM10 levels. We also examine the impact of the jet positions on the full distribution of PM10 as well as on the odds of PM10 extremes (exceedances of the local winter 95th percentiles). The latter is done through a logistic regression model which considers the effect of the persistence of extremes and different time lags for the jet position. The northern position is associated with enhanced PM10 concentrations (on average  $\sim 9 \mu\text{g m}^{-3}$ ) over northwestern/central Europe and threefold increases in the odds of PM10 extremes at most sites in the region. Similar increases have been found for PM10 in southern Europe when the jet is in its central-northern position. In both cases, the rise in the PM10 concentrations is associated with anticyclonic conditions over those regions and the impact on PM10 extremes is maximised for time lags of around 1–2 days. On the other hand, the central-southern and southern jet positions yield large PM10 decreases (on average around  $-9 \mu\text{g m}^{-3}$ ) in northwestern/central Europe and southern Europe, respectively.

**Keywords:** PM<sub>10</sub>, Particulate matter, Jet stream, Synoptic meteorology, Air quality.

---

## **Particulate matter bound polycyclic aromatic hydrocarbons: Toxicity and health risk assessment of exposed inhabitants**

**RitwikaRoy<sup>a</sup>, RohiJan<sup>a</sup>, GayatriGunjal<sup>a</sup>, RenukaBhor<sup>b</sup>, KalpanaPai<sup>b</sup>, P. GursumeeranSatsangi<sup>a</sup>**

**Source:** Atmospheric Environment, Volume 210, 1 August 2019, Pages 47-57

In the present study, the toxicological profile of 13 polycyclic aromatic hydrocarbons (PAHs) associated with airborne particulate matter (PM) was assessed. The average concentration of both PM10 and PM2.5 exceeded the Indian National Ambient Air Quality Standards. Amongst 13 analyzed PAHs, Naphthalene (Nap) was found to be the most dominant in both size fraction of PM whereas Indeno (1, 2, 3-cd) pyrene (IP) exhibited the least concentration. The relative % distribution of Low molecular weight (LMW) three ring PAHs were found to be predominant in both sized PM. The combined results derived from diagnostic ratios and factor analysis suggested that the vehicular emission (Diesel + gasoline) and coal combustion in the vicinity of study province are probable sources of PM

bound PAHs. Maximum contribution towards the carcinogenicity has been found for Benzo (a) pyrene [B(a)p] for both size PM. The cytotoxic profile of PAHs determined by MTT assay demonstrated significant decrease in cell viability and PAHs associated with PM10 samples exhibited higher cytotoxic response. The redox activity measured by DTT assay exhibited the oxidative nature of PAHs associated with both sized PM. The interaction study between the PAHs and BSA resulted in substantial decrease in fluorescence intensity of BSA, indicating that PM bound PAHs could quench intrinsic fluorescence of the protein through successive molecular interaction and further conformational changes of protein was confirmed by circular dichroism spectra. Results obtained in the present study provide a valuable approach to evaluate the toxicological profile of PAHs encountered in the atmosphere of Pune.

**Keywords:** Particulate matter, PAHs, Source identification, Carcinogenicity, Cytotoxicity, DTT.

---

## **Relationship between long-range transported atmospheric black carbon and carbon monoxide at a high-altitude background station in East Asia**

**Shantanu KumarPani<sup>a</sup> Chang-FengOu-Yang<sup>a</sup> Sheng-HsiangWang<sup>a</sup> John A.Ogren<sup>b</sup>  
Patrick J.Sheridan<sup>b</sup> Guey-RongSheu<sup>a</sup> Neng-HueiLin<sup>a</sup>**

**Source :** Atmospheric Environment, Volume 210, 1 August 2019, Pages 86-99

Lulin Atmospheric Background Station (LABS, 23.47°N, 120.87°E; 2862 m above sea level) at the summit of Mount Lulin in central Taiwan was established in spring 2006 and is the only high-altitude background station over western Pacific region in East Asia to study the impact of various air pollutants through long-range transport. Continuous in-situ measurements of equivalent black carbon (EBC) and carbon monoxide (CO) concentrations were made at LABS from June 2012 to May 2014 and their association was investigated in this study. The highest monthly concentration of EBC (median; 840 ng m<sup>-3</sup>) and CO (212 ppbv) in March were primarily attributed to the westerly winds coupled with biomass-burning (BB) emissions from Southeast Asia (SEA) region. The association of EBC and CO was weak at LABS possibly due to the influence of dissimilar air masses from various sources, and scavenging or dilution of EBC during the long-range atmospheric transport to Mt. Lulin. The mean  $\Delta\text{EBC}/\Delta\text{CO}$  ratio (slope of least-squares regression line of  $\Delta\text{EBC}-\Delta\text{CO}$  scatterplot; where  $\Delta$  indicates surplus amounts with respect to the background value) was found the most significant in March (5.3 ng m<sup>-3</sup> ppbv<sup>-1</sup> or  $7.3 \times 10^{-3}$  g of carbon as EBC per gram of carbon as CO). On the basis of episodic cases, the mean  $\Delta\text{EBC}/\Delta\text{CO}$  ratios at LABS were estimated to be 6.1, 8.0, and 2.4 ng m<sup>-3</sup> ppbv<sup>-1</sup> for SEA BB emissions,

southern China mixed pollution, and northern China mixed pollution, respectively. A total of 32% loss in EBC aerosols (6.4% of EBC removal per day) was estimated for the atmospheric transport of BB emissions from SEA region to LABS. This study provides needful information to understand the  $\Delta\text{EBC}/\Delta\text{CO}$  ratios at a remote site and would be used in model simulations to evaluate BC aging and scavenging over western Pacific region in East Asia.

**Keywords :** Mount lulin, Equivalent black carbon, Carbon monoxide, Long-range transport, Southeast Asia biomass-burning.

---

## **Distribution, source and transport of the aerosols over Central Asia**

**Y.Liu, Q.Zhu, R.Wang, K.Xiao, P.Cha**

**Source :** Atmospheric Environment, Volume 210, 1 August 2019, Pages 120-131

Limited by scarce observations, the sources and transport of aerosols over Central Asia are relatively unclear. In this study, using Terra and Aqua satellite images, Moderate Resolution Imaging Spectroradiometer (MODIS) data, Cloud-Aerosol Lidar and Infrared Pathfinder Satellite Observations (CALIPSO) satellite observations and meteorological reanalyze data, the distribution, source and transport of aerosols over Central Asia are investigated. We find that there are 227 aerosol events occurred in Central Asia during 2000–2017 and the aerosols which can be transported from outside to Central Asia are dominated by dust and smoke (organic carbon and black carbon) particles. Statistical analyses show that the contribution of the sources outside of Central Asia (76 times) to all aerosol events (122 times) is greater than that of local emissions in Central Asia (46 times) in the spring and summer during 2000–2017. The smoke events (39 times), sourcing from Russia and Europe with strong northwest wind, account for 51.3% of total aerosol events contributed by sources outside of Central Asia. Additionally, the dust events (37 times), which mainly source from the northern Arabia Peninsula and North Africa with strong southwest wind, account for 48.7% of the total aerosol events contributed by the sources outside of Central Asia. On the contrary, the contribution of local emissions in Central Asia (90 times) to all aerosol events (105 times) is greater than that of outside sources (15 times) in the autumn and winter. Result of clustering analyses for all 157 aerosol events during 2005–2017 is in agreement with the conclusion of statistical analyses based on observations. This study can provide some evidence to understand the aerosol properties over the Central Asia.

**Keywords :** Dust, Smoke, Source, Transport, Central Asia.

---



## **PM<sub>2.5</sub> and PM<sub>10</sub> oxidative potential at a Central Mediterranean Site: Contrasts between dithiothreitol- and ascorbic acid-measured values in relation with particle size and chemical composition**

**Maria Rita Perrone<sup>a</sup>, Ilaria Bertoli<sup>b</sup>, Salvatore Romano<sup>a</sup>, Mara Russo<sup>b</sup>, Gennaro Rispoli<sup>a</sup>,  
Maria Chiara Pietrogrande<sup>b</sup>**

**Source :** Atmospheric Environment, Volume 210, 1 August 2019, Pages 143-155

In this study, PM<sub>2.5</sub> airborne particulate matter was collected over a full year at a costal site of the Central Mediterranean Sea and analysed for its chemical composition and oxidative potential (OP), determined by the dithiothreitol (DTT) and the ascorbic acid (AA) assays. In autumn-winter, the volume normalized oxidative OP (OPV) were  $0.29 \pm 0.03 \text{ nmol min}^{-1} \text{ m}^{-3}$  and  $0.21 \pm 0.03 \text{ nmol min}^{-1} \text{ m}^{-3}$  for the DTT (OPDTTV) and AA (OPA AV) assay, respectively. In spring-summer the OPDTTV values were higher than OPA AV responses, i.e.,  $0.19 \pm 0.02 \text{ nmol min}^{-1} \text{ m}^{-3}$  vs.  $0.09 \pm 0.01 \text{ nmol min}^{-1} \text{ m}^{-3}$ . Overall, marked seasonality was observed with higher values in Autumn-Winter (AW) than in Spring-Summer (SS), i.e., 1.5 and 2.3 times increase for OPDTTV and OPA AV, respectively.

In the cold season, the OPV activity was broadly correlated with metals and carbon species, such as K<sup>+</sup>, NO<sub>3</sub><sup>-</sup>, Ba, Cd, Cu, Fe, Mn, P, V, OC, EC, Acetate, Oxalate and Glycolate ( $p < 0.05$ ). This suggested the main contribution of a “mixed anthropogenic” source, consisting of the biomass burning (K<sup>+</sup>, OC and EC) and traffic (Ba, Cu, Fe, Mn, V, EC) emissions. In SS, OPV was significantly correlated with only few species i.e., OC, EC, Cu, and NO<sub>3</sub><sup>-</sup>, suggesting main association with the “mixed anthropogenic” and the “reacted dust” sources.

For each sampling day, PM<sub>2.5</sub> and PM<sub>10</sub> samples were simultaneously collected and analysed to investigate the variation of the OP activity in relation with the particle size and chemical composition.

OPDTTV values exhibited a poor particle-size dependence, with similar values close to  $0.20 \pm 0.04 \text{ nmol min}^{-1} \text{ m}^{-3}$  in both fractions. This could be explained by the association of OPDTTV with species mainly accumulated in the fine fraction, i.e., OC, POC and EC and K<sup>+</sup>. Otherwise, the OPA AV responses exhibited a clear particle-size dependence, with significantly higher values for PM<sub>10</sub> than for PM<sub>2.5</sub>, i.e.,  $0.35 \pm 0.06$  vs.  $0.21 \pm 0.03 \text{ nmol min}^{-1} \text{ m}^{-3}$  in AW and  $0.23 \pm 0.04$  vs.  $0.09 \pm 0.01$  in SS. This may be supported by the strong correlation of OPA AV with Cu and Fe, which were most abundant metals in the PM<sub>10</sub> fraction.

The data of specific monitoring days were investigated in detail to better highlight the impact of some individual redox active species on the OPDTTV and OPA AV responses.

**Keywords :** Oxidative potential, PM<sub>2.5</sub> particulate matter, PM<sub>2.5</sub> and PM<sub>10</sub> size distribution, Dithiothreitol assay, Ascorbic acid assay, PM<sub>2.5</sub> and PM<sub>10</sub> chemical composition.

## **Spatial and temporal distribution of open bio-mass burning in China from 2013 to 2017**

**HuabingKe<sup>a</sup>, SunlingGong<sup>a</sup>, JianjunHe<sup>a</sup>, ChunhongZhou<sup>a</sup>, LeiZhang<sup>ab</sup>, YikeZhou<sup>a</sup>**

**Source :** Atmospheric Environment, Volume 210, 1 August 2019, Pages 156-165

Open bio-mass burning plays an important role in the formation of heavy pollution events during harvest seasons in China by releasing the trace gases and particulate matters into the atmosphere. A better understanding of spatial-temporal variations of open bio-mass burning in China is required to assess its impacts on the air quality and especially on the heavy haze pollution. The MODIS fire spots data and the calculated burned areas were used in this research, which shows the varying number of fire spots in China from 2013 to 2017, with the highest in 2014 and the lowest in 2016. Meanwhile, the fire spots were found mainly concentrated in three key periods (March–April, June and October–November) and two zones (Zone 1 and Zone 2) with inter-annual variations of burned areas. In addition, the contribution of major vegetation types burning was studied, the cropland occupied the largest proportion of burned area of more than 70% in any period time, followed by forest. Finally, from the perspective of climate and human activities, the causes of inter-annual variations were discussed. By comparing the average temperature and precipitation in the two zones from 2013 to 2017, it was found that the burned forest area is positively correlated with the average temperature of the zones and negatively correlated with the average precipitation. Meanwhile, the relationship between the El Niño events and the bio-mass burning was discussed.

**Keywords :** Open bio-mass burning, Spatial-temporal variations, MODIS, Vegetation types, El Niño.

---

## **Impact of emission controls on air quality in Beijing during APEC 2014: Implications from water-soluble ions and carbonaceous aerosol in PM<sub>2.5</sub> and their precursors**

**WenXu<sup>a</sup>, XuejunLiu<sup>a</sup>, LeiLiu<sup>b</sup>, Anthony J.Dore<sup>c</sup>, AohanTang<sup>a</sup>, LiLu<sup>d</sup>, QinghuaWu<sup>a</sup>, YangyangZhang<sup>a</sup>, TianxiangHao<sup>a</sup>, YuepengPan<sup>e</sup>, JianminChen<sup>f</sup>, FusuoZhang<sup>a</sup>**

**Source :** Atmospheric Environment, Volume 210, 1 August 2019, Pages 241-252

Stringent emission controls during the Asia Pacific Economic Cooperation Summit (APEC; November 5–11, 2014) provide a valuable opportunity to examine the impact of such measures on the chemical properties of PM<sub>2.5</sub> and other air pollutants. Here, we measured the water-soluble inorganic ions (WSII) and carbonaceous species in PM<sub>2.5</sub>, NH<sub>3</sub> and NO<sub>2</sub> at multiple sites in Beijing between September and November 2014. Relative to the pre-APEC period (September and October 2014), significant reductions in the average concentrations of WSII (69% for NO<sub>3</sub><sup>-</sup>, 68% for SO<sub>4</sub><sup>2-</sup>, 78% for NH<sub>4</sub><sup>+</sup>, and 29–71% for

other species), elemental carbon (EC, 43%) and organic carbon (OC, 45%) in PM<sub>2.5</sub> were found during the APEC period. The contributions of secondary inorganic ions (SIA, including SO<sub>4</sub><sup>2-</sup>, NO<sub>3</sub><sup>-</sup>, and NH<sub>4</sub><sup>+</sup>) to PM<sub>2.5</sub> were significantly lower during the APEC period (9–44%), indicating a combination of lower gaseous precursor emissions and a relative weak secondary aerosol formation. Ion-balance calculations indicated that the PM<sub>2.5</sub> sample in the pre-APEC period was alkaline but was acidic during the APEC period. Relatively lower mean concentrations of EC (1.5 µg m<sup>-3</sup>), OC (10.5 µg m<sup>-3</sup>), secondary organic carbon (SOC, 3.3 µg m<sup>-3</sup>), secondary organic aerosol (SOA, 5.9 µg m<sup>-3</sup>) and primary organic aerosol (POA, 10.0 µg m<sup>-3</sup>) appeared during the APEC period. The average concentrations of NH<sub>3</sub> and NO<sub>2</sub> at all road sites were significantly reduced by 48 and 60% during the APEC period, which is consistent with clear reductions in satellite NH<sub>3</sub> columns over Beijing city in the same period. This finding suggests that reducing traffic emissions could be a feasible method to control urban NH<sub>3</sub> pollution. During the APEC period, concentrations of PM<sub>2.5</sub>, PM<sub>10</sub>, NO<sub>2</sub>, SO<sub>2</sub> and CO from the Beijing city monitoring network showed significant reductions at urban (20–60%) and rural (18–57%) sites, whereas O<sub>3</sub> concentrations increased significantly (by 93% and 53%, respectively). The control measures taken in the APEC period substantially decreased PM<sub>2.5</sub> pollution but can increase ground O<sub>3</sub>, which also merits attention.

**Keywords :** PM<sub>2.5</sub>, Ammonia, Chemical components, Air pollution, Emission control.

---

## **New method for evaluating winter air quality: PM<sub>2.5</sub> assessment using Community Multi-Scale Air Quality Modeling (CMAQ) in Xi'an**

**XiaochunYang<sup>abc</sup>, QizhongWu<sup>ac</sup>, RongZhao<sup>b</sup>, HuaqiongCheng<sup>ac</sup>, HuijuanHe<sup>d</sup>, QianMa<sup>ac</sup>, LanningWang<sup>ac</sup>, HuiLuo<sup>b</sup>**

**Source :** Atmospheric Environment, Volume 211, 15 August 2019, Pages 18-28

Particulate matter is the main air pollutant in China, especially in Xi'an in recent years. Since 2013, the WRF-SMOKE-CMAQ model system has been used to build an air quality model system for daily air quality forecasting in Xi'an. The emission inventory was built based on several anthropogenic emission inventories and open access emission datasets, and the model evaluation is presented to verify the emission inventory for particulate matter in Xi'an. Comparing the daily observed and simulated fine particulate (PM<sub>2.5</sub>) concentrations for four winters in different years (from 2014 to 2017), the model performs well in all studied time periods. The correlation coefficient of the simulated daily PM<sub>2.5</sub> concentration data are all larger than 0.58, reaches 0.80 in 2016, and the fraction of predictions within a factor of two of observations (FAC2) are all above 66%. The differences of simulated results based on emission-unchanged system between 2014 and 2015 indicate that the slightly deteriorating air quality of 2015 is affected by the unfavorable air diffusion condition. The PM<sub>10</sub> concentration increases from 95.9 µg/m<sup>3</sup> to 110.3 µg/m<sup>3</sup>, and the PM<sub>2.5</sub> from 82.4 µg/m<sup>3</sup> to 95.4 µg/m<sup>3</sup>. According to the error

analysis in model performance, the serious polluted situation of 2016 is mostly because of the sharp increased dust emissions. The emission-unchanged simulated particulate matter concentrations have little variation from 2015 to 2016, but the observation data increase obviously, that results in dramatically change of Mean Bias (MB). The absolute MB of PM10 increase from 70.3  $\mu\text{g}/\text{m}^3$  to 135.2  $\mu\text{g}/\text{m}^3$ , and PM2.5 from 0.46  $\mu\text{g}/\text{m}^3$  to 69.9  $\mu\text{g}/\text{m}^3$ . While the improved air quality in 2017 is attributed to both the better weather condition and the emission-reductions. The emission-unchanged simulated results decrease, and the absolute MB even have bigger decrease, that of the PM10 concentration reduce by 47  $\mu\text{g}/\text{m}^3$ , and PM2.5 by 37  $\mu\text{g}/\text{m}^3$ .

**Keywords :** PM<sub>10</sub>, PM<sub>2.5</sub>, CMAQ, Xi'an, Model assessment.

---

## **Measurement-based assessment of the regional contribution and drivers of reduction in annual and daily fine particulate matter impact metrics in Paris, France (2009–2018)**

**Christopher S.Malley<sup>a</sup>, Elsa N.Lefèvre<sup>b</sup>**

**Source :** Atmospheric Environment, Volume 211, 15 August 2019, Pages 38-54

Health effects from long- and short-term exposure to fine particulate matter (PM<sub>2.5</sub>) have resulted in an annual average PM<sub>2.5</sub> standard across Europe and World Health Organisation guidelines for annual (10  $\mu\text{g m}^{-3}$ ) and 24 h PM<sub>2.5</sub> concentrations (25  $\mu\text{g m}^{-3}$ ). Developing strategies to reduce both annual and 24 h average PM<sub>2.5</sub> requires that the conditions that produce the magnitude of these metrics are understood. This paper presents a standard and replicable set of statistics that link the magnitude of annual and daily PM<sub>2.5</sub> metrics to variation in i) hourly PM<sub>2.5</sub> concentrations, ii) geographic regions traversed by air mass back trajectories, and iii) the 'urban increment' and 'regional contribution' to urban PM<sub>2.5</sub> concentrations. These statistics are calculated between 2009 and 2018 at monitoring sites across Paris and the Île-de-France region, France, where there is a national objective to achieve the WHO annual PM<sub>2.5</sub> guideline, and where short-term PM<sub>2.5</sub> episodes still occur. The aim is to investigate changes in the conditions producing annual average, and 24 h PM<sub>2.5</sub> concentrations exceeding 25  $\mu\text{g m}^{-3}$ , and how these long- and short-term metrics could be reduced further. The statistics indicate that reductions between 2009 and 2018 in both annual PM<sub>2.5</sub> concentrations (PM<sub>2.5AA</sub>, -0.79  $\mu\text{g m}^{-3} \text{ y}^{-1}$  averaged across 3 urban background sites (33% average 2009–2018 reduction)) and the number of days with 24 h PM<sub>2.5</sub> concentrations above 25  $\mu\text{g m}^{-3}$  (D24h25, -6 days  $\text{y}^{-1}$  (62% average 2009–2018 reduction)), were driven by reductions in local emissions in Paris and the Île-de-France region. For example, reduction in PM<sub>2.5AA</sub> and D24h25 were greater at urban traffic sites, and between 2009 and 2018 the highest hourly PM<sub>2.5</sub> concentrations occurred less frequently during rush hour periods, while the lowest hourly PM<sub>2.5</sub> concentrations occurred more frequently during the day. In addition, when relatively moderate and high hourly PM<sub>2.5</sub> concentrations were measured, air mass back trajectories spent more time (during the 4 preceding days) over European geographic

regions, compared to the ocean indicating an increased relative contribution from regional transport to these hourly PM<sub>2.5</sub> concentrations. Consequently, there is now a greater difference in the contribution of different hourly PM<sub>2.5</sub> concentrations to annual and 24 h PM<sub>2.5</sub> compared with 2009, with relatively high hourly PM<sub>2.5</sub> concentrations having a larger contribution to D24h25, and moderate hourly PM<sub>2.5</sub> concentrations having a larger contribution to PM<sub>2.5AA</sub>. Strategies to reduce PM<sub>2.5</sub> concentrations in Paris should consider how mitigation measures will affect different ranges of hourly PM<sub>2.5</sub> concentrations to understand the (potentially differing) effect on long- and short-term PM<sub>2.5</sub> impact metrics. Comparison of hourly PM<sub>2.5</sub> concentrations at urban sites and upwind rural sites showed regional contributions to PM<sub>2.5AA</sub> of approximately 50% and 70% at urban traffic and urban background sites, respectively. The largest regional contributions were also estimated for the highest hourly PM<sub>2.5</sub> concentrations, compared to moderate hourly PM<sub>2.5</sub> concentrations. Regional emission reductions could therefore make a substantial contribution to achieving the WHO air quality guidelines in Paris.

**Keywords :** Fine particulate matter,,Air pollution,Air quality monitoring,Chemical climatology,Paris,Trends.

---

## **An advanced spatio-temporal model for particulate matter and gaseous pollutants in Beijing, China**

**JiaXu<sup>ab</sup>, WenYang<sup>b</sup>, BinHan<sup>ba</sup>, MengWang<sup>cda</sup>, ZhanshanWang<sup>b</sup>, ZhipingZhao<sup>b</sup>, ZhipengBai<sup>b</sup>, SverreVedal<sup>ab</sup>**

**Source :** Atmospheric Environment, Volume 211, 15 August 2019, Pages 120-127

Modeling fine-scale spatial and temporal patterns of air pollutants can be challenging. Advanced spatio-temporal modeling methods were used to predict both long-term and short-term concentrations of six criteria air pollutants (particulate matter with aerodynamic diameter less than or equal to 10 and 2.5  $\mu\text{m}$  [PM<sub>10</sub> and PM<sub>2.5</sub>], SO<sub>2</sub>, NO<sub>2</sub>, ozone and carbon monoxide [CO]) in Beijing, China. Monitoring data for the six criteria pollutants from April 2014 through December 2017 were obtained from 23 administrative monitoring sites in Beijing. The dimensions of a large array of geographic covariates were reduced using partial least squares (PLS) regression. A land use regression (LUR) model in a universal kriging framework was used to estimate pollutant concentrations over space and time. Prediction ability of the models was determined using leave-one-out cross-validation (LOOCV). Prediction accuracy of the spatio-temporal two-week averages was excellent for all of the pollutants, with LOOCV mean squared error-based R<sup>2</sup> (R<sup>2</sup><sub>mse</sub>) of 0.86, 0.95, 0.90, 0.82, 0.94 and 0.95 for PM<sub>10</sub>, PM<sub>2.5</sub>, SO<sub>2</sub>, NO<sub>2</sub>, ozone and CO, respectively. These models find ready application in making fine-scale exposure predictions for members of cohort health studies and may reduce exposure measurement error relative to other modeling approaches.

**Keywords :** Particulate matter, Air pollution, Spatio-temporal model, Geo-statistical model, Beijing.

---

## **Meteorological parameters and gaseous pollutant concentrations as predictors of daily continuous PM<sub>2.5</sub> concentrations using deep neural network in Beijing–Tianjin–Hebei, China**

**Xinpeng Wang Wenbin Sun**

**Source :** Atmospheric Environment, Volume 211, 15 August 2019, Pages 128-137

The deep learning model can simulate the complex nonlinear relationship between PM<sub>2.5</sub> and aerosol optical depth (AOD), and has great application potentiality in PM<sub>2.5</sub> inversion. However, the underestimation of high PM<sub>2.5</sub> concentrations problem is still exist in heavily polluted Beijing–Tianjin–Hebei (JingJinJi) region due to AOD cannot adequately represent the correlation between high PM<sub>2.5</sub> concentrations and independent variables and neglected the effects of missing AOD. Thus, the long- and short-term PM<sub>2.5</sub> exposure risk estimate was reduced. This work introduces gaseous pollutant data (NO<sub>2</sub>, SO<sub>2</sub>, CO, and O<sub>3</sub>) related to primary emission and secondary transformation of pollutants as predictors into a deep neural network model to improve the underestimation of high PM<sub>2.5</sub> concentrations based on AOD and meteorological factors. We predicted the PM<sub>2.5</sub> concentration in the missing AOD areas, generated a daily continuous PM<sub>2.5</sub> spatial distribution, and reduced estimated bias due to AOD deficiency. Grid-based 10-fold cross-validation (CV) was used to test the model performance. Results show that daily PM<sub>2.5</sub> concentration CV R<sup>2</sup> is 0.87 and the root-mean-square prediction error (RMSE) is 27.11 µg/m<sup>3</sup>. The CV R<sup>2</sup> and RMSE are higher by 0.12 and lower by 9.72 µg/m<sup>3</sup> than the model without gaseous pollutants (GASS) as predictors. In including the missing AOD, the average concentration of PM<sub>2.5</sub> CV R<sup>2</sup> is 0.86 and the RMSE is 16.95 µg/m<sup>3</sup> in heavy polluted winter; the CV R<sup>2</sup> and RMSE are higher by 0.07 and lower by 3.95 µg/m<sup>3</sup>, respectively, than when the missing AOD was excluded. Prediction results of PM<sub>2.5</sub> spatial distribution show that the model has high prediction accuracy and provides a complete and highly accurate spatiotemporal distribution characteristics for long- and short-term PM<sub>2.5</sub> exposure studies, and reduces exposure misclassification of PM<sub>2.5</sub> in heavily polluted areas.

**Keywords :** PM<sub>2.5</sub>, Aerosol optical depth, Gaseous pollutants, Deep neural network, AOD deficiency.

---

## **Fine and ultrafine particles concentrations in vape shops**

**Charlene Nguyen Liqiao Li Chanbopha Amy Sen Emilio Ronquillo Yifang Zhu**

**Source :** Atmospheric Environment, Volume 211, 15 August 2019, Pages 159-169

Vape shops are widespread due to the popularity of electronic cigarettes (e-cigs) as an alternative to tobacco cigarettes. In this study, sixty-seven Southern California vape shops were randomly surveyed for building characteristics, ventilation, and business patterns. Based on the survey results, six representative shops were recruited for real-time measurements of indoor and outdoor fine and ultrafine particles concentrations on a busy and less busy day. Occupancy, vaping frequency, and opening and closing of doors were recorded, and shop air exchange rate was determined. Indoor CO<sub>2</sub>, relative humidity, and temperature were also recorded. In addition, simultaneous measurements were taken at increasing distances away from a vaping area to assess the mixing and spatial profiles of particle levels inside the shops. During active vaping, real-time indoor particle number concentration and gravimetric-corrected PM<sub>2.5</sub> mass concentration across the six vape shops varied from  $1.3 \times 10^4$  to  $4.8 \times 10^5$  particles/cm<sup>3</sup> and from 15.5 to 37,500  $\mu\text{g}/\text{m}^3$ , respectively. The spatial profiles of particle number and mass were more uniformly mixed than expected in an indoor environment. Total vaping frequency was the main predictor of particle concentrations inside the vape shops when indoor-outdoor particle mass transfer is minimal (doors closed).

**Keywords :** Vape shop, Electronic cigarette, Secondhand vaping, Ultrafine, PM<sub>2.5</sub>.

---

## **Short-term responses of greenhouse gas emissions and ecosystem carbon fluxes to elevated ozone and N fertilization in a temperate grassland**

**JinyangWang<sup>a</sup>FelicityHayes<sup>b</sup>David R.Chadwick<sup>a</sup>Paul W.Hill<sup>a</sup>GinaMills<sup>b</sup>Davey L.Jones<sup>ac</sup>**

**Source :** Atmospheric Environment, Volume 211, 15 August 2019, Pages 204-213

Growing evidence suggests that tropospheric ozone has widespread effects on vegetation, which can contribute to alter ecosystem carbon (C) dynamics and belowground processes. In this study, we used intact soil mesocosms from a semi-improved grassland and investigated the effects of elevated ozone, alone and in combination with nitrogen (N) fertilization on soil-borne greenhouse gas emissions and ecosystem C fluxes. Ozone exposure under fully open-air field conditions was occurred during the growing season. Across a one-year period, soil methane (CH<sub>4</sub>) and nitrous oxide (N<sub>2</sub>O) emissions did not differ between treatments, but elevated ozone significantly depressed soil CH<sub>4</sub> uptake by 14% during the growing season irrespective of N fertilization. Elevated ozone resulted in a

15% reduction of net ecosystem exchange of carbon dioxide, while N fertilization significantly increased ecosystem respiration during the growing season. Aboveground biomass was unaffected by elevated ozone during the growing season but significantly decreased by 17% during the non-growing season. At the end of the experiment, soil mineral N content, net N mineralization and extracellular enzyme activities (i.e., cellobiohydrolase and leucine aminopeptidase) were higher under elevated ozone than ambient ozone. The short-term effect of single application of N fertilizer was primarily responsible for the lack of the interaction between elevated ozone and N fertilization. Therefore, results of our short-term study suggest that ozone exposure may have negative impacts on soil CH<sub>4</sub> uptake and C sequestration and contribute to accelerated rates of soil N-cycling.

**Keywords :** Air pollutant, Fertilizer management, Ground level O<sub>3</sub>, Plant-soil feedbacks, Soil nutrient cycling.

---

## **Multiple perspectives for modeling regional PM<sub>2.5</sub> transport across cities in the Beijing–Tianjin–Hebei region during haze episodes**

**HanyuZhang<sup>a</sup>, ShuiyuanCheng<sup>ab</sup>, SenYao<sup>a</sup>, XiaoqiWang<sup>a</sup>, JunfengZhang<sup>a</sup>**

**Source :** Atmospheric Environment, Volume 212, 1 September 2019, Pages 22-35

Regional transport always plays a crucial role in the formation and dissipation of haze over the Beijing–Tianjin–Hebei (BTH) region. This study, conducted using pollution and meteorological observations and the Weather Research and Forecasting model (WRF) coupled with the Comprehensive Air Quality Model with Extensions (CAMx), investigated the possible meteorological causes for the occurrence of haze pollution and quantitatively assessed the PM<sub>2.5</sub> transport contribution to haze episodes that occurred in Beijing in January and July 2015. The results indicated that modeling system reproduced the spatial-temporal variation in PM<sub>2.5</sub> concentrations in the BTH region well. During the study period, haze episodes were primarily attributed to meteorological conditions such as planetary boundary layer height, relative humidity, wind vector, and temperature inversion, in the context of pollution emissions. Analysis of surface PM<sub>2.5</sub> transport showed that 62.89% of the surface PM<sub>2.5</sub> in Beijing was came from local emissions, with the remaining 23.69% and 13.42%, on average, originating from short- and long-range transport during the study period. The percentage of contribution varied with the evolutionary stage of the haze episodes, showing the joint influence of local emissions and regional transport on haze pollution in Beijing. Additionally, investigation of vertical PM<sub>2.5</sub> transport identified the following three major pathways: a northwest–southeast pathway in January (at all layers below 1200 m, though it was stronger above 600 m), a southeast–northwest pathway in July (at all layers below 800 m), and a southwest–northeast pathway during both months (at a height of 200–1200 m). Moreover, the magnitude of daily PM<sub>2.5</sub> transport fluxes during the haze episodes was generally stronger than the corresponding



monthly average. These results provide a scientific basis for strategic control of both multiple cities and provinces and in-depth knowledge of the mechanisms and sources of haze pollution in the BTH region.

**Keywords :** PM<sub>2.5</sub> transport, Modeling system, Meteorological causes, Haze episodes, The Beijing–Tianjin–Hebei region.

---

## **Design and application of a hybrid assessment of air quality models for the source apportionment of PM<sub>2.5</sub>**

**Hsin-ChihLai<sup>a</sup>, Hwong-WenMa<sup>b</sup>, Chih-RungChen<sup>b</sup>, Min-ChuanHsiao<sup>c</sup>, Bo-HanPan**

**Source :** Atmospheric Environment, Volume 212, 1 September 2019, Pages 116-127

Increasing levels of air pollution greatly affect the environment and human health; air quality control is therefore of particular importance. To improve the efficiency of air pollution control, reliable air quality models for source apportionment are critically in need. The multitude of air quality models to find the sources of air pollution, however, have their own limitations. Hence, this study seeks to integrate different air quality models, including a diffusion model (AERMOD) and a grid model (CMAQ), employing initial meteorological fields provided by the Weather Research and Forecasting (WRF) model. Using the advantages of these models, this study builds a hybrid air quality model, which provides a more effective analysis of the distribution of primary pollutants, secondary pollutants, and other environmental information. Two significant fine particulate matter (PM<sub>2.5</sub>) events were selected in this study to discuss the influence of the Taichung coal-fired power plant and the Taichung traffic source on the PM<sub>2.5</sub> in the Taichung area, as well as to evaluate the performance of the hybrid model. Simulation results for the two cases show that if the coal-fired power loads are reduced by 20% (around 1100 MW), the concentration of PM<sub>2.5</sub> in the Taichung area will decrease by 0.5%; such decrease will reach 1.25% when the power load reduction is 40%. If the traffic source is reduced by 20%, the concentration of PM<sub>2.5</sub> in the Taichung area will decrease by 4.3%, and by 6.6% with 30% traffic source reduction. The hybrid model shows that the contribution of different pollution sources can be illuminated to support air quality control strategies.

**Keywords :** Hybrid air quality model, Source apportionment, Primary PM<sub>2.5</sub>, Secondary PM<sub>2.5</sub>, CMAQ, AERMOD.

---

## **Assessment and mitigation of indoor human exposure to fine particulate matter (PM<sub>2.5</sub>) of outdoor origin in naturally ventilated residential apartments: A case study**

**Ruchi Sharma Rajasekhar Balasubramanian**

**Source :** Atmospheric Environment, Volume 212, 1 September 2019, Pages 163-171

Emissions of fine particulate matter (PM<sub>2.5</sub>) from on-road traffic and their influence on air quality and human health are of major concern in urban areas. Exposure to traffic-related PM<sub>2.5</sub> indoors has received considerable attention as people spend about 80% of their time in indoor environments, but little information is currently available on the assessment and mitigation of this exposure. A systematic field study was conducted with the key objective to assess and mitigate indoor human exposure to traffic-related PM<sub>2.5</sub> in a typical naturally ventilated residential apartment. Results indicated that traffic-related PM<sub>2.5</sub> levels indoors exceeded the air quality guidelines (12 µg/m<sup>3</sup>), and the PM<sub>2.5</sub> levels decreased significantly (74%) while using an indoor air cleaner. The human health risk assessment based on the bioavailable fraction of toxic trace elements revealed a substantial reduction in potential health risk while using the air cleaner. Overall, the major outcomes of this study would help develop effective air pollution control strategies to reduce indoor human exposure to PM<sub>2.5</sub> and potential human health risk caused by vehicular pollution in urban areas.

**Keywords :** Vehicular emissions, Fine particulate matter, Air cleaner, Bioavailable toxic trace elements, Potential carcinogenic health risk.

---

## **China's black carbon emission from fossil fuel consumption in 2015, 2020, and 2030**

**YanLu<sup>ab</sup>Qin'gengWang<sup>ac</sup>XiaohuiZhang<sup>a</sup>YuQian<sup>a</sup>XinQian<sup>ac</sup>**

**Source :** Atmospheric Environment, Volume 212, 1 September 2019, Pages 201-207

Black carbon (BC) emissions in China have been changing significantly due to rapid evolution of fuel consumption. In this study, BC emissions from fossil fuel consumption in different sectors were estimated in 2015 based on up-to-date activity data and emission factors (EFs). While for the future scenarios in 2020 and 2030, it was estimated according to relative changes in the activity level and EFs. In 2015, total BC emissions were estimated to be 1.48 Tg, mostly from the industrial, residential, and transportation sectors. Emission fluxes were found to have remarkable spatial features, where high fluxes generally located in eastern China. About 25% of the terrestrial area of China showed an annual flux above 0.2 t km<sup>-2</sup>. Total BC emissions will be decreased to 1.33 (2020) and 1.16 Tg (2030). Most

reduction will occur in the industrial and residential sectors, while the transportation sector will see an obvious increase. The dramatic reduction of BC emissions in future is a new indication to our current understanding of the emission and its effects as well, and it may provide guidance for future scientific research and policy making in the field of climate change and air quality control.

**Keywords :** BC, Emission inventory, Energy consumption, Scenario projection.

---

## **Influence of atmospheric PM<sub>2.5</sub>, PM<sub>10</sub>, O<sub>3</sub>, CO, NO<sub>2</sub>, SO<sub>2</sub>, and meteorological factors on the concentration of airborne pollen in Guangzhou, China**

**AnannaRahman<sup>abc</sup>, ChuanxiuLuo<sup>ab</sup>, Md Hafijur RahamanKhan<sup>abc</sup>, JinzhaoKe<sup>d</sup>,  
VidusankaThilakanayaka<sup>abc</sup>, SazalKumar<sup>abc</sup>**

**Source :** Atmospheric Environment, Volume 212, 1 September 2019, Pages 290-304

The existence of biological (pollen and spore) and non-biological (PM<sub>2.5</sub>, PM<sub>10</sub>, O<sub>3</sub>, CO, NO<sub>2</sub>, SO<sub>2</sub>, etc.) particles in the atmosphere is connected to the frequency of adverse allergenic reactions affecting human health. Considering all probable effects of atmospheric pollutants and airborne pollen on allergic reactions, the present study mainly examines the influence of non-biological pollutants and weather parameters on the concentration of airborne pollen in the Guangzhou city area by using Pearson's correlation, Spearman's rho test, and multiple linear regressions. Accordingly, we analyze the seasonal variation of non-biological pollutants, meteorological parameters, and airborne pollen during 2017 from two districts (Haizhu and Panyu) of Guangzhou, China. The airborne pollen data were collected using the volumetric method. Spring and autumn were the primary seasons for most of the pollen identification in this area. Pearson's correlation and Spearman's rho test revealed that pollen dispersion was significantly correlated with non-biological pollutants and meteorological parameters. Among them, PM<sub>2.5</sub> and O<sub>3</sub> were positively correlated with pollen concentration and NO<sub>2</sub> was negatively correlated. A significant positive correlation was observed between temperature and wind speed with pollen concentration. Precipitation and relative humidity were negatively correlated with pollen concentration during the study period. In contrast, multiple linear regressions revealed a minor effect among these parameters on pollen concentration. However, the meteorological parameter shows more valid regression than the air pollutants. Some inconsistent results were discovered, which might be due to differences in climate, vegetation type, and rapid urbanization. Therefore, considering the long periods needed to collect data on pollen, further research is necessary to investigate the allergenic effects and health burden due to atmospheric pollutants.

**Keywords :** Atmospheric pollutants, Meteorological parameters, Airborne pollen , Statistical analysis, Guangzhou.

---

## **Collective impacts of biomass burning and synoptic weather on surface PM2.5 and CO in Northeast China**

**YichenLi<sup>a</sup>, JaneLiu<sup>ab</sup>HanHan<sup>a</sup>, TianliangZhao<sup>c</sup>, XunZhang<sup>ad</sup>, BingliangZhuang<sup>a</sup>, TijianWang<sup>a</sup>, HuiminChen<sup>a</sup>, YueWu<sup>a</sup>MengmengLi<sup>a</sup>**

**Source :** Atmospheric Environment, Volume 213, 15 September 2019, Pages 64-80

Biomass burning has become one of the prominent sources of air pollution in Northeast China, where the land is largely covered by forest, grasslands, and agricultural crops. Nevertheless, the impact of biomass burning on air quality and the sensitivity of such impact to weather are rarely documented. In this study, we addressed these issues using satellite fire radiative power (FRP) and surface PM<sub>2.5</sub> and CO data at 24 stations during fire seasons (March, April, October and November) in Northeast China from 2015 to 2017. Fire-polluted days were identified by tracing air parcels at the stations back to fire regions using a trajectory model, the Hybrid Single-Particle Lagrangian Integrated Trajectory (HYSPLIT) model. The results show that 60–80% the polluted days in Northeast China can be attributed to biomass burning in the fire seasons, varying among subregions due to the differences in landscapes, fire activities, and weather conditions. On fire-polluted days, the mean PM<sub>2.5</sub> and CO concentrations from all observation stations in Northeast China reached 111  $\mu\text{g m}^{-3}$  and 1.3  $\text{mg m}^{-3}$ , respectively. The hourly PM<sub>2.5</sub> and CO concentrations on fire-polluted days could reach as high as 1000  $\mu\text{g m}^{-3}$  and 10  $\text{mg m}^{-3}$ , respectively. By subregions, the mean PM<sub>2.5</sub> concentrations were 128, 112, 102, 106  $\mu\text{g m}^{-3}$ , respectively, in the central, eastern, northern, and southern subregions, while mean CO concentrations were 1.2, 1.3, 0.8, 1.5  $\text{mg m}^{-3}$ , respectively, in the four corresponding subregions. On average, PM<sub>2.5</sub> and CO concentrations on fire-polluted days elevated, respectively, by 22–54% and 4–11% from those on no-fire-polluted days, with the largest enhancement in the central subregion and the least in the southern subregion. We classified six predominant weather patterns during the fire seasons. When Northeast China was ahead of a strong Siberian High, fire-polluted days were least and FRP was weakest among the six patterns in most subregions, leading to lowest enhancement of PM<sub>2.5</sub> and CO in the subregions. In contrast, two weather patterns exacerbated PM<sub>2.5</sub> and CO pollution the most during fire episodes. Under one of the weather patterns, Northeast China was under a stagnant high-pressure system, resulting in poor dispersion conditions and thus high PM<sub>2.5</sub> and CO pollution. The other pattern was characterized with high humidity and southwesterlies ahead of a trough, which brought about strong hygroscopic growth and regional transport of fire emissions. The degree to which the weather patterns impacted air pollution during fires varied largely among subregions. This study highlights the combined impacts of biomass burning and weather on air pollution. The findings and the developed methodology are helpful for forecasting air quality and implementing mitigation strategies during biomass burning.

**Keywords :** Biomass burning, Air quality, Particulate matter, Carbon monoxide, Northeast China

---

## **Oral bioavailability estimation of toxic and essential trace elements in PM<sub>10</sub>**

**Jorge Moreda-Piñeiro, Lucía, Dans-Sánchez, Joel Sánchez-Piñero, Isabel Turnes-Carou, Soledad Muniategui-Lorenzo, Purificación, López-Mahía**

**Source :** Atmospheric Environment, Volume 213, 15 September 2019, Pages 104-115

Oral bioavailability of essential and toxic elements has been assessed in particulate matter samples (PM<sub>10</sub>) at several sites (industrial, urban and sub-urban sites) by using an in-vitro model that combines simulated gastric/intestinal fluids and physiologically based extraction conditions which simulate human digestive system. Metals concentrations in bioavailable fractions will allow to a real human health-risk assessment associated to toxic metals. High oral bioavailability percentages were found for metals such as Cu, Mn, Ni, Pb and Sb (oral bioavailability ratios in the range of 39.7–45.7%). Al and V are less bioavailable (oral bioavailability ratios in the range of 1.8–9.2%). The influence of chemical composition (major ions, carboxylic acids and black carbon (BC)) on bioavailability ratios was assessed. Fe, Ni, V and Zn bioavailability ratios was found to be affected by the K<sup>+</sup>, NH<sub>4</sub><sup>+</sup>, acetate and BC contents of PM<sub>10</sub>; while a correlation was found between marine content (Cl<sup>-</sup> and Na<sup>+</sup>) of PM<sub>10</sub> and Cu, Fe and Mn dialyzability ratios. Zn and Sr bioavailability ratios were correlated with crustal contribution of PM<sub>10</sub>. Principal Component Analysis (PCA) results also showed that Fe, Mn, Ni, Pb, Sb, Sr and V bioavailability are dependent on BC and NH<sub>4</sub><sup>+</sup> contents and Cu and Zn bioavailability are dependent on sea salt content of PM<sub>10</sub>. Predicted bioavailability for some metals after applying a quadratic surface model based on crustal, marine and anthropogenic content of PM<sub>10</sub> could also be established. Toxicity prediction of target metals, by using hazard quotient/index values, suggested potential non-carcinogenic risk for Pb and Sb.

**Keywords :** Oral bioavailability, Dialyzability, Essential/toxic minerals, Particulate matter, Toxicity prediction.

---

## **The transport of PM<sub>10</sub> over Cape Town during high pollution episodes**

**Koketso M.Molepo<sup>a</sup>Babatunde J.Abiodun<sup>a</sup>Rembu N.Magoba<sup>b</sup>**

**Source :** Atmospheric Environment, Volume 213, 15 September 2019, Pages 116-132

---

This study investigates the influence of PM<sub>10</sub> from remote sources on PM<sub>10</sub> episodes over the city of Cape Town. For the study, we analysed observation data from Cape Town's air quality monitoring stations as well as high-resolution simulation data from the Weather Research and Forecasting model with Chemistry (WRF-Chem). The observation data were used to identify PM<sub>10</sub> episodes during the study period (2008–2014) and WRF-Chem was applied to simulate the atmospheric conditions and PM<sub>10</sub> transport over southern Africa during each episode. The capability of WRF-Chem to simulate the wind and PM<sub>10</sub> concentration over Cape Town was quantified and the paths of air parcels over Cape Town during each episode were tracked. Results of the study show that WRF-Chem gives a realistic simulation of observed wind (speed and direction) over the city during the episodes, but the model struggles to reproduce the observed PM<sub>10</sub> concentration. For most episodes, the magnitude of the simulated PM<sub>10</sub> is lower than the observed due to lack of local emissions in the simulations. In some cases, the model reproduces the peak in PM<sub>10</sub> concentration some days earlier or later than observed. The simulations show that most air parcels over Cape Town during the episodes have travelled over major dust source regions (i.e., the Kalahari or Namib Desert) before reaching the city. Most of episodes are associated with a southward transport of a plume of PM<sub>10</sub> from the north-west coast of southern Africa to Cape Town. This PM<sub>10</sub> plume is induced by a coastal trough and a continental high pressure system. In some cases, local topography influences the intrusion of the PM<sub>10</sub> plume into Cape Town by blocking some of the pollution, thereby minimising the amount of PM<sub>10</sub> that reaches the city. Results of the study suggest that the transport of PM<sub>10</sub> from the north-west coast of southern Africa may contribute to PM<sub>10</sub> episodes in Cape Town.

**Keywords :** PM<sub>10</sub>, Cape town, Atmospheric transport, WRF-Chem, HYSPLIT.

---

## **Investigating secondary organic aerosol formation pathways in China during 2014**

**WenyiYang<sup>ab</sup>JieLi<sup>abc</sup>WeigangWang<sup>d</sup>JunlingLi<sup>d</sup>MaofaGe<sup>d</sup>YeleSun<sup>abc</sup>XueshunChen<sup>ab</sup>BaozhuGe<sup>a</sup>ShengruiTong<sup>d</sup>QingqingWang<sup>a</sup>ZifaWang<sup>abc</sup>**

**Source :** Atmospheric Environment, Volume 213, 15 September 2019, Pages 133-147

The concentrations of organic aerosol (OA) in central and eastern China are much higher than those in Europe and North America. Compared with observations, recent numerical modeling studies have largely underestimated the concentrations of OA, especially the secondary components. Based on the volatility basis set framework, a secondary OA (SOA) module is developed and coupled into the nested air quality prediction modeling system

(NAQPMS). This model is applied to investigate the concentration and formation pathways of SOA in central and eastern China during 2014, and the simulation performance is validated through observation. The oxidation of intermediate volatile organic compounds (IVOCs) is significant to SOA formation and could reduce the great discrepancy between simulations and observations. In winter, the contribution of IVOCs accounted for 60%–80% of SOA formation. In spring and autumn, IVOCs and volatile organic compounds (VOCs) have a considerable effect on SOA formation. In summer, the contributions of VOCs reach 40%–60% due to an increase in the emissions of biogenic VOCs. The mass yields and other parameters of IVOCs remain largely uncertain. By using the latest mass yields obtained from chamber experiments, the simulated SOA concentrations in winter increase by 10–20  $\mu\text{g m}^{-3}$  compared with the base scenario. To more thoroughly understand SOA formation in China, further research on the emission sources and mass yields of IVOCs is warranted.

**Keywords** : NAQPMS, Secondary organic aerosol, Intermediate volatile organic compounds, Mass yield.

---

## **A high-resolution inventory of air pollutant emissions from crop residue burning in China**

**XiaohuiZhang<sup>a</sup>, YanLu<sup>ac</sup>, Qin'gengWang<sup>ab</sup>, XinQian<sup>ab</sup>**

**Source** : Atmospheric Environment, Volume 213, 15 September 2019, Pages 207-214

Crop residue burning is an important source of air pollutants and strongly affects the regional air quality and global climate change. This study presents a detailed emission inventory of major air pollutants from crop residue burning for the year of 2014 in China by the bottom-up method. Activity data were investigated for 296 prefecture-level cities. Emission factors were determined for indoor and in-field burning separately. Regional differences were considered for the proportion of residue burned (PCRB), the ratio between indoor and in-field burning, and the ratio of straw to grain production. The emissions were estimated at prefecture-city level as the first step; then they were redistributed within a city based on 1-km resolution land-use, MODIS fire counts, and rural population. Temporal variation was determined according to farming practices in different regions and MODIS fire counts. Uncertainties were estimated using the Monte Carlo method. The total emissions from crop residue burning in China were estimated to be 0.13 (–47–92%) for BC, 0.71 (–48–92%) for OC, 1.77 (–48–91%) for PM<sub>2.5</sub>, 2.04 (–50–100%) for PM<sub>10</sub>, 0.16 (–59–133%) for SO<sub>2</sub>, 0.53 (–55–105%) for NO<sub>x</sub>, 0.12 (–47–93%) for NH<sub>3</sub>, 1.07 (–55–102%) for CH<sub>4</sub>, 1.85 (–43–74%) for NMVOC, 18.33 (–46–85%) for CO and 305.20 (–45–80%) for CO<sub>2</sub>, in unit of Tg yr<sup>-1</sup>. Our results are remarkably lower than those reported in previous studies, mainly because of the PCRB has decreased significantly in recent years. For most of the pollutants, indoor burning accounted for about 50–70% of the emissions. Rice, wheat and corn contributed more than 85% of the emissions, but their relative contributions varied a lot with region and season. High emissions were mostly located in the eastern China, central China and northeastern China, and temporally peaked

in April, June and October, with different intensities in the north and the south. This study provides a useful basis for air quality modeling and the policy making of pollution control strategies.

**Keywords :** Crop straw, Biomass burning, Air pollutants, Emission inventory, Spatial and temporal distribution.

---

## **Analysis of aerosol scattering properties and PM10 concentrations at a mountain site influenced by mineral dust transport**

**J.F.Nicolás, R.Castañer, N.Galindo, E.Yubero, J.Crespo, A.Clemente**

**Source :** Atmospheric Environment, Volume 213, 15 September 2019, Pages 250-257

Aerosol scattering properties (ASP) i.e., scattering and backscattering coefficients ( $\sigma_{sp}$ ,  $\sigma_{bsp}$ , 525 nm), scattering Ångström exponent (SAE, 450–635 nm) and backscatter ratio ( $b$ , 525 nm) along with PM10 concentrations were measured from November 2015 to October 2016 at a mountain site (1558 m a.s.l) located in the southwestern Mediterranean. ASP and PM10 average values obtained for the whole period were: 26.2 Mm<sup>-1</sup>, 3.5 Mm<sup>-1</sup>, 1.42, 0.139 and 12.4 µg/m<sup>3</sup>, respectively. The study was aimed at analyzing: a) the seasonal variability of the measured parameters, b) the impact of mineral dust from North Africa on PM10 and optical properties and c) the variation of ASP values and PM10 concentrations as a function of the mixing layer height. The extensive scattering properties had values ~35% higher during the warm period, while SAE and  $b$  were similar during both the cold and warm seasons.  $\sigma_{sp}$  and  $\sigma_{bsp}$  increased under Saharan dust events (SDE). In contrast, SAE and  $b$  values showed a decrease due to the increase in coarse particle concentrations during this type of event. On non-event days, the lowest values of  $\sigma_{sp}$  and PM10 were recorded under free troposphere (FT) conditions (10.5 Mm<sup>-1</sup>, 3 µg/m<sup>3</sup>). Conversely, SAE recorded its highest value (~2.00) under these conditions, pointing to a predominance of fine particles in this layer. Average values of  $\sigma_{sp}$  and PM10 increased with the increase in the height of the Planetary Boundary Layer (PBL), while the SAE value progressively decreased to a steady value of 1.50–1.60. The average value of the mass scattering efficiency (MSE) during the study period was 1.35 m<sup>2</sup>/g.

**Keywords :** Light scattering, PM<sub>10</sub>, Mass scattering efficiency, Free troposphere, Mountain site, Saharan dust events.

---



## **Regional air pollution mixtures across the continental US**

**Weeberb J.Requia<sup>a</sup>, Brent A.Coull<sup>b</sup>, PetrosKoutrakis<sup>a</sup>**

**Source :** Atmospheric Environment, Volume 213, 15 September 2019, Pages 258-272

A limited literature body have estimated regional differences in air pollution mixtures. More comprehensive analyses are necessary to accurately depict differences in air pollution characteristics over space and time. Our objective is to further these efforts by investigating spatial differences of air pollution mixtures across the US. We employed spatially constrained clustering approach (based on k-means algorithm) to group air pollution monitoring sites that exhibit distinct pollutant profiles or mixtures in the US over 9 years (2008–2016). We accounted for 20 chemical components of PM<sub>2.5</sub>. The resulting clusters of pollution mixtures are characterized and validated based on source emissions represented by land-use information. Our analysis resulted in 27 clusters with different number of sites. For example, the cluster 1 has 14 sites and it covers part of the southeast, including the states of North Carolina, South Carolina, Georgia, and Florida. The southwest has a very prominent cluster with 8 sites (cluster 26), covering part of the Louisiana, Mississippi, Texas, and Arkansas. In the west coast, two clusters were highlighted in our analysis, cluster 3 in California and cluster 7 in Washington and part of Oregon. Both clusters with 5 sites. We estimated that Cu, Se, NO<sub>3</sub><sup>-</sup>, Cr, and Ba were the top five species that divided the study area into cluster of sites more effectively. Observing the concentration ratios (concentrations of the species *i*/concentration of PM<sub>2.5</sub>) for some of these clusters, our results show that clusters 3 and 7 in the west coast represent sites with high Na ratios. Cluster 13 in the northwest and part of the Midwest represents sites with high SO<sub>4</sub><sup>2-</sup> ratio. The cluster 16 with a single site in northeast has the highest SO<sub>4</sub><sup>2-</sup> ratio, representing almost the third quartile of the SO<sub>4</sub><sup>2-</sup> ratio. This is one of the few studies focused on spatial patterns analysis to estimate regions that exhibit distinct pollutant mixtures on a large scale. We expect that further investigations can use our findings to analyze the relationship between areas that exhibit distinct pollutant mixtures and the impact of regulations, climate change, and health effects in the US.

**Keywords :** Air pollution, Pollutant mixtures, Spatiotemporal analysis, Cluster analysis.

---

## **Analysis of PM<sub>2.5</sub> pollution episodes in Beijing from 2014 to 2017: Classification, interannual variations and associations with meteorological features**

**JinSun<sup>ab</sup>, JianhuaGong<sup>ac</sup>, JiepingZhou<sup>a</sup>, JiantaoLiu<sup>d</sup>, JianmingLiang<sup>ac</sup>**

**Source :** Atmospheric Environment, Volume 213, 15 September 2019, Pages 384-394

Ambient PM<sub>2.5</sub> pollution has been a major environmental concern in recent years. Beijing, the capital of China, is enduring frequent and severe PM<sub>2.5</sub> pollution. In this study, 186 valid PM<sub>2.5</sub> pollution episodes during the 2014-2017 period were identified and classified into four categories according to the mechanism of pollution formation and evolution. Category I often occurs in autumn, winter and early spring, depending on accumulation during stagnant weather. Category II featured by photochemistry is dominant in summer, and category III caused by dust storms occasionally occurs in spring. Category IV represents a combination during transition periods. Interannual variations show that particulate pollution decreased from 2014 to 2017, and the decline in categories I and II played the most important role. To further understand the PM<sub>2.5</sub> pollution patterns in Beijing, the temporal and spatial characteristics and relationships between PM<sub>2.5</sub> levels and meteorological features were analyzed. Category I is the main pollution type that brings forth heavy or severe pollution and has the longest duration in those cases, while category II often leads to light or moderate pollution. There is a north-south gap in the PM<sub>2.5</sub> levels in Beijing. The high-level pollution in category I tends to evolve northward, while the low-level pollution in category I and category II pollution tend to evolve southward and widen the north-south gap, affected by the regional transport and more local emissions in the south. Additionally, the relationship between the concentrations and meteorology also vary with the pollution categories. High relative humidity, low wind speeds and low boundary layer heights are likely to lead to category I or II pollution, but category III requires high winds. These results provide insights into the annual tendency and characteristics of Beijing's particulate pollution in recent years.

**Keywords :** Fine particles, Meteorological conditions, Mechanisms, Gravity centers, Beijing.

---

## **Understanding the washoff processes of PM<sub>2.5</sub> from leaf surfaces during rainfall events**

**ChangkunXie<sup>ab</sup>, LubingYan<sup>b</sup>, AnzeLiang<sup>b</sup>, ShengquanChe<sup>a</sup>**

**Source :** Atmospheric Environment, Volume 214, 1 October 2019, 116844

The PM on plant surface being washed into soil during the rain is one of the key processes for plants to reduce atmospheric PM. This study attempted to explore the PM<sub>2.5</sub> washoff processes from different tree leaves during rain events (<16 mm/h) using an artificial rainfall simulation experiment. We aimed to improve our knowledge of processes associated with PM<sub>2.5</sub> reduction and to provide a basis for accurately evaluating the ability of plants to reduce PM<sub>2.5</sub>. This is the first study showing that the PM<sub>2.5</sub> washoff processes from leaves follow quartic functions and 4 pattern curves under different conditions were categorized. They respectively explained the PM<sub>2.5</sub> washoff processes in broad-leaved trees with large leaves and simple crowns (bimodal curved), in conifer species with small leaves and complex crowns under high rainfall intensity (unimodal curved), in trees with extremely complex crowns under high rainfall intensity (continually-rising curved), and in conditions under which extremely high water interception efficiency but rather low water

storage capacity occur (U-shaped curved). These curves indicate that the amount of PM<sub>2.5</sub> on leaves was not necessarily reduced in rainfall events. The general ranking of the average values of PM<sub>2.5</sub> number on leaves surface during rain events was Cedrus Deodara ( $40.3 \times 10^3/\text{cm}^2$ ), Japanese Maple ( $33.0 \times 10^3/\text{cm}^2$ ) > Dragon Juniper ( $14.7 \times 10^3/\text{cm}^2$ ), Dawn Redwood ( $12.6 \times 10^3/\text{cm}^2$ ) > Common Boxwood ( $6.4 \times 10^3/\text{cm}^2$ ), Lotus Magnolia ( $4.1 \times 10^3/\text{cm}^2$ ). The cycles of PM<sub>2.5</sub> accumulation and removal on broad-leaved trees might be shorter than that of conifers, meaning that they may have a better PM<sub>2.5</sub> washoff efficiency during rain, which is opposite to the PM<sub>2.5</sub> deposition efficiency. Higher rainfall intensity can reduce the cycle length and enhance the PM<sub>2.5</sub> washoff efficiency.

**Keywords :** Particulate matter, Air pollution, PM<sub>2.5</sub> washoff processes, Rainfall, Leaves.

---

## **Study on the contribution of transport to PM<sub>2.5</sub> in typical regions of China using the regional air quality model RAMS-CMAQ**

**RongLiab, XinMeiab, LifeiWeiab, XiaoHanc, MeigenZhangcde, YingyingJingf**

**Source :** Atmospheric Environment, Volume 214, 1 October 2019, 116856

Regional transport plays a significant role in the air pollution in China, which is characterized by diverse emission sources and distinct distributions. To improve the understanding of factors determining the PM<sub>2.5</sub> level in China, a source apportionment tool coupled with the RAMS-CMAQ model (CMAQ-ISAM) was used to quantify the contribution of transport to PM<sub>2.5</sub> and its major components during 2017 in the North China Plain (NCP), Yangtze River Delta (YRD), Pearl River Delta (PRD), and Chengyu area. It is found that transport accounts for a predominant fraction of the PM<sub>2.5</sub> in Beijing, Tianjin, and Shanghai with relatively low PM<sub>2.5</sub> levels. Transport in the NCP is mainly at intraregional scale and comparable to local emissions. In contrast, the contributions of interregional transport from the NCP to the YRD (~10–25%) and from NCP and YRD to PRD and Chengyu (~5–25%) is at similar level to those of intraregional transport and local emissions in winter and fall, but are lower in spring and summer. It is worth noting that particle components have very different transport capabilities. Nitrate exhibits much stronger intraregional transport than other components in the NCP, and much higher concentration than other components during winter. In contrast, the concentration of sulfate is higher than that of nitrate during spring and summer in most provinces. In addition, the transport potential of primary OC, EC, and ammonia are relatively weaker, but these compounds can still have considerable contributions. Our results reveal that the notable contributions of regional transport to PM<sub>2.5</sub> should be addressed according to targeted emission sources in order to improve air quality efficiently.

**Keywords :** PM<sub>2.5</sub>, CMAQ-ISAM, Regional transport, Air quality, China.

---

# Contributions of local and regional sources to PM<sub>2.5</sub> and its health effects in north India

HaoGuo<sup>a</sup>Sri HarshaKota<sup>bc</sup>Shovan KumarSahu<sup>d</sup>HongliangZhang<sup>e</sup>

**Source** : Atmospheric Environment, Volume 214, 1 October 2019, 116867

Air quality in India, especially in north India, is increasingly severe due to rapid growth of industrialization and urbanization in past decades. Very few studies were conducted in the recent past to quantify regional contributions to high pollutant concentrations for designing effective control strategies. In this paper, source-oriented versions of Community Multi-scale Air Quality (CMAQ) model were applied to quantify the contributions of nine source regions (Delhi, Haryana & Rajasthan, Uttar Pradesh & Uttarakhand, Himachal Pradesh & Punjab, Central India, West India, South India, East & Northeast India and Outside India) to fine particulate matter (PM<sub>2.5</sub>) and its components including primary PM (PPM) and secondary inorganic aerosol (SIA) i.e. sulfate, nitrate and ammonium ions, in Delhi and three surrounding cities, Chandigarh, Lucknow and Jaipur in 2015. PPM is dominated by local sources (>70%), with Delhi as the top contributor in Delhi contributing to a maximum of 90 µg/m<sup>3</sup> in winter. Unlike PPM, SIA contributions from non-local sources are more significant. Delhi, Haryana & Rajasthan, Uttar Pradesh & Uttarakhand, and Himachal Pradesh & Punjab contribute to ~4 µg/m<sup>3</sup> SIA concentrations in North India. In Delhi, local sources contribute to over 70% of total PM<sub>2.5</sub>, but the non-local sources are still important (over 30%) especially in winter. Furthermore, local emissions contribute less in highly polluted days compared to less polluted days indicating the importance of regional transport on high pollution episodes in Delhi. Overall, while local sources contribute to 1.495 × 10<sup>4</sup> premature deaths in Delhi, non-local sources contribute to 0.483 × 10<sup>4</sup> premature deaths.

**Keywords** : Regional transport, PM<sub>2.5</sub>, North India, Delhi, Premature mortality

---

## Assessing PM<sub>2.5</sub> model performance for the conterminous U.S. with comparison to model performance statistics from 2007-2015

James T.Kelly<sup>a</sup>, Shannon N.Koplitz<sup>a</sup>, Kirk R.Baker<sup>a</sup>, Amara L.Holder<sup>b</sup>, Havala O.T.Pye<sup>b</sup>, Benjamin N.Murphy<sup>b</sup>, Jesse O.Bash<sup>b</sup>, Barron H.Henderson<sup>a</sup>, Norman C.Possiel<sup>a</sup>, HeatherSimon<sup>a</sup>, Alison M.Eyth<sup>a</sup>, CareyJanga<sup>a</sup>, SharonPhillips<sup>a</sup>, BrianTimin<sup>a</sup>

**Source** : Atmospheric Environment, Volume 214, 1 October 2019, 116872

Previous studies have proposed that model performance statistics from earlier photochemical grid model (PGM) applications can be used to benchmark performance in

new PGM applications. A challenge in implementing this approach is that limited information is available on consistently calculated model performance statistics that vary spatially and temporally over the U.S. Here, a consistent set of model performance statistics are calculated by year, season, region, and monitoring network for PM<sub>2.5</sub> and its major components using simulations from versions 4.7.1-5.2.1 of the Community Multiscale Air Quality (CMAQ) model for years 2007–2015. The multi-year set of statistics is then used to provide quantitative context for model performance results from the 2015 simulation. Model performance for PM<sub>2.5</sub> organic carbon in the 2015 simulation ranked high (i.e., favorable performance) in the multi-year dataset, due to factors including recent improvements in biogenic secondary organic aerosol and atmospheric mixing parameterizations in CMAQ. Model performance statistics for the Northwest region in 2015 ranked low (i.e., unfavorable performance) for many species in comparison to the 2007–2015 dataset. This finding motivated additional investigation that suggests a need for improved speciation of wildfire PM<sub>2.5</sub> emissions and modeling of boundary layer dynamics near water bodies. Several limitations were identified in the approach of benchmarking new model performance results with previous results. Since performance statistics vary widely by region and season, a simple set of national performance benchmarks (e.g., one or two targets per species and statistic) as proposed previously are inadequate to assess model performance throughout the U.S. Also, trends in model performance statistics for sulfate over the 2007 to 2015 period suggest that model performance for earlier years may not be a useful reference for assessing model performance for recent years in some cases. Comparisons of results from the 2015 base case with results from five sensitivity simulations demonstrated the importance of parameterizations of NH<sub>3</sub> surface exchange, organic aerosol volatility and production, and emissions of crustal cations for predicting PM<sub>2.5</sub> species concentrations.

**Keywords :** CMAQ, Model evaluation, Crustal cations, Ammonia, Organic aerosol.

---

## **Characteristics of six criteria air pollutants before, during, and after a severe air pollution episode caused by biomass burning in the southern Sichuan Basin, China**

**YangZhou<sup>a</sup>, BinLuo<sup>b</sup>, JingLi<sup>ac</sup>, YufangHao<sup>a</sup>, WenwenYang<sup>a</sup>, FangtianShi<sup>a</sup>, YijiaChen<sup>a</sup>, MaimaitiSimayi<sup>a</sup>, ShaodongXie<sup>a</sup>**

**Source :** Atmospheric Environment, Volume 215, 15 October 2019, 116840

Biomass burning (BB) seriously affect air pollution, human health and global climate. A severe pollution episode (PE) caused by BB was investigated in the southern Sichuan Basin (SSB), one of the most polluted areas in China. Hourly variations in criteria air pollutants (PM<sub>2.5</sub>, PM<sub>10</sub>, SO<sub>2</sub>, NO<sub>2</sub>, CO, and O<sub>3</sub>), chemical components, and sources of PM<sub>2.5</sub> before, during, and after the severe regional air PE were characterized at three sites, namely Neijiang (NJ), Zigong (ZG), and Yibin (YB). The results showed that combination of intensive pollution from BB, stable meteorological conditions, and the basin topography

caused this severe regional PE in the SSB. The average daily concentrations of PM<sub>2.5</sub> during the PE were 1.8–6 times those measured during the periods before and after the PE, and 4.0–7.4 times that of World Health Organization air quality guidelines in the SSB. The highest PM levels occurred in ZG, where the peak values of PM<sub>2.5</sub> and PM<sub>10</sub> reached 536  $\mu\text{g m}^{-3}$  and 578  $\mu\text{g m}^{-3}$  at night, respectively. PM<sub>10</sub>, NO<sub>2</sub>, and CO also increased dramatically at night in the SSB. O<sub>3</sub> formation was affected by BB, showing lower levels at night but higher levels in the day during the PE than before and after the PE, whereas SO<sub>2</sub> levels were not affected. Sulfate–nitrate–ammonium in PM<sub>2.5</sub> was the main chemical compositions before the PE, whereas organic matter (OM) and K<sup>+</sup> became characteristics compositions during and after the PE. Higher OC/EC and K<sub>excess</sub>/EC ratios were observed during the PE and K<sub>excess</sub>/EC ratio was a better indicator of BB in the SSB than OC/EC ratio. The results of a positive matrix factorization model indicated that BB was the most significant contributor to PM<sub>2.5</sub> during the PE, accounting for 58% in NJ, 65% in ZG, and 56% in YB. Backward trajectory analysis confirmed that the SSB is susceptible to pollutants from Chongqing and other surrounding cities, especially in ZG and NJ, due to the unique topography of the basin. Our findings suggest that BB in the basin topography can cause severe regional air pollution events at night, thus supporting the critical need for BB control in the basin to improve regional air quality.

**Keywords :** Biomass burning, Chemical components, Criteria air pollutants, Source apportionment, Southern sichuan basin.

---

## **Analysis of exposure to fine particulate matter using passive data from public transport**

**BenjamínTrehwela<sup>ab</sup>, NicolásHuneus<sup>bc</sup>, MarcelaMunizaga<sup>ab</sup>, AndreaMazzeo<sup>b1</sup>, LaurentMenut<sup>d</sup>, SylvainMailler<sup>d</sup>, MyrtoValari<sup>d</sup>, CesarOrdoñez<sup>b2</sup>**

**Source :** Atmospheric Environment, Volume 215, 15 October 2019, 116878

The city of Santiago experiences extreme pollution events during winter due to particulate matter and the associated health impact depends on the exposure to this pollutant, particularly to PM<sub>2.5</sub>. We present and apply a method that estimates the exposure of users of the public transport system of Santiago by combining smart card mobility data with measured surface concentrations from the monitoring network of Santiago and simulated concentrations by the CHIMERE model. The method was applied between July 20th and 24th of 2015 to 105,588 users corresponding to 12% of the frequent users of the public transport system and approximately 2% of the total population of Santiago. During those five days, estimated exposure based on measured concentrations varied between 44 and 75  $\mu\text{g}/\text{m}^3$  while exposure based on simulated concentrations varied between 45 and 89  $\mu\text{g}/\text{m}^3$ . Furthermore, including socioeconomic conditions suggests an inverse relationship between exposure and income when measured concentrations are used, i.e. the lower the income the higher the exposure, whereas no such relationship is observed

when using simulated concentrations. Although only exposure to PM<sub>2.5</sub> was considered in this study, the method can also be applied to estimate exposure to other urban pollutant such as ozone.

**Keywords :** Air quality, Exposure, Mobility, PM<sub>2.5</sub>, Public transport users.

---

## **A study on the short-term impact of fine particulate matter pollution on the incidence of cardiovascular diseases in Beijing, China**

**YuxiaMa<sup>a1</sup>, SixuYang<sup>ab1</sup>, ZhiangYu<sup>a</sup>, HaoranJiao<sup>a</sup>, YifanZhang<sup>a</sup>, BingjiMa<sup>a</sup>**

**Source :** Atmospheric Environment, Volume 215, 15 October 2019, 116889

Recently, air pollution has been substantially decreased in China, including particulate matter (PM) pollution in Beijing. However, PM pollution still has a great impact on human health, as stated in several epidemiological studies. In this paper, we used a generalized additive model (GAM) to evaluate the associations between PM<sub>2.5</sub> and cardiovascular diseases from 2009 to 2012 in the Beijing metropolitan area. In GAM, we controlled the confounding factors, such as day of the week and long-term trends. We used the number of daily hospital emergency room (ER) visits to represent the incidence of the studied diseases. We divided the entire study group by gender (i.e., male and female) and age (i.e., 15–60 yr, 60–75 yr, and ≥75 yr). The results showed strong links were observed between increase in PM<sub>2.5</sub> concentration and the number of hospital ER visits for cardiovascular diseases. For each interquartile range (IQR) increase in PM<sub>2.5</sub>, the relative risks (RRs) of the incidence of ischemic heart disease, arrhythmia, high blood pressure, and cerebrovascular disease were 1.023 (95% CI: 1.007–1.040), 1.019 (95% CI: 0.992–1.047), 1.082 (95% CI: 0.985–1.188), 0.976 (95%CI: 0.957–0.996), and 1.038 (95% CI: 1.005–1.072), respectively. Overall, the short-term impact of PM<sub>2.5</sub> on the incidence of cardiovascular diseases was the strongest for the 60–75 yr subgroup. For the two different gender subgroups, the short-term impact of PM<sub>2.5</sub> on ischemic heart disease and high blood pressure was relatively stronger for the females than for the males, while the opposite was true for arrhythmia and cerebrovascular disease.

**Keywords :** Fine particulate matter, Cardiovascular disease, Hospital emergency room visits, Air pollution, Generalized additive model.

---

## **Surveillance efficiency evaluation of air quality monitoring networks for air pollution episodes in industrial parks: Pollution detection and source identification**

**ZihanHuang<sup>a</sup>, QiYu<sup>abc</sup>, WeichunMa<sup>abc</sup>, LiminChen<sup>a</sup>**

**Source :** Atmospheric Environment, Volume 215, 15 October 2019, 116874

Both air pollution detection and source identification for air pollution episodes are highly desirable for detecting and controlling industrial air pollution. Surveillance of air pollution episodes in industrial parks is the focus of this article. The surveillance in this study consists of air pollution detection and subsequent source identification. The Gaussian puff model is applied to simulate the dispersion of air pollution, and the source area analysis method is used to reconstruct unknown source terms. A case study involving hydrogen sulfide emissions in a typical chemical industrial park is presented. The long-term efficiencies of both pollution detection and source identification of a developing planning of boundary-type air quality monitoring network (AQMN) are evaluated. Five typical scenarios are identified for the evaluation. Moreover, several key factors for the surveillance efficiency variation (i.e., meteorological conditions, monitor number and distance between sources) are discussed. The efficiency of pollution detection increases with the number of monitors. The efficiency of source identification increases with the number of monitors and the distance between sources.

**Keywords :** Air pollution episodes, Boundary-type monitoring network, Gaussian puff model, Source area analysis, Hydrogen sulfide.

---

## **Characterization of pollutants emitted during burning of eight main tree species in subtropical China**

**XiajieYang<sup>a</sup>, YuanfanMa<sup>a</sup>, GuangyuWang<sup>b</sup>, Ernesto C.Alvarado<sup>c</sup>, Mulualetigabu<sup>ad</sup>, YuanhuaJu<sup>a</sup>, FutaoGuo<sup>ab</sup>**

**Source :** Atmospheric Environment, Volume 215, 15 October 2019, 116899

Understanding the chemical composition of pollutants released from forest fuel burning is crucial for revealing the effects of forest fire on the atmosphere and ecosystem. However, relevant studies exploring this aspect in China are rare. The emission factors (EFs) of five key pollutants (CO, CO<sub>2</sub>, NO<sub>x</sub>, PM<sub>2.5</sub>), non-methane hydrocarbons (NMHCs) and oxygenated volatile organic compounds (OVOCs) from different components of eight dominant tree species in sub-tropical China were determined under both smoldering and flaming stages using a self-designed combustion system. Results demonstrate that the emissions factors of different pollutants varied by tree component under both combustion stages. The average EFs of gaseous pollutants and PM<sub>2.5</sub> of leaves, branches, and bark from the eight tree species under two combustion stages equaled  $230.49 \pm 17.61$  (smoldering)



vs.  $154.35 \pm 15.61$  (flaming, g/kg) for CO;  $1018.23 \pm 48.77$  vs.  $1307.86 \pm 76.99$  (g/kg) for CO<sub>2</sub>;  $1.16 \pm 0.16$  vs.  $1.42 \pm 0.23$  (g/kg) for NO<sub>x</sub>; and  $18.62 \pm 4.30$  vs.  $9.51 \pm 2.75$  (g/kg) for PM<sub>2.5</sub>. Under different combustion stages, leaves and branches from these different tree species released 48 types of NMHCs, including 19 alkanes, 15 alkenes, and 14 aromatic compounds. The total EF of NMHCs ranged from 841.35 to 1846.46 mg/kg (smoldering) to 754.32–1128.88 mg/kg (flaming) for leaves, and from 539.50 to 2907.14 mg/kg (smoldering) to 698.11–1013.49 mg/kg (flaming) for branches. The NMHCs released from the combustion of leaves and branches under smoldering stage were more harmful to the environment and human health than flaming stage, with the most threatening NMHCs released by forest fires being alkenes and i-butane, 1-butene, 1,3-butadiene, benzene, and p-xylene. Acetic acid was found to be the most abundant species among OVOCs, followed by Glycolaldehyde, Formaldehyde, Phenol, and Furan. Our findings are an important step towards further understanding the ecological and health implications of forest fires in subtropical China.

**Keywords :** Forest fire, Emission factors, Combustion conditions, Gaseous pollutants, Particulate pollutants, NMHCs.

---

## **Numerical assessment of PM<sub>2.5</sub> and O<sub>3</sub> air quality in Continental Southeast Asia: Impacts of potential future climate change**

**Giang Tran**

**HuongNguyen<sup>ab</sup>HikariShimadera<sup>a</sup>KatsushigeUranishi<sup>a</sup>TomohitoMatsuo<sup>a</sup>AkiraKondo<sup>a</sup>**

**Source :** Atmospheric Environment, Volume 215, 15 October 2019, 116901

Changing climate will impact future air quality. In this study, an online coupled meteorology and chemistry WRF-CMAQ model was applied to simulate such impacts on future O<sub>3</sub> and PM<sub>2.5</sub> air quality over Continental Southeast Asia. Simulations were conducted for present (2006–2015) and future (2046–2055) years under two climate scenarios, RCP4.5 and RCP8.5. Future climate projections were obtained by implementing a downscaling dynamical method based on pseudo global warming technique. In order to estimate the impacts of climate change alone, anthropogenic and biomass burning emissions were held constant at present level while biogenic emissions varying with climate were used. The model results indicated a future regional meteorology characterized by a warmer and more humid atmosphere, increased precipitation, and more stagnant condition. Affected by climate change, NO<sub>x</sub> and NMVOCs biogenic emissions increase which contribute to the increasing effects on O<sub>3</sub> and PM<sub>2.5</sub> precursors concentrations. Subsequently, the changes in meteorology and biogenic emission affect air quality. These influence on ground level O<sub>3</sub> and PM<sub>2.5</sub> are different between the two climate scenarios. Under RCP4.5 scenario, future atmosphere appears to be reduced in O<sub>3</sub> and PM<sub>2.5</sub> concentrations, suggesting a potential “climate benefit” for air quality. At four target countries, namely Cambodia, Laos, Thailand,

and Vietnam, O<sub>3</sub> concentration decreases by -0.76 ppb (-2.40%), PM<sub>2.5</sub> concentration decreases by -0.95 µg/m<sup>3</sup> (-4.32%) on average for the entire year. However, climate change worsen O<sub>3</sub> and PM<sub>2.5</sub> air pollution under RCP8.5 scenario. O<sub>3</sub> concentration increases by +0.26 ppb (+0.84%), PM<sub>2.5</sub> concentration increases by +0.92 µg/m<sup>3</sup> (+4.20%) on average for the entire year. Significant increases were generally located in northern Vietnam (for O<sub>3</sub>) and southern Vietnam (for PM<sub>2.5</sub>) during the dry season. The analysis suggests that the decrease in O<sub>3</sub> concentration is due to the dominance of the negative effect of water vapor increase and the increase in O<sub>3</sub> concentration is affected largely by the temperature increase, stagnant condition, and biogenic emission increase. The responses of PM<sub>2.5</sub> to climate change depend on the physical and chemical characteristics of each PM<sub>2.5</sub> species. The major climate change effect on PM<sub>2.5</sub> is the physical effect, rather than the chemical effect.

**Keywords :** Online coupled WRF-CMAQ model, Climate change impacts, Fine particulate matter, Ozone, Continental Southeast Asia.

---

## Characteristics and sources of volatile organic compounds (VOCs) in Shanghai during summer: Implications of regional transport

YuehuiLiu<sup>ab</sup>, HongliWang<sup>b</sup>, ShengaoJing<sup>b</sup>, YaqinGao<sup>b</sup>, YarongPeng<sup>ab</sup>, ShengrongLou<sup>b</sup>, TiantaoCheng<sup>cd</sup>, ShikangTao<sup>b</sup>, LiLi<sup>b</sup>, YingjieLi<sup>b</sup>, DandanHuang<sup>b</sup>, QianWang<sup>b</sup>, JingyuAn<sup>b</sup>

**Source :** Atmospheric Environment, Volume 215, 15 October 2019, 116902

Intensive field measurements were carried out in urban Shanghai between 20th and 30th of May 2017, and the VOC characteristics and sources were investigated with a focus on the relative contributions of local emissions and regional transport, as well as on the potential source regions. The VOC characteristics and sources largely depended on the meteorological conditions, especially wind direction and wind speed. Generally, two kinds of episodes were associated with regional transport. In one scenario, pollutants were transported from areas upwind (north-to-northwest) of Shanghai, specifically the Suzhou-Wuxi-Changzhou and Nantong city clusters and were characterized by combustion emissions and aged air masses. In the other scenario, pollutants were transported from areas upwind (south-to-southeast) of Shanghai, specifically Ningbo-Zhoushan port, and were characterized by industrial emissions and aged air masses. Additionally, an episode associated with air masses from the clean area over the sea provided an opportunity to study the local emissions of VOCs in Shanghai. Vehicle exhaust and chemical industries, especially solvent usage, contributed a majority of the VOCs in urban Shanghai in summer, together accounting for more than 55%. The aromatic fraction of the PAMS in Shanghai was significantly higher than that in other regions in China. Regional transport and secondary formation were also important sources of VOCs, and their contribution ranged from ~15% to ~25% depending on the meteorological conditions, with an hourly maximum contribution as high as 67%. Fuel evaporation, especially leakage emissions, should be

addressed in Shanghai. The present study highlights the fact that joint control of VOCs in conjunction with surrounding cities is critical for Shanghai.

**Keywords :** VOCs, Emission, Source, Regional transport.

---

## **Emission inventory of key sources of air pollution in Lebanon**

**AbdelkaderBaayoun<sup>a</sup>, WaelItani<sup>a</sup>, JadEl Helou<sup>a</sup>, LamaHalabi<sup>a</sup>, SajedMedleja<sup>a</sup>, MaryaEl Malki<sup>b</sup>, AliMoukhadder<sup>b</sup>, Lea KaiAboujaoude<sup>c</sup>, VahaknKabakian<sup>de</sup>, HalaMounajed<sup>f</sup>, TharwatMokalled<sup>f</sup>, AlanShihadeh<sup>a</sup>, IssamLakkis<sup>a</sup>, Najat A.Saliba<sup>g</sup>**

**Source :** Atmospheric Environment, Volume 215, 15 October 2019, 116871

Exposure to air pollutants has been associated with deleterious health effects that cause premature mortality and a range of morbidities. Air quality in the Mediterranean is of particular interest due to an array of environmental and anthropogenic conditions that make it an air-pollution hotspot. However, the scarcity of data for the region's emission inventories inhibits accurate and holistic assessment. Lebanon, located on the eastern board of the Mediterranean, faces several challenges including an unsustainable transport sector, an unregulated power generation sector, and high urban densities, all of which amplify the air-quality crisis. This paper presents an air pollutant emission inventory for two major emission sources in Lebanon, diesel generators and light duty vehicles (LDVs) of the transport sector, and uncovers trends for over a decade. The exhaust emissions for carbon dioxide, nitrogen oxide, carbon monoxide, sulfur dioxide, and fine particulate matter for diesel generators and for LDVs were estimated by assimilating different approaches and data sources through the use of survey data and national statistics for a higher tier. Our results uncovered that diesel generators consumed almost 1.6 million tons of fuel and emitted about 2 Gg of fine particulate matter in 2016. LDVs doubled in number over a decade and were responsible for approximately 0.20 Gg of fine particulate matter emissions in 2015. While the market for diesel generators appeared to have saturated, ownership of passenger cars per passengers continued to increase, while vehicle age, conditions, and, thus, emissions continued to augment. The results highlight the need for greater government intervention to meet the national electricity demand and promote public transportation and discourage private transportation, especially for energy-inefficient vehicles

**Keywords :** East Mediterranean, Emission inventory, Beirut, Light duty vehicles, Diesel generators.

---

## **Emission inventory research of typical agricultural machinery in Beijing, China**

**Xiuning HouJinling TianChangbo SongJie WangJiyun ZhaoXuemin Zhang**

**Source** : Atmospheric Environment, Volume 216, 1 November 2019, 116903

Non-road mobile machinery, especially agricultural machinery, has increasingly become an important source of air pollution in China. Hence, it is important to study these emissions. In this study, Beijing is used as an example, and the emission characteristics of 22 types of agricultural machinery (tractors, combine harvesters, and micro-tillers) in idling mode, moving mode, and working mode were tested using a portable emission measurement system (PEMS). The results indicate that the net power-based emission factor in working mode was larger than that in the idling and moving modes. Based on information from actual emission factors, ownership and activity levels, a typical agricultural machinery emission inventory for Beijing from 2006 to 2016 is established using the complex method from the *Technical Guidelines for Compiling Non-Road Mobile Source Emission Inventory*. In addition, the spatial distribution of the emission inventory is analyzed using Geographic Information System (GIS). Typical agricultural machinery in Beijing emitted carbon monoxide (CO), hydrocarbons (HC), nitrogen oxides (NO<sub>x</sub>), particulate matter (PM), and the total, and these decreased by 63.11%, 62.93%, 72.07%, 74.67%, and 68.66%, respectively, from 2006 to 2016, which proved the validity of emission control technologies and relevant regulations in China. In addition, the emission intensities of the different agricultural machines and different regions differed significantly. In 2016, the overall contribution of tractor emissions accounted for more than 80%. In the Yanqing District, Shunyi District, and Miyun District, the total emissions reached nearly 50%. The Chaoyang District was less than 1%. Therefore, in the future, government should pay more attention to high emission intensity agricultural machinery and its regional impacts.

**Keywords** : PEMS, Agricultural machinery, Emission factor, Emission inventory.

---

## **Traffic source impacts on chlorinated polycyclic aromatic hydrocarbons in PM<sub>2.5</sub> by short-range transport**

**RyosukeOishi<sup>a</sup>Yukilmai<sup>b</sup>Fumikazulkemori<sup>c</sup>TakeshiOhura<sup>ab</sup>**

**Source** : Atmospheric Environment, Volume 216, 1 November 2019, 116944

Chlorinated polycyclic aromatic hydrocarbons (ClPAHs) are recognized as ubiquitous hazardous pollutants in the environment, whereas their behavior in local areas remains unclear. Additionally, there is limited information on the sources in local areas. Here, we investigated the seasonal trends of ClPAHs associated with fine particles (PM<sub>2.5</sub>) at two sites near heavy traffic roads to evaluate the local atmospheric behaviors and sources. The annual mean concentrations of total ClPAHs at the north (site A) and south side (site B) across a heavy traffic road were 12.0 and 19.2 pg/m<sup>3</sup>, respectively. The higher concentration at site B was further emphasized during the winter season; at that time the site was located beneath the wind from the traffic road. In addition, for individual ClPAHs, the behaviors of 8-chlorofluoranthene (8-ClFluor) and 7-chlorobenz[a]anthracene (7-ClBaA) were consistent with the frequency of the north wind, suggesting that 8-ClFluor and 7-ClBaA have the ability to be indicators of vehicle exhaust. Diagnostic ratios using these specific ClPAHs during high-traffic activities provided the specific values to differentiate the impacts.

**Keywords :** ClPAHs, Biomarkers, PM<sub>2.5</sub>, Diagnostic ratio, Vehicle exhaust.

---

## **Performance evaluation of twelve low-cost PM<sub>2.5</sub> sensors at an ambient air monitoring site**

**Brandon Feenstra<sup>abc</sup>, Vasileios Papapostolou<sup>a</sup>, Sina Hasheminassab<sup>a</sup>, Hang Zhang<sup>a</sup>, Berj DerBoghossian<sup>a</sup>, David Cocker<sup>bc</sup>, Andrea Polidori<sup>a</sup>**

**Source :** Atmospheric Environment, Volume 216, 1 November 2019, 116946

A variety of low-cost sensors are now available on the consumer market for measuring air pollutants. The use of these low-cost sensors for ambient air monitoring applications is increasing and includes fence-line or near-source monitoring, community monitoring, emergency response, hot-spot identification, mobile monitoring, epidemiological studies, and supplemental monitoring to improve the spatial-temporal resolution of current monitoring networks. Evaluating and understanding the performance of these devices is necessary to properly interpret the results and reduce confusion when low-cost sensor measurements are not in agreement with measurements from regulatory-grade instrumentation. Systematic and comprehensive field and laboratory studies comparing low-cost sensors with regulatory-grade instrumentation are necessary to characterize sensor performance. This paper presents the results of 12 particulate matter (PM) sensors measurement of PM<sub>2.5</sub> (particles with aerodynamic diameter less than 2.5 μm) tested under ambient conditions against a federally equivalent method (FEM) instrument at an ambient air monitoring station in Riverside, CA spanning over a 3-year period from 02/05/15 to 03/27/18. Sensors were evaluated in triplicate with a typical time duration of 8-week. Performance evaluation results found 6 of the 12 sensor triplicates with average R<sup>2</sup> values ≥ 0.70 for PM<sub>2.5</sub> concentrations less than 50 μg/m<sup>3</sup>. Within this subset, the Mean

Absolute Error (MAE) ranged from 4.4 to 7.0  $\mu\text{g}/\text{m}^3$  indicating the need for caution when interpreting data from these sensors. Additional analysis revealed that the impact of relative humidity on sensor performance varied between models with several models exhibiting increased bias error with increasing humidity. Results indicate that a number of these sensors have potential as useful tools for characterizing PM<sub>2.5</sub> levels in ambient environments when data is interpreted and understood correctly with regard to existing ambient air quality networks. The performance evaluation results are specific for Riverside, CA under non-repeatable ambient weather conditions and particle properties with the expectation that performance evaluation testing at other locations with different particle properties and weather conditions would yield similar but non-identical results.

**Keywords :** Air quality, Fine particulate matter, Low-cost sensors, Optical particle counter, Performance evaluation.

---

## **Investigation of long-range transported PM<sub>2.5</sub> events over Northern Taiwan during 2005–2015 winter seasons**

**Wei-TingHung<sup>a</sup>, Cheng-Hsuan (Sarah)Lu<sup>a</sup>, Sheng-HsiangWang<sup>b</sup>, Sheng-PoChen<sup>ac</sup>, FujungTsai<sup>d</sup>, Charles C.-K.Chou<sup>e</sup>**

**Source :** Atmospheric Environment, Volume 217, 15 November 2019, 116920

In-situ PM<sub>2.5</sub> observations and the Modern-Era Retrospective analysis for Research and Applications, Version 2 (MERRA-2) aerosol reanalysis were analyzed to characterize long-range transported high PM<sub>2.5</sub> events over Northern Taiwan during winter seasons. MERRA-2 aerosol composition was evaluated using independent in-situ observations at the Cape Fuguei (CAFE) site. Results showed that MERRA-2 was able to distinguish the contribution of different species within complicated aerosol mixtures. Fifty transported high PM<sub>2.5</sub> events were identified during the winters of 2005–2015. To investigate the transport characteristics associated with Asian continental outflow, these events were further classified into sulfate-dominated, dust-dominated and mixed-composition events. More than 80% of transported events were influenced by Asian dust and 20% of them were dust-dominated. Both sulfate-dominated and dust-dominated events showed similar average PM<sub>2.5</sub> concentrations ( $\sim 44 \mu\text{g m}^{-3}$ ), while dust-dominated events showed a higher average PM<sub>10</sub> concentration ( $114 \mu\text{g m}^{-3}$ ) and thus a lower PM<sub>2.5</sub>/PM<sub>10</sub> ratio (0.41) compared to sulfate-dominated events ( $94 \mu\text{g m}^{-3}$  and 0.46, respectively). Results indicated that the low-level trough at 700 hPa plays a critical role in determining the transport paths of dust aerosols and their impact on local air quality. Therefore, the influence of Asian dust over Northern Taiwan cannot be neglected during winter seasons, and could potentially offset the effectiveness of emission controls and pollutant reductions. Such potential impacts could occur over vast areas affected by Asian continental outflow. The utilization of aerosol reanalysis provided valuable insights for long-range transport studies in the regions with complicated aerosol compositions.

**Keywords :** PM<sub>2.5</sub>, Long-range transport, Aerosol composition analysis, Chinese haze, Asian dust.

---

## **Effects of meteorological factors to reduce large-scale PM<sub>10</sub> emission estimation errors on unpaved roads**

**Tse-HuaiLiuYoojungYoon**

**Source :** Atmospheric Environment, Volume 217, 15 November 2019, 116956

Unpaved roads are one of the major sources of the particulate matter (PM) known to negatively affect human health, environment, and vegetation. The control of PM<sub>10</sub> and PM<sub>2.5</sub> (i.e., aerodynamic diameter < 10 μm and < 2.5 μm, respectively) is an increasing concern among many local agencies. The U.S. Environmental Protection Agency (EPA) provided the first emission factor equation for unpaved roads in 1975, and there are also several large-scale or site-specific PM<sub>10</sub> estimation models. These models are mostly based on linear regression models, which relate the PM<sub>10</sub> emission to the multiple input variables that represent the physical and operational characteristics of vehicles (e.g., vehicle speed, passes, and weights) as well as road surface material properties (e.g., silt and moisture content). Scientific knowledge is still lacking, however, pertaining to the potential effects of meteorological factors such as wind speed, temperature, and cloud cover, which could enhance the quality of PM<sub>10</sub> estimation models for unpaved roads. Therefore, this paper presents the results of a study investigating the potential effects of the meteorological factors to reduce the performance errors of large-scale PM<sub>10</sub> estimation models for unpaved roads employing a hypothesis test. The PM<sub>10</sub> models for the performance analysis in this study were developed using Principal Component Analysis (PCA) and Artificial Neural Network (ANN). The raw data were retrieved from the EPA report, "Emission Factor Documentation for AP-42," published in 1998, and two weather-related input variables (e.g., mean wind speed and temperature) were identified with other vehicle- and road-related input variables. The performance analysis results and hypothesis test based on the two common error measures (e.g., root mean square error and mean absolute error) indicated that there was no advantage in the inclusion of either one or both of the two weather-related variables as far as enhancing the predictive ability of large-scale PM<sub>10</sub> estimation models.

**Keywords :** Unpaved roads, Meteorological factors, Wind speed, Temperature, Particulate matter.

---

## Characteristics and sources of PM<sub>2.5</sub> and reactive gases near roadways in two metropolitan areas in Canada

EwaDabek-Zlotorzynska<sup>a</sup>, ValbonaCelo<sup>a</sup>, LuyiDing<sup>a</sup>, DennisHerod<sup>a</sup>, Cheol-HeonJeong<sup>b</sup>, GregEvans<sup>b</sup>, NathanHilker<sup>b</sup>

**Source :** Atmospheric Environment, Volume 218, 1 December 2019, 116980

With concern in recent years about adverse health effects for populations living or spending significant amounts of time near large roadways, an investigation of the air quality characteristics and potential sources influencing levels of PM and its chemical composition was undertaken in Toronto and Vancouver. Three near-road monitoring stations were established in the downtown area and beside a large highway in Toronto, and beside a major trucking route in Vancouver. 24-hour integrated samples were concurrently collected at these near-road and nearby urban background sites. This study has provided detailed chemical data for PM<sub>2.5</sub> and reactive gases (NH<sub>3</sub>, HONO and HNO<sub>3</sub>) for a year in 2015–2016. Differences between pollutant concentrations at the near-road and background urban sites were identified, and compared with observations at other urban locations. The traffic contribution was quantified as the concentration increment between the near-road and background sites. The highest increments due to traffic were observed for elemental carbon, select trace metals (e.g. Fe, Ba, Cu, Sb, Zn) and reactive gases (NH<sub>3</sub>, HONO). In general, the percent contribution of local traffic-related emissions followed a descending order of Toronto highway > Vancouver truck route > downtown Toronto for most of these pollutants. It appears that the influence of traffic-related emissions on air pollution near roads depends more on the proportion of large trucks in the fleet than the total traffic volume. Application of principal component analysis (PCA) coupled with multi-linear regression (MLR) analysis to the local traffic increment pollutant data, as well as knowledge of chemical markers representative of different sources, helped to identify the possible sources of traffic-related PM<sub>2.5</sub>. These sources include non-exhaust (brake wear abrasion, resuspended road dust) and vehicular exhaust (mixed gasoline/diesel, diesel and lubricating oil combustion) emissions. The contribution of each of the sources varied between sites. In particular, the contribution of diesel exhaust emissions, presumably from highly polluting heavy-duty vehicles and trucks, was significant at the truck route (Vancouver) and the highway (Toronto) sites. Furthermore, the substantial contribution of non-exhaust emissions (brake wear and resuspension of road dust) to PM<sub>2.5</sub>, and thus metals, with differences between sites due to traffic characteristics or local meteorology was identified. Emissions related to lube oil combustion were not statistically significant. Overall, this work delivered valuable information that serves as input for further studies involving other roads and cities in order to generate reliable and representative results for air quality management and associated health outcomes.

**Keywords :** Traffic-related air pollution, PM<sub>2.5</sub> speciation, Exhaust emissions, Non-exhaust emissions, Source apportionment.



## **Monitoring on-road air quality and measuring vehicle emissions with remote sensing in an urban area**

**R.Smit<sup>abc</sup>, P.Kingston<sup>a</sup>, D.W.Neale<sup>a</sup>, M.K.Brown<sup>a</sup>, B.Verran<sup>a</sup>, T.Nolan<sup>a</sup>**

**Source :** Atmospheric Environment, Volume 218, 1 December 2019, 116978

Simultaneous day-time measurement (8 a.m.–5 p.m.) of on-road air quality and emissions (remote sensing) on an urban road with traffic volumes varying between approximately 400-800 vehicles per hour and an average speed of about 40 km/h has been used to compare multiple measurement techniques and assess on-road air quality. It was found that observed daytime concentration levels of CO, NO<sub>x</sub>, NO<sub>2</sub>, O<sub>3</sub>, PM<sub>10</sub> and PM<sub>2.5</sub> are below current WHO health based guideline values, varying from a few percent (CO) to above 60% (O<sub>3</sub> and PM<sub>2.5</sub>) of the guideline values. NO<sub>2</sub> to NO<sub>x</sub> ratios were about a factor of two higher than measured in a previous tunnel study, which indicates that about half of measured NO<sub>2</sub> concentrations are due to urban background levels. Statistical analysis suggest that on-road NO<sub>2</sub> and ozone concentrations are largely driven by atmospheric chemistry processes, and not significantly affected by variation in local traffic volume and fleet mix. A significant positive weighted correlation ( $r = 0.71-0.74$ ) between remote sensing and air concentration monitoring is observed for CO in calm conditions. Speciated VOC measurements on the road show large discrepancies with current COPERT (Australia) vehicle emission factors, confirming the results from an earlier tunnel study. The weight of evidence suggests that the current (EU based) VOC speciation in COPERT Australia is likely not appropriate for the Australian on-road fleet.

**Keywords :** Motor vehicle, Emissions, Road traffic, On-road air quality, VOCs, Remote sensing, Tunnel, COPERT, Ozone, NO<sub>2</sub>.

---

## **Interactions between rainfall and fine particulate matter investigated by simultaneous chemical composition measurements in downtown Beijing**

**BingGao<sup>a</sup>, WeiOuyang<sup>a</sup>, HongguangCheng<sup>a</sup>, YiXu<sup>a</sup>, ChunyeLin<sup>a</sup>, JingChen<sup>ab</sup>**

**Source :** Atmospheric Environment, Volume 218, 1 December 2019, 117000

Rainfall can directly remove atmospheric pollutants through the below-cloud scavenging process, and the atmospheric particles also affect the chemical composition of rainfall. Therefore, the interactions between rainfall properties and fine particulate matter (PM<sub>2.5</sub>) need deep investigation. Based on simultaneous in situ measurements of PM<sub>2.5</sub> and rainfall samples during May–October in 2017 and 2018, their chemical composition dynamics and the relationship were identified. It was found that NO<sub>3</sub><sup>-</sup> and SO<sub>4</sub><sup>2-</sup> were predominant in PM<sub>2.5</sub>, whereas NO<sub>3</sub><sup>-</sup> and Ca<sup>2+</sup> were the main ionic species in rainfall. The characteristics of ions in rainfall and PM<sub>2.5</sub> showed that Beijing was heavily affected by mobile sources and by anthropogenic pollution. The PM<sub>2.5</sub> was most effectively removed from the

atmosphere by rainfall and the responses of the ionic compositions of PM<sub>2.5</sub> to the washing effect were much different. Simultaneously, PM<sub>2.5</sub> posed a significant impact on Ca<sup>2+</sup> and K<sup>+</sup> in rainwater. The effect of PM<sub>2.5</sub> 1 day before rain on the Ca<sup>2+</sup> in rainwater was more prominent than the effect of the chemical species in PM<sub>2.5</sub> on the day of the rainfall, while the trend was the opposite for K<sup>+</sup>. The key factors affecting the characteristics of ions in PM<sub>2.5</sub> and rainfall were rainfall amount, duration and relative humidity. The wind direction also have big impacts on NH<sub>4</sub><sup>+</sup>. The findings provide more scientific supports the rainfall pollution and PM<sub>2.5</sub> management in the urban.

**Keywords :** PM<sub>2.5</sub>, Rainwater, Washing effect, Correlation analysis, Diffuse pollution.

---

### **Mode-specific, semi-volatile chemical composition of particulate matter emissions from a commercial gas turbine aircraft engine**

**ZhenhongYu<sup>a</sup>, Michael T.Timko<sup>b</sup>, Scott C.Herndon<sup>a</sup>, Richard, C.Miake-Lye<sup>a</sup>, Andreas J.Beyersdorf<sup>c</sup>, Luke D.Ziemba<sup>d</sup>, Edward L.Winstead<sup>e</sup>, Bruce E.Anderson<sup>d</sup>**

**Source :** Atmospheric Environment, Volume 218, 1 December 2019, 116974

We measured and characterized semi-volatile chemical composition of particulate matter (PM) in aircraft engine exhaust plumes in a dedicated aircraft PM emission study (NASA's AAFEX 1 field measurement campaign). Mode-specific organic and sulfate components were observed with a compact time-of-flight aerosol mass spectrometer (C-ToF-AMS). Nitrate components in both the nucleation and soot mode particles were negligible. The organic composition for the nucleation mode particles decreases with increasing engine power. For the soot mode, organic fraction initially decreases with increasing engine power but then slightly increases again above 45% engine thrust, probably due to the increasing contribution from lubrication oil emissions. These results show that an appreciable amount of semi-volatile PM can be generated in the exhaust plumes from a commercial aircraft engine. Thus, volatile PM must be studied as carefully as non-volatile soot emissions to fully address local air quality and human health impacts of aviation.

**Keywords :** Aviation, Emission, Nucleation, Soot, Particulate matter, Chemical composition.

---

### **Source identification of personal exposure to fine particulate matter (PM<sub>2.5</sub>) among adult residents of Hong Kong**

**Xiao-CuiChen<sup>a</sup>, Tony J.Ward<sup>b</sup>, Jun-JiCao<sup>cd</sup>, Shun-ChengLee<sup>e</sup>, Ngar-CheungLau<sup>af</sup>, Steve HL.Yim<sup>af</sup>, Kin-FaiHo<sup>acgh</sup>**

**Source :** Atmospheric Environment, Volume 218, 1 December 2019, 116999

---

Epidemiological studies provide evidence of the harmful effects of source-specific fine particulate matter (PM<sub>2.5</sub>) on human health. Studies regarding relative contributions of multiple sources to personal exposure are limited and inconsistent. Personal exposure monitoring for PM<sub>2.5</sub> was conducted in 48 adult subjects (ages 18–63 years) in Hong Kong between June 2014 and March 2015. We identified seven sources of personal PM<sub>2.5</sub> exposure using Positive Matrix Factorization (PMF). These sources included regional pollution (associated with coal combustion and biomass burning), secondary sulfate, tailpipe exhaust, secondary nitrate, crustal/road dust, and shipping emission sources. For personal PM<sub>2.5</sub> exposure, one additional source related to individuals' activities was found: non-tailpipe pollution (characterized by Fe, Mn, Cr, Cu, Sr). We also applied principal component analysis (PCA) for PM<sub>2.5</sub> source identification. The results revealed similar factor/component profiles using PMF and PCA, with some discrepancies in the number of factors. PCA/absolute principal component scores (PCA/APCs) coupled with a linear mixed-effects model (LMM) was applied to the same dataset for source apportionment, adjusting for temperature and relative humidity. Furthermore, stratified PCA/APCs-LMM models were applied to estimate season- and group-specific source contributions of personal PM<sub>2.5</sub> exposure. A mixed source contributions of secondary sulfate, secondary nitrate, and regional pollution were shown (35.1–43.6%), with no seasonal or subject group differences ( $p > 0.05$ ). Shipping emissions were ubiquitous, contributing 6.3–8.8% of personal PM<sub>2.5</sub> exposure for all subjects. Tailpipe exhaust and traffic-related particles varied by season ( $p < 0.01$ ) and subject group ( $p < 0.05$ ). Caution should be taken when using source-specific PM<sub>2.5</sub> as proxies for the corresponding personal exposures in epidemiological studies.

**Keywords :** Personal fine particles exposure, Ambient air pollution, Positive matrix factorization, Principal component analysis/absolute principal component scores, Mixed-effects model.

---

## **Insights into the temporal and spatial characteristics of PM<sub>2.5</sub> transport flux across the district, city and region in the North China Plain**

**Hanyu Zhang Shuiyuan Cheng Sen Yao Xiaoqi Wang Chuanda Wang**

**Source :** Atmospheric Environment, Volume 218, 1 December 2019, 117010

The Beijing–Tianjin–Hebei (BTH) region in the North China Plain (NCP) is significantly affected by inter–district, city and region transport, but systematic works on this aspect using flux calculation method remain insufficient. To obtain further insights into the temporal and spatial characteristics of PM<sub>2.5</sub> flux, the Weather Research and Forecasting (WRF) model and the Comprehensive Air Quality Model with Extensions (CAMx) have been applied during January, April, July and October 2016. The results demonstrated that the modeling flux calculation method was suitable for investigating the evolutionary trend of PM<sub>2.5</sub> flux by comparing cross–district simulations and observations. The total of monthly inflow, outflow and net flux indicated the intensive interactions and prominent temporal

and spatial variations of PM<sub>2.5</sub> transport through the boundary segment of the district, city and region. The vertical distribution analysis of net flux shows that PM<sub>2.5</sub> net flux between target megacity/region and surroundings differed with the altitude, and the altitude at which its maximum intensity was closely related to neighboring areas and occurrence of month. Notably, three main transport pathways during four months have been identified based on the investigation of cross-city transport, namely the northwest-southeast (NW-SE) for January and April, the southeast-northwest (SE-NW) for July and October, the southwest-northeast (SW-NE) for all months, which were further confirmed by cross-region transport. Additionally, summer and winter monsoon have significant influences on the SE-NW and NW-SE pathway, respectively. Furthermore, this research draws upon a typical process of PM<sub>2.5</sub> haze episodes from 11 to 17 October in Beijing, Tangshan and Shijiazhuang, with the aim of demonstrating flux intensity variations in different stages of haze episodes. Overall, the evolution of flux intensity at the higher-altitude layer have similar pattern to that of lower-altitude layer, in which the former was approximately 2 times the latter. Furthermore, inter-city transport along the SW-NE pathway played a crucial role before reaching the most severe stage of pollution, while the local emissions were more conducive to forming heavy pollution extremes. Overall, flux intensity calculations provide scientific support to put forward effective joint control measures and acquire a better understanding of evolutionary mechanism of haze episodes in the NCP.

**Keywords :** WRF-CAMx, PM<sub>2.5</sub> flux, Transport pathway, Haze episodes, The North China Plain.

---

## **Black carbon and PM<sub>2.5</sub> monitoring campaign on the roadside and residential urban background sites in the city of Tehran**

**Ahmad Taheri Pourya Aliasghari Vahid Hosseini**

**Source :** Atmospheric Environment, Volume 218, 1 December 2019, 116928

Fine particulate matter characterized as PM<sub>2.5</sub> is the most important criteria air pollutant in the city of Tehran. Tehran is one of the most polluted cities of the Middle East based on annual mean PM<sub>2.5</sub> concentrations. Tehran emission inventory shows the large contribution of mobile sources to the total particles. PM<sub>2.5</sub> source apportionment studies show large fraction of black carbon (BC) in the total mass of PM<sub>2.5</sub>, especially during the cold seasons. BC is the product of incomplete combustion that is mainly derived from diesel engines and rich-burned gasoline carburetor engines on scooters and light-duty vehicles. The present study shows the results of a large experimental campaign in which BC concentration data along with PM<sub>2.5</sub> mass concentration data were collected at various sites in the city of Tehran for a period of a year. The effect of heavy-duty diesel vehicle traffic on fresh BC and on the mass fraction of BC to PM<sub>2.5</sub> was observed. Nearly 17% of total mass of PM<sub>2.5</sub> was identified as BC. During the night hours the BC/PM<sub>2.5</sub> mass ratio was increased to more than 4 times than that of day hours due to heavy-duty diesel traffic restrictions during the day. More detailed analyses based on absorption characteristics of

BC showed that by increasing heavy diesel vehicle traffic during the night hours, more fresh BC was collected compared to that of aged BC collected during the day time. A city wide temporary ban of heavy-duty diesel traffic during an air pollution episode resulted in a sudden reduction of BC concentration in Tehran air, while the total mass of PM<sub>2.5</sub> remained constant. This shows the direct contribution of diesel fleet to BC. It shows the necessity of introducing more accurate and relevant pollutant indicators such as BC mass instead of total PM<sub>2.5</sub> mass for better and more effective policies.

**Keywords :** Air quality, Black carbon, Diesel pollution, Particulate matter, Traffic, Tehran.

---

## **Age-specific seasonal associations between acute exposure to PM<sub>2.5</sub> sources and cardiorespiratory hospital admissions in California**

**KeitaEbisu<sup>a</sup>, BrianMaliga<sup>a</sup>, SinaHasheminassab<sup>b</sup>, ConstantinosSioutas<sup>b</sup>**

**Source :** Atmospheric Environment, Volume 218, 1 December 2019, 117029

Numerous studies have explored the relationships between short-term exposure to fine particulate matter (PM<sub>2.5</sub>) and morbidity. However, few studies have investigated which PM<sub>2.5</sub> sources and constituents contribute to the health associations, and even fewer studies are available which explored age or seasonal effect modification for the associations between PM<sub>2.5</sub> sources and health. We explored age-specific associations between short-term exposure to PM<sub>2.5</sub> chemical constituents and its sources, and hospital admissions in California. We linked hospital admission data (n = 1,679,094) with PM<sub>2.5</sub> chemical constituents and source apportionment data for eight sites in California for the period of 2002–2009. Site-specific source apportionment was conducted using Positive Matrix Factorization, and five PM<sub>2.5</sub> sources were commonly identified in most sites (biomass burning, soil, secondary ammonium nitrate, secondary ammonium sulfate, and vehicular emissions). Age-stratified Poisson time-series regression was conducted for each site, and the health risk estimates were combined to generate overall age-specific associations with cardiovascular- and respiratory-related hospital admissions. We further conducted seasonal interaction models to assess seasonal effect modification. An interquartile range increase in PM<sub>2.5</sub> vehicular emissions was associated with increased risk of cardiovascular-related hospital admission at lag 0 (1.32% [95% confidence interval (CI): 0.16, 2.49]) for elderly people (≥65 years old). Exposure to PM<sub>2.5</sub> vehicular emissions increased the risk of respiratory-related hospitalizations at lag 2 (3.58% [95% CI: 0.90, 6.33]) for children (0–18 years old). Risk estimates of PM<sub>2.5</sub> total mass, vehicular emissions, and its related constituents (e.g., iron) for respiratory admissions were higher in the warm season among children. Heterogeneous seasonal estimates were not observed for other age groups. Our results suggest that short-term exposures to several PM<sub>2.5</sub> sources and their related constituents are more harmful than exposures to other pollutants, particularly for children in summer. Identifying toxic sources is important for developing effective interventions and protecting susceptible populations.

**Keywords :** Fine particulate matter, PM<sub>2.5</sub> sources, Hospital admissions, Season, Children's health.

---

## **Primary particulate matter emissions and estimates of secondary organic aerosol formation potential from the exhaust of a China V diesel engine**

**HuaZhou<sup>ac</sup>, HongweiZhao<sup>a</sup>, JieHu<sup>b</sup>, MengliangLi<sup>c</sup>, QianFeng<sup>c</sup>, JingyuQi<sup>b</sup>, ShiZongbo<sup>df</sup>, HongjunMao<sup>be</sup>, TaoshengJin<sup>be</sup>**

**Source :** Atmospheric Environment, Volume 218, 1 December 2019, 116987

Vehicle emissions contribute to ambient particulate matter (PM) pollution directly via emissions of PM and indirectly by secondary aerosol formation, as a result of trace gas emissions. In this paper, we determined the emission factors of primary pollutants and estimated the secondary organic aerosol (SOA) formation potential of a China V heavy-duty diesel engine tested under ETC (European Transient Cycle) and ESC (European Stationary Cycle) with different types of fuels using an engine dynamometer. Volatile organic compounds (VOCs) emission factors were 55.7–121 mg/kwh, while primary PM emission factors were 15.0–26.8 mg/kwh. These values were substantially lower than those of older diesel vehicles that met pre-China V standards. Based on the SOA yields of the measured VOCs, the SOA formation potential of diesel engines were estimated to be 2.8–15.9 mg/kg fuel. The ratios of potential SOA/primary PM ranged from 0.07 to 0.16. We further showed that VOCs emission factors, SOA formation potential and the ratios of SOA/primary PM were highly dependent on the test cycle, whereas the primary PM emission factors on both test cycles and fuel quality.

**Keywords :** Vehicle emission, Secondary organic aerosol, Diesel particulate matter, Volatile organic compounds, Driving test cycles, Fuel quality.

---

## **Reducing PM<sub>2.5</sub> and secondary inorganic aerosols by agricultural ammonia emission mitigation within the Beijing-Tianjin-Hebei region, China**

**ZhilanYe<sup>a</sup>, XiuruiGuo<sup>a</sup>, LongCheng<sup>a</sup>, ShuiyuanCheng<sup>a</sup>, DongshengChen<sup>a</sup>, WenlinWang<sup>b</sup>, BoLiu<sup>c</sup>**

**Source :** Atmospheric Environment, Volume 219, 15 December 2019, 116989

The contribution to fine particulate air pollution (PM<sub>2.5</sub>) from ammonia emissions has been proven to be significant. In China, agricultural sources contribute to the majority of ammonia emissions. It is necessary and valuable to explore air quality improvements



caused by the mitigation of agricultural ammonia emissions. The purpose of this study was to quantify the reduction effects on PM<sub>2.5</sub> and secondary inorganic aerosols by performing air quality simulations based on the developed agricultural ammonia emission inventory at the county-level within the Beijing-Tianjin-Hebei (BTH) region. The results demonstrated that the total NH<sub>3</sub> emission in the BTH region was 1625.03 Gg in 2015. Livestock manure spreading represented 58% of the total emissions (941.79 Gg NH<sub>3</sub>), while synthetic fertilizer applications accounted for the remaining 42% of the emissions. Spatially, the agricultural ammonia emissions were generally distributed over the southern BTH regions (Handan and Shijiazhuang) due to the intensive agricultural activities in this area. Temporally, the agricultural ammonia emissions peaked during summer, consistent with variations in temperature and agricultural practices. Compared to the baseline scenario, the annual average PM<sub>2.5</sub> concentrations in the BTH region were reduced by 2.57%, 5.08%, and 5.71%, respectively, under the Progressive (NH<sub>3</sub> emission cut by 21.26%), Stringent (NH<sub>3</sub> emission cut by 45.58%), and Complex (NH<sub>3</sub> emission cut by 46.63%) scenarios. Moreover, under the same conditions, secondary inorganic aerosols such as sulfate, nitrate, and ammonium were alleviated by 2.94–6.85%, 3.45–17.9%, and 4.24–23.32%, respectively. The results confirmed that mitigating ammonia emissions could lead to the considerable reduction of nitrate, followed by ammonium. In contrast, the impact on sulfate was relatively limited. This study could provide helpful and reliable evidence to determine effective mitigation measures and control strategies for policy makers.

**Keywords :** Agricultural ammonia emission, Reduction effect, WRF-CMAQ, PM<sub>2.5</sub>, Secondary inorganic aerosols.

---

## **Numerical assessment of PM<sub>2.5</sub> and O<sub>3</sub> air quality in continental Southeast Asia: Baseline simulation and aerosol direct effects investigation**

**Giang Tran HuongNguyen<sup>ab</sup>, HikariShimadera<sup>a</sup>, KatsushigeUranishi<sup>a</sup>, TomohitoMatsuo<sup>a</sup>, AkiraKondo<sup>a</sup>, SarawutThepanondh<sup>c</sup>**

**Source :** Atmospheric Environment, Volume 219, 15 December 2019, 117054

An online coupled modeling system composed of Weather Research and Forecasting (WRF) model and Community Multiscale Air Quality (CMAQ) model was applied to assess aerosol direct effects on meteorology and air quality with the focus on particulate matter with an aerodynamic diameter of 2.5 μm or less (PM<sub>2.5</sub>) and ozone (O<sub>3</sub>) in Continental Southeast Asia. Comprehensive model evaluations demonstrated that the modeling system had the capacity to reproduce the observations, and could capture the temporal and spatial variations of temperature, radiation, humidity, wind speed, wind direction, PM<sub>2.5</sub> concentration, and O<sub>3</sub> concentration. The performance of the two-way online simulation was slightly better than that of the one-way online simulation. The aerosol direct effects on the meteorology and air quality were calculated by taking the differences between the

results of the two-way online simulation and the one-way online simulation. Over four target countries, namely Laos, Cambodia, Thailand, and Vietnam, the aerosol direct effects moderately decreased the shortwave radiation, temperature, planetary boundary layer (PBL) height, and wind speed by  $-10.98 \text{ W/m}^2$  ( $-5.17\%$ ),  $-0.21 \text{ }^\circ\text{C}$  ( $-0.85\%$ ),  $-27.25 \text{ m}$  ( $-6.13\%$ ), and  $-0.03 \text{ m/s}$  ( $-1.29\%$ ), respectively. These percentages were  $-17.80 \text{ W/m}^2$  ( $-7.71\%$ ),  $-0.39 \text{ }^\circ\text{C}$  ( $-1.67\%$ ),  $-48.33 \text{ m}$  ( $-8.89\%$ ), and  $-0.06 \text{ m/s}$  ( $-2.01\%$ ) during the dry season, and  $-4.31 \text{ W/m}^2$  ( $-2.22\%$ ),  $-0.03 \text{ }^\circ\text{C}$  ( $-0.12\%$ ),  $-6.71 \text{ m}$  ( $-1.92\%$ ), and  $-0.01 \text{ m/s}$  ( $-0.50\%$ ) during the wet season, respectively. Consequently, the meteorological response to direct effects led to changes in the ground-level PM<sub>2.5</sub> and O<sub>3</sub> concentrations. The PM<sub>2.5</sub> concentration was found to increase by  $+1.21 \text{ } \mu\text{g/m}^3$  ( $+5.36\%$ ) and the O<sub>3</sub> concentration was found to decrease by  $-0.40 \text{ ppb}$  ( $-1.26\%$ ) over the entire year. For each season, the PM<sub>2.5</sub> concentration increased by  $+2.09 \text{ } \mu\text{g/m}^3$  ( $+6.75\%$ ) during the dry season and  $+0.15 \text{ } \mu\text{g/m}^3$  ( $+1.42\%$ ) during the wet season. The O<sub>3</sub> concentration decreased by  $-0.96 \text{ ppb}$  ( $-2.41\%$ ) during the dry season and slightly increased by  $+0.13 \text{ ppb}$  ( $+0.55\%$ ) during the wet season. The direct effects were large during high PM<sub>2.5</sub> polluted periods and locations. A correlation matrix clarified that the increasing effect of aerosol on the PM<sub>2.5</sub> concentration was attributed to the decrease in the above-mentioned meteorological variables. The increase or decrease in the O<sub>3</sub> concentration depended on the responses of the atmospheric dynamics as well as the photolysis rates.

**Keywords :** Online coupled WRF-CMAQ model, Aerosol direct effects, Fine particulate matter, Ozone, Continental southeast asia.

---

## **A fast forecasting method for PM<sub>2.5</sub> concentrations based on footprint modeling and emission optimization**

**Mingyuan Yu Xuhui Cai Yu Song Xuesong Wang**

**Source :** Atmospheric Environment, Volume 219, 15 December 2019, 117013

We propose a method for fast forecasting of PM<sub>2.5</sub> concentrations in the North China Plain based on footprint (source–receptor relationship) modeling and emission inventory inversion. A backward Lagrangian stochastic particle dispersion model was employed to derive the footprint, using meteorological fields and boundary layer parameters provided by the WRF model. An analytical Bayesian inversion model was used to optimize existing emission inventories using long-term, multi-site PM<sub>2.5</sub> monitoring data. The fast simulation of PM<sub>2.5</sub> concentrations was based on the optimized inventory and the footprint results. Two-year simulations were carried out for six cities (Baoding, Beijing, Dezhou, Shijiazhuang, Tianjin, and Tangshan), with model establishment and emission inversion in the first year (2015) and test forecasting in the second year (2016). Promising simulation results were obtained even when using the primary emission inventory. For all six cities, the fractions of simulations of measurements within a factor of two ranged from 0.49 to 0.68, and the correlation coefficients ranged from 0.40 to 0.56 in 2015. The model



also well reproduced temporal variations in PM<sub>2.5</sub> concentrations in Beijing during severe haze episodes in the winter of 2015. Great improvement was achieved for the simulations by using the optimized emission inventory. The proportion of samples that met the PM model criteria increased from 88% to 97%, and the proportion that achieved the modeling goal increased from 25% to 44%. This method maintained its high forecasting skill in 2016, with 92% and 46% of samples meeting the PM model criteria and achieving the modeling goal, respectively. However, the corresponding values were 86% and 39% if emission optimization was not applied.

**Keywords :** PM<sub>2.5</sub> forecasting, Footprint model, Emission inventory, Inversion method.

---

#### 4. Atmospheric Research- 3.778

### Carbonaceous components and major ions in PM<sub>10</sub> from the Amazonian Basin

Danilo Custodio<sup>abc</sup>, Célia Alves<sup>b</sup>, Yendry Jomolca<sup>a</sup>, Pérolade Castro Vasconcellos<sup>a</sup>

**Source :** Atmospheric Research, Volume 215, 1 January 2019, Pages 75-84

Air pollution mainly resulting from deforestation and agricultural activities has become one of the major concerns in the Amazonian Basin. A detailed analysis of the PM<sub>10</sub> chemical composition is critical for devising pollution control measures and improving climate models. In this study, daily 24-h filter samples were collected and analyzed in different sites of the Amazon Basin between 2008 and 2016 (over 200 samples). The six sampling sites were classified into two groups, one in South Amazonia, a region with strong influence of land occupation, and another in a remote forest region to the North. The high mean concentrations of PM<sub>10</sub> and the occurrences of extreme events at the Southern site denote air pollution episodes. High correlations between the temporal trends of PM<sub>10</sub> and primary species linked to soil re-suspension and biomass burning highlight the contribution of these sources of air pollution in the region. Significant differences between PM<sub>10</sub> in the South and North regions were observed, for which levels of  $72.6 \pm 66.5 \mu\text{g m}^{-3}$  and  $8.9 \pm 4.2 \mu\text{g m}^{-3}$ , respectively. The average concentrations of organic carbon (OC) and elemental carbon (EC) in the aerosol were  $5.81 \pm 4.18 \mu\text{g m}^{-3}$ ,  $2.43 \pm 1.65 \mu\text{g m}^{-3}$  and  $5.17 \pm 5.54 \mu\text{g m}^{-3}$ ,  $0.51 \pm 0.41 \mu\text{g m}^{-3}$ , respectively, for the Southern and Northern Amazonia sampling sites. The aerosol was largely composed of inorganic species in Southern Amazonia, whose carbonaceous matter accounted for 16% of the gravimetrically measured PM<sub>10</sub>. However, in the forest region, the contribution of carbonaceous species, mainly OC, accounted for >90% and remained more constant throughout the seasons. Na<sup>+</sup> was the dominant water soluble ion in samples from the Southern region, followed by SO<sub>4</sub><sup>2-</sup>, NO<sub>3</sub><sup>-</sup>, Ca<sup>2+</sup> and K<sup>+</sup>. High levels of carbonate (CC) were also observed for these samples. For the Northern region, SO<sub>4</sub><sup>2-</sup> was the

dominant soluble ion, followed by  $K^+$  and  $NH_4^+$ . Some of these species exhibited a clear seasonal trend during the study period. This study provides a better understanding of the current state of air pollution in diversified Amazon basin sites.

**Keywords :** Amazon air pollution, Amazonia aerosol, Aerosol composition, Air quality, Atmospheric chemistry

---

## **Background concentrations of PMs in Xinjiang, West China: An estimation based on meteorological filter method and Eckhardt algorithm**

**YaqianWang<sup>a</sup>, JieqiongZhang<sup>a</sup>, ZhipengBai<sup>ab</sup>, WenYang<sup>b</sup>, HuiZhang<sup>a</sup>, JianMao<sup>a</sup>, YanLingSun<sup>a</sup>, ZhenxingMa<sup>a</sup>, JianXiao<sup>c</sup>, ShuangGao<sup>a</sup>, LiChen<sup>a</sup>**

**Source :** Atmospheric Research, Volume 215, 1 January 2019, Pages 141-148

Quantitative evaluation of background concentrations of pollutants in atmospheric field can help us implement effective measures to improve air quality. The aim of this study was to estimate background concentrations of PM<sub>10</sub> and PM<sub>2.5</sub> in Xinjiang using meteorological filter and the Eckhardt algorithm. In this study, the meteorological factors including wind direction, wind speed and temperature were used to filter the background periods. Results showed that annual average background concentrations of PM<sub>10</sub> and PM<sub>2.5</sub> in Xinjiang were 112  $\mu\text{g}/\text{m}^3$  and 39  $\mu\text{g}/\text{m}^3$  in 2016, respectively. There were seasonal differences on background concentrations of PMs in Northern and Southern Xinjiang, and the background concentrations in Southern Xinjiang were much higher than those in Northern Xinjiang. Background concentrations from easterly wind (49  $\mu\text{g}/\text{m}^3$  for PM<sub>10</sub> and 29  $\mu\text{g}/\text{m}^3$  for PM<sub>2.5</sub>) and westerly wind (179  $\mu\text{g}/\text{m}^3$  for PM<sub>10</sub> and 63  $\mu\text{g}/\text{m}^3$  for PM<sub>2.5</sub>) were the highest in Northern Xinjiang and Southern Xinjiang, respectively. Dust from Taklimakan Desert had great contribution to the background concentrations of PMs in Southern Xinjiang area. Good correlations were obtained when comparing the two methods. The differences of annual average background concentrations in Xinjiang between two methods were 9  $\mu\text{g}/\text{m}^3$  for PM<sub>10</sub> and 4  $\mu\text{g}/\text{m}^3$  for PM<sub>2.5</sub>. The estimated background concentrations by the proposed method can be used by local government to develop more efficient pollution control policies.

**Keywords :** Background concentration, PM<sub>10</sub> and PM<sub>2.5</sub>, Xinjiang, Meteorological filter method, Eckhardt algorithm.

---

## Comparing the impact of strong and weak East Asian winter monsoon on PM2.5 concentration in Beijing

ChaoWang<sup>ab</sup>, XingqinAn<sup>ab</sup>, PeiqunZhang<sup>c</sup>, ZhaobinSun<sup>d</sup>, MengCui<sup>e</sup>, LinMa

Source : Atmospheric Research , Volume 215, 1 January 2019, Pages 165-177

We investigate the relationship between the wintertime PM2.5 concentration in Beijing from 2005 to 2016 and the East Asian winter monsoon (EAWM) strength based on PM2.5 observations and the National Centers for Environmental Prediction/National Center for Atmospheric Research (NCEP/NCAR) reanalysis data. The large-scale atmospheric circulations are compared and the differences in spatial distribution and source areas of Beijing PM2.5 concentration are studied in depth combined with GRAPES-CUACE atmospheric chemistry model and its aerosol adjoint model in strong and weak EAWM years. The results show that the monthly Beijing PM2.5 concentration in winter is significantly anti-correlated with the individual EAWM indices of winter month. According to three EAWM indices, December 2014 and 2016 are selected as the representatives of strong and weak EAWM years for further comparison. In December 2014, the strong EAWM circulation was characterized by the strengthened subtropical westerly jet stream at 300 hPa, the deepened 500 hPa East Asian trough, the strengthened northwesterly wind at 850 hPa in North China, and the developed Siberian High. Conversely, these anomalous patterns in December 2016 were much weaker, resulting in lower boundary layer height, more stable atmosphere stratification and more frequent inversion. The simulated PM2.5 concentration in the northern and southern part of Beijing were affected by the EAWM to different extents, with the values of 55–75  $\mu\text{g}/\text{m}^3$  in the north and 95–125  $\mu\text{g}/\text{m}^3$  in the south. There was no obvious difference in the locations of sensitive source areas between December 2014 and 2016. However, compared to December 2014, the accumulated sensitivity coefficients of Beijing, Tianjin, Hebei and Shanxi sources at 72 h ahead of the objective time period were 2.2, 5.9, 1.6, and 1.4 times higher, and the key discharge period was 2.6 times longer in December 2016. The contributions of Beijing and Tianjin sources had greater increase rates, stressing the importance of sensitive source areas in the direction of southeast Beijing in weak EAWM year.

**Keywords :** PM<sub>2.5</sub>, East Asian winter monsoon (EAWM), Tracking source areas with adjoint model, Beijing.

---

## Natural and anthropogenic contributions to long-term variations of SO<sub>2</sub>, NO<sub>2</sub>, CO, and AOD over East China

HanqingKang<sup>ab</sup>, BinZhu<sup>ab</sup>, Ronald J.van der A<sup>bc</sup>, ChunmaoZhu<sup>bd</sup>, Gerritde Leeuwe<sup>e</sup>,  
XueweiHou<sup>ab</sup>, JinhuiGao<sup>ab</sup>

Source : Atmospheric Research, Volume 215, 1 January 2019, Pages 284-293

Concentrations of atmospheric pollutants over East China have varied considerably during the past decades. These variations are partly due to variations of human activities, e.g., increasing energy consumption and implementation of government emission control policies, and partly to natural fluctuations. This study aims to separate the effects of natural processes and anthropogenic activities on the increase/decrease of the concentrations of some of the most important pollutants (SO<sub>2</sub>, NO<sub>2</sub>, CO and aerosols) over East China in the last decade. This was achieved by the comparison of the temporal variations in long-term time series of satellite-retrieved aerosol optical depth (AOD) and vertical column densities (VCDs) of SO<sub>2</sub>, NO<sub>2</sub>, and CO, with those in model-simulated time series of the natural variations only. The latter were created by the use of the same anthropogenic emissions throughout the whole simulation, while using re-analysis data (MERRA) to describe meteorological processes and natural emissions. Thus, the comparison between observed and simulated temporal variations reveals the effects due to anthropogenic emissions only, assuming that the atmospheric processes affect natural and anthropogenic species in the same way. In the analysis, a Kolmogorov–Zurbenko (KZ) filter is used to extract long-term components from both the observed and simulated data and normalization to the situation at a certain reference point is used to eliminate bias between observations and simulations. By this new method, natural and anthropogenic contributions to long-term variations of trace gases and AOD are quantitatively estimated. The results show that NO<sub>2</sub> VCDs increased from 2004 to 2011 by 76% and of the overall increase in this period only 1% ± 1% was attributed to natural factors, 99% ± 1% attributed to anthropogenic factors. AOD increased by 24% between 2001 and 2011 and of the overall increase 24% ± 32% was due to natural factors and 76% ± 32% was due to anthropogenic factors. SO<sub>2</sub> VCDs decreased by 15% from 2007 to 2013, natural and anthropogenic factors contributed respectively 16% ± 14% and 84% ± 14% to the overall decrease in this period. CO decreased since 2003 with 13% and of the overall decrease 6% ± 6% was due to natural factors and 94% ± 6% was due to anthropogenic factors.

**Keywords :** Natural, Anthropogenic, Contribution, Pollutants, Long-term variation.

---

## **Atmosphere boundary layer height and its effect on air pollutants in Beijing during winter heavy pollution**

**YanXiang<sup>ab</sup>, TianshuZhang<sup>b</sup>, JianguoLiu<sup>b</sup>, LihuiLv<sup>ab</sup>, YunshengDong<sup>b</sup>, ZhenyiChen<sup>b</sup>**

**Source :** Atmospheric Research, Volume 215, 1 January 2019, Pages 305-316

Beijing is suffering from serious particulate matter pollution, and the atmosphere boundary layer (ABL) has important direct and indirect effects on human activities. This research analyzed the characteristics of the ABL in Beijing and discussed the impacts of meteorological factors on atmosphere boundary layer height (ABLH) during winter heavy pollution events in Beijing. The data observed by Mie lidar in the winter of 2014 to 2016 were used to estimate the ABLH by employing image edge detection. In addition, a weather

research and forecasting (WRF) model was used to simulate the meteorological field in the same period. Ground and vertical data indicated that the average ABLH decreased from 0.63 km to 0.53 km in three consecutive years. In addition, a significant negative correlation existed between ABLH and PM<sub>2.5</sub>, and the effect of low ABLH on the vertical diffusion capacity of pollutants was greater than that of high ABLH. Relative humidity was negatively correlated with ABLH, increasing during the three years at a rate of 61%. In the winter of 2014, the atmosphere was dominated by instability, which was beneficial to the development of ABL. In contrast, many stable stratifications occurred in the upper air during the winters of 2015 and 2016; however, these were not conducive to the development of ABL. The northwest wind decreased by 11.35% and the south wind increased by 11.41%. Moreover, the time of near-surface wind speed below 2 m s<sup>-1</sup> increased by 34.74%, and the frequency of occurrence above 4 m s<sup>-1</sup> decreased by 8.19%. The decrease in ground wind speed was unfavorable for the development of ABL. The sea level pressure remained at 1027.68 ± 17.32 hPa, and the ABLH was found to be generally positively correlated with sea level pressure.

**Keywords :** Atmosphere boundary layer height, Lidar, PM<sub>2.5</sub>, Meteorological factors, WRF model.

---

## **Consensus in climate classifications for present climate and global warming scenarios**

**Francisco J.TapiadorRaúlMorenoAndrésNavarro**

**Source :** Atmospheric Research, Volume 216, 1 February 2019, Pages 26-36

Climate classifications of climate models' outputs have been used to assess environmental changes but systematic analyses of the differences between models, scenarios and classification methods are scarce. Here, the results of applying the most commonly used climate classifications to the outputs of 47 Global Climate Models (GCM) of different physical parameterizations and varied grid size are presented. The extent and intensity of changes for present climate, three different Representative Pathways Scenarios (RCP26, RCP45 and RCP85) and three increasingly-fine classification methods show that there is a consensus between models, and that climate classifications are indeed useful tools to translate physical climatology variables into environmental changes. The main conclusions are that climate classifications can indeed be used to gauge model performance at several grid sizes and that the classification method does not decisively affects the potential global changes in future climates under increasing greenhouse gas emissions. The analyses also reveal that there are several uncertainties that are not attributable to model grid size or to

limitations in the reference datasets but more likely to deficiencies in the physics of the models.

**Keywords :** Amazon air pollution, Amazonia aerosol, Aerosol composition, Air quality, Atmospheric chemistry.

---

## **Sources and spatial distribution of PM<sub>2.5</sub>-bound polycyclic aromatic hydrocarbons in Zhengzhou in 2016**

**Qiang Li Nan Jiang Xue Yu Zhe Dong Shiguang Duan Leishi Zhang Ruiqin Zhang**

**Source :** Atmospheric Research, Volume 216, 1 February 2019, Pages 65-75

Atmospheric polycyclic aromatic hydrocarbons (PAHs) in PM<sub>2.5</sub> were analyzed in 2016 at five representative sites in Zhengzhou, China to determine their seasonal and spatial characteristics. The annual PM<sub>2.5</sub> concentration of all sites ( $114 \pm 85 \mu\text{g}/\text{m}^3$ ) was 2.3 times higher than the Chinese National Ambient Air Quality Standard (NAAQS) (annual standard:  $35 \mu\text{g}/\text{m}^3$ ). The total PAH level was highest at traffic site ( $46.2 \pm 21.4 \text{ ng}/\text{m}^3$ ), followed by urban center site ( $40.1 \pm 18.7 \text{ ng}/\text{m}^3$ ), industrial site ( $38.8 \pm 17.2 \text{ ng}/\text{m}^3$ ), urban site ( $37.8 \pm 10.3 \text{ ng}/\text{m}^3$ ) and background site ( $34.0 \pm 19.4 \text{ ng}/\text{m}^3$ ) with an annual concentration of  $39.1 \pm 17.6 \text{ ng}/\text{m}^3$  for all sites. The seasonal variation was in the order of winter > autumn > spring > summer. Among 16 PAHs, BbF, Ind, BkF, Chry, and BghiP were more abundant species with an integral trend of 5–6 rings > 4 rings > 2–3 rings. The annual BaP concentration ( $2.1 \text{ ng}/\text{m}^3$ ) exceeded the limit of the annual average BaP ( $1.0 \text{ ng}/\text{m}^3$ ) given by the NAAQS, and the BaP<sub>eq</sub> concentration was at a high level, which indicated a severe health risk of PAHs. The incremental lifetime cancer risk results showed that the risk level was acceptable level in the study area. Diagnostic ratios analysis demonstrated that PAHs in the study area were produced by the common outcome of the fossil fuel, petroleum, biomass, and coal combustions. Four sources determined by positive matrix factorization were coal combustion, motor vehicles, biomass burning, and industry, which respectively accounted for 37.9%, 26.9%, 19.7% and 15.4% of the annual total PAHs in Zhengzhou. The contribution of motor vehicles/aircraft fuel source was the highest at the traffic site (29.7%) and the contribution of industry was higher at industrial site (21.4%). The contribution of biomass burning in autumn was greater than that in other seasons because open burning of straws increased during harvest season while the contribution of coal combustion increased in winter due to concentrated heating.

**Keywords :** PM<sub>2.5</sub>, PAHs, Health risk, Diagnostic ratios, PMF.

---

## **Open cut black coal mining: Empirical verification of PM<sub>2.5</sub> air emission estimation techniques**

**ClaireRichardson<sup>a</sup>, ShannonRutherford<sup>b</sup>, Igor E.Agranovski<sup>a</sup>**

**Source :** Atmospheric Research, Volume 216, 1 February 2019, Pages 151-159

There is a paucity of empirical data relating to PM<sub>2.5</sub> emissions from open cut coal mines. Availability of high quality emission data is fundamental to the completion of robust analyses of the potential future impacts of particulate emissions from open cut coal mining operations. This study presents PM<sub>2.5</sub> emission rates determined on the basis of empirical data from open cut coal mining operations located in two regions of Australia. These data are used to validate the currently adopted PM<sub>2.5</sub> emission estimation methodologies, which are based on total suspended particulate measurements adjusted for PM<sub>2.5</sub> size fraction. The emission rates determined in this study demonstrate that regional differences between emission rates may be significant for specific activities. Measured average PM<sub>2.5</sub> emission rates are compared to rates calculated using existing available emissions estimation methodologies. This reveals that for dragline operation and coal dumping there are significant differences between the measured emission rates and emission rates calculated using currently available methodologies. This study identifies that the existing adopted US EPA and Australian emissions estimation methods for PM<sub>2.5</sub> emissions from coal haul routes, which are one of the most significant sources of PM<sub>2.5</sub> emissions at open cut mines, are reliable if the surface moisture content and dust control watering regimes are appropriately accounted for. The Australian estimation method is also considered reliable for overburden haul routes, however the US EPA method over predicts the measured PM<sub>2.5</sub> emission rate by a factor of 3.

Further, the study highlights that there is a high degree of inherent uncertainty in empirically derived emissions estimates for fugitive dust sources of this type. This uncertainty should be considered when completing emissions calculations, particular where these estimations are subsequently the basis for impact assessment and health risk analysis.

**Keywords :** Open cut mining, Air quality, PM<sub>10</sub> emission, PM<sub>2.5</sub> emission.

---

## **Variation tendency of pollution characterization, sources, and health risks of PM<sub>2.5</sub>-bound polycyclic aromatic hydrocarbons in an emerging megacity in China: Based on three-year data**

**NanJiang Liping LiShanshan WangQiang LiZhe Dong Shiguang Duan RuiqinZhang ShengliLi**

**Source :** Atmospheric Research, Volume 217, 1 March 2019, Pages 81-92

In this study, a total of 180 PM<sub>2.5</sub> samples were collected from December 3, 2013 to October 20, 2016 in an urban area in Zhengzhou, China, and 16 polycyclic aromatic hydrocarbons (PAHs) in PM<sub>2.5</sub> were analyzed. Diagnostic ratio and positive matrix factorization (PMF) were used for annual PAH source identification, and health risks and source regions of PM<sub>2.5</sub>-bound PAHs were also investigated. Results showed high pollution levels of PM<sub>2.5</sub>, in which all annual average concentrations substantially exceeded the Chinese standard. Although the PAH concentrations exhibited an evident decreasing trend, PAH pollution remained serious, especially in winter. Combustion, particularly coal combustion and vehicle emission, which were relative sources of 4–5-ring PAHs, played important roles in PAH pollution associated with PM<sub>2.5</sub> by diagnostic ratios. PMF results showed that coal combustion had the highest contribution to PM<sub>2.5</sub>-bound PAHs at 39.6%, 39.6%, and 42.6% and traffic at 29.3%, 25.4%, and 27.9% in 2014–2016, respectively. Biomass burning and coking plants were also important sources of PAHs in PM<sub>2.5</sub>, with an average contribution of 16.4% ± 1.3% and 15.4% ± 3.5%, respectively. The surrounding region in Henan Province was the key potential source area for PM<sub>2.5</sub>. However, the northwest and adjoining regions of Zhengzhou were the vital potential sources for PAHs during the entire study period. The concentration levels of benzo[*a*]pyrene (BaP),  $\sum_{16}\text{PAHs}_{\text{TEQ}}$ , and carcinogenic PAHs remained high, especially for BaP, which had an annual concentration (1.9–5.5 ng/m<sup>3</sup>) that was considerably higher than the Chinese standard. Carcinogenic risks existed in the order of ingestion > dermal absorption > inhalation and adults > children > seniors > adolescents (except for naphthalene). The risk for females was slightly high, and no remarkable non-carcinogenic risk from PAHs were found.

**Keywords :** PM<sub>2.5</sub>-bound PAH, Diagnostic ratio, Positive matrix factorization, Carcinogenic risk, Potential source contribution function.

---

## **Characteristics of gaseous and particulate ammonia and their role in the formation of secondary inorganic particulate matter at Delhi, India**

**Saraswati<sup>ab</sup>, S.K.Sharma<sup>ab</sup>, MohitSaxena<sup>c</sup>, T.K.Mandal<sup>ab</sup>**

**Source :** Atmospheric Research, Volume 218, 1 April 2019, Pages 34-49

Chemical characteristics of ambient ammonia (NH<sub>3</sub>), other trace gases (NO, NO<sub>2</sub>, SO<sub>2</sub>, and HNO<sub>3</sub>) and ionic species (NH<sub>4</sub><sup>+</sup>, SO<sub>4</sub><sup>2-</sup>, NO<sub>3</sub><sup>-</sup> and Cl<sup>-</sup> etc.,) of PM<sub>2.5</sub> were estimated from January 2013 to December 2015 at an urban site of Delhi, India to evaluate the role of ambient NH<sub>3</sub> in the formation of secondary inorganic aerosols over Delhi. The average mixing ratios of ambient NH<sub>3</sub>, NO, NO<sub>2</sub>, SO<sub>2</sub> and HNO<sub>3</sub> were recorded as 19.6 ± 3.5 (ppb),



20.4 ± 6.2 (ppb), 19.7 ± 5.3 (ppb), 1.7 ± 0.5 (ppb) and 1.2 ± 0.3 (ppb), respectively during the entire study period. The mixing ratios of NH<sub>3</sub>, other trace gases (SO<sub>2</sub>, NO and NO<sub>2</sub>) and ionic species of PM<sub>2.5</sub> were recorded higher during winter season (except HNO<sub>3</sub>). The result reveals that the increased relative humidity (RH) during winter season plays a major role in the formation of NH<sub>4</sub><sup>+</sup> aerosol over the observational site of Delhi. The annual average concentration of total water soluble inorganic ionic components (WSIC) in PM<sub>2.5</sub> was 69.1 ± 38.1 μg m<sup>-3</sup> accounting for ~60% of PM<sub>2.5</sub> concentration. The secondary aerosol components i.e. NH<sub>4</sub><sup>+</sup>, SO<sub>4</sub><sup>2-</sup>, NO<sub>3</sub><sup>-</sup> and Cl<sup>-</sup> shared the largest part of the total water soluble ions (61%) and PM<sub>2.5</sub> concentration (36%). Among the secondary inorganic aerosol components in PM<sub>2.5</sub>, SO<sub>4</sub><sup>2-</sup> was the most abundant component followed by NO<sub>3</sub><sup>-</sup> and Cl<sup>-</sup>. Ion balance and molar equivalent ratios indicated that the sufficient amount of NH<sub>4</sub><sup>+</sup> was available to neutralize SO<sub>4</sub><sup>2-</sup>, NO<sub>3</sub><sup>-</sup> and Cl<sup>-</sup> in the winter season followed by summer and monsoon seasons. The formation of NH<sub>4</sub>NO<sub>3</sub> was higher in winter due to low temperature and high humid conditions that drives the reaction between NH<sub>3</sub> and HNO<sub>3</sub> in forward direction.

**Keywords :** Trace gases, Mixing ratio, Ion-balance, Precursor gases, Seasonal variation.

---

## **Weekly cycle assessment of PM mass concentrations and sources, and impacts on temperature and wind speed in Southern Italy**

**Maria Rita Perrone<sup>a</sup>, Roberta Vecchi<sup>b</sup>, Salvatore Romano<sup>a</sup>, Silvia Becagli<sup>c</sup>, Rita Traversi<sup>c</sup>, Fabio Paladini<sup>a</sup>**

**Source :** Atmospheric Research , Volume 218, 1 April 2019, Pages 129-144

A methodology to detect the weekly cycle impact of the particulate matter (PM), and PM sources on the near surface temperature and wind speed is discussed in the paper. Chemically-specified PM<sub>10</sub> and PM<sub>2.5</sub> samples are analyzed to detect the weekly cycle of both the PM mass concentrations and the PM sources identified by the Positive Matrix Factorization technique. The average percent departure (APD) of the PM mass concentration from the mean value calculated for each day of the week shows that a positive (higher values during midweek) and a negative (higher values during weekend) weekly cycle characterizes the PM<sub>10</sub> and PM<sub>2.5</sub> mass concentrations in Autumn-Winter (AW, September–February) and Spring-Summer (SS, March–August), respectively. The westerly transport of pollution seems to have a role on the negative PM weekly cycle found in SS. The analysis of the six identified aerosol sources indicates that in SS the mixed anthropogenic and the reacted dust sources likely impact the PM<sub>10</sub> negative weekly cycle and that the mixed anthropogenic source likely impacts the PM<sub>2.5</sub> negative weekly cycle. The mixed anthropogenic and soil dust sources likely affect in AW the positive weekly cycle of the PM<sub>10</sub> mass concentration. Both sources in addition to the reacted dust source seem to affect the PM<sub>2.5</sub> mass concentration in AW. The APD analysis of the temperature (T) and wind speed (WS) at the surface from measurements co-located in space and time with the

PM ones reveals that the WS and T values are characterized by a negative weekly cycle in AW. Conversely, in SS, the WS-APD value decreases on Sunday and the T-APD values increase in the second half of the week. These last results likely give evidence of the PM impact on the near-surface temperature and wind speed

**Keywords :** Weekly cycles, PM mass concentration, Temperature and wind speed, Positive Matrix Factorization, Long-range transport.

---

## Temporal distribution and source apportionment of PM<sub>2.5</sub> chemical composition in Xinjiang, NW-China

YusanTurap<sup>a</sup>, DilinuerTalifu<sup>a</sup>, XinmingWang<sup>b</sup>, AbulikemuAbulizi<sup>a</sup>,  
MailikezhatiMaihemuti<sup>a</sup>, YalkunjanTursun<sup>a</sup>, XiangDing<sup>b</sup>, TuergongAierken<sup>a</sup>,  
SuwubinuerRekefu<sup>a</sup>

**Source :** Atmospheric Research , Volume 218, 1 April 2019, Pages 257-268

Daily fine particulate matter samples were collected in Dushanzi district within four months from September 2015 to August 2016 and represent the four seasons. The samples were determined for major chemical components in PM<sub>2.5</sub>, including elements, water-soluble ions (WSIs) and the organic/elemental carbon (OC/EC). The results indicated that the annual mean PM<sub>2.5</sub> concentration was  $62.85 \pm 43.5 \mu\text{g m}^{-3}$  in the Dushanzi district, with the highest seasonal average in winter ( $95.47 \pm 61.7 \mu\text{g m}^{-3}$ ) and the lowest in summer ( $33.22 \pm 17.7 \mu\text{g m}^{-3}$ ). The crustal elements were the most abundant elements and accounted for 96.51% of the total analyzed elements. Carcinogenic metals, such as Cr, Pb, As and Cd, originated from human activity, especially during winter. The highest total WSI concentration was  $68.99 \mu\text{g m}^{-3}$  in winter, followed by autumn ( $16.32 \mu\text{g m}^{-3}$ ), spring ( $10.23 \mu\text{g m}^{-3}$ ) and summer ( $7.06 \mu\text{g m}^{-3}$ ). SO<sub>4</sub><sup>2-</sup>, NO<sub>3</sub><sup>-</sup> and NH<sub>4</sub><sup>+</sup> were the most abundant WSIs in Dushanzi. Ion balance calculations showed that PM<sub>2.5</sub> in winter was acidic; in autumn and spring alkaline; and in summer nearly neutral. Total carbonaceous aerosol (TCA) accounted for 34% of the PM<sub>2.5</sub>. The chemical mass closure (CMC) indicated that minerals and WSIs were the major fraction, accounting for 33.58% and 23.17% of PM<sub>2.5</sub> mass concentration, respectively. Dushanzi was controlled by four major air masses, and the relative contributions of these air masses differ by season. Positive matrix factorization (PMF) analysis identified six sources including vehicle emission, biomass burning, coal combustion, industrial pollution, secondary aerosols and soil dust, with annual mean contributions of 9.43%, 10.86%, 18.45%, 12.15%, 18.26% and 30.85%, respectively. Moreover, the relative contributions of these identified sources varied significantly with the changing seasons.

**Keywords :** Fine particulate matter, Chemical composition, Hysplit trajectory model, Sources apportionment.

## **Characterization of individual particles and meteorological conditions during the cold season in Zhengzhou using a single particle aerosol mass spectrometer**

**ShenboWang<sup>a</sup>, BingHe<sup>b</sup>MinghaoYuan<sup>b</sup>, FangchengSu<sup>a</sup>, ShashaYin<sup>a</sup>, QisheYan<sup>a</sup>,  
NanJiang<sup>a</sup>, RuiqinZhang<sup>a</sup>, XiaoyanTang<sup>a</sup>**

**Source :** Atmospheric Research, Volume 219, 1 May 2019, Pages 13-23

To investigate the formation of haze during the cold season, continuous ambient air measurements were taken at an urban site in Zhengzhou from October 10, 2016 through December 31, 2016 using a single particle aerosol mass spectrometer. In total, 4,099,800 particles were analyzed and classified into eight major particle types: elemental carbon (EC, 36.7%), organic carbon (OC, 30.0%), ECOC (8.6%), K-rich (13.0%), levoglucosan (1.2%), metal (2.2%), NH<sub>4</sub>-K (2.1%), and dust (6.2%). By combining these measurements with correlation analysis and wind data, particle sources were determined to be vehicles, industrial emissions, coal combustion, biomass burning, secondary aerosols, agriculture, and dust. Additionally, analysis of mixing states indicated that particles underwent substantial aging and secondary OC particles were dominant OC species. Temporal profiles of meteorological parameters, mixing states, and particle types during a typical haze episode revealed that EC and OC particles were dominant components during haze formation, and a northeastern transport route (Anyang-Zhengzhou and Puyang-Xuchang) for OC particles was identified by potential source contribution function and concentration weighted trajectory analysis. Relatively higher humidity and lower temperature favored the formation of secondary inorganic aerosol. Wind direction and speed determined the transport, formation, and elimination of stagnant weather conditions.

In sum, heavy haze during the cold season in Zhengzhou was observed due to extensive aerosol aging under adverse weather conditions (i.e., northeastern wind direction, wind speed <2 m s<sup>-1</sup>, temperature < 10 °C, relative humidity >60%, temperature inversion, and uniform pressure field).

**Keywords :** Single particles, SPAMS, Mixing states, Formation mechanisms, Heavy haze.

---

## **Long-term variations of the PM<sub>2.5</sub> concentration identified by MODIS in the tropical rain forest, Southeast Asia**

**YiningMa<sup>ab</sup>, JinyuanXin<sup>bc</sup>, WenyuZhang<sup>a</sup>, ZiruiLiu<sup>b</sup>, YongjingMa<sup>ab</sup>, LingbinKong<sup>ab</sup>,  
YuesiWang<sup>b</sup>, YunDeng<sup>d</sup>, ShuhengLin<sup>e</sup>, ZhimingHe<sup>f</sup>**

**Source :** Atmospheric Research, Volume 219, 1 May 2019, Pages 140-152

Aerosol and particulate matter are playing significant roles in the regional climate and environment in the tropical rain forest of Southeast Asia. Both satellite and ground observations showed significant seasonal variations in the PM<sub>2.5</sub> concentration and the aerosol optical properties during 2012–2014 in the Xishuangbanna tropical rain forest. The annual mean values of the PM<sub>2.5</sub>, aerosol optical depth (AOD), and the Ångström exponent ( $\alpha$ ) were  $34.3 \pm 19.7 \mu\text{g}\cdot\text{m}^{-3}$ ,  $0.54 \pm 0.37$ , and  $1.36 \pm 0.20$  in the dry season and  $16.90 \pm 5.08 \mu\text{g}\cdot\text{m}^{-3}$ ,  $0.37 \pm 0.10$ , and  $1.07 \pm 0.25$  in the wet season, respectively. The results showed that 46.9% and 56.5% of the moderate-resolution imaging spectroradiometer (MODIS) C6 AOD data met the NASA accuracy requirements in the dry and wet season respectively and 17.1% and 17.7% of the seasonal mean systematically underestimated the ground-based data. There was a high correlation between PM<sub>2.5</sub> and AOD. The range of the correlation coefficient (R<sup>2</sup>) was 0.69–0.85 in the dry season and 0.33–0.39 in the wet season. Linear regression functions of PM<sub>2.5</sub> and MODIS AOD were developed and used to retrieve the spatial and temporal distributions of the PM<sub>2.5</sub> in the tropical rain forest over the last decade (2006–2015). The annual mean PM<sub>2.5</sub> increased slightly in the region. The range of the PM<sub>2.5</sub> was 20–40  $\mu\text{g}\cdot\text{m}^{-3}$  in the wet season and 25–80  $\mu\text{g}\cdot\text{m}^{-3}$  in the dry season. In northern Thailand, northern Vietnam and the central district of Laos, PM<sub>2.5</sub> was up to the range of 50–80  $\mu\text{g}\cdot\text{m}^{-3}$ , which was mainly attributed to biomass burning in these areas.

**Keywords :** PM<sub>2.5</sub>, Aerosol optical depth (AOD), MODIS, Biomass burning, The tropical rain forest, Southeast Asia.

---

## **Impacts of urban expansion on fog types in Shanghai, China: Numerical experiments by WRF model**

**YingGu<sup>a</sup>, HiroyukiKusaka<sup>b</sup>, Van QuangDoan<sup>c</sup>, JianguoTan<sup>d</sup>**

**Source :** Atmospheric Research, Volume 220, 15 May 2019, Pages 57-74

Fog is a hazard to transportation activities in Shanghai, China, but it is not known how this fog is influenced by urban expansion. Here we use a numerical model to run, for the first time for Shanghai, sensitivity experiments of the fog response to urban expansion, including the changes of land use and anthropogenic heat. Instead of using ‘fog days’ as a measure, we use the 29-year (1989–2017) meteorological observations of fog events at Hongqiao International Airport in central Shanghai, and classify the fog into radiation, advection, advection–radiation, and precipitation types. The results show that (1) Fog events generally decrease over these 29 years, with the decline in winter accounting for 50.2% of the total reduction. (2) Radiation fog decreases the most, but remains the most common type throughout the period. (3) Numerical sensitivity experiments show that the urban expansion in the past 29 years caused both an increase in surface air temperature and a decrease in water-vapor mixing ratio, resulting in a decrease in relative humidity and an increase in visibility for radiation fog. (4) For advection fog, the increased surface air

temperature allowed an increase in water-vapor mixing ratio, but a decrease in liquid water. (5) Due to warmer near-surface air, the inversion layer weakened. Hence, urban expansion in Shanghai has reduced the amount of not only radiation fog, but also advection fog.

**Keywords :** Urban expansion, WRF, Climatological characteristics, Fog event, Fog type, Shanghai.

---

## **Comparing mountain breezes and their impacts on CO<sub>2</sub> mixing ratios at three contrasting areas**

**C.RománCascón<sup>ab</sup>, C.Yagüe<sup>a</sup>, J.A.Arrillaga<sup>a</sup>, M.Lothon<sup>b</sup>, E.R.Pardyjak<sup>c</sup>, F.Lohou<sup>b</sup>, R.M.Inclán<sup>d</sup>, M.Sastre<sup>a</sup>, G.Maqueda<sup>a</sup>, S.Derrien<sup>b</sup>, Y.Meyerfeld<sup>b</sup>, C.Hang<sup>ce</sup>, P.Campargue-Rodríguez<sup>b</sup>, I.Turki<sup>b</sup>**

**Source :** Atmospheric Research, Volume 221, 1 June 2019, Pages 111-126

This work presents the characterisation and comparison of daytime and nighttime mountain breezes observed at three sites through the analysis of tower data. The sites are located: (i) in the foothills of the Guadarrama Mountains in Spain, (ii) on a plateau adjacent to the Pyrenees in France, and (iii) in the Salt Lake Valley (SLV) in the southwest of the United States. The thermally-driven winds are detected through a systematic algorithm which considers both synoptic and local meteorological conditions. The characteristics of the mountain breezes depend on the scale of the breeze at each site. Nighttime events are associated with stronger wind speeds at the two sites located farther away from the mountains due to larger-scale phenomena (valley winds and mountain-plain winds). The arrival of both nighttime and daytime flows to the sites are observed approximately when the buoyancy heat flux changes sign, being a few hours delayed at the sites farther from the mountains.

In addition, the impacts of these breezes on CO<sub>2</sub> mixing ratios are analysed. The characteristic increase of CO<sub>2</sub> mixing ratio observed during the evening transition takes place approximately when the nocturnal breeze arrives at the site. Nonetheless, both processes are not always simultaneous, indicating that CO<sub>2</sub> advection is not the main mechanism controlling the drastic CO<sub>2</sub> increase. An analogous result is obtained for the CO<sub>2</sub> decrease at the morning transition. However, we have found that the CO<sub>2</sub> mixing ratio is sensitive to wind direction (horizontal advection) in highly heterogeneous areas like the SLV, where CO<sub>2</sub> emissions from the nearby city centre play an important role.

Finally, a clear relationship is found between the CO<sub>2</sub> mixing ratio and near-surface turbulence at night. Maximum CO<sub>2</sub> mixing ratios are found for specific turbulence thresholds, which depend on the height of the CO<sub>2</sub> sensor. Conditions associated with both stronger and weaker turbulence levels lead to reduced CO<sub>2</sub> mixing ratios at the local measurement height due to excessive and ineffective mixing, respectively.

**Keywords :** Thermally-driven flows, Downslope, Upslope, CO<sub>2</sub>, Advection, Turbulent mixing.

---

## **Regional CO emission estimated from ground-based remote sensing at Hefei site, China**

**ChanggongShan<sup>ab</sup>, WeiWang<sup>b</sup>, ChengLiu<sup>bcd</sup>, YouwenSun<sup>b</sup>, QihouHu<sup>b</sup>, XingweiXu<sup>b</sup>, YuanTian<sup>b</sup>HuifangZhang<sup>b</sup>, IsamuMorino<sup>e</sup>, David W.T.Griffith<sup>f</sup>, Voltaire A.Velazco<sup>f</sup>**

**Source :** Atmospheric Research, Volume 222, 1 July 2019, Pages 25-35

Carbon monoxide (CO) is regarded as a useful tracer of biomass burning and anthropogenic pollution, so CO measurements can provide valuable information about the intensity of various anthropogenic activities. However, the emission estimates of CO based on inventories are associated with high uncertainties, especially in China. As CO is co-emitted with CO<sub>2</sub> in the combustion of carbonaceous fuels, the relationship between CO and CO<sub>2</sub> is often used to estimate regional CO emissions. Hefei is located in the area of eastern central China, which is one of the most industrialized regions in China, with severe regional air pollution. The enhancement slopes of  $\Delta\text{CO}$  to  $\Delta\text{CO}_2$  were calculated and compared from ground-based remote sensing observations, surface in-situ measurements, satellite and emission inventory data at the Hefei site during the period from September 2015 to August 2017. Both inventory based ratios of  $\Delta\text{CO}$  to  $\Delta\text{CO}_2$  are significantly larger than the ratios based on the observation data, including Fourier Transform Spectrometer (FTS) data, in-situ data, and satellite data. Further the CO emissions in the central China were estimated from the enhancement slopes of  $\Delta\text{CO}/\Delta\text{CO}_2$  combined with the CO<sub>2</sub> emission inventory. The CO emission estimated from the ground-based FTS observations and the Peking University (PKU) inventory based CO<sub>2</sub> emission is about  $10.96 \pm 0.88$  and  $11.95 \pm 0.71$  Tg CO yr<sup>-1</sup> during the 2015–2016 and the 2016–2017 period, respectively. The CO emission estimated from the ground-based FTS observations and the Emission Database for Global Atmospheric Research (EDGAR) inventory based CO<sub>2</sub> emission is about  $11.27 \pm 0.91$  and  $12.35 \pm 0.74$  Tg CO yr<sup>-1</sup>, respectively. So the CO emissions estimated from the ground-based FTS data and the different inventory based CO<sub>2</sub> emission show a good agreement. However, CO emissions derived from FTS data are substantially lower than those calculated directly from the inventories, i.e. there is a large difference between CO emissions derived from FTS and CO emissions directly derived from the two inventories. The phenomenon suggests that the emission inventories greatly overestimate the actual CO emission in the study area. This study estimates the regional CO emissions from ground-based remote sensing observations and investigates how much the difference is between the emissions from inventories and ground-based measurements.

---

## **Characterizing the regional contribution to PM<sub>10</sub> pollution over northern France using two complementary approaches: Chemistry transport and trajectory-based receptor models**

**E.Potier<sup>ac</sup>, A.Waked<sup>b</sup>, A.Bourin<sup>b</sup>, F.Minvielle<sup>a</sup>, J.C.Péré<sup>a</sup>, E.Perdrix<sup>b</sup>, V.Michoud<sup>bd</sup>, V.Riffault<sup>b</sup>, L.Y.Alleman<sup>b</sup>, S.Sauvage<sup>b</sup>**

**Source :** Atmospheric Research, Volume 223, 15 July 2019, Pages 1-14

Atmospheric pollution is a striking regional issue for public health and ecosystems and has major global impacts on climate. Particulate matter (PM) can be of primary or secondary origin and its sources, both natural and anthropogenic, are very heterogeneous in space and time. Hence, many efforts have been made worldwide to get a better knowledge of PM sources, in order to set effective reduction strategies. To this end, several distinct approaches may be used among which: (i) the localization of potential source areas with trajectory-based statistical receptor models (TRMs) which combine PM concentrations observed at receptor sites with computed back trajectories (BTs) of air masses, and (ii) the estimation of PM source contribution and chemical speciation with deterministic chemistry transport models (CTMs) based on emission inventories and detailed chemistry-transport processes. This study aims at testing the coherence between two independent approaches, CTMs and TRMs, for the geographical localization of the sources impacting a region of study. The case study refers to PM<sub>10</sub> pollution in the Hauts-de-France region (HdF) in the North of France for the year 2010. The considered TRMs are multi-site Concentration Field (CF) and Potential Source Contribution Function (PSCF) applied to 12 receptor sites using the Zefir package. The considered CTM is CHIMERE using detailed EDGAR European emission data. First, TRMs showed that some given far-located European countries (named “Far-East” countries) could have a strong but infrequent impact on PM<sub>10</sub> levels in the study region, while some given nearer European countries (named “Near-East” countries) had a frequent and predominant impact. Then, the contributions of each of these TRM-highlighted regions to PM<sub>10</sub> concentrations over the study area were analyzed by CHIMERE simulations. The potential influence of another non TRM-highlighted region (i.e. the “British Isles”) was also studied for comparison. The CTM results confirmed the prevalence of the Near-East source area in terms of mass contribution throughout the year and particularly during high-concentration periods. Therefore results obtained from CHIMERE CTM and multi-site CF and PSCF TRMs showed consistency, highlighting the interest for further comparison of both CTMs and TRMs independent approaches in other regions as well as for other pollutants.

**Keywords :** CHIMERE, Receptor model, PSCF, Concentration field, PM<sub>10</sub> sources.

---

## **C-Sr-Pb isotopic characteristics of PM2.5 transported on the East-Asian continental outflows**

**Chien-ChengJung<sup>a</sup>, Charles C.-K.Chou<sup>a</sup>, Chuan-YaoLin<sup>a</sup>, Chuan-ChouShen<sup>bc</sup>, Yu-ChiLin<sup>a</sup>, Yi-TangHuang<sup>a</sup>, Chao-YangTsai<sup>a</sup>, Pei-HsuanYao<sup>bc</sup>, Ci-RongHuang<sup>bc</sup>, Wei-RuHuang<sup>a</sup>, Mei-JuneChen<sup>a</sup>, Shu-HuiHuang<sup>a</sup>, Shuen-ChinChang<sup>de</sup>**

**Source :** Atmospheric Research, Volume 223, 15 July 2019, Pages 88-97

This study investigated isotopic signatures of carbon (C), lead (Pb) and strontium (Sr) in PM2.5 samples collected from two paired sites (urban vs. rural/background) in northern Taiwan during the summer of 2015 and the spring of 2016, respectively. Significant seasonality was revealed in the isotopic signatures of C and Pb, whereas no seasonal difference was observed in 87Sr/86Sr ratio. The values of  $\delta^{13}\text{C}$ , 206Pb/207Pb, and 208Pb/207Pb were more diverse and exhibited local features in summer. However, during the episodes of continental pollution outbreaks in springtime, the  $\delta^{13}\text{C}$  and Pb isotope ratios of PM2.5 shifted and converged consistently toward the documented characteristics of particulate matters in northern China. Moreover, the results showed that the differences in the Pb and Sr isotopic characteristics between the paired urban and rural sites were statistically insignificant, whereas marginally lower  $\delta^{13}\text{C}$  values were observed at the urban site. It was inferred accordingly that a substantial amount of gaseous hydrocarbons emitted in local urban areas could have been converted to secondary organic aerosols with lower  $\delta^{13}\text{C}$ . On the contrary, the consistency in the spatial and temporal variations of mass concentration and isotope ratios of Pb at the two sites suggested that East-Asian continental pollution outbreak was the major source of Pb-containing particles in the northern Taiwan during springtime. It is noteworthy that there was neither seasonal nor spatial differences in the 87Sr/86Sr ratio observed in this study, which suggested that the Sr-containing particles collected in this study could be originating from a common mixture of sources, including not only natural dust but also the anthropogenic emissions, coal-combustion for instance. This investigation upon the C-Pb-Sr isotopic features evidenced the substantial impacts of the continental pollution outbreaks on the aerosol composition and air quality in the downwind areas of the East-Asian winter monsoons.

**Keywords :** Fine particulate matters, Isotopic signatures, Asian continental outflows.

---

## **The hourly characteristics of aerosol chemical compositions under fog and high particle pollution events in Kinmen**

**Yu-ChiehChen<sup>a</sup>, Charles C.-K.Chou<sup>b</sup>, Yu-JenTsai<sup>a</sup>, Shih-YuChang<sup>ac</sup>, Wei-NaiChen<sup>b</sup>**

**Source :** Atmospheric Research, Volume 223, 15 July 2019, Pages 132-141



The hourly measurement of inorganic soluble ions in PM<sub>10</sub> aerosols was conducted with new in situ air composition measuring equipment (ACME) from March 15 to April 15, 2016, on Kinmen Island. The purposes of this study are to understand the influences of fog on secondary aerosol formation and to determine the impacts of air pollutants on haze formation under different relative humidity conditions.

The hourly measurements showed that the mass fraction of sulfate in PM<sub>10</sub> increased with increases in the liquid water content of fog and decreases in the gaseous concentrations of SO<sub>2</sub>. The value of the SO<sub>4</sub><sup>2-</sup>/PM<sub>10</sub> ratio is also affected by the concentration of SO<sub>2</sub> before the fog occurs and the level of the fog. This finding indicates that a humid environment is important for enhancing the heterogeneous reaction of sulfate formation. The nitrate concentrations were related to the ratio of NH<sub>4</sub><sup>+</sup> to SO<sub>4</sub><sup>2-</sup> during fog episodes. The formation of particulate NO<sub>3</sub><sup>-</sup> was associated with ammonium formation under ammonium-rich conditions (NH<sub>4</sub><sup>+</sup>/SO<sub>4</sub><sup>2-</sup> > 1.5). The gas-phase nitrate was usually observed under ammonium-poor conditions. During periods of high particle pollution, the air mass was from near the ground surface in the mainland coastal areas and transported more pollution to Kinmen. The concentrations of NO<sub>2</sub><sup>-</sup> were higher during periods of high particle pollution, which means that the secondary aerosol formation in the nearby areas also strongly affected the air quality degradation. The short-term and rapid change in the north-south wind system not only brings water vapor from the south but also delivers accumulated pollutants via the transport of northern pollution at low wind speeds.

**Keywords :** Fog, Haze, Relative humidity, Heterogeneous, NO<sub>x</sub>.

---

## **A modelling study of assessment of the effectiveness of combining foreign and local emission control strategies**

**Tu-FuChenKen-HuiChangChang-YouTsai**

**Source :** Atmospheric Research, 1 August 2019, Pages 114-126

In order to improve the atmospheric PM<sub>2.5</sub> levels of Taiwan, the Taiwanese government has developed a number of detailed emission reduction measures based on a highly detailed emission database, hoping to meet stringent air quality standards (15 µg/m<sup>3</sup>) by 2020. Past studies have shown that Chinese pollutants have a significant impact on Taiwanese air quality; fortunately, China has also been actively promoting various emission control. This study used an air quality model to simulate and evaluate improvements under three emission control scenarios, and assessed the possibility of achieving governmental air quality standards across the various regions of Taiwan under these scenarios. The simulation results show that under the implementation of the expected Taiwan and China emission control strategies (Scenario 3), all regions in Taiwan can reach the 1-Hour O<sub>3</sub> standard (120 ppb) by 2020, but since the 8-Hour O<sub>3</sub> standard (60 ppb) is considerably stricter, with strategies biased toward PM<sub>2.5</sub> improvement, most areas, particularly western

Taiwan, will still be unable to meet the standards by 2020. For PM<sub>2.5</sub>, regulatory responses have significantly improved Annual PM<sub>2.5</sub> and 24-Hour PM<sub>2.5</sub> in each region, especially in southern Taiwan, however in most regions such as western Taiwan there are still pockets of pollutants where Annual PM<sub>2.5</sub> (15 µg/m<sup>3</sup>) and 24-Hour PM<sub>2.5</sub> (35 µg/m<sup>3</sup>) rise well above the desired threshold to 2–14 µg/m<sup>3</sup> and 3–30 µg/m<sup>3</sup> respectively. It is suggested that Taiwan should propose more intensive emission control measures and strengthen the implementation of such measures. This will be required in addition to the continued emission reductions policy currently in place in domestic China.

**Keywords :** Fine particulate matter, Ozone, Air quality standard, Emission control strategy, Air quality modeling.

---

## **Biomass burning in the northern peninsular Southeast Asia: Aerosol chemical profile and potential exposure**

**Shantanu KumarPani<sup>a</sup>, SompornChantara<sup>bc</sup>, ChanakarnKhamkaew<sup>c</sup>, Chung-TeLee<sup>d</sup>, Neng-HueiLin<sup>a</sup>**

**Source :** Atmospheric Research, Volume 224, 1 August 2019, Pages 180-195

This study aimed to characterize the PM<sub>2.5</sub> (particulate matter ≤ 2.5 µm in aerodynamic diameter) chemical components obtained at Doi Ang Khang (DAK; high mountain and near-source of biomass-burning (BB) emissions) and Chiang Mai University (CMU; foothill site and an urban location) in northern peninsular Southeast Asia (PSEA) during dry BB season of 2015 through the analysis of water-soluble inorganic ions, organic carbon (OC), and elemental carbon (EC) contents. The 24-h average PM<sub>2.5</sub> levels (µg m<sup>-3</sup>) at DAK (118 ± 36) and CMU (113 ± 45) were about 4 folds greater than the WHO health-based guideline (25 µg m<sup>-3</sup>). Major diagnostics ratios between selected ions and carbonaceous fractions showed the significant BB influence on ambient aerosols. Enriched tracers in collected aerosols, such as NO<sub>3</sub><sup>-</sup>, OC<sub>3</sub> (evolved at 280–480 °C), and EC<sub>1</sub>-OP (EC evolved at 580 °C minus the pyrolyzed OC) confirmed that the samples were influenced by significant BB emissions. OC was the most abundant component in PM<sub>2.5</sub> and the contribution of BB to OC was estimated to be ~90%. For the first time, the conversion factor of OC to organic matter was estimated on the basis of mass closure approach to be 1.7 ± 0.3 and 1.6 ± 0.3 at DAK and CMU, respectively. Effective carbon ratio, which indicates an association between carbonaceous particles and climatic impact, at DAK revealed the significant atmospheric warming due to the presence of more absorbing aerosols attributed to near-source BB emissions at the high mountain site. The estimated inhalation dose of PM<sub>2.5</sub> and EC indicated severe health risk for local inhabitants during their outdoor activities. This study enhances the knowledge of aerosol chemical characterization and also addresses exposure to fine aerosols for local inhabitants during intense BB emissions in northern PSEA.

**Keywords :** 7-SEAS, Aerosol chemistry, PM<sub>2.5</sub>, OC to OM conversion factor, Effective carbon ratio, Exposure dose.

---

## **Nocturnal fine particulate nitrate formation by N<sub>2</sub>O<sub>5</sub> heterogeneous chemistry in Seoul Metropolitan Area, Korea**

**Hyun-YoungJo<sup>a</sup>, Hyo-JungLee<sup>a</sup>, Yu-JinJo<sup>a</sup>, Jong-JaeLee<sup>a</sup>, SoojinBan<sup>b</sup>, Jin-JuLee<sup>b</sup>, Lim-SeokChang<sup>b</sup>, GookyounHeo<sup>b</sup>, Cheol-HeeKim<sup>a</sup>**

**Source :** Atmospheric Research, Volume 225, 1 September 2019, Pages 58-69

This study investigated the potential of fine nitrate (NO<sub>3</sub><sup>-</sup> in PM<sub>2.5</sub>) formation in Seoul Metropolitan Area (SMA) by nighttime dinitrogen pentoxide (N<sub>2</sub>O<sub>5</sub>) heterogeneous chemistry during March 16–18, 2016, relatively dry and stagnant early spring days, by intervening N<sub>2</sub>O<sub>5</sub> uptake coefficients (reactive uptake probability,  $\gamma$ N<sub>2</sub>O<sub>5</sub>) in modeling with WRF-CMAQ. Simulations of a base case and two sensitivity tests with default (Davis et al., 2008), zero and decupled (tenfold)  $\gamma$ N<sub>2</sub>O<sub>5</sub> showed that impacts of  $\gamma$ N<sub>2</sub>O<sub>5</sub> on NO<sub>3</sub><sup>-</sup> and PM<sub>2.5</sub> are sensitive to relative humidity (RH) and sulfate-nitrate-ammonium (SNA) conditions. The base case simulation generally underestimated NO<sub>3</sub><sup>-</sup> and PM<sub>2.5</sub> levels in comparison to observations. Even with decupled  $\gamma$ N<sub>2</sub>O<sub>5</sub>, modeled NO<sub>3</sub><sup>-</sup> and PM<sub>2.5</sub> concentrations showed relatively small increases under conditions that RH is relatively low in the range of 20 to 40% and SNA levels are severely underestimated (e.g., lower by one third) in the base case simulation. Comparisons of NO<sub>3</sub><sup>-</sup> and PM<sub>2.5</sub> concentrations in SMA between simulations with differently specified  $\gamma$ N<sub>2</sub>O<sub>5</sub> indicated that N<sub>2</sub>O<sub>5</sub> heterogeneous chemistry has potential to (1) form additional nitric acid (HNO<sub>3</sub>), (2) further react with ammonia (NH<sub>3</sub>) emitted from various sources including agricultural sources outside of SMA urban-core areas, and (3) contribute to NO<sub>3</sub><sup>-</sup> and PM<sub>2.5</sub> formation in SMA. Additional modeling and observational studies on heterogeneous N<sub>2</sub>O<sub>5</sub> chemistry are needed to improve our understanding of NO<sub>3</sub><sup>-</sup> and PM<sub>2.5</sub> formation and better forecast PM<sub>2.5</sub> pollution levels over SMA or other urban areas with abundant nitrogen oxides emissions and ammonia emissions such as agricultural emissions from surrounding areas.

**Keywords :** N<sub>2</sub>O<sub>5</sub> heterogeneous chemistry, Nitrate aerosol, Secondary inorganic aerosol, PM<sub>2.5</sub> forecasting, Seoul Metropolitan Area, CMAQ model.

---

## **Gaseous and speciated particulate emissions from the open burning of wastes from tree pruning**

**Célia A.Alves<sup>a</sup>, Estela D.Vicente<sup>a</sup>, MargaritaEvtyugina<sup>a</sup>, AnaVicente<sup>a</sup>, CasimiroPio<sup>a</sup>, María FernándezAmado<sup>b</sup>, Purificación LópezMahía<sup>b</sup>**

**Source :** Atmospheric Research, Volume 226, 15 September 2019, Pages 110-121

---

Open-air burning of wastes from tree pruning is a common practice in many regions worldwide. However, this practice degrades air quality and contributes to the greenhouse effect. Aiming at characterizing particle (PM<sub>10</sub>) and gaseous emissions, the smoke from the open burning of vine, olive, willow and acacia branches was sampled and then analyzed by multiple techniques. Emission factors of gaseous compounds were as follows (g kg<sup>-1</sup> biofuel, dry basis): 1564–1663 CO<sub>2</sub>, 40.6–87.7 CO, 2.06–5.82 CH<sub>4</sub>, 0.91–3.73 ethane, <0.99 ethylene, and <1.80 formaldehyde. PM<sub>10</sub>, organic carbon (OC) and elemental carbon (EC) emissions were in the ranges 8.76–20.1, 2.70–7.44, and 0.32–1.18 g kg<sup>-1</sup> biofuel, dry basis, respectively. From the PM<sub>10</sub> emitted, water soluble ions represented from 5.3% (vines) to 13.6% (acacia). Potassium was the dominant ionic species, accounting for a PM<sub>10</sub> content from 1.4 to 4.7% wt. While in smoke from vines and olive combustion the NaCl mass fractions were lower than 0.9%, higher weight percentages were obtained for willow (3.6) and acacia (6.7). On average, OC accounted for PM<sub>10</sub> mass fractions of 33.4, 19.3, 32.3 and 36.5%, while EC represented 5.04, 2.34, 3.53 and 7.32% for willow, acacia, vines and olive combustion, respectively. Emissions of polycyclic aromatic hydrocarbons (PAHs) from the combustion of vines and olive branches were one order of magnitude higher than those from acacia and willow. Mean levoglucosan mass fractions of 18.1, 13.2, 17.1 and 12.4 mg g<sup>-1</sup> PM<sub>10</sub> were obtained in samples from the combustion of vines, olive, willow and acacia, respectively. Smoke particles also encompassed several other polar constituents, such as various types of acids, phenolic compounds, sterols, and polyols, whose contribution to the PM<sub>10</sub> mass varied with the biofuel burned.

**Keywords :** Agricultural burning, Gaseous emissions, PM<sub>10</sub>, Water soluble ions, Carbonaceous compounds.

---

## **Air quality during and after festivals: Aerosol concentrations, composition and health effects**

**AjitSingh<sup>a</sup>, PallaviPant<sup>b</sup>, Francis D.Pope<sup>a</sup>**

**Source :** Atmospheric Research, Volume 227, 1 October 2019, Pages 220-232

Ambient particulate matter (PM) continues to be among the top environmental health concerns globally; in 2017, nearly 3 million deaths were attributed to exposure to PM<sub>2.5</sub> around the world (HEI, 2019). While much attention is paid towards point and mobile sources of PM (e.g., power plants, vehicles), episodic/periodic events such as dust storms, use of fireworks etc. can also increase ambient PM levels and lead to adverse effects on air quality, visibility, and human health, albeit in the short-term. Fireworks and bonfires are commonly used during religious and cultural festivals including Diwali (India), Lunar New Year (China), Bastille Day (France), Guy Fawkes Night (UK), Australia Day (Australia), Fourth of July/Independence Day (USA), New Year's Eve (worldwide) as well as large sporting and other events. During these events, use of fireworks results in smoke plumes

which can raise the PM concentration levels for short periods of time. This review article summarizes the current body of literature on the role of fireworks use (and bonfires) on air quality, visibility, and human health. A summary of distinct type of fireworks and existing legislations/laws in different countries is also presented. Overall, there is clear evidence that such events produce exceptionally high level of pollutants, and as a result there can be intense exposures to a multipollutant mixture. In particular, the sharpest spikes are found in pollutant concentrations (such as PM<sub>2.5</sub>, PM<sub>10</sub>, and NO<sub>x</sub>) during and immediately after the firework event, followed by a decrease in the concentrations back to background levels, typically within 24 h. Peak concentrations of pollutants during firework events can exceed ambient levels by 2–8 times. As a result, overall visibility also decreases significantly, and in some cases, by as much as 92% during fireworks events. Moreover, significant health risks due to fireworks activities are also reported, although limited research has been conducted on this type of rapid air pollution exposure. The review concludes with a list of suggested future research priorities required to better understand the impacts of fireworks and bonfires on human and environmental health.

**Keywords :** Particulate matter, Fireworks, Air quality, Trace metals, Visibility.

---

## **Characterization of particle size distributions during winter haze episodes in urban air**

**YanCheng<sup>ab</sup>, LuYana<sup>a</sup>, YuHuang<sup>bc</sup>, QiyuanWang<sup>bc</sup>, LidiaMorawska<sup>d</sup>, ZhaolinGu<sup>a</sup>, JunjiCao<sup>bc</sup>, LiyuanZhang<sup>e</sup>, BoweiLi<sup>a</sup>, YelinWang<sup>a</sup>**

**Source :** Atmospheric Research, Volume 228, 1 November 2019, Pages 55-67

Detail characterization of particle size distribution and its temporal evolution is one of the critical elements towards uncovering mechanisms behind haze formation, yet rarely conducted. To address this deficiency, we conducted comprehensive characterization of particle size distribution during winter in Xi'an, China. Real-time measurements were conducted using a TSI Fast Mobility Particle Sizer Model 3091 (FMPS, from 5.6 to 523 nm) in the Qujiang campus of Xi'an Jiaotong University in the period from December 4th, 2015 to January 8th, 2016. The FMPS readings were adjusted by factors derived from an intercomparison with a TSI Scanning Mobility Particle Sizer (consisting of a TSI DMA 3081 and a CPC 3772, from 15.1 to 850.8 nm). Seven haze episodes and two new particle formation episodes were recorded during the sampling campaign. Two (E1 and E6) of the seven haze episodes are investigated in this study. E1 was an prolonged episode starting from a new particle formation (NPF) episode, followed by low, sustained PM<sub>2.5</sub> increase at an average growth rate of 2  $\mu\text{g m}^{-3}$  per hour (from 37  $\mu\text{g m}^{-3}$  to 262  $\mu\text{g m}^{-3}$  within 155 h), while E6 was a short-term haze episode starting from a rapid increase in PM<sub>2.5</sub> at an rapid growth rate of 27  $\mu\text{g m}^{-3}$  (from 79  $\mu\text{g m}^{-3}$  to 213  $\mu\text{g m}^{-3}$  within only 5 h). The average total particle number concentrations (PNC) were  $3.35 \times 10^4 \text{ cm}^{-3}$ ,

$4.14 \times 10^4 \text{ cm}^{-3}$  and  $3.99 \times 10^4 \text{ cm}^{-3}$  during normal days, E1, and E6, respectively, showing an increase in particle number concentration from normal days to haze days ( $p < .000$  for E1 and  $p < .002$  for E6, two-tailed t-test). While statically significant, the magnitude of the increase was not as large as of the increase in PM<sub>2.5</sub> concentration. On normal days, the peak in particle number size distribution (PNSD) was centered at smaller particle sizes (around 60–70 nm, computed based on a normal distribution) and shifted towards larger sizes during the night (139 nm at 0:00 and 168 nm at 4:00 am). The diurnal variations of PNSD during E1 and E6 episodes were not as evident as the variations on normal days, with the centers of the major peaks at 179 nm for E1 and 137 nm for E6. It was found that significant changes in PNC and PNSD occurred during the PM<sub>2.5</sub> increase phase of severe haze episodes, but not during the high concentration phase. Since the growth rates of PM<sub>2.5</sub> varied during increase phase between E1 and E6, PM<sub>2.5</sub> pollution formation mechanisms were different throughout evaluating growth rates as it relates to PM<sub>2.5</sub>, gaseous pollutants, PNC, PNSD, and meteorological variables in these processes.

**Keywords :** Particle number concentration (PNC), Particle number size distribution (PNSD), New particle formation (NPF), Haze.

---

## **Synoptic circulation pattern and boundary layer structure associated with PM<sub>2.5</sub> during wintertime haze pollution episodes in Shanghai**

**NingLiu<sup>ab</sup>, ShaZhou<sup>ab</sup>, ChaoshunLiu<sup>ab</sup>, JianpingGuo<sup>c</sup>**

**Source :** Atmospheric Research, Volume 228, 1 November 2019, Pages 186-195

Rapid industrialization and urbanization have caused severe air pollution in Shanghai, China, which occurs frequently in recent winters. Here, the relationships between boundary layer structure and PM<sub>2.5</sub> under different synoptic patterns were analysed. Firstly, the wintertime synoptic circulation patterns in Shanghai have been classified into seven types using the obliquely rotated Principal Components in T-mode (PCT) method based on the 925 hPa geopotential data. Then, the fine-resolution sounding-derived structures of planetary boundary layer (PBL) in these patterns, including PBL height (PBLH), inversion base height, and inversion intensity, combined with the relative humidity (RH) and temperature were analysed with respect to PM<sub>2.5</sub>. The results showed that three typical patterns, including high pressure located to the west, and those to the southwest and south of Shanghai, accounted for 62.17% of the total number of cases characterized by high PM<sub>2.5</sub> concentrations. The north-westerly winds were found to dominate these specific synoptic patterns, causing severe pollution when polluted air masses from the northwest region of China were brought into Shanghai. The local meteorological factors within the PBL also influenced PM<sub>2.5</sub> to varying extent in Shanghai under different synoptic conditions. Particularly, the PM<sub>2.5</sub> concentrations were anti-correlated with PBLH ( $R = -0.2$  at 0800 Beijing Local Time (BJT);  $R = -0.3$  at 2000 BJT). Also, temperature inversion played an important role in aerosol pollution. The intensity of temperature inversion was slightly correlated with PM<sub>2.5</sub> ( $R = 0.13$ ). The base height of the

temperature inversion was more closely anti-correlated with PM<sub>2.5</sub> ( $R = -0.25$ ). The frequent near-surface temperature inversions in the latter two synoptic patterns were unfavourable for the spread and dispersion of aerosol pollutants in the PBL, thus leading to severe aerosol pollution. This study has important implications for better understanding of the association of atmospheric circulation patterns with air pollution episodes in Shanghai.

**Keywords :** Synoptic circulation pattern, PM<sub>2.5</sub>, Planetary boundary layer, Inversion, Shanghai.

---

## **Evolution of the vertical structure of air pollutants during winter heavy pollution episodes: The role of regional transport and potential sources**

**QianqianHong<sup>a</sup>, ChengLiu<sup>abcd</sup>, QihouHu<sup>a</sup>, ChengzhiXing<sup>b</sup>, WeiTan<sup>a</sup>HaoranLiu<sup>b</sup>,  
YongHuang<sup>e</sup>, YuZhu<sup>f</sup>, JinsongZhang<sup>f</sup>, TianzhaoGeng<sup>f</sup>, JianguoLiu<sup>ac</sup>**

**Source :** Atmospheric Research, Volume 228, 1 November 2019, Pages 206-222

Knowledge of vertical distribution of air pollutants is important for understanding the mechanisms underlying haze pollution. In this paper, we characterize the vertical structure of air pollutants based on ground-based Multi-Axis Differential Optical Absorption Spectroscopy (MAX-DOAS) measurements in the wintertime in Hefei, East China. Both NO<sub>2</sub> and aerosol show exponentially decreasing profile with high concentrations concentrated close to the surface, suggesting the major emissions are at ground level. SO<sub>2</sub> profiles extend to slightly higher altitudes than NO<sub>2</sub>, which might be due to the SO<sub>2</sub> emissions from elevated point sources (e.g., power plants). Elevated HCHO was observed in the middle layer during noon time, probably indicating that the larger effect of the photochemical formation of atmospheric HCHO rather than direct HCHO emissions. Potential source contribution function (PSCF) and concentration-weighted trajectory (CWT) models were used to evaluate the potential sources of Hefei's air pollution in the lower, middle and upper boundary layer. The results revealed that the major regional source of NO<sub>2</sub> and aerosol were located in the northern and eastern part of Anhui and the transport mainly occurred in the lower layer. Transported SO<sub>2</sub> from the northwestern regions in the middle layer made great contribution to SO<sub>2</sub> in Hefei. HCHO was mostly produced locally while the transport of HCHO from potential source areas was negligible. To further explore the potential source contributions affecting haze pollution, PSCF and CWT analysis for heavy haze episodes suggested that the potential source areas for aerosol were almost located in the northern region, the northwestern region, and the YRD region. Our findings provide a more comprehensive understanding for regional transport through the study on potential sources at different altitudes, which are useful for designing collaborative air pollution control strategies on a regional scale.

**Keywords :** MAX-DOAS instrument, Vertical distribution, NO<sub>2</sub>, SO<sub>2</sub>, HCHO, Aerosol, Regional transport.

---

## **Polycyclic aromatic hydrocarbons in atmospheric PM<sub>2.5</sub> and PM<sub>10</sub> in the semi-arid city of Xi'an, Northwest China: Seasonal variations, sources, health risks, and relationships with meteorological factors**

**LijunWang<sup>ab</sup>, ShuzhenDong<sup>a</sup>, MengmeiLiu<sup>a</sup>, WendongTao<sup>c</sup>, BoXiao<sup>d</sup>, ShengweiZhang<sup>a</sup>, PanqingZhang<sup>a</sup>, XiaopingLi<sup>ab</sup>**

**Source :** Atmospheric Research, Volume 229, 15 November 2019, Pages 60-73

Atmospheric particulate matter (PM<sub>2.5</sub> and PM<sub>10</sub>) samples were collected at urban and suburban sites in Xi'an City from December 2016 to November 2017. Sixteen priority polycyclic aromatic hydrocarbons (PAHs) associated with PM<sub>2.5</sub> and PM<sub>10</sub> were analyzed for their seasonal variations, sources, health risks, and influencing factors. The results showed that the annual average concentrations of PM<sub>2.5</sub> and PM<sub>10</sub> were 111 and 185 µg/m<sup>3</sup>, respectively, exceeding the National Ambient Air Quality Standard of China (35 µg/m<sup>3</sup> for PM<sub>2.5</sub> and 70 µg/m<sup>3</sup> for PM<sub>10</sub> in Grade II). The annual averages of PM<sub>2.5</sub>- and PM<sub>10</sub>-bound total PAHs were 63.1 and 66.8 ng/m<sup>3</sup>, respectively, with a PM<sub>2.5</sub> decrease in the order of winter (115 ng/m<sup>3</sup>) >> spring (47.6 ng/m<sup>3</sup>) > summer (33.2 ng/m<sup>3</sup>) > autumn (30.8 ng/m<sup>3</sup>) and a PM<sub>10</sub> decrease in the order of winter (127 ng/m<sup>3</sup>) >> spring (55.6 ng/m<sup>3</sup>) > autumn (32.6 ng/m<sup>3</sup>) > summer (30.2 ng/m<sup>3</sup>). The most abundant PAHs were benzo[a]anthracene, benzo[b]fluoranthene, and fluoranthene. The PM<sub>2.5</sub>- and PM<sub>10</sub>-bound PAHs were originated mainly from traffic emissions (51.0% and 43.4%), followed by combustion of biomass (20.4% and 23.6%) and coal (16.8% and 23.1%). Pressure and relative humidity were positively correlated with PM<sub>2.5</sub> and PM<sub>10</sub> as well as PM<sub>2.5</sub>- and PM<sub>10</sub>-bound PAHs, while temperature, visibility and wind speed had negative correlations. The annual means of TEQs (toxic equivalency quantities) for the 16 PAHs in PM<sub>2.5</sub> and PM<sub>10</sub> were 10.1 and 10.2 ng/m<sup>3</sup>, respectively, being attributed to 7 carcinogenic PAHs (> 95%). The ECRs (lifetime excess cancer risks) for PM<sub>2.5</sub>- and PM<sub>10</sub>-bound PAHs were  $1.12 \times 10^{-3}$  and  $1.17 \times 10^{-3}$ , i.e., 1125 and 1169 lung cancer cases per million, respectively. The ILCRs (incremental lifetime cancer risks) due to PM<sub>2.5</sub>- and PM<sub>10</sub>-bound PAHs for adults ( $1.21 \times 10^{-6}$  and  $1.26 \times 10^{-6}$ ) were larger than those for children ( $2.09 \times 10^{-7}$  and  $2.17 \times 10^{-7}$ ), with acceptable carcinogenic risks. The ambient levels of PM and most PM-bound PAHs as well as their TEQs, ECRs and ILCRs exhibited a spatial pattern of the suburban site > the urban site and a seasonality with winter and spring > summer and autumn. The results suggest that it is important to control PM<sub>2.5</sub> and PM<sub>10</sub> for local air quality improvement and special attention should be paid to PM and PM-bound PAHs in suburban areas, particularly in winter and spring.

**Keywords :** Polycyclic aromatic hydrocarbon, Particulate matter, Source, Health risk.

---



# **Changes in concentrations of fine and coarse particles under the CO<sub>2</sub>-induced global warming**

**DongdongYang<sup>abc</sup>, HuaZhang<sup>ab</sup>, JiangnanLi<sup>c</sup>**

**Source :** Atmospheric Research, Volume 230, 1 December 2019, 104637

Using an aerosol-climate coupled model, we have investigated the climate response to increases in atmospheric carbon dioxide (CO<sub>2</sub>) levels and the resulting changes in the column concentrations of anthropogenic and natural particulate matters. Special attention has been paid on the fine particulate matters (PM<sub>2.5</sub>, particulate matters with aerodynamic diameters  $\leq 2.5 \mu\text{m}$ ) and coarse particles of non-PM<sub>2.5</sub> (NPM, particulate matters with aerodynamic diameters  $> 2.5 \mu\text{m}$ ). Rising CO<sub>2</sub> levels led to significant effects on surface air temperature, large scale circulation, surface water flux, precipitation, etc., which considerably affect the column concentrations of anthropogenic and natural particulate matters, for both fine and coarse modes. Changes in burden of fine particles are major contributions to that of total anthropogenic particulate matters by CO<sub>2</sub>-induced global warming. The anthropogenic PM<sub>2.5</sub> burden was found to decrease in the regions with latitudes  $> 30^\circ\text{N}$ , whereas in the rest areas increase. The geographical distributions of changes in the column concentrations of fine and coarse natural particles were found in the same order of magnitude in most regions, and the particle size distribution shifted to the coarse mode. The physical mechanisms are analyzed to explain the changes in aerosol local column concentrations due to CO<sub>2</sub>-induced climate change.

**Keywords :** Aerosol, PM<sub>2.5</sub>, Coarse particle, CO<sub>2</sub>, Climate response.

---

## **5. Environmental Science and pollution Research**

### **Short-term effects of ambient air pollution and cardiovascular events in Shiraz, Iran, 2009 to 2015**

**Zahra Soleimani, Ali Darvishi Boloorani, Reza Khalifeh, Dale W. Griffin & Alireza Mesdaghinia**

**Source :** Environmental Science and Pollution Research volume 26, pages6359–6367(2019)

Air pollution and dust storms are associated with increased cardiovascular hospital admissions. The aim of this study was to investigate the association between short-term exposure to ambient air pollutants and CVD (cardiovascular disease) events in a long-term observational period. The study included the events of cardiovascular diseases (namely coronary artery disease, ischemic heart disease, myocardial infarction, and pneumo thrombo embolism) within the population of Shiraz, from March 21, 2009 to March 20,

2015. Also, each patient's demographics were recorded. Main meteorological variables and five ambient pollutants (CO, O<sub>3</sub>, SO<sub>2</sub>, NO<sub>2</sub>, and PM<sub>10</sub>) were recorded. Statistical analysis was performed using linear regression (GLM) and a generalized additive model (GAM) estimating Poisson distribution and adjusted for the main risk factors and ambient meteorological variables. A mild prevalence (51.5%) of coronary artery disease (CAD) was registered in 6425 events. In GLM analysis, we observed an association among the pollutants with the coronary artery disease hospital admissions which was in the order of CO, NO<sub>2</sub>, and PM<sub>10</sub>. The highest association of each pollutant with hospital admission was observed as PM<sub>10</sub> at lag 4 (RR = 1.08; 95% CI 1.02, 1.14 and p < 0.05), NO<sub>2</sub> at lag 0 (RR = 1.22; 95% CI 1.00, 1.48), and CO at lag 0 (RR = 1.52 95% CI = (1.16, 1.99)). However, on dusty days, there were significantly higher numbers of referrals of cardiovascular patients (mean = 7.54 ± 4.44 and p = 0.002,) than on non-dusty days. According to these data, dust storms and some types of pollutants in the air are responsible for more admissions to hospitals for cardiovascular problems.

**Keywords :** Air pollution, Cardiovascular, Shiraz, Hospital admission.

---

## **Impact of air pollution on hospital admissions with a focus on respiratory diseases: a time-series multi-city analysis**

**Alessandro Slama, Andrzej Śliwczyński, Jolanta Woźnica, Maciej Zdrolik, Bartłomiej Wiśnicki, Jakub Kubajek, Olga Turżańska-Wieczorek, Dariusz Gozdowski, Waldemar Wierzba & Edward Franek**

**Source :** Environmental Science and Pollution Research volume 26, pages16998–17009(2019)

Together with the growing availability of data from electronic records from healthcare providers and healthcare systems, an assessment of associations between different environmental parameters (e.g., pollution levels and meteorological data) and hospitalizations, morbidity, and mortality has become possible. This study aimed to assess the association of air pollution and hospitalizations using a large database comprising almost all hospitalizations in Poland. This time-series analysis has been conducted in five cities in Poland (Warsaw, Białystok, Bielsko-Biała, Kraków, Gdańsk) over a period of almost 4 years (2014–2017, 1255 days), covering more than 20 million of hospitalizations. The hospitalizations have been extracted from the National Health Fund registries as daily summaries. Correlation analysis and distributed lag nonlinear models have been used to investigate for statistically relevant associations of air pollutants on hospitalizations, trying by various methods to minimize potential bias from atmospheric parameters, days of the week, bank holidays, etc. A statistically significant increase of respiratory disease hospitalizations has been detected after peaks of particulate matter concentrations (particularly PM<sub>2.5</sub>, between 0.9 and 4.5% increase per 10 units of pollutant increase, and PM<sub>10</sub>, between 0.9 and 3.5% per 10 units of pollutant increase), with a typical time lag between the pollutant peak and the event of 2 to 6 days. For other pollution parameters

and other types of hospitalizations (e.g., cardiovascular events, eye and skin diseases, etc.), a weaker and ununiform correlations were recorded. Ambient air pollution exposure increases are associated with a short-term increase of hospitalizations due to respiratory tract diseases. The most prominent effect was recorded with the correlation of PM<sub>2.5</sub> and PM<sub>10</sub>. There is only weak evidence indicating that such short-term associations exist between peaks of air pollution concentrations and increased hospitalizations for other (e.g., cardiovascular) diseases. The obtained information could be used to better predict hospitalization patterns and costs for the healthcare system and perhaps trigger additional vigilance on particulate matter pollution in the cities.

**Keywords :** Air pollution, Respiratory health, Hospital admissions, Multi-city time-series, analysis, Particulate matter.

---

## **Association between particulate matter air pollution and cardiovascular disease mortality in Lanzhou, China**

**Tingting Wu, Yuan Ma, Xuan Wu, Ming Bai, Yu Peng, Weiting Cai, Yongxiang Wang, Jing Zhao & Zheng Zhang**

**Source :** Environmental Science and Pollution Research volume 26, pages15262–15272(2019)

Ambient particulate matter (PM) pollution has been linked to elevated mortality, especially from cardiovascular diseases. However, evidence on the effects of particulate matter pollution on cardiovascular mortality is still limited in Lanzhou, China. This research aimed to examine the associations of daily mean concentrations of ambient air pollutants (PM<sub>2.5</sub>, PM<sub>10</sub>, and PM<sub>2.5-10</sub>) and cardiovascular mortality due to overall and cause-specific diseases in Lanzhou. Data representing daily cardiovascular mortality rates, meteorological factors (daily average temperature, daily average humidity, and atmospheric pressure), and air pollutants (PM<sub>2.5</sub>, PM<sub>10</sub>, SO<sub>2</sub>, NO<sub>2</sub>) were collected from January 1, 2014, to December 31, 2017, in Lanzhou. A quasi-Poisson regression model combined with a distributed lag non-linear model (DLNM) was used to estimate the associations. Stratified analyses were also performed by different cause-specific diseases, including cerebrovascular disease (CD), ischemic heart disease (IHD), heart rhythm disturbances (HRD), and heart failure (HF). The results showed that elevated concentration of PM<sub>2.5</sub>, PM<sub>10</sub>, and PM<sub>2.5-10</sub> had different effects on mortality of different cardiovascular diseases. Only cerebrovascular disease showed a significant positive association with elevated PM<sub>2.5</sub>. Positive associations were identified between PM<sub>10</sub> and daily mortality rates from total cardiovascular diseases, cerebrovascular diseases, and ischemic heart diseases. Besides, increased concentration of PM<sub>10</sub> was correlated with increased death of cerebrovascular diseases and ischemic heart diseases. For cerebrovascular disease, each 10 µg/m<sup>3</sup> increase in PM<sub>2.5</sub> at lag<sub>4</sub> was associated with increments of 1.22% (95% CI 0.11–2.35%). The largest significant effects for PM<sub>10</sub> on cardiovascular diseases and ischemic heart diseases were both observed at lag<sub>0</sub>, and a 10 µg/m<sup>3</sup> increment in concentration of PM<sub>10</sub> was associated with 0.47% (95% CI 0.06–0.88%) and 0.85% (95% CI 0.18–1.52%) increases in cardiovascular mortality and

ischemic heart diseases. In addition, it exhibited a lag effect on cerebrovascular mortality as well, which was most significant at lag6d, and an increase of 10  $\mu\text{g}/\text{m}^3$  in PMC was associated with a 0.76% (95% CI 0.16–1.37%) increase in cerebrovascular mortality. The estimates of percentage change in daily mortality rates per 10  $\mu\text{g}/\text{m}^3$  increase in PM10 were 0.52% (95% CI 0.05–1.02%) for cerebrovascular disease at lag6 and 0.53% (95% CI 0.01–1.05%) for ischemic heart disease at lag0, respectively. Our study suggests that elevated concentration of atmospheric PM (PM2.5, PMC, and PM10) in Lanzhou is associated with increased mortality of cardiovascular diseases and that the health effect of elevated concentration of PM2.5 is more significant than that of PMC and PM10.

**Keywords :** Air pollution, Particulate matter, Cardiovascular diseases, Mortality, Death, Time-series study.

---

## **Short-term effects of ambient fine particulate air pollution on inpatient visits for myocardial infarction in Beijing, China**

**Yao Wu, Man Li, Yaohua Tian, Yaying Cao, Jing Song, Zhe Huang, Xiaowen Wang & Yonghua Hu**

**Source :** Environmental Science and Pollution Research volume 26, pages14178–14183(2019)

The effects of ambient fine particulate matter (PM2.5) on the incidence of myocardial infarction have been reported, but little is known about this association in China. We conducted a time-series study of ambient PM2.5 concentrations and inpatient visits for myocardial infarction in Beijing. A generalized additive model with a Poisson link was applied to estimate the percentage change in inpatient visits for myocardial infarction following a 10- $\mu\text{g}/\text{m}^3$  increase in PM2.5 concentrations. A total of 15,432 inpatient visits for myocardial infarction were identified between January 1, 2010, and June 30, 2012. A 10- $\mu\text{g}/\text{m}^3$  increase in PM2.5 concentrations was associated with a 0.46% ( $P \leq 0.001$ ) increase in daily inpatient visits for myocardial infarction. Males were more sensitive to the adverse effects, and the association was more significant during the warm season (May through October). Short-term exposure to PM2.5 was associated with increased risk of inpatient visits for myocardial infarction in Beijing. The findings may be useful in developing more accurate targeted interventions.

**Keywords :** Myocardial infarction, PM2.5, Air pollution, Inpatient visits, Generalized, additive model, Hospitalization.

---

## **Effect of O<sub>3</sub>, PM<sub>10</sub> and PM<sub>2.5</sub> on cardiovascular and respiratory diseases in cities of France, Iran and Italy**

**Pierre Sicard, Yusef Omid Khaniabadi, Sandra Perez, Maurizio Gualtieri & Alessandra De Marco**

**Source :** Environmental Science and Pollution Research volume 26, pages32645–32665(2019)

At present, both tropospheric ozone (O<sub>3</sub>) and particulate matters (PM) are among the most threatening air pollutants for human health in cities. The air pollution effects over public health include increased risk of hospital admissions and mortality for respiratory and cardiovascular diseases even when air pollutant concentrations are below European and international standards. The aim of this study was to (i) estimate the burden of mortality and morbidity for cardiovascular and respiratory diseases attributed to PM<sub>2.5</sub>, PM<sub>10</sub> and O<sub>3</sub> in nine selected cities in France, Iran and Italy in 2015 and 2016 and to (ii) compare estimated burdens at current O<sub>3</sub> and PM levels with pre-industrial levels. The selected Mediterranean cities are among the most affected by the air pollution in Europe, in particular by rising O<sub>3</sub> while the selected Iranian cities rank as the most polluted by PM in the world. The software AirQ+ was used to estimate the short-term health effects, in terms of mortality and morbidity by using in situ air quality data, city-specific relative risk values and baseline incidence. Compared to pre-industrial levels, long-term exposures to ambient PM<sub>2.5</sub>, PM<sub>10</sub> and O<sub>3</sub> have substantially contributed to mortality and hospital admissions in selected cities: about 8200 deaths for non-accidental causes, 2400 deaths for cardiovascular diseases, 540 deaths for respiratory diseases, 220 deaths for chronic obstructive pulmonary diseases as well as 18,800 hospital admissions for cardiovascular diseases and 3400 for respiratory diseases were reported in 2015. The study supports the need of city-specific epidemiological data and urgent strategies to mitigate the health burden of air pollution.

**Keywords :** Air pollution, AirQ, Mortality, Hospital admission, Risk assessment, Particulate matter, Ozone.

---

## **Characterization of aerosol particles during the most polluted season (winter) in urban Chengdu (China) by single-particle analysis**

**Jinqi Luo, Xiaojuan Huang, Junke Zhang, Bin Luo, Wei Zhang & Hongyi Song**

**Source :** Environmental Science and Pollution Research volume 26, pages17685–17695(2019)

Chengdu, the capital city of Sichuan Province, is one of the most polluted cities in China. We used single-particle aerosol mass spectrometer to monitor particulate matter pollution in an urban area of Chengdu from December 9, 2015 to January 4, 2016 to determine the characteristics of air pollution during the winter months. The mass concentrations of

particulate matter were high during the whole observation period, with mean values for PM<sub>2.5</sub> and PM<sub>10</sub> of  $101 \pm 60$  and  $162 \pm 99 \mu\text{g m}^{-3}$ , respectively. The particles were clustered into nine distinct particle types: dust (3%), potassium-elemental carbon (KEC) (24%), organic carbon (OC) (12%), combined OC and EC (OCEC) (6%), K-organic nitrogen (KCN) (10%), K-nitrate (KNO<sub>3</sub>) (12%), K-sulfate (KSO<sub>4</sub>) (18%), K-sulfate and nitrate (KSN) (12%), and metal (3%) particles. Analysis on different types of day showed that: (1) from “excellent” (days with PM<sub>2.5</sub> lower than  $35 \mu\text{g m}^{-3}$ ) to “light pollution” (PM<sub>2.5</sub> between 75 and  $115 \mu\text{g m}^{-3}$ ) days, local/regional combustion was the major contributor, whereas the aggravation of pollution from light pollution to “heavy pollution” (PM<sub>2.5</sub> higher than  $150 \mu\text{g m}^{-3}$ ) days was mainly determined by the combined effect of local/regional combustion and long-distance transport; (2) as the air quality deteriorated, the mixing of sulfate and nitrate in particles increased sharply, especially sulfate; and (3) the relative aerosols acidity increased from excellent to light pollution days, while decreased significantly from light pollution to heavy pollution days. Backward trajectory analysis showed that there were significant differences in PM<sub>2.5</sub> concentrations and particle compositions between clusters of trajectories, which affected the level and evolution of PM<sub>2.5</sub> pollution in Chengdu. These results give a deeper understanding of PM<sub>2.5</sub> pollution in Chengdu and the Sichuan Basin.

**Keywords :** Single particles, Mixing state, Pollution evolution, SPAMS, Chengdu.

---

## **Levels and health risk assessments of particulate matters (PM<sub>2.5</sub> and PM<sub>10</sub>) in indoor/outdoor air of waterpipe cafés in Tehran, Iran**

**Gholamreza Heydari, Farhad Taghizdeh, Mehdi Fazlzadeh, Ahmad Jonidi Jafari, Zahra Asadgol, Ehsan Abouee Mehrizi, Masoud Moradi & Hossein Arfaeinia**

**Source :** Environmental Science and Pollution Research volume 26, pages7205–7215(2019)

To determine the concentration of particulate matters (PM<sub>2.5</sub> and PM<sub>10</sub>), 36 samples were collected from indoor/outdoor air of hookah cafés (HS), cigarette cafés (CS), both hookah and cigarette (HCS), and no-smoking building (NS) in Tehran City from December 2017 to March 2018. The mean  $\pm$  SD of PM<sub>10</sub> concentration in the indoor air of the cafés in terms of HS, CS, HCS, and NS sites has been 702.35, 220.20, 1156.60, and  $60.12 \mu\text{g}/\text{m}^3$ , while for PM<sub>2.5</sub>, the values have been 271.92, 111.80, 619.10, and  $22.25 \mu\text{g}/\text{m}^3$ , respectively. It was also found that the PM concentration inside the cafés was higher during weekend session (with a higher number of active smokers), than during the weekday sessions. Moreover, the PM levels in the indoor air of the cafés were considerably higher than those of the outdoors ( $p < 0.05$ ). Based on path analysis, the number of “active smokers” had the highest influence on production of PM inside the cafés, followed by the tobacco type. Finally, the mean excess lifetime cancer risk (ELCR) for PM<sub>2.5</sub> in the indoor air of cafés was observed in the range of  $0.64 \times 10^{-5}$ – $14.98 \times 10^{-5}$ . Also, the mean of hazard quotient (HQ) for PM<sub>2.5</sub> and PM<sub>10</sub> was calculated in range of 0.82–18.4 and 0.16–3.28, respectively, which corresponds to an unacceptably high risk for human health. The PM levels in the indoor air of smoking cafés

in Tehran are significantly high, such that it can cause serious risks for the health of both the customers and personnel. Thus, it is necessary that suitable controlling strategies be adopted for this public health threat.

**Keywords:** Air quality, PM2.5, PM10, Waterpipe cafés, Risk assessment, Tehran.

---

## **Field assessment of the effects of land-cover type and pattern on PM10 and PM2.5 concentrations in a microscale environment**

**Shuxin Fan, Xiaopeng Li & Li Dong**

**Source :** Environmental Science and Pollution Research volume 26, pages2314–2327(2019)

The microscale environment is a very important human-scale outdoor spatial unit. Aimed at investigating the effects of microscale land-cover type and pattern on levels of PM10 and PM2.5, we monitored PM10 and PM2.5 concentrations among different land-cover type and pattern sites through field measurements, during four seasons (December 2015 to November 2016) in Beijing, China. Differences of daily PM10 and PM2.5 concentrations among seven typical land-cover types, and correlations between daily two-sized PM levels and various microscale land-cover patterns as explained by landscape metrics were analyzed. Results show that concentrations of the two-sized particles had stable daytime and seasonal trends. During the four seasons, there were various differences in daily PM10 and PM2.5 levels among the seven land-cover types. Overall, bare soil always had the highest daily PM10 level, whereas high canopy density vegetation and water bodies had low levels. Maximum PM2.5 levels were always found in high canopy density vegetation. Moderate canopy density vegetation and water bodies had lower concentrations. Correlations between different landscape metrics and daily levels of two-sized PM varied by season. Metrics reflecting the dominance and distribution of land-cover classifications had closer relationships with particle concentrations in the microscale environment. The patterns of pavement along with low and moderate canopy density vegetation had a greater impact on PM10 level. The responses of PM2.5 level to patterns of building and low and moderate canopy density vegetation were sensitive. Reasonable design of land-cover structure would be conducive to ameliorate air particle concentrations in the microscale environment.

**Keywords:** Microscale environment, PM10, PM2.5, Land-cover type, Land-cover pattern.

---

## **Characterization of chemical components and cytotoxicity effects of indoor and outdoor fine particulate matter (PM<sub>2.5</sub>) in Xi'an, China**

**Xinyi Niu, Kin Fai Ho, Tafeng Hu, Jian Sun, Jing Duan, Yu Huang, Ka Hei Lui & Junji Cao**

**Source :** Environmental Science and Pollution Research volume 26, pages31913–31923(2019)

The chemical and cytotoxicity properties of fine particulate matter (PM<sub>2.5</sub>) at indoor and outdoor environment were characterized in Xi'an, China. The mass concentrations of PM<sub>2.5</sub> in urban areas (93.29~96.13  $\mu\text{g m}^{-3}$  for indoor and 124.37~154.52  $\mu\text{g m}^{-3}$  for outdoor) were higher than suburban (68.40  $\mu\text{g m}^{-3}$  for indoor and 96.18  $\mu\text{g m}^{-3}$  for outdoor). The PM<sub>2.5</sub> concentrations from outdoor environment due to fossil fuel combustion were higher than indoor environment. An indoor environment without central heating demonstrated higher organic carbon-to-elemental carbon (OC / EC) ratios and n-alkanes values that potentially attributed to residential coal combustion activities. The cell viability of human epithelial lung cells showed dose-dependent decrease, while nitric oxide (NO) and oxidative potential showed dose-dependent increase under exposure to PM<sub>2.5</sub>. The variations of bioreactivities could be possibly related to different chemical components from different sources. Moderate ( $0.4 < R < 0.6$ ) to strong ( $R > 0.6$ ) correlations were observed between bioreactivities and elemental carbon (EC)/secondary aerosols (NO<sub>3</sub><sup>-</sup>, SO<sub>4</sub><sup>2-</sup>, and NH<sub>4</sub><sup>+</sup>)/heavy metals (Ni, Cu, and Pb). The findings suggest PM<sub>2.5</sub> is associated with particle induced oxidative potential, which are further responsible for respiratory diseases under chronic exposure.

**Keywords:** PM<sub>2.5</sub>, Indoor and outdoor, Oxidative stress, Inflammation.

---

## **Spatial and temporal variations of PM<sub>2.5</sub> mass closure and inorganic PM<sub>2.5</sub> in the Southeastern U.S.**

**Bin Cheng, Lingjuan Wang-Li, Nicholas Meskhidze, John Classen & Peter Bloomfield**

**Source :** Environmental Science and Pollution Research volume 26, pages33181–33191(2019)

Fine particulate matter (i.e., PM<sub>2.5</sub>) has gained extensive attention owing to its adverse effects. The impacts of PM<sub>2.5</sub> may vary in time and space due to the spatiotemporal variations of PM<sub>2.5</sub> number size distribution and chemical compositions. This research analyzed the latest PM<sub>2.5</sub> chemical compositions measurements with an aim to better understand the dynamic changes of PM<sub>2.5</sub> in response to emission reductions due to the new regulations. The particulate measurements from the Southeastern Aerosol Research and Characterization (SEARCH) network between 2001 and 2016 were analyzed for the spatiotemporal variations of PM<sub>2.5</sub> and inorganic PM<sub>2.5</sub> (iPM<sub>2.5</sub> = SO<sub>4</sub><sup>2-</sup> + NH<sub>4</sub><sup>+</sup> + NO<sub>3</sub><sup>-</sup>) chemical compositions in the Southeastern United States (U.S.). It was discovered that PM<sub>2.5</sub> and iPM<sub>2.5</sub> mass concentrations exhibited significant downward trends in 2001–2016. Both PM<sub>2.5</sub> and iPM<sub>2.5</sub> mass concentrations were higher at urban and inland sites



than rural/suburban and coastal sites. The higher iPM<sub>2.5</sub> concentrations at agricultural sites were attributed to the influences of ammonia (NH<sub>3</sub>) emissions from animal feeding operations (AFOs). The iPM<sub>2.5</sub> was the dominant contributor to PM<sub>2.5</sub> in 2001–2016 at the coastal sites, whereas organic carbon matter (OCM) was the major contributor to PM<sub>2.5</sub> after 2011 at the inland sites. Our data analysis suggests that significant decrease of PM<sub>2.5</sub> concentrations is attributed to the reductions in nitrogen oxides (NO<sub>x</sub>) and sulfur dioxide (SO<sub>2</sub>) emissions in 2001–2016. Findings from this research provide insights into the development of effective PM<sub>2.5</sub> control strategies and assessment of air pollutants exposure.

**Keywords:** Chemical compositions, Gas-particle partitioning, Inorganic aerosols, Mass closure, PM<sub>2.5</sub>, Spatiotemporal variations.

---

## 6. Science of Total Environment- 4.9

### **Effects of wood moisture on emission factors for PM<sub>2.5</sub>, particle numbers and particulate-phase PAHs from Eucalyptus globulus combustion using a controlled combustion chamber for emissions**

**FabiánGuerrero<sup>ac</sup>, KarenYáñez<sup>a</sup>, VíctorVidal<sup>ab</sup>, FranciscoCereceda-Balic<sup>ab</sup>**

**Source :** Science of The Total Environment, Volume 648, 15 January 2019, Pages 737-744

Polycyclic aromatic hydrocarbons, PM<sub>2.5</sub> and micrometer-sized particles are mainly emitted by residential wood combustion, affecting air pollution in the cities of Chile. Eucalyptus globulus (EG) at 0% and 25% wood moisture was burning using a new controlled combustion chamber for emissions (3CE) to determine the emission factors of PM<sub>2.5</sub>, micrometer-sized particle numbers (0.265 μm to 34.00 μm) and 16 EPA-PAHs plus retene adsorbed on PM<sub>2.5</sub> quartz filters. A method using accelerated solvent extraction, concentration, clean-up and GC–MS is proposed for determining emission factors for 16 EPA-PAHs for the concentration from biomass combustion. Chromatographic conditions and analytical steps were optimized in terms of linearity, selectivity, limits of detection and quantification, precision and accuracy. The recovery obtained from urban dust SRM 1649A (NIST reference material) analyses was between 63% (benzo[b]fluoranthene) and 102% (benzo[k]fluoranthene). In this investigation, it was shown that increasing the wood moisture in combustion tests decreased combustion efficiency (93% to 49%) and increased the emission factors of total PAHs (5215.47 ng g<sup>-1</sup> to 7644.48 ng g<sup>-1</sup>), the gravimetric PM<sub>2.5</sub> (2.01 g kg<sup>-1</sup> to 22.90 g kg<sup>-1</sup>) and the total number of measured micrometer-sized particles (3.15 × 10<sup>12</sup> particles kg<sup>-1</sup> to 1.33 × 10<sup>13</sup> particles kg<sup>-1</sup>) due to incomplete combustion. The PM<sub>2.5</sub> emission rates (ERs) were estimated using EG at 0% WM (2.39 g h<sup>-1</sup> to 3.15 g h<sup>-1</sup>) and 25% WM (27.32 g h<sup>-1</sup> to 35.77 g h<sup>-1</sup>) for three regions of Chile. In almost all regions, the Chilean emission regulations were exceeded for PM<sub>2.5</sub> from wood combustion in the heater (stove with thermal power ≤8 kW and emission limit of 2.5 g h<sup>-1</sup>).

Finally, when using wet wood for residential combustion, the amount of PAHs on the PM<sub>2.5</sub> increased, presenting a potential hazard to population health. Therefore, improvements are necessary in the current regulation of PM emissions.

**Keywords:** Eucalyptus wood combustion, Polycyclic aromatic hydrocarbons, Combustion chamber, Wood humidity, Emission factors, Emission rates PM<sub>2.5</sub>.

---

## **Temporal variation of oxidative potential of water soluble components of ambient PM<sub>2.5</sub> measured by dithiothreitol (DTT) assay**

**JingpengWang<sup>a</sup>, XinLin<sup>b</sup>, LipingLu<sup>ac</sup>, YujieWu<sup>ac</sup>, HuanxinZhang<sup>d</sup>, QiLv<sup>a</sup>, WeipingLiu<sup>ac</sup>, YanlinZhang<sup>b</sup>, ShulinZhuang<sup>ae</sup>**

**Source :** Science of The Total Environment, Volume 649, 1 February 2019, Pages 969-978

The exposure to ambient fine particulate matter (PM<sub>2.5</sub>) can induce oxidative stress, contributing to global burden of diseases. The evaluation of the oxidative potential (OP) of PM<sub>2.5</sub> is thus critical for the health risk assessment. We collected ambient PM<sub>2.5</sub> samples in Hangzhou city, China for four consecutive quarters in the year 2017 and investigated the oxidation property of PM<sub>2.5</sub> components by the dithiothreitol (DTT) assay. The annual mean of ambient PM<sub>2.5</sub> mass concentrations in 2017 was 63.05  $\mu\text{g m}^{-3}$  (median: 57.34, range: 6.67–214.33  $\mu\text{g m}^{-3}$ ) with the significant seasonal variations ranking as winter > spring > summer > autumn. Secondary inorganic aerosol (SIA) species including SO<sub>4</sub><sup>2-</sup>, NO<sub>3</sub><sup>-</sup> and NH<sub>4</sub><sup>+</sup> totally account for >50% of PM<sub>2.5</sub> mass. The annual mean volume-normalized DTT activity (DTTv) showed a relatively high value of 0.62 nmol/min/m<sup>3</sup> (median: 0.62, range: 0.11–1.66 nmol/min/m<sup>3</sup>) and DTTv of four seasons was roughly at the same level, indicating a high annual exposure level of ambient PM<sub>2.5</sub>. SIA species were correlated well with the corresponding DTTv and showed significant diurnal variations with strong or moderate correlations at day and weak correlations at night, suggesting strong secondary formation in daytime with contribution to the particulate OP. The annual mean mass-normalized DTT activity (DTTm) had a relatively low value of 6.39 pmol/min/ $\mu\text{g}$  (median: 5.63, range: 1.99–22.70 pmol/min/ $\mu\text{g}$ ), indicating low intrinsic oxidative toxicity. The DTTm of four seasons ranked as autumn > winter > spring > summer, indicating seasonal variations of the DTT-active components. The PM<sub>2.5</sub> mass concentration is more related to exposure levels than intrinsic properties of components, while OP is determined by the components rather than PM<sub>2.5</sub> mass concentration. Our results provide an insight into reactive oxygen species-induced health risk of PM<sub>2.5</sub> exposure and decision for subsequent emission control.

**Keywords:** Fine particulate matter, Reactive oxygen species, Temporal variation, Secondary inorganic aerosol.

---

## **Chemical source profiles of urban fugitive dust PM<sub>2.5</sub> samples from 21 cities across China**

**JianSun<sup>ab</sup>, ZhenxingShen<sup>ab</sup>, LeimingZhang<sup>c</sup>, YaliLei<sup>a</sup>, XuesongGong<sup>a</sup>, QianZhang<sup>a</sup>TianZhang<sup>a</sup>, HongmeiXu<sup>a</sup>SongCui<sup>d</sup>, QiyuanWang<sup>b</sup>, JunjiCao<sup>b</sup>, JunTao<sup>e</sup>, NingningZhang<sup>b</sup>, RenjianZhang<sup>f</sup>**

**Source :** Science of The Total Environment, Volume 649, 1 February 2019, Pages 1045-1053

Urban fugitive (road and construction) dust PM<sub>2.5</sub> samples were collected in 21 cities of seven regions in China. Seven water-soluble ions, eight sub-fractions of carbonaceous components, and 19 elements were determined to investigate the chemical profiles of urban fugitive dust. Among the analyzed chemical compositions and on regional average, the elemental compositions showed the highest proportion (12.5–28.9% in road dust (RD) and 13.1–38.0% in construction dust (CD)), followed by water-soluble ions (5.1–19.0% in RD and 4.2–16.4% in CD) and carbonaceous fractions (5.4–9.6% in RD and 4.9–9.3% in CD). Chemical compositions measured in CD were all slightly lower than those in RD although statistically insignificant ( $p > 0.05$ ). Soil dust, which was estimated from Fe concentration, was proved to be the biggest contributor to urban fugitive dust PM<sub>2.5</sub> mass. While, it showed a higher contribution in Northern China (71.5%) than in Southern China (52.1%). Higher enrichment factors were found for elemental S, Zn and Pb in RD than CD, reflecting stronger anthropogenic sources (i.e. vehicle exhaust) in RD. Low NO<sub>3</sub><sup>-</sup>/SO<sub>4</sub><sup>2-</sup> and high SO<sub>4</sub><sup>2-</sup>/K<sup>+</sup> ratios both indicated that fugitive dust was strongly influenced by stationary sources (e.g. coal combustion), and this influence was especially strong in Northern China. Coefficients of divergence proved that dust profiles within the same region were more similar than across regions, reflecting that urban fugitive dust was influenced more by local sources than long-range transport.

**Keywords:** Urban fugitive dust, Chemical profiles, Source identification.

---

## **PM<sub>2.5</sub> source apportionment for the port city of Thessaloniki, Greece**

**Dikaia E.Saraga<sup>ab</sup>, Evangelos I.Tolis<sup>b</sup>, ThomasMaggos<sup>a</sup>, ChristosVasilakos<sup>a</sup>, John G.Bartzis<sup>b</sup>**

**Source :** Science of The Total Environment, Volume 650, Part 2, 10 February 2019, Pages 2337-2354

This paper aims to identify the chemical fingerprints of potential PM<sub>2.5</sub> sources and estimate their contribution to Thessaloniki port-city's air quality. For this scope, Positive Matrix Factorization model was applied on a comprehensive PM<sub>2.5</sub> dataset collected over a one-year period, at two sampling sites: the port and the city center. The model indicated six and five (groups of) sources contributing to particle concentration at the two sites, respectively. Traffic and biomass burning (winter months) comprise the major local PM

sources for Thessaloniki (their combined contribution can exceed 70%), revealing two of the major control-demanding problems of the city. Shipping and in-port emissions have a non-negligible impact (average contribution to PM<sub>2.5</sub>: 9–13%) on both primary and secondary particles. Road dust factor presents different profile and contribution at the two sites (19.7% at the port; 7.4% at the city center). The secondary-particle factor represents not only the aerosol transportation over relatively long distances, but also a part of traffic-related pollution (14% at the port; 34% at the city center). The study aims to contribute to the principal role of quantitative information on emission sources (source apportionment) in port-cities for the implementation of the air quality directives and guidelines for public health.

**Keywords:** PMF, Urban sources, Ship and harbor emissions, Wind pattern.

---

## **Removal of PM<sub>2.5</sub> and secondary inorganic aerosols in the North China Plain by dry deposition**

**JiaoDu<sup>a</sup>, XiaodongZhang<sup>a</sup>, TaoHuang<sup>a</sup>, HongGao<sup>a</sup>, JingyueMo<sup>a</sup>, XiaoxuanMao<sup>a</sup>, JianminMa<sup>a</sup>**

**Source :** Science of The Total Environment, Volume 651, Part 2, 15 February 2019, Pages 2312-2322

The North China Plain (NCP) has experienced heavy air pollution in the past several decades featured by high levels of fine particulate matter (PM<sub>2.5</sub>). PM<sub>2.5</sub> removal from the atmosphere in the NCP by dry deposition was estimated from 1999 through 2013 using the inferential method, which combined PM<sub>2.5</sub> air concentrations retrieved from satellite remote sensing and dry deposition velocities (V<sub>d</sub>) calculated using a bulk particle dry deposition model. Dry deposition of the three major inorganic ions in PM<sub>2.5</sub>, namely NH<sub>4</sub><sup>+</sup> (ammonium), NO<sub>3</sub><sup>-</sup> (nitrate), and SO<sub>4</sub><sup>2-</sup> (sulfate), with their concentrations in 2000 and 2010 obtained from WRF-Chem model simulations, were also investigated considering their important roles in PM<sub>2.5</sub> formation and ecosystem health. High levels of modeled and satellite-retrieved PM<sub>2.5</sub> air concentrations, the secondary inorganic aerosols (the sum of NH<sub>4</sub><sup>+</sup>, NO<sub>3</sub><sup>-</sup>, and SO<sub>4</sub><sup>2-</sup>), and their respective deposition fluxes were identified from the southern NCP to Beijing-Tianjin metropolitans. The deposition fluxes derived from the inferential method and WRF-Chem increased considerably in the 2000s due to rising PM<sub>2.5</sub> atmospheric levels across the NCP. The enhancement of dry deposition velocities of PM<sub>2.5</sub> and three aerosol species in the NCP were associated nicely with increasing vegetation coverage and wind speed. We show that both air concentrations of PM<sub>2.5</sub> and secondary inorganic aerosols and rising dry deposition velocities related to extensive afforestation activities contributed to their deposition fluxes and an inclining trend of PM<sub>2.5</sub> removal from the atmosphere.

**Keywords:** North China Plain, PM<sub>2.5</sub>, Secondary inorganic aerosols, Dry deposition.

---

## **PM2.5 concentration and composition in the urban air of Nanjing, China: Effects of emission control measures applied during the 2014 Youth Olympic Games**

**MirellaMiettinen<sup>a</sup>, AriLeskinen<sup>bc</sup>, GülcinAbbaszade<sup>d</sup>, JürgenOrasche<sup>de</sup>, MaijaSainio<sup>a</sup>,  
SanttuMikkonen<sup>c</sup>, HannaKoponen<sup>a</sup>, TeemuRönkkö<sup>a</sup>, JarnoRuusunen<sup>a</sup>, KariKuuspalo<sup>a</sup>,  
PetriTiitta<sup>a</sup>, PasiJalava<sup>a</sup>, LiqingHao<sup>c</sup>, DieFang<sup>f</sup>, QingengWang<sup>f</sup>, ChengGu<sup>f</sup>, YuZhao<sup>f</sup>,  
BernhardMichalke<sup>g</sup>, ...OlliSippula<sup>a</sup>**

**Source :** Science of The Total Environment, Volume 652, 20 February 2019, Pages 1-18

Industrial processes, coal combustion, biomass burning (BB), and vehicular transport are important sources of atmospheric fine particles (PM<sub>2.5</sub>) and contribute to ambient air concentrations of health-hazardous species, such as heavy metals, polycyclic aromatic hydrocarbons (PAH), and oxygenated-PAHs (OPAH). In China, emission controls have been implemented to improve air quality during large events, like the Youth Olympic Games (YOG) in August 2014 in Nanjing. In this work, six measurement campaigns between January 2014 and August 2015 were undertaken in Nanjing to determine the effects of emission controls and meteorological factors on PM<sub>2.5</sub> concentration and composition. PAHs, OPAHs, hopanes, n-alkanes, heavy metals, and several other inorganic elements were measured. PM<sub>2.5</sub> and potassium concentrations were the highest in May–June 2014 indicating the prevalence of BB plumes in Nanjing. Emission controls substantially reduced concentrations of PM<sub>2.5</sub> (31%), total PAHs (59%), OPAHs (37%), and most heavy metals (44–89%) during the YOG compared to August 2015. In addition, regional atmospheric transport and meteorological parameters partly explained the observed differences between the campaigns. The most abundant PAHs and OPAHs were benzo[b,k]fluoranthenes, fluoranthene, pyrene, chrysene, 1,8-naphthalic anhydride, and 9,10-anthracenedione in all campaigns. Carbon preference index and the contribution of wax n-alkanes indicated mainly biogenic sources of n-alkanes in May–June 2014 and anthropogenic sources in the other campaigns. Hopane indexes pointed to vehicular transport as the major source of hopanes, but contribution of coal combustion was detected in winter 2015. The results provide evidence to the local government of the impacts of the air protection regulations. However, differences between individual components were observed, e.g., concentrations of potentially more harmful OPAHs decreased less than concentrations of PAHs. The results suggest that the proportions of hazardous components in the PM<sub>2.5</sub> may also change considerably due to emission control measures.

**Keywords:** Air quality, Aerosol, Fine particles, Chemical composition, Health effects.

---

## **Factors controlling the long-term (2009–2015) trend of PM<sub>2.5</sub> and black carbon aerosols at eastern Himalaya, India**

**ChirantanSarkar<sup>a1</sup>, ArindamRoy<sup>a</sup>, AbhijitChatterjee<sup>ab</sup>, Sanjay K.Ghosh<sup>abc</sup>, SibajiRaha<sup>bc</sup>**

**Source :** Science of The Total Environment, Volume 656, 15 March 2019, Pages 280-296

A first-ever long-term (2009–2015) study on the fine particulate matter (PM<sub>2.5</sub>) and black carbon (BC) aerosol were conducted over Himalaya in order to investigate the characteristics, temporal variations and the important factors regulating the long-term trend. The study was conducted over a high altitude station, Darjeeling (27°01'N, 88°15'E, 2200 m asl) representing a typical high altitude urban atmosphere at eastern Himalaya in India. The average concentrations of PM<sub>2.5</sub> and BC over a period of seven years were  $25.2 \pm 5.6 \mu\text{g m}^{-3}$  (ranging between 2.2 and 220.4  $\mu\text{g m}^{-3}$ ) and  $3.4 \pm 0.7 \mu\text{g m}^{-3}$  (0.4 to 15.6  $\mu\text{g m}^{-3}$ ) respectively. We observed decreasing trends in both PM<sub>2.5</sub> (49% at a rate of 170  $\text{ng m}^{-3} \text{ month}^{-1}$ ) and BC (34% at the rate of 20  $\text{ng m}^{-3} \text{ month}^{-1}$ ) mass concentration over this region from 2009 to 2015. We extensively studied the impact of micrometeorological parameters on the long-term trend in PM<sub>2.5</sub> and BC through the correlation analysis. The significant changes in boundary layer dynamics over this region played a major role in the decreasing trend of aerosols. The concentration weighted trajectory analysis revealed that the important contributory long-distant source regions for PM<sub>2.5</sub> and BC over eastern Himalaya were Indo Gangetic Plane and Nepal. The contributions from these regions were found to be decreased significantly from 2009 to 2015. Investigations on the fire counts associated with the forest fire, and open burning activities through the satellite observations revealed that the decreasing trend in PM<sub>2.5</sub> and BC over eastern Himalaya is well correlated to the decreasing trend in the fire counts over IGP and Nepal. We also explored that the changes and up gradation of the domestic fuel at the Indo Gangetic Plane regions in recent years not only improved the regional air quality but also affected the atmospheric environment over the eastern part of Himalaya.

**Keywords:** Trend analysis, PM<sub>2.5</sub>, Black carbon, Eastern Himalaya.

---

## **Chemical composition and source apportionment of PM<sub>1</sub> and PM<sub>2.5</sub> in a national coal chemical industrial base of the Golden Energy Triangle, Northwest China**

**XiaoxueLiang<sup>a</sup>, TaoHuang<sup>a</sup>, SiyingLin<sup>a</sup>, JinxiangWang<sup>c</sup>, JingyueMo<sup>d</sup>, HongGao<sup>a</sup>, ZhanxiangWang<sup>a</sup>, JixiangLi<sup>a</sup>, LuluLian<sup>a</sup>, JianminMa<sup>ab</sup>**

**Source :** Science of The Total Environment, Volume 659, 1 April 2019, Pages 188-199

As part of the Energy Golden Triangle in northwest China and the largest coal-to-liquids industry in the world, the emission and contamination of fine particles in the Ningdong National Energy and Chemical Industrial Base (NECIB) are unknown. There are also large knowledge gaps in the association of air pollution with coal-to-liquids industry. This paper

reports the chemical composition and source apportionment of PM<sub>1</sub> and PM<sub>2.5</sub> collected at two industrial sites Yinglite (YLT) and Baofeng (BF) from a field campaign during summer 2016 and winter 2017. Major chemical components in PM<sub>1</sub> and PM<sub>2.5</sub>, including carbonaceous aerosols, water-soluble inorganic ions, and metal elements were analyzed. The Positive Matrix Factorization (PMF) model and the ISORROPIA II thermodynamic equilibrium model were used to track possible sources and contributions of these chemical components to the formation of the two fine particles. The results identified four primary sources of the fine particles, including vehicle emissions, biomass burning and waste incineration, the secondary aerosols and coal combustion, and soil dust. The PM<sub>1</sub> and PM<sub>2.5</sub> concentrations were higher in winter than summer. The summed secondary inorganic and carbonaceous aerosols accounted for 36.1–40.0% of PM<sub>2.5</sub> mass. The total mass of chemical components identified in the source apportionment only explained about 64.2 to 72.4% of the PM<sub>2.5</sub> mass. These results imply some missing sources in this large-scale coal chemical industry base. A coupled weather forecasting and atmospheric chemistry model WRF-Chem was employed to simulate the PM<sub>2.5</sub> mass and concentrations of OC and EC, and to examine the origins of PM<sub>2.5</sub> across the NECIB. The modeled concentrations of OC and EC were consistent with the sampled data, but the modeled mass of PM<sub>2.5</sub> is lower considerably than the measurements, again suggesting unknown sources of fine particles in this energy industrial base.

**Keywords:** Coal chemical industry, PM<sub>1</sub> and PM<sub>2.5</sub>, Source apportionment, Mass reconstruction, WRF-chem modeling.

---

## **Temporal variations of PM<sub>2.5</sub>-bound organophosphate flame retardants in different microenvironments in Beijing, China, and implications for human exposure**

**DouWang<sup>ab</sup>, PuWang<sup>a</sup>, YiwenWang<sup>c</sup>, WeiweiZhang<sup>ab</sup>, ChaofeiZhu<sup>d</sup>, HuizhongSun<sup>ab</sup>, JuliusMatsiko<sup>ab</sup>, YingZhu<sup>a</sup>YingmingLi<sup>a</sup>, WenyingMenge<sup>e</sup>, QinghuaZhang<sup>ab</sup>, GuibinJiang<sup>ab</sup>**

**Source :** Science of The Total Environment, Volume 666, 20 May 2019, Pages 226-234

In the present study, the temporal distribution of PM<sub>2.5</sub>-bound organophosphate flame retardants (OPFRs) was comprehensively investigated in various indoor environments as well as outdoor air in Beijing, China over a one-year period. The mean concentrations of  $\Sigma$ 9OPFRs were 22.7 ng m<sup>-3</sup> and 1.40 ng m<sup>-3</sup> in paired indoor and outdoor PM<sub>2.5</sub>, respectively. The concentrations of tri-n-butyl phosphate (TNBP), tris (2-chloroethyl) phosphate (TCEP) and tris (2-chloroisopropyl) phosphate (TCIPP) in indoor PM<sub>2.5</sub> were significantly correlated with those in outdoor PM<sub>2.5</sub>. For different indoor microenvironments, mean concentrations of  $\Sigma$ 9OPFRs were in the order of office (29.0 ± 11.7 ng m<sup>-3</sup>) > home (24.0 ± 9.4 ng m<sup>-3</sup>) > dormitory (19.4 ± 4.9 ng m<sup>-3</sup>) > activity room (14.4 ± 3.1 ng m<sup>-3</sup>). TCIPP was the most abundant compound in the indoor PM<sub>2.5</sub>, followed by TCEP. Significantly higher concentrations of OPFRs were observed in indoor environments with more furnishing, electronics or other materials (p < 0.05). Moreover,

lower levels of OPFRs in indoor air were observed at well-ventilated (with higher air exchange rate) indoor sampling sites. Concentrations of  $\Sigma$ 9OPFRs in the activity room, dormitory, homes and outdoor sites generally increased in summer and heating seasons (November 2016 to February 2017). Significant correlations ( $p < 0.05$ ) were observed between temperatures and mass concentrations of OPFRs with higher vapor pressures, i.e. TNBP, TCEP and TCIPP in all indoor and outdoor samples. Seasonal differences in human exposure were observed and the highest daily exposure dose occurred in summer. Toddlers may suffer the highest exposure risk of PM<sub>2.5</sub>-bound OPFRs via inhalation among all age groups. This is one of the very few studies that have revealed the seasonal variation and human exposure of PM<sub>2.5</sub>-bound OPFRs in different microenvironments, which shed light on emission sources and fate of OPFRs and potential human exposure pathway.

**Keywords:** Organophosphate flame retardants, PM<sub>2.5</sub>, Microenvironment, Seasonal variation, Human exposure.

---

## **Impacts of the near-surface urban boundary layer structure on PM<sub>2.5</sub> concentrations in Beijing during winter**

**LinlinWang<sup>ab</sup>, HongWang<sup>b</sup>, JunkaiLiu<sup>a</sup>, ZhiqiuGao<sup>a</sup>, YuanjianYang<sup>bc</sup>, XiaoyeZhang<sup>d</sup>, YubinLi<sup>b</sup>, MengHuang<sup>b</sup>**

**Source :** Science of The Total Environment, Volume 669, 15 June 2019, Pages 493-504

The Urban Boundary layer (UBL) structure plays an important role in the accumulation of air pollutants in cities. To understand how the near-surface UBL structure affects air pollutants, we analyzed 40-day vertical observations collected at a 325-m meteorology tower in Beijing from 1 December 2016 to 9 January 2017. The occurrences of heavy pollution episodes (HPEs) in the study period were closely associated with weak wind speed (WS), high temperature, high relative humidity, weak friction velocity ( $u^*$ ) and weak turbulence kinetic energy (TKE) in near-surface UBL. In particular, the thickness and intensity of the temperature inversions were enhanced during all HPEs at nighttime. In addition, the PM<sub>2.5</sub> concentration at the ground was significantly negative/positive correlation with vertical dynamic factors (e.g., WS,  $u^*$  and TKE)/temperature inversion in the near-surface UBL. Diurnal variations in the vertical WS, potential temperature ( $\theta$ ),  $u^*$  and TKE were less evident on the 23 polluted days than those on the 14 clean days; specifically, there were larger differences in the WS and  $\theta$  between polluted and clean days at higher levels. Note that the varying quantitative relationships between the observed PM<sub>2.5</sub> concentration and UBL dynamic factors during the daytime were much more significant than those at nighttime at all vertical levels. Compared with the WS,  $u^*$  and TKE, the PM<sub>2.5</sub> concentration showed a much more sensitive change with  $u^*$  (WS) during the daytime (at nighttime).

**Keywords:** PM<sub>2.5</sub>, Boundary layer structure, Mixing turbulence, Near-surface layer, Beijing.

---



## **Differences in concentration and source apportionment of PM<sub>2.5</sub> between 2006 and 2015 over the PRD region in southern China**

**XingchengLu<sup>a</sup>, YiangChen<sup>a</sup>, YeqiHuang<sup>a</sup>, ChangqingLin<sup>b</sup>, ZhiyuanLi<sup>a</sup>, Jimmy C.H.Fung<sup>ac</sup>, Alexis K.H.Lau<sup>abd</sup>**

**Source :** Science of The Total Environment, Volume 673, 10 July 2019, Pages 708-718

During China's 11th Five Year Plan (FYP) and 12th FYP (2006–2015), a series of air pollution control measures was implemented in the Pearl River Delta (PRD) region. Therefore, it is vital to determine how the concentration and sources of fine particulate matter (PM<sub>2.5</sub>) in this region changed between 2006 and 2015. In this work, using 2006 and 2015 emission inventories, the concentration and source apportionment of PM<sub>2.5</sub> were simulated using the Weather Research and Forecast - Comprehensive Air Quality Model with Extensions (WRF-CAMx) for January, April, July and October in the PRD region. The PM<sub>2.5</sub> in 10 cities and the contributions made by sources in six major categories were tracked using the Particulate Source Apportionment Technology (PSAT) module. The results showed that the PM<sub>2.5</sub> concentration was lower across the entire PRD region in the 2015 emission scenario than in the 2006 scenario, and that the degree of this reduction exceeded 40 µg/m<sup>3</sup> in some places. The PM<sub>2.5</sub> contributed by mobile emissions decreased the most, especially in Guangzhou, Foshan and Shenzhen, where mobile contributions decreased from 15.0, 17.9 and 13.0 µg/m<sup>3</sup> in 2006 to 2.6, 3.1 and 4.1 µg/m<sup>3</sup> in 2015, respectively. The PM<sub>2.5</sub> contributed by power plants also decreased, and in Dongguan and Guangzhou, the extent of this reduction reached 2.5 and 3.4 µg/m<sup>3</sup> respectively. However, due to an increase in industrial production and population size, the PM<sub>2.5</sub> from industrial point sources and area sources also increased between 2006 and 2015 in some of the cities. Investigation of the source apportionment for city centers yielded similar results. In addition to emissions within the PRD region, outside-PRD non-local contribution is still an important PM<sub>2.5</sub> contributor. Hence, more stringent policies for controlling industrial and area sources and deepening province-to-province cooperation are urgently needed as the next step in PM<sub>2.5</sub> control.

**Keywords:** PM<sub>2.5</sub>, WRF-CAMx, Source apportionment, Anthropogenic source, Control efficacy.

---

## **Ground-level PM<sub>2.5</sub> estimation over urban agglomerations in China with high spatiotemporal resolution based on Himawari-8**

**TaixinZhang<sup>a</sup>, LinZang<sup>b</sup>, YouchuanWan<sup>a</sup>, WeiWang<sup>c</sup>, YiZhang<sup>a</sup>**

**Source :** Science of The Total Environment, Volume 676, 1 August 2019, Pages 535-544

High concentrations of particulate matter with diameter of <2.5 µm (PM<sub>2.5</sub>) demonstrate severe effects on human health, especially in the metropolitan agglomerations of China. Estimating PM<sub>2.5</sub> based on satellite aerosol optical depth (AOD) is a widely used method.

AOD data from Himawari-8, a geostationary satellite, enable improvement of the temporal resolution of PM<sub>2.5</sub> estimates to the hourly level, thereby reflecting diurnal variations of pollutants compared with AOD products from polar orbit satellites, which only have one value per day. In this study, PM<sub>2.5</sub> concentrations are estimated based on Himawari-8 AOD and other ancillary data by constructing spatiotemporal linear mixed effects model in Central China (CCH), Beijing–Tianjin–Henan (BTH), Yangtze River Delta (YRD) and Pearl River Delta (PRD) regions, respectively. The determination coefficient (R<sup>2</sup>) between the measurements and estimates of PM<sub>2.5</sub> calculated with the tenfold cross-validation method are 0.82, 0.84, 0.80 and 0.74 in CCH, BTH, YRD and PRD, respectively. The spatial distributions of PM<sub>2.5</sub> present large regional variation, which is highly correlated with land-use type. Heavily polluted zones are mainly located in urban or rural areas, which have dense population and high anthropogenic emissions. Comparisons among different seasons show that particle pollution during the cold seasons (autumn and winter) is relatively severe with an average PM<sub>2.5</sub> of >60 µg/m<sup>3</sup> in CCH, BTH and YRD, whereas the level does not greatly change throughout the year in the PRD region. During the daytime, particulate pollution levels are generally high in the morning.

**Keywords:** Himawari-8 AOD, Hourly PM<sub>2.5</sub>, Linear mixed-effects model, Spatiotemporal variation.

---

## **Characteristics of chemical composition and seasonal variations of PM<sub>2.5</sub> in Shijiazhuang, China: Impact of primary emissions and secondary formation**

**YuzhuXie<sup>ag</sup>, ZiruiLiu<sup>a</sup>, TianxueWen<sup>a</sup>, XiaojuanHuang<sup>ab</sup>, JingyunLiu<sup>ac</sup>, GuiqianTang<sup>a</sup>, YangYang<sup>d</sup>, XingruLi<sup>e</sup>, RongrongShen<sup>a</sup>, BoHu<sup>a</sup>, YuesiWang<sup>afg</sup>**

**Source :** Science of The Total Environment, Volume 677, 10 August 2019, Pages 215-229

North China registers frequent air pollution episodes from high PM<sub>2.5</sub> concentrations. Shijiazhuang is located at the intensive industrial zone of this region, but there is insufficient data on the chemical composition of PM<sub>2.5</sub> and its sources in this city. In this study, the chemical and seasonal characteristics of PM<sub>2.5</sub> in Shijiazhuang were investigated based on 12-h integrated PM<sub>2.5</sub> measurements made over eight 1-month periods in each season between June 2014 and April 2016 (486 samples). The eight-season average concentration of PM<sub>2.5</sub> was 138.8 µg m<sup>-3</sup>, and the major chemical components were secondary inorganic aerosol (SIA) species of sulfate, nitrate, and ammonium (41.5%), followed by organic matter (25.9%). The mass concentration and most of the chemical components of PM<sub>2.5</sub> showed clear seasonal variation, with a winter-high and summer-low pattern. SO<sub>4</sub><sup>2-</sup> and NO<sub>3</sub><sup>-</sup> were the dominant components at each pollution level in summer and autumn (18.1%–30.6% and 14.2%–27.0%, respectively). Sufficient gaseous oxidants (O<sub>3</sub>) concentrations and suitable meteorology conditions were observed in these two seasons. Highest SOR (0.61), SO<sub>4</sub><sup>2-</sup>/EC(10.8) and NOR (0.58), NO<sub>3</sub><sup>-</sup>/EC (5.9) were found in summer and autumn, which indicated intense secondary transformation in these two seasons. Organic matter was the dominant species in winter, which increased from

17.1  $\mu\text{g m}^{-3}$  for clean days (28.7% of PM<sub>2.5</sub>) to 169.1  $\mu\text{g m}^{-3}$  (38.4% of PM<sub>2.5</sub>). The accumulation of primary emissions (coal combustion and biomass burning) was responsible for the increasing OM trend (especially for POC). The highest and leading proportion of mineral dust occurred in spring (20.3%–46.5%) as a result of higher wind speeds (up to 3 m/s). Potential source contribution function (PSCF) analyses implied that the border areas of Hebei, Henan and Shandong Provinces, together with the central area of Shanxi Province, contributed significantly to the PM<sub>2.5</sub> pollution in Shijiazhuang, especially in autumn and winter.

**Keywords:** PM<sub>2.5</sub>, Chemical composition, Secondary formation, Primary emission.

---

## **In-vehicle PM<sub>2.5</sub> personal concentrations in winter during long distance road travel in India**

**Soma Sekhara Rao, Kolluru<sup>a</sup>, Aditya KumarPatra<sup>ab</sup>, Ravish ShailendraDubey<sup>a</sup>**

**Source :** Science of The Total Environment, Volume 684, 20 September 2019, Pages 207-220

During travel, passengers are exposed to high concentrations of PM which constitute a significant fraction of daily personal exposures. We carried out comprehensive mobile monitoring for a distance of 400 km on an Indian National Highway during the winter season to evaluate the PM<sub>2.5</sub> Personal Concentrations (PC) and mass exposure in three traffic microenvironments (public bus, car with AC (Car CW) and car without AC (Car OW)) and to quantify the key factors that influence it. The mean concentrations were highest inside Car OW ( $175.3 \pm 142.7 \mu\text{g m}^{-3}$ ) followed by bus ( $134.0 \pm 113.9 \mu\text{g m}^{-3}$ ) and lowest in Car CW ( $78.8 \pm 37.1 \mu\text{g m}^{-3}$ ). PC during in-city highway sections were greater than out-city highway sections during Bus and Car OW journeys. PC were higher during morning than evening journeys in Bus and Car OW. Mean PC in different seating positions in Bus followed the trend: middle > rear > front. Results of the Linear Mixed-Effects Models (LMM) indicated that journey timings were the significant predictors of PC for Bus and Car OW. The exposures per unit time followed trend: Car OW > Bus > Car CW. Total mass of inhaled exposures however followed a different trend: Bus > Car OW > Car CW, because Bus needed longer duration to cover the entire distance. Car CW users experienced both the least PC and mass exposures. We estimated that the road repairing works contributed ~22% in Bus and Car OW, and ~12% in Car CW increment in mass exposures. These findings indicate that management of exposures needs to consider mass exposures in addition to PC, for curtailing the adverse health effects relating to long distance journeys. Highway authorities should focus on early completion of construction and repairing activities to reduce exposures to passengers.

**Keywords:** Air pollution, Personal concentrations, PM<sub>2.5</sub>, Mass exposures, Travel modes.

---

## **PM2.5 vertical variation during a fog episode in a rural area of the Yangtze River Delta, China**

**JunZhu<sup>ab</sup>, BinZhu<sup>ab</sup>, YongHuang<sup>cd</sup>, JunlinAn<sup>ab</sup>, JiapingXu<sup>e</sup>**

**Source :** Science of The Total Environment, Volume 685, 1 October 2019, Pages 555-563

A dense radiation fog event occurred at the Shouxian site, Anhui Province, China, from the evening of January 2 to noon on January 3, 2017. During this event, vertical profiles of particulate matter (PM) and meteorological parameters within the lower troposphere (0–1000 m) were collected using a tethered balloon. This study assessed the evolution of the PM2.5 profile with the planetary boundary layer (PBL) structure and the effects of fog on the PM2.5 concentration. The results showed the following: (1) At the surface, the average diurnal variation in Aitken mode, accumulation mode and coarse mode particles had bimodal patterns before fog formation and was mainly influenced by diurnal variation in the mixing level depth (MLD). The aerosol number concentrations decreased remarkably, and the PM2.5 was strongly scavenged from 150 µg/m<sup>3</sup> to 45 µg/m<sup>3</sup> during the fog process. (2) In the vertical direction, the PM2.5 distribution was affected by the PBL height and the vertical fog structure. At 05:00 LT (local time) (i.e., early morning before the fog event), the PM2.5 concentration was slightly higher in the stable layer (260 µg/m<sup>3</sup>) than in the residual layer (200 µg/m<sup>3</sup>). At 14:00 LT (haze period), PM2.5 was well mixed below 500 m, with a concentration of 310 µg/m<sup>3</sup>. After 20:00 LT, when fog formed, PM2.5 was scavenged from the surface to the upper layers, and the scavenging height was controlled by the fog top height. (3) The vertical development of fog was promoted by turbulent mixing and radiation cooling at the fog top. Turbulent mixing enhanced the particle scavenging efficiency of fog droplets by the collision-coalescence process. The PM2.5 scavenging height was corresponded to the turbulence height. Therefore, turbulence development in the fog was the essential dynamic factor driving PM2.5 reduction.

**Keywords:** Radiation fog, PM<sub>2.5</sub> profile, Planetary boundary layer structure, Turbulence, Scavenging of PM<sub>2.5</sub>.

---

## **Characterization of polycyclic aromatic hydrocarbon (PAHs) source profiles in urban PM2.5 fugitive dust: A large-scale study for 20 Chinese cities**

**XuesongGong<sup>ab</sup>, ZhenxingShen<sup>abc</sup>, QianZhang<sup>d</sup>, YalingZeng<sup>a</sup>, JianSun<sup>a</sup>, Steven Sai HangHo<sup>e</sup>, YaliLei<sup>a</sup>, TianZhang<sup>a</sup>, HongmeiXu<sup>a</sup>, SongCui<sup>c</sup>, YuHuang<sup>b</sup>, JunjiCao<sup>b</sup>**

**Source :** Science of The Total Environment, Volume 687, 15 October 2019, Pages 188-197

Polycyclic aromatic hydrocarbons (PAHs) in road dust (RD) and construction dust (CD) in PM2.5 were quantified in the samples collected in 20 Chinese cities. The PAHs profiles in urban PM2.5 fugitive dusts were determined and their potential health risks were evaluated. Seven geographical regions in China were identified as northwest China (NWC),

the North China Plain (NCP), northeast China (NEC), central China (CC), south China (SC), southwest China (SWC), and east China (EC). The overall average concentrations of total quantified PAHs ( $\Sigma$ PAHs) were  $23.2 \pm 18.9$  and  $22.8 \pm 29.6 \mu\text{g}\cdot\text{g}^{-1}$  in RD and CD of PM<sub>2.5</sub>, indicating that severe PAHs pollution to urban fugitive dusts in China. The differences of  $\Sigma$ PAHs between RD and CD were minor in northern and central regions of China but much larger in southern and east regions. The  $\Sigma$ PAHs for RD displayed a pattern of “high in northern and low in southern”, and characterized by large abundance of high molecular weights (HMWs) PAHs, indicating that vehicle emission was the predominant pollution origin. Additionally, higher diagnostic ratios of fluoranthene/(fluoranthene + pyrene) in NCP, CC, and SWC suggest critical contributions of biomass burning and coal combustion for RD in these areas. In comparison, gasoline combustion was the major pollution source for CD PAHs in NWC, NCP, NEC, and CC, whereas industrial emissions such as cement production and iron smelting had strong impacts in the heavy industrial regions. The total benzo[a]pyrene (BaP) carcinogenic potency concentrations (BaPTEQ) for RD and CD both showed the lowest in SC (0.05 and 0.07, respectively) and the highest in NCP (10.99 and 7.67, respectively). The highest and lowest incremental life cancer risks (ILCR) were found in NCP and SC, coinciding with the spatial distributions of ambient PAHs levels. The total CD-related cancer risks for adults and children ( $\sim 10^{-4}$ ) suggest high potential health risks in NCP, SWC, and NWC, whereas the evaluated values in EC and SC indicate virtual safety ( $\leq 10^{-6}$ )

**Keywords:** Urban fugitive dust, Polycyclic aromatic hydrocarbons (PAHs), Source identification, Health risk evaluation, Chinese cities.

---

## **Characteristics and human inhalation exposure of ionic per- and polyfluoroalkyl substances (PFASs) in PM<sub>10</sub> of cities around the Bohai Sea: Diurnal variation and effects of heating activity**

**YangLiu<sup>a</sup>, WeiJianLiu<sup>a</sup>, YunSongXu<sup>a</sup>, YongZhiZhao<sup>b</sup>, PeiWang<sup>c</sup>, ShuangYuYu<sup>a</sup>, JiaoDiZhang<sup>a</sup>, YiTang<sup>d</sup>, GuanNanXiong<sup>a</sup>, ShuTao<sup>a</sup>, WenXinLiu<sup>a</sup>**

**Source :** Science of The Total Environment, Volume 687, 15 October 2019, Pages 177-187

Atmospheric PM<sub>10</sub> (particulate matter with aerodynamic diameter <10  $\mu\text{m}$ ) samples were collected in the cities along the Bohai Sea Rim during heating and non-heating periods, and ionic per- and polyfluoroalkyl species (PFASs) in the PM<sub>10</sub> were measured. The total concentration of ionic PFASs ranged from 21.8 to 87.0  $\text{pg}/\text{m}^3$ , and the mean concentration of ionic PFASs during the day (42.6  $\text{pg}/\text{m}^3$ ) was slightly higher than that at night (35.1  $\text{pg}/\text{m}^3$ ). Generally, diurnal variations in the levels of ionic PFASs were consistent with those in the PM<sub>10</sub> concentrations. Perfluorooctanoic acid (PFOA, 23.5–33.7%), perfluoropentanoic acid (PFPeA, 28.3–39.9%) and perfluorobutyric acid (PFBA, 17.1–20.1%) accounted for the dominant compositional contributions. Significant positive correlations ( $p < 0.05$ ) between the main components of PFASs and O<sub>3</sub> implied that oxidative degradation (O<sub>3</sub> served as the main oxidant) in the period of non-heating may affect the short-chain PFASs. The clustering analysis of a 72-h backward trajectory

indicated that cross-provincial transport contributed to ionic PFASs at the sampling sites. Compared with ingestion via daily diet, the inhalation of PM<sub>10</sub> exhibited an insignificant contribution to the estimated average daily intakes (ADIs) of PFASs by different age groups. In addition, the calculated hazard ratios (HRs) for the non-cancer respiratory risk, based on the air concentrations of PFOA and perfluorooctane sulfonate (PFOS), also manifested lower non-cancer risk through inhalation exposure.

**Keywords:** Ionic PFASs in PM<sub>10</sub>, Bohai Sea Rim, Heating activity, Diurnal variation, Potential source, Health risk.

---

## Short-term and long-term effects of PM<sub>2.5</sub> on acute nasopharyngitis in 10 communities of Guangdong, China

LingliZhang<sup>ab1</sup>, YinYang<sup>a1</sup>, YanhongLi<sup>c1</sup>, Zhengmin (Min)Qian<sup>d</sup>, WanliXiao<sup>e</sup>, XiaojieWang<sup>b</sup>, Craig A.Rolling<sup>d</sup>, EchuLiu<sup>d</sup>, JianpengXiao<sup>f</sup>, WeilinZeng<sup>f</sup>, TaoLiu<sup>fg</sup>, XingLi<sup>f</sup>, ZhenjiangYao<sup>b</sup>, HaoWang<sup>b</sup>, WenjunMa<sup>fg</sup>, HualiangLin<sup>a</sup>

**Source :** Science of The Total Environment, Volume 688, 20 October 2019, Pages 136-142

### Objectives

We aimed to assess the effects of short-term and long-term exposure to ambient fine particle matter (PM<sub>2.5</sub>) on acute nasopharyngitis.

### Methods

A total of 9468 participants aged 18 years and above were recruited from 10 communities in four cities of Guangdong, China during the baseline survey in 2014, and they were followed-up from January 2015 to December 2016. Air pollution exposure was assessed based on the daily concentrations (short-term) and annual concentrations (long-term) of the nearby air monitoring station and the survey date. A mixed-effect logistic model and Cox proportional hazards model were used to quantify the short-term and long-term associations after adjustment for potential confounding factors.

### Results

Significantly positive associations were found between both short-term and long-term exposures of PM<sub>2.5</sub> and acute nasopharyngitis. The adjusted odds ratio was 1.15 (95% CI: 1.07, 1.23) for each 10 µg/m<sup>3</sup> increase in daily PM<sub>2.5</sub> at lag2 day (short-term effects), and the hazard risk was 1.18 (95% CI: 1.10, 1.25) for each 10 µg/m<sup>3</sup> increase in annual PM<sub>2.5</sub> (long-term effects). Stronger associations between short-term PM<sub>2.5</sub> exposure and acute nasopharyngitis were observed among men (OR = 1.10; 95% CI: 1.04, 1.17) and participants aged above 65 years (OR = 1.13; 95% CI: 1.04, 1.23) in the stratified analyses. No significant association was found in women (OR = 1.00; 95% CI: 0.92, 1.10) or young participants ≤65 years (OR = 0.96; 95% CI: 0.88, 1.04). However, for the long-term exposure, the hazard risk was higher for participants younger than 65 years (OR = 1.22; 95% CI: 1.12, 1.32) than the older group (OR = 1.11; 95% CI: 1.00, 1.24).

## **Conclusion**

This study indicates that both short-term and long-term exposures to higher concentrations of PM<sub>2.5</sub> could increase the risk of acute nasopharyngitis.

**Keywords:** Air pollution, PM<sub>2.5</sub>, Acute nasopharyngitis, Effect modification.

---

## **Molecular characterization of dissolved organic matters in winter atmospheric fine particulate matters (PM<sub>2.5</sub>) from a coastal city of northeast China**

**CuipingNing<sup>ab</sup>, YuanGao<sup>a</sup>, HaijunZhang<sup>a</sup>, HaoranYu<sup>ab</sup>, LeiWang<sup>c</sup>, NingboGeng<sup>a</sup>, RongCao<sup>a</sup>, JipingChen<sup>a</sup>**

**Source :** Science of The Total Environment, Volume 689, 1 November 2019, Pages 312-321

Dissolved organic matters (DOMs) in fine particulate matters (PM<sub>2.5</sub>) play a crucial role in global climate change and carbon cycle. However, the chemical components of DOMs are poorly understood due to its ultra-complexity. In this study, DOMs in atmospheric PM<sub>2.5</sub> collected during the heating period in coastal city Dalian were analyzed with ultrahigh resolution Fourier transform ion cyclotron resonance mass spectrometer, and the molecular composition was characterized. A large number of monoisotopic molecular formulas were assigned to DOMs, which could be classified into CHO, CHNO, CHOS, and CHNOS subgroups. A total of 4228 molecular formulas were identified in DOMs collected in hazy days, while only 2313 components were found in DOMs collected in normal days. CHO group was the dominated components in normal days, whereas CHNO group gave significantly higher contributions in hazy days. The S-containing (CHOS and CHNOS) groups posed the highest relative percentages in both normal and hazy days. In addition, potential emission sources were discussed according to the chemical component analysis. The van Krevelent diagram illustrated that lignin-like and protein/amino sugar family species were the most abundant subclasses in DOMs; and 78% and 94% of DOMs in atmospheric PM<sub>2.5</sub> collected from Dalian could come from biogenic origins in hazy and normal days, respectively. More compounds in hazy days were derived from anthropogenic emissions.

**Keywords:** PM<sub>2.5</sub>, DOMs, FT-ICR MS, Molecular characteristics.

---

## **PM<sub>2.5</sub> generated during rapid failure of fiber-reinforced concrete induces TNF-alpha response in macrophages**

**Lupita D.Montoya<sup>a</sup>, Harish K.Gadde<sup>a</sup>, Wyatt M.Champion<sup>a</sup>, NingLi<sup>b</sup>, Mija H.Hubler<sup>a</sup>**

**Source :** Science of The Total Environment, Volume 690, 10 November 2019, Pages 209-216

Failure of large, concrete structures can lead to the generation of very small fragments, including aerosols in the fine fraction, which have aerodynamic diameters of  $\leq 2.5 \mu\text{m}$  (PM<sub>2.5</sub>). These aerosols can persist in the environment, pose exposure risks, and potentially cause negative health effects. New trends in construction favor the use of concrete reinforced with steel fibers, but little is known about the nature of the fragments generated during its failure. This study investigated the fragmentation of several steel-fiber reinforced concrete formulations using dynamic compression testing. The release of tumor necrosis factor alpha (TNF- $\alpha$ ), an inflammatory marker widely used in both human and animal studies, was then analyzed to determine the effects of the fragments in the aerosol fine fraction on mouse macrophages (RAW 264.7). All concrete formulations studied showed statistically increased TNF- $\alpha$  release, which was inversely correlated with fiber length and fiber content (% weight). In addition, results from a select set of concrete formulations also showed a clear dose-response relationship. This paper postulates the fracture mechanisms by which concrete parameters (i.e., fiber length and content) lead to the generation of PM<sub>2.5</sub>, producing the observed TNF- $\alpha$  release.

**Keywords:** Reinforced concrete, Concrete aerosols, Inflammation, Tumor necrosis factor alpha, Construction particles.

---

## **Approaches for identifying PM<sub>2.5</sub> source types and source areas at a remote background site of South China in spring**

**KaiZhang<sup>a</sup>, XiaonaShang<sup>a</sup>, HartmutHerrmann<sup>b</sup>, FanMeng<sup>a</sup>, ZhaoyuMo<sup>c</sup>, JianhuaChen<sup>a</sup>, WenliLv<sup>a</sup>**

**Source :** Science of The Total Environment, Volume 691, 15 November 2019, Pages 1320-1327

The receptor model is an effectively and widely used tool for analyzing the source of PM<sub>2.5</sub>, and its development and improvement have always been focused and challenged. In this study, approaches of source analysis is applied and compared. The PM<sub>2.5</sub> samples were collected in spring of 2015 at a remote background site of Weizhou, South China and were analyzed for water-soluble ions, trace metals, and sugars. The 28 measurement species were introduced into the positive matrix factorization (PMF) and a non-negative matrix factorization (NMF) model for inter-comparison of PM<sub>2.5</sub> prediction. Results showed that the NMF model is a more robust tool to identify source types and source apportionment in the case of a small sample size ( $n = 31$ ). In NMF, four source variants were obtained as dust (15.6%), biomass combustion (11.8%), secondary formation (17.6%), and coal combustion (54.9%), corresponding to four main source areas. These were Southeast Asia, South China Sea, Taiwan Strait, as well as Pearl River Delta, respectively. The areas were distinguished based on hybrid receptor models, potential source contribution function (PSCF) and concentration weighted trajectory (CWT), by introducing the daily loadings of each source factor from NMF method. These model results were highly consistent with categorized chemical characteristics of PM<sub>2.5</sub>, suggesting that NMF linking with hybrid receptor models provides valuable implications for exploring source types and source areas of



PM<sub>2.5</sub>. Meanwhile, biomass combustion and coal combustion comparably contributed to the high PM<sub>2.5</sub> concentrations indicating control strategy in South China in spring.

**Keywords:** PM<sub>2.5</sub>, Source types, Source areas, NMF, PMF, Hybrid receptor models.

---

## **Energy and emission pathways towards PM<sub>2.5</sub> air quality attainment in the Beijing-Tianjin-Hebei region by 2030**

**DanTong<sup>ab</sup>, GuannanGeng<sup>b</sup>, KejunJiang<sup>c</sup>JingChen, g<sup>a</sup>, YixuanZheng<sup>a</sup>, ChaopengHong<sup>ab</sup>, LiuYan<sup>a</sup>, YuxuanZhang<sup>a</sup>, XiaotingChen<sup>b</sup>, YuBo<sup>d</sup>, YuLei<sup>e</sup>, QiangZhang<sup>a</sup>, KebinHe<sup>b</sup>**

**Source :** Science of The Total Environment, Volume 692, 20 November 2019, Pages 361-370

In 2013, the Chinese government announced its first air quality standard for PM<sub>2.5</sub> (particulate matter with a diameter < 2.5 μm) which requires annual mean PM<sub>2.5</sub> concentration to achieve the World Health Organization (WHO) interim target 1 of 35 μg/m<sup>3</sup> nationwide including the most polluted region of Beijing-Tianjin-Hebei (BTH). Here, we explore the future mitigation pathways for the BTH region to investigate the possibility of air quality attainment by 2030 in that region, by developing two energy scenarios (i.e., baseline energy scenario and enhanced energy scenario) and two end-of-pipe scenarios (i.e., business as usual scenario and best available technology scenario) and simulating future air quality for different scenarios using the WRF/CMAQ model. Results showed that without stringent energy and industrial structure adjustment, even the most advanced end-of-pipe technologies did not allow the BTH region to attain the 35 μg/m<sup>3</sup> target. Under the most stringent scenario that coupled the enhanced structure adjustment measures and the best available end-of-pipe measures, the emissions of SO<sub>2</sub>, NO<sub>x</sub>, PM<sub>2.5</sub> and NMVOCs (nonmethane volatile organic compounds) were estimated to be reduced by 85%, 74%, 82% and 72%, respectively, in 2030 over the BTH region. As a result, the simulated annual mean PM<sub>2.5</sub> concentrations in Beijing, Tianjin and Hebei could decline to 23, 28 and 28 μg/m<sup>3</sup>, respectively, all of which achieved the 35 μg/m<sup>3</sup> target by 2030. Our study identified a feasible pathway to achieve the 2030 target and highlighted the importance of reshaping the energy and industrial structure of the BTH region for future air pollution mitigation.

**Keywords:** Emission scenarios, Beijing-Tianjin-Hebei, PM<sub>2.5</sub>, Air quality improvement.

---

# Particulate air pollution and ischemic stroke hospitalization: How the associations vary by constituents in Shanghai, China

WeidongWang<sup>a1</sup>, CongLiu<sup>a1</sup>, ZhekangYing<sup>a</sup>, XiaoningLei<sup>a</sup>, CuipingWang<sup>a</sup>, JuntaoHuo<sup>b</sup>, QianbiaoZhao<sup>b</sup>, YihuaZhang<sup>b</sup>, YusenDuan<sup>b</sup>, RenjieChen<sup>ac</sup>, QingyanFu<sup>b</sup>, HaoZhang<sup>d</sup>, HaidongKan

**Source :** Science of The Total Environment, Volume 695, 10 December 2019, 133780

## Background

The identification of constituents of fine particulate matter (PM<sub>2.5</sub>) air pollution that had key impacts of ischemic stroke (the predominant subtype of stroke) is important to understand the underlying biological mechanisms and develop air pollution control policies.

## Objectives

To explore the associations between PM<sub>2.5</sub> constituents and hospitalization for ischemic stroke in Shanghai, China.

## Methods

We conducted a time-series study to explore the associations between 27 constituents of PM<sub>2.5</sub> and hospitalization for ischemic stroke in Shanghai, China from 2014 to 2016. The over-dispersed generalized additive models with adjustment for time, day of week, holidays, and weather conditions were used to estimate the associations. We also evaluated the robustness of the effect estimates for each constituent after adjusting for the confounding effects of PM<sub>2.5</sub> total mass and gaseous pollutants and the collinearity (the residual) between this constituent and PM<sub>2.5</sub> total mass. We also compared the associations between seasons.

## Results

In total, we identified 4186 ischemic stroke hospitalizations during the study period. The associations of ischemic stroke were consistently significant with elemental carbon and several elemental constituents (Chromium, Iron, Copper, Zinc, Arsenic, Selenium, and Lead) at lag 1 day in single-constituent models, models adjusting for PM<sub>2.5</sub> total mass or gaseous pollutants and models adjusting for collinearity. The associations were much stronger in cool season than in warm season.

## Conclusions

The current study provides suggestive evidence that elemental carbon and some metallic elements may be mainly responsible for the risks of ischemic stroke hospitalization induced by short-term PM<sub>2.5</sub> exposure.

**Keywords:** PM<sub>2.5</sub>, Chemical constituent, Ischemic stroke, Morbidity, Time-series.

## Characteristics and health effects of PM<sub>2.5</sub> emissions from various sources in Gwangju, South Korea

InjeongKim<sup>a</sup>, KwangyulLee<sup>b</sup>, SunhongLee<sup>c</sup>, Sang DonKim<sup>ad</sup>

**Source :** Science of The Total Environment, Volume 696, 15 December 2019, 133890

Increasing evidence suggests that the toxicity of fine dust particles (PM<sub>2.5</sub>) is linked to specific components rather than their mass. However, research on the chemical composition and health risk of PM<sub>2.5</sub> is insufficient. This study analyzed the metals, polycyclic aromatic hydrocarbon (PAHs), organochlorine pesticides (OCPs), and polychlorinated biphenyls (PCBs) present in PM<sub>2.5</sub> and evaluated their risk to health during outdoor activities. The concentration of metals was one order of magnitude higher than that of PAHs and the concentration and detection frequency of OCPs and PCBs were considerably lower than those of metals and PAHs. The lifetime excess cancer risk (LECR) for carcinogens in PM<sub>2.5</sub> exceeded de minimis risk ( $1 \times 10^{-6}$ ) as  $1.33\text{--}3.44 \times 10^{-6}$  (at 5th–95th percentile) as Cr(VI), As, and Cd showed high contributions. Children in the 2 < years <18 age group had a high risk of cancer due to early-life susceptibility. The proportion of  $\sum$ Metals to LECR was approximately 95%, while  $\sum$ PAHs attributed to 5% of total LECR. The effects of  $\sum$ OCPs and 2,3',4,4',5'-Pentachlorobiphenyl (PCB-123) on LECR were negligible. The hazard quotient (HQ) for non-carcinogens was <1, and non-carcinogenic effects were not expected. Mn, BaP, Pb, As, and Cd were the key determinants of the HQ values and among the identified PM<sub>2.5</sub> sources they are closely related to industrial activities, oil combustion, and gasoline exhaust. Therefore, control strategies for these sources can effectively reduce PM<sub>2.5</sub> risk. This study measured the concentrations of toxic compounds in ambient PM<sub>2.5</sub> and considered only PM<sub>2.5</sub> exposure during outdoor activities. PM<sub>2.5</sub> health risk during the entire day would be higher than the PM<sub>2.5</sub> risk determined in this study, and further research is required for this evaluating this risk.

**Keywords:** PM<sub>2.5</sub>, Metals, Polycyclic aromatic hydrocarbon, Organochlorine pesticides, Risk assessment.

---

## Short-term effects of real-time personal PM<sub>2.5</sub> exposure on ambulatory blood pressure: A panel study in young adults

MengRen<sup>a</sup>, HuanhuanZhang<sup>a</sup>, TarikBenmarhnia<sup>b</sup>, BinJalaludin<sup>c</sup>, HaotianDong<sup>a</sup>,  
KaipuWu<sup>a</sup>, QiongWang<sup>ad</sup>, CunruiHuang<sup>ad</sup>

**Source :** Science of The Total Environment, Volume 697, 20 December 2019, 134079

### Background

Short-term exposure to PM<sub>2.5</sub> has been shown to be associated with changes in blood pressure. However, most of the evidence is based on PM<sub>2.5</sub> measurements from fixed stations and resting blood pressure measured at a regular time.

## **Objectives**

To evaluate the short-term daily and hourly effects of real-time personal PM<sub>2.5</sub> exposure on ambulatory blood pressure, and to compare the effects with those of PM<sub>2.5</sub> exposure from fixed stations.

## **Methods**

Between April 2017 and December 2017, 37 young adults were recruited in a panel study from a central urban area and a suburban area, to measure personal hourly PM<sub>2.5</sub> and ambulatory systolic blood pressure (SBP) as well as diastolic blood pressure (DBP) for three consecutive days. Hourly PM<sub>2.5</sub> concentrations were also obtained from the nearest monitoring station operated by Guangdong Environmental Monitoring Center. Generalized additive mixed model was employed to evaluate the effects of PM<sub>2.5</sub> on ambulatory blood pressure.

## **Results**

During the study period, the mean concentration of personal PM<sub>2.5</sub> exposure was  $60.30 \pm 52.14 \mu\text{g}/\text{m}^3$ , while the value of PM<sub>2.5</sub> from fixed stations was  $36.77 \pm 21.52 \mu\text{g}/\text{m}^3$ . Both personal PM<sub>2.5</sub> exposure and exposure from fixed stations averaged over the previous 1 to 3 days decreased blood pressure. During daytime, a  $10 \mu\text{g}/\text{m}^3$  increase in 1-day moving average of personal PM<sub>2.5</sub> was associated with a 0.54 mmHg (95% CI: -1.03, -0.05) and 0.22 mmHg (95% CI: -0.59, 0.15) decrease in SBP and DBP, respectively. When using PM<sub>2.5</sub> exposures from fixed stations, the decrease in SBP and DBP were 0.95 mmHg (95% CI: -1.82, -0.07) and 0.74 mmHg (95% CI: -1.46, -0.03). Stratified analysis showed stronger effects in the central urban area and among males.

## **Conclusions**

Both personal PM<sub>2.5</sub> exposure and exposure from fixed stations averaged over the previous 1 to 3 days decreased blood pressure. Stronger effects were found in a central urban area and among males.

**Keywords:** PM<sub>2.5</sub>, Personal exposure, Ambulatory blood pressure, Panel study.

---



**Indian Institute of Tropical Meteorology**  
**Dr. Homi Bhabha Road, Pashan, Pune - 411 008, India**  
**Telephone: +91-20-2590-4200**  
**E-mail: [iitm-env@nic.in](mailto:iitm-env@nic.in)**  
**Website: [www.iitmenvis.nic.in](http://www.iitmenvis.nic.in)**